Physical and Engineering Sciences in Medicine (2023) 46:413–519
https://doi.org/10.1007/s13246-023-01228-5

EPSM 2022, Engineering and Physical Sciences in Medicine

13–16 November 2022, Adelaide, Australia

Published online: 10 March 2023

O1. [Plenary] The way to radiotheranostics: IJB as a center of excellence

Zena Wimana[1,*]

[1]Institut Jules Bordet, Bruxelles, Belgium

O2. [Plenary] Motion correction in MRI

Ernesta Meintjes[1,*]

[1]University of Cape Town, Cape Town, South Africa

O3. [Plenary] Fun with 4D images

Marcel van Herk[1,*]

[1]University of Manchester, Manchester, UK

O4. [Plenary] FLASH radiotherapy—a myth or reality?

Magdalena Bazalova-Carter[1,*]

[1]University of Victoria, Victoria BC, Canada

O5. [Invited] Medical Device Production and Software Development at Point-of-Care: Achieving Regulatory Conformity

Scott Crowe[1,2,3,4,*]

[1]Royal Brisbane & Women's Hospital, Brisbane, Australia, [2]Herston Biofabrication Institute, Brisbane, Australia, [3]University of Queensland, Brisbane, Australia, [4]Queensland University of Technology, Brisbane, Australia

Medical physicists are often "custodians" of quality within their workplaces [1], having a scope of practice that covers many aspects of quality management, including assessment and mitigation of risk, the evaluation of new technologies, quality control and assurance testing, and ongoing monitoring and quality improvement [2]. It is in this capacity that they often lead or contribute to the development of new medical devices or software to improve clinical practices. 3D printing, open-source software development libraries, and the wealth of guidance available online have removed barriers of entry, accelerating these activities at point-of-care. Physicists, however, are not necessarily familiar with the regulatory environment surrounding the development and supply of these devices. In a 2022 ACPSEM webinar, 72% of attendees reported they were "not at all" or only "slightly" confident in their understanding of the definition of a medical device, and what is subject to TGA or Medsafe regulation [2]. Anecdotally, similar uncertainties exist around what constitutes software as a medical device. This presentation will share the experiences of the Royal Brisbane and Women's Hospital and Herston Biofabrication Institute Cancer Care program in quality management of medical device development and achieving regulatory conformity.

References

1. Zellars R, Njeh C, Marquette S (2022) The need for dedicated time for medical physicists practice quality improvement efforts in radiation oncology department: a commentary. J Appl Clin Med Phys 23(3): e135115. https://doi.org/10.1002/acm2.13515
2. Simpson-Page E, Coogan P, Kron T, et al. (2022) Webinar and survey on quality management principles within the Australian and New Zealand ACPSEM Workforce. Phys Eng Sci Med (in press). https://doi.org/10.1007/s13246-022-01160-0

O6. An evaluation of novel additive manufacturing processes in the production of combined shielding and bolus in megavoltage electron treatments

Daniel Thommen[1], **Ashley Cullen**[2], **Will Lewin**[3], **Robin Hill**[1,2,3,*]

[1]Institute of Medical Physics, School of Physics, University of Sydney, Sydney, Australia, [2]Department of Radiation Oncology, Chris O′Brien Lifehouse, Camperdown, Australia, [3]Biomedical Innovation Hub, Chris O'Brien Lifehouse, Camperdown, Australia

Introduction Megavoltage electron beams are an effective treatment modality for superficial lesions. To improve the dose homogeneity as well as reduce dose to healthy tissue, bolus and shielding devices are commonly used. A 3D printed filament device may provide superior conformation to the patient contour and be more efficient in manufacturing. In this project, we evaluate the dosimetric characteristics of a novel combined shield and bolus device, co-printed using different filament materials.

Method Percentage depth dose (PDD) and transmission measurements were performed on a Varian TrueBeam accelerator. Surface contours for device design were obtained by both CT scans (Toshiba Aquilon) and optical imaging (EinScan Pro 2X) of an Alderson-Rando head phantom. The device was 3D modelled in Autodesk MeshMixer software and produced using a Raise3D Pro2 Plus FDM printer with Bilby3D TPU and ColorFabb BronzeFill filaments. Treatment planning was implemented using Varian Eclipse TPS, and verification performed using Gafchromic EBT3 film.
Results The printed TPU exhibited similar radiological properties to conventional bolus in terms of mass and relative electron densities. Approximately 10 mm of printed shielding was required to reduce the relative dose by 95% for the 6 MeV beam, while 15 mm was required for a 9 MeV beam. A combined bolus/shielding device was created with initial results showing acceptable conformability to the phantom.
Conclusion Both the TPU and metal filaments exhibited appropriate radiological properties for their intended use as bolus and shielding materials within the lower electron beam energies. Using a novel production method, both materials were successfully incorporated into a combined bolus and shielding device.

	CT Number (HU)	Mass Density ($g{\cdot}cm^{-3}$)	Electron Density (relative to water)
TPU Slabs	105 ± 5	1.090 ± 0.05	1.070 ± 0.05
TPU Bolus	-5 ± 85	1.015 ± 0.075	1.000 ± 0.075

Fig. 1. Radiological properties of printed TPU samples.

Fig. 2. Comparison of traditional versus additive manufacturing production of combined bolus and shielding devices.

O7. Towards an open source AI medical device: creating a new paradigm for commercial software

Simon Biggs[1,*], May Whitaker[1]

[1]Radiotherapy AI, Tatton, Australia

Introduction Translating research into clinical practice is a lengthy and opaque process. In 2021 the TGA introduced new Software as a Medical Device (SaMD) regulation. This brought in new requirements for software developers, both clinical and commercial, who create and supply software to support radiotherapy. When solving new problems there are often precedents that may be used as guides. There are not, as yet, transparent examples to assist in becoming a regulated medical device in the radiotherapy space. Sharing regulated, open source, software would forge a path for other developers to follow, and create a new paradigm for collaborative research with the aim of expediting the translation from development to clinical use.
Method Consultation was undertaken to ascertain the TGA classification of an autocontouring SaMD. The product was then developed and the associated quality management and technical documents were produced. Iterative feedback from the TGA was sought to ensure regulatory requirements were met at each phase.
Results Autocontouring products are classified as a clinical decision support software in Australia, as a Class IIb Medical Device. This is the same medical device classification as treatment planning systems and linear accelerators. The process for creating a transparent and reproducible path for the regulation of an open source Class IIb SaMD is currently in progress. There have been some initial successes in pilot and feasibility studies in preparation for sharing the code.
Conclusion Translating research into clinical practice is difficult. There are no clear, transparent and reproducible examples for how to achieve this in the radiotherapy space. In creating a new path towards the regulation of SaMDs, it is hoped that researchers and developers will have a framework to guide them, encouraging collaborative research to be translated into better patient care.

O8. Investigations into 3 mm bolus use for breast radiation therapy

Izabela Junis[1]

[1]Blacktown Cancer and Haematology Centre, Blacktown, Australia

Introduction 5 mm thick Superflab bolus is applied to the skin surface of post mastectomy radiotherapy breast plans to boost surface dose. Currently, the bolus is used for certain VMAT plans and the open tangent fields of hybrid IMRT plans. 3 mm thick bolus was purchased to see if it could be used as a replacement, as it could potentially reduce skin desquamation, and is more pliable, making it easier to conform to the skin surface. Another part of this study was to investigate if 3 mm bolus could be used for the full duration of treatment without removal for the IMRT component.
Methods Tangent and VMAT plans were mocked up in Eclipse. These plans were delivered to a thorax phantom and measured with OSLD's with scenarios no bolus, 3 mm bolus and 5 mm bolus. Eclipse TPS (AAA and AXB) dose and physical delivered dose was calculated for a range of bolus combinations.
Results Considering OSLD measurements and Eclipse TPS calculated dose analysis, it was found that 3 mm bolus for all fractions is approximately 5.0%(6X) and 7.0%(10X) cooler than 5 mm bolus for all fractions. 3 mm bolus for all portions of the treatment plan (IMRT + open field) is on average 8.2%(6X) and 7.6%(10X) hotter than 5 mm bolus on just the open portion of the plan. When 3 mm bolus replaces 5 mm keeping with current practice, on average, the 3 mm bolus plans are 2.1%(6X) and 4.1%(10X) cooler. This compares to no bolus use being 30.4%(6X) 34.8%(10X) cooler than the current practice of 5 mm bolus on 60% of the plan.
Conclusion It is recommended that to not exceed current surface doses, the practice of bolus on open fields and off IMRT fields is maintained. For modest surface dose reduction $\sim$ 5%, 3 mm can be used for the open fields instead of 5 mm. 3 mm bolus on all fields will increase surface dose compared to current practice.

O9. Construction of Hybrid Software Phantoms for Theragnostic Dosimetry

Erin Mckay[1,*]

[1]South Eastern Sydney Local Health District, Kogarah, Australia

Introduction Radiopharmaceutical dosimetry for theragnostics often involves either adjusting target organ masses for a pre-defined anthropomorphic model using a software tool such as OLINDA/EXM

[1] or applying dose kernel convolution or Monte Carlo simulation to estimate voxel-level distributions of dose directly from tomographic images using tools like 3D-ID/RD [2]. Voxel-based approaches provide a close approximation of individual anatomy for large, solid structures. They also provide an indication of the distribution of absorbed dose within sufficiently large targets. However, model-based approaches may better represent hollow organs such as the gut and small-scale structures such as bone marrow and bone surfaces. This work enables a hybrid approach based on pre-defined anthropomorphic models that may be partially customised with individual anatomy using clinical image segmentation and Monte Carlo simulation.

Method The MrVoxel [3] image processing software is used to specify source and target volumes of interest in clinical anatomy, calling the GATE Monte Carlo simulation software [4] to establish the associated dose factors for a nominated radionuclide. Dose calculations incorporating the new or updated sources and targets are performed using MrVoxel's "MIRD Phantom Dose" plug-in module [5] which replaces or complements dose factors generated on-the-fly in a selected OpenDose Calculator [6] internal dosimetry phantom.

Results In combination, these software tools allow for the incorporation of customised dose factors into a pre-defined anthropomorphic phantom prior to performing an internal dose calculation. The utility of the method is limited by an assumption that the activity distribution within source regions is uniform and the contribution to the radiation dose received by new or modified targets from pre-defined phantom sources is not calculated.

Conclusion Software has been developed to facilitate the modification of MIRD-style dosimetry phantoms by adjusting existing dose factors and/or adding new ones on-the-fly. This capability opens up new possibilities for individual internal radionuclide dosimetry.

References

1. Stabin M.G., Sparks R.B., Crowe E., 2005. "OLINDA/EXM: The Second-Generation Personal Computer Software for Internal Dose Assessment in Nuclear Medicine". J Nucl Med; 46:1023–1027.
2. Sgouros G., et al., 2008. "3-D Imaging Based, Radiobiological Dosimetry". Semin Nucl Med; 38(5): 321–334.
3. McKay E., 2003. "A Software Tool for Specifying Voxel Models for Dosimetry Estimation". Cancer Biotherapy & Radiopharmaceuticals;18(3).
4. Villoing D, et al., 2017 "Internal dosimetry with the Monte Carlo code GATE: validation using the ICRP/ICRU female reference computational model". Phys Med Biol; 62(5):1885–1904.
5. McKay E., 2022. "Combining Individual and Model-Based Internal Dosimetry Calculation for Radionuclide Therapy using MrVoxel/OCD". Abstract for ANZSNM 2022.
6. McKay E., MalarodaA., 2019. "OpenDose: an extensible, open-source internal dosimetry calculator". Australas Phys Eng Sci Med; 42: 285–401.

O10. From cancer to cardiac arrhythmias: how we can use our expertise to help another patient cohort

Suzanne Lydiard[1,2,*]

[1]Kathleen Kilgour Centre, Tauranga, New Zealand, [2]Cancer & Blood, Radiation Oncology, Auckland City Hospital, Auckland, New Zealand

Stereotactic ablative radiotherapy (SABR) is now recommended and/or supported for a range of primary tumour sites. The successful widespread implementation of SABR is at least partially attributable to technology advancements that enable the accurate treatment delivery of high doses per fraction, even for tumours sites that previously challenged radiotherapy. A timely and current question is "has radiotherapy technology advanced enough to be an efficacious treatment for cardiac arrhythmias?" Cardiac radioablation has been proposed as a new non-invasive treatment alternative for two cardiac arrhythmias; ventricular tachycardia (VT) and atrial fibrillation (AF). Cardiac radioablation has the potential to significantly advance [1] and expand the clinical care available to those suffering from cardiac arrhythmias and is already being implemented within clinical trials globally. However, this treatment presents possibly the most challenging treatment scenario yet encountered in radiotherapy; $\geq$ 25 Gy needs to be precisely delivered to cardiac sub-structures whilst sparing critical structures in close proximity, treatment targets undergo complex cardio-respiratory target motion and often lack inherent contrast from surrounding tissue, and successful treatments require clear communication and collaboration between Radiation Oncology and Cardiology colleagues [2]. This talk will introduce cardiac radioablation, illustrate how our radiation oncology expertise could help those suffering from cardiac arrhythmias, highlight the status and challenges of cardiac radioablation for AF compared to VT, and explore the possibility of MRI-guided cardiac radioablation treatments.

References

1. Cuculich S, Schill MR, Kashani R, Mutic S, Lang A, Cooper D, et al. Noninvasive Cardiac Radioablation for Ablation of Ventricular Tachycardia. N Engl J Med. 2017;377(24):2325–36.
2. Lydiard S, Blanck O, Hugo G, O'Brien R, Keall P. A Review of Cardiac Radioablation for Arrhythmias: Procedures, Technology, and Future Opportunities. Int J Radiat Oncol Biol Phys. 2021;109(3):783–800.

O11. How consistent are heart contours and associated dosimetry?

Lois Holloway[1,2,3,4], Robert Finnegan[1,3,5], Vicky Chin[1,2], Phillip Chlap[1,2,*], Daniel Al Mouiee[1,2], Matthew Field[1,2], Xinyi (Janet) Cui[1,2], Amir Anees[1,2], Fahim Alam[1,2], Nicholas Hardcastle[4,6], David Porter[7], Martin Carolan[4,8], Michael Bailey[8], Senthilkumar Gandhidasan[8], Jonathan Sykes[3,9], Verity Ahern[9,10], Eric Hau[9,10], Joerg Lehmann[3,11,12], John Simpson[11,12], [11]Jane Ludbrook, Jothy Selvaraj[2,13], Angela Rezo[14,15], David Thwaites[3,16], Shalini Vinod[1,2], Geoff Delaney[1,2]

[1]South Western Sydney Cancer Services, NSW Health and Ingham Institute, Sydney, Australia, [2]South Western Sydney Clinical Campus, School of Clinical Medicine, University of New South Wales, Sydney, Australia, [3]Institute of Medical Physics, University of Sydney, Sydney, Australia, [4]Centre for Medical Radiation Physics, University of Wollongong, Wollongong, Australia, [5]Royal North Shore Hospital, Sydney, Australia, [6]Department of Physical Sciences, Peter MacCallum Cancer Centre, Melbourne, Australia, [7]School of Science, RMIT University, Melbourne, Australia, [8]Illawarra and Shoalhaven Cancer Care Centres, Wollongong, Australia, [9]Western Sydney Local Health District, Sydney, Australia, [10]Westmead Clinical School, University of Sydney, Sydney, Australia, [11]Radiation Oncology Department, Calvary Mater, Newcastle, Australia, [12]School of Mathematical and Physical Sciences, University of Newcastle, Newcastle, Australia, [13]Medical Physics and Radiation Engineering, Canberra Health Services, Canberra, Australia, [14]The Canberra Hospital, Canberra, Australia, [15]Medical School, Australian National University, Canberra,

Australia, [16]Leeds Institute of Medical Research, School of Medicine, University of Leeds, Leeds, United Kingdom

Introduction Understanding the impact of radiation dose to the heart has evolved in recent years. Although acknowledged that whole heart is perhaps not the most appropriate target, mean heart dose is commonly included in prognostic models and used for plan optimization [1]. However, little is known on the consistency of heart contours and associated dose metrics across clinics. In this work an auto-segmentation tool was used to assess contour consistency across clinics.
Method Using a recently released open-access, deep learning heart auto-segmentation model[2], heart volumes were segmented on lung and breast datasets from two clinics with existing clinical heart volumes. 98/100 breast patients receiving either 40 Gy/15 fractions or 42.5 Gy/16 fractions and 100/76 lung patients receiving 60-66 Gy/30–33 fractions and recently treated were selected from clinic 1 and 2 respectively. The average Dice similarity coefficient (DSC), mean distance to agreement (MDA) and volume as well as the difference in mean heart dose, V20Gy(breast) and V5Gy(lung) between the automated and clinical heart contours were calculated. Distributions of these metrics were compared between the clinics.
Results Tables 1 and 2 show the average and standard deviation of contour comparison metrics, and differences in dose metrics for the lung and breast cohorts respectively. For both cohorts high DSC and low MDA was observed, and good agreement between dose metrics. The average difference in mean heart dose, a significant factor in cardiotoxicity, was 0.1 Gy or less for the breast cohort. Pearson's correlation between auto and mean heart doses was above 0.95 for both clinics.
Conclusion Difference in contouring and dose metrics for lung and breast cohorts from different clinics between automatically and clinically defined heart contours were shown to be small from this initial comparison, implying that cardiac dose comparison metrics can be used consistently between clinics and in modelling studies. Future work will incorporate a wider range of clinics.
Acknowledgements
Australian Research Data Commons and NSW Cancer Institute for grant funding.
References

1. Darby SC, Ewertz M, McGale P, Bennet AM, Blom-Goldman U, Brønnum D, Correa C, Cutter D, Gagliardi G, Gigante B, Jensen MB (2013) Risk of ischemic heart disease in women after radiotherapy for breast cancer. New England Journal of Medicine 368:987–98.
2. Finnegan R, Dowling J, Koh ES, Tang S, Otton J, Delaney G, Batumalai V, Luo C, Atluri P, Satchithanandha A, Thwaites D, Holloway L (2019) Feasibility of multi-atlas cardiac segmentation from thoracic planning CT in a probabilistic framework. Physics in Medicine & Biology. 64:085,006.
3. https://pyplati.github.io/platipy/cardiac.html

Table 1 Comparison metrics for auto-segmented and manually defined heart contours for the lung cohort.

	Clinic 1		Clinic 2	
	Average	Std Dev	Average	Std Dev
DSC	0.92	0.04	0.92	0.03
MDA (mm)	2.6	1.2	2.7	1.0
HD (mm)	14.9	7.2	18.0	24.7
Vol_manual (cc)	664.6	169.5	701.7	198.5
Vol_auto (cc)	701.3	156.2	738.2	185.9
Vol_diff (manual-auto) (cc)	6.7	76.0	36.4	78.4
MeanDose_manual (Gy)	8.5	5.8	12.0	9.9
MeanDose_auto (Gy)	9.0	6.2	12.6	10.0
MeanDosediff (manual-auto) (Gy)	-0.5	1.4	0.6	1.6
V5Gy_manual (%)	37.1	27.0	40.5	29.6
V5Gy_auto (%)	37.8	26.9	42.0	29.2
V5Gy_diff (%)	-0.6	3.7	1.5	4.1

Table 2 Comparison metrics for auto-segmented and manually defined heart contours for the breast cohort.

	Clinic 1		Clinic 2	
	Average	Std Dev	Average	Std Dev
DSC	0.92	0.05	0.92	0.04
MDA (mm)	2.5	1.3	2.4	1.1
HD (mm)	14.5	7.5	14.7	7.0
Vol_manual (cc)	615.5	166.9	586.7	101.3
Vol_auto (cc)	638.4	128.3	612.1	92.6
Vol_diff (manual-auto) (cc)	-22.9	88.0	25.5	60.1
MeanDose_manual (Gy)	1.4	0.9	1.8	1.2
MeanDose_auto (Gy)	1.4	1.0	1.8	1.1
MeanDosediff (manual-auto) (Gy)	0.0	0.3	-0.1	0.2
V20Gy_manual (%)	0.5	0.9	1.5	1.9
V20Gy_auto (%)	0.4	0.7	1.4	1.9
V20Gy_diff (%)	0.1	0.3	-0.1	0.4

O12. The application of metal artifact reduction algorithms in planning computed tomography scans for ultrasound-guided cardiac radioablation using protons

Sathyathas Puvanasunthararajah[1,2,*], Saskia Camps[3], Marie-Luise Wille[4,5], Davide Fontanarosa[1,2]

[1]School of Clinical Sciences, Queensland University of Technology, Brisbane, Australia, [2]Centre for Biomedical Technologies, Queensland University of Technology, Brisbane, Australia, [3]EBAMed SA, Geneva, Switzerland, [4]School of Mechanical, Medical & Process Engineering, Faculty of Engineering, Queensland University of Technology, Brisbane, Australia, [5]ARC ITTC

for Multiscale 3D Imaging, Modelling, and Manufacturing, Queensland University of Technology, Brisbane, Australia

Introduction Cardiac radioablation is a promising treatment for cardiac arrhythmias, but accurate dose delivery can be affected by heart motion. For this reason, real-time cardiac motion monitoring during radioablation is of paramount importance. Real-time ultrasound (US) guidance can be a solution. The US-guided cardiac radioablation workflow can be simplified by the simultaneous US and planning computed tomography (CT) acquisition, which can result in US transducer-induced metal artifacts on the planning CT scans. To reduce their impact, a new metal artifact reduction (MAR) algorithm, named Combined Clustered Scan-based MAR (CCS-MAR) has been developed and compared with iMAR, (Siemens) and MDT (ReVision Radiology) algorithms.
Method CT scans from a Model ART-211 male phantom with and without Terason XY Biplane phased array US transducer induced artifacts (CT_{art} and CT_{ref}, respectively), were used (see Fig. 1). The mean absolute percentage (MAP) error of CT_{art} and the corrected CT scans was calculated and compared to CT_{ref} in the heart, lung, and bone (Fig. 1).
Results In all three regions, CCS-MAR reduced the artifacts caused by the US transducer more efficiently than the other MAR algorithms. For example, in the heart region, the calculated MAP error was 29% on CT_{art} and it was reduced to 17%, 12% and 10% after iMAR, MDT, and CCS-MAR application, respectively.
Conclusion The application of MAR algorithms reduces the negative impact of US transducer-induced metal artifacts on planning CT scans. In comparison to iMAR and MDT, CCS-MAR performs better or comparably in reducing these metal artifacts.
References

1. Perrin R, Maguire P, Garonna A, Weidlich G, Bulling S, Fargier-Voiron M, De Marco C, Rossi E, Ciocca M, Vitolo V and Mirandola A 2022 Case Report: Treatment Planning Study to Demonstrate Feasibility of Transthoracic Ultrasound Guidance to Facilitate Ventricular Tachycardia Ablation with Protons. Front. Cardiovasc. Med. 9 Online: https://www.frontiersin.org/article/10.3389/fcvm.2022.849247
2. Ipsen S, Bruder R, García-Vázquez V, Schweikard A and Ernst F 2019 Assessment of 4D Ultrasound Systems for Image-guided Radiation Therapy—Image Quality, Framerates and CT Artifacts Curr. Dir. Biomed. Eng. 5 245–8.

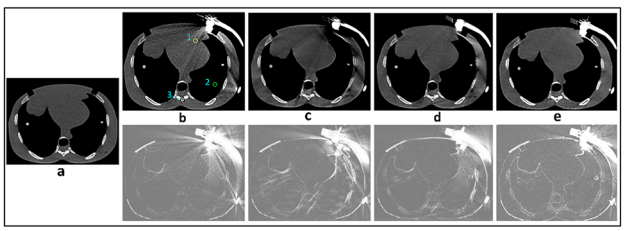

Fig. 1. **a** (CT_{ref}), **b** (CT_{art}) and artifact corrected CT scans by **c** (iMAR), **d** (MDT) and **e** (CCS-MAR). The absolute differences of **b**, **c**, **d**, and **e** with the **a** is given below them. The positions of region of interest (1: heart, 2: lung, 3: bone) for the Hounsfield unit measurements are shown in CT_{art}.

O13. Is this the end of CT? Consumer smartphones for 3D printing bolus and surface mould applicators for radiation oncology

Corey Bridger[1,2,*], Alexandre Santos[1,2], Paul Reich[1,2], Michael Douglass[1,2]

[1]Department of Medical Physics, Royal Adelaide Hospital, Adelaide, Australia, [2]School of Physical Sciences, The University of Adelaide, Adelaide, Australia

Introduction With recent advancements in phone-based technology, photographic and LIDAR-based applications are more readily available than ever before and to a high level of quality. In this work, we aim to determine if smartphones can be used by radiation oncologists to scan patients for 3D printed bolus and surface applicators.
Method This work involved two separate studies, a phantom and human study. For the phantom study, 3D models of the nose region of a RANDO anthropomorphic phantom were generated using three different imaging techniques: CT scan, smartphone-based photogrammetry and LIDAR applications. Virtual boli were designed in Blender and 3D printed with PLA plastic. The conformity of each boli was assessed by air gap volume measurements using a CT scan of each boli on the RANDO phantom. For the human study, photographs and a LIDAR scan of four volunteers were captured using an iPhone 13 to assess their feasibility for generating human models. Each 3D model was visually assessed to identify any issues in their reconstruction. The LIDAR models were registered to the photogrammetry models where a distance to agreement analysis was performed to assess their level of similarity.
Results The photogrammetry derived bolus showed comparable conformity to the CT derived bolus while the LIDAR derived bolus showed significantly poorer conformity. Both the photogrammetry and LIDAR models of the volunteers showed poor reconstruction quality in regions of facial hair and occlusion. The LIDAR models were reconstructed with less detail than the photogrammetry models and their level of similarity varied in quality between each volunteer model.
Conclusion Smartphone-based photogrammetry and LIDAR software show great potential for future use in generating 3D models for radiation oncology purposes. However, in their current state, their uses are limited but will greatly improve as new technology is made available.

O14. Comparing multi-leaf collimator jaws to improve radiotherapy access in low- and middle-income countries

Gregory Peiris[1,*]

[1]The University of Melbourne, Parkville, Australia

Introduction It is projected that by 2030, Low- and Middle-Income Countries (LMICs) will contribute to 75% of cancer related deaths worldwide. This is due to a growing shortfall of radiotherapy linear accelerators (LINACs) in these nations, leading to a substantial barrier in cancer care. Existing research has characterised the higher failure frequency and downtimes between LMICs (Nigeria, Botswana) compared to High-Income Countries (HIC, the UK) and identified the Multi-Leaf Collimator (MLC) as a component in need of re-evaluation [1]. There is some evidence to suggest that thinner leaves correspond to a higher failure rate [2], but how it affects treatment plan quality in a LMIC context is yet to be explored.

Method Using anonymized patient data generously provided by Peter MacCallum Cancer Centre, we compare the effect of MLC leaf width on clinical metrics. Variables such as target volume and anatomical site are controlled to reflect the caseload in LMICs. We investigate target related dose metrics, such as PTV D98% and plan quality metrics like Conformity Index and Monitor Units per Grey. The dose metrics for relevant Organs-At-Risk (OARs) are also monitored and compared between varying leaf widths.
Results We expect to see no clinically significant differences in treatment plan quality between leaf widths, especially for larger tumor volumes. The lack of any discernable advantage of thinner leaves would motivate a shift to more reliable MLC jaws with fewer and wider leaves for LMICs.
Conclusion To address the dramatic shortfall of Radiotherapy LINAC access in LMICs is crucial with the gap widening the longer we wait. These results will motivate the need and highlight the benefits of a more reliable MLC with fewer leaves.
References

1. L. Wroe, T. Ige, O. Asogwa, et al. "Comparative analysis of radiotherapy linear accelerator downtime and failure modes in the UK, Nigeria and Botswana," Clinical Oncology, vol. 32, no. 4, pp. e111–e118, 2020. https://doi.org/10.1016/j.clon.2019.10.010
2. G. S. Peiris, S. A. Pawiro, M. F. Kasim, and S. L. Sheehy, "Failure modes and downtime of radiotherapy linear accelerators and multi-leaf collimators in Indonesia," 2021. arXiv:2105.08906v2.

O15. [Invited] A renaissance of relevance – new molecular cancer treatment options in the twenty-first century

Dale Bailey[1,2,*]

[1]Department of Nuclear Medicine, Royal North Shore Hospital, Sydney, [2]Faculty of Medicine & Health, University of Sydney, Sydney

Driven by the last half century of discoveries in molecular biology and, in particular, signalling pathways and genomic profiles in cancer, nuclear medicine is enjoying a renaissance of relevance as more accurately targeted radiopharmaceutical probes are combined with higher performance imaging equipment leading to a number of new therapeutic opportunities. Radiolabelled peptides, monoclonal antibodies or diabodies and nanoparticles allow precision targeting of receptors and pathways in cells to intervene in abnormal cell behaviour. Increasingly, radiodiagnostic agents can be alternately labelled to be a radiotherapeutic, which can greatly accelerate the treatment planning and delivery paradigm (*i.e.*, "see it, treat it"). Instrumentation has moved forward fundamentally also with now ultra-high sensitivity Total Body PET (TB-PET) systems available. Further, we are starting to see the evolution from standard gamma cameras to dedicated SPECT imaging devices capable of whole-body scans in times comparable to PET scanning. What this means for our patients will be better outcomes based on more precise treatment planning and an increased understanding of the inherent nature of radionuclide therapy using particles emitted by therapeutic radiopharmaceuticals. This effect will likely be further enhanced by combination of radionuclide therapy with other treatments such as immunotherapies exploiting the inflammatory or apoptotic processes initiated by the ionising radiation damage.

O16. Integrating PET and MALDI-2 imaging for discovery of a theranostic probe for brain endocannabinoid α/β-hydrolase domain 6 (ABHD6)

Muneer Ahamed[1,*]

[1]MITRU, South Australian Health and Medical Research Institute (SAHMRI), Adelaide, Australia

Introduction Serine hydrolase α/β-Hydrolase Domain 6 (ABHD6) is an endocannabinoid and responsible for metabolizing endogenous cannabinoid ligand 2-arachidonoyglycerol (2-AG). Blockade of ABHD6 increases 2-AG levels marginally, resulting in mild activation of the endocannabinoid system without exerting any psychoactive effects. Recently, ABHD6 has emerged as a novel therapeutic strategy to treat drug addiction, inflammation, epilepsy, glucose dependent diabetes, and other neurodegenerative diseases. The mapping of ABHD6 by positron emission tomography (PET) studies will allow a thorough understanding of ABHD6 mediated lipid metabolism and neurotransmission. Here we show discovery and validation of a first theranostic probe targeting ABHD6 by combining PET and matrix-assisted laser desorption/ionisation (MALDI)-mass spectrometry imaging.
Method We used comprehensive pharmacological assays to determine affinity and selectivity for the probe. The potent probe was radiolabeled using ^{18}F-fluoride and ex vivo and in vivo PET imaging was performed in small animals and non-human primates. We also imaged a pharmacological response by MALDI imaging of key lipid on ABHD6 inhibition, in mouse brain tissues ex vivo.
Results The reported ligand JZP-MA-11 is potent and highly selective for ABHD6 with greater than 100-fold selectivity compared to other endocannabinoid hydrolases in mouse proteome profiling. Radiosynthesis of [^{18}F]JZP-MA-11 was carried out using copper mediated ^{18}F-aromatic fluorination method. The ABHD6 specific uptake of [^{18}F]JZP-MA-11 in ABHD6-rich peripheral tissues and major brain regions was demonstrated both ex vivo and in vivo using PET in small animals and non-human primates. MALDI-2 imaging showed an elevated 2-AG (a lipid) levels in mouse brain tissues of JZP-MA-11 treated animals.
Conclusion The demonstrated image-based features can be collectively used to identify biological information which cannot be obtained by a single imaging modality. These synergistic imaging efforts hold promise for improving the understanding the brain endocannabinoids and related lipid metabolism in peripheral and central nervous system disorders and accelerating drug and theranostics discovery.

O17. In vitro characterisation of 225Ac-DOTA-C595 as targeted alpha therapy for pancreatic cancer

Ashleigh Hull[1,2,*], William Hsieh[1,2], William Tieu[3], Artem Borysenko[4], Dylan Bartholomeusz[2,3], Yanrui Li, Eva Bezak[1,3]

[1]University of South Australia, Adelaide, Australia, [2]SA Medical Imaging, Royal Adelaide Hospital, Adelaide, Australia, [3]The University of Adelaide, Adelaide, Australia, [4]Environment Protection Authority, Adelaide, Australia.

Introduction Pancreatic cancer is a highly aggressive malignancy with poor prognosis. Targeted alpha therapy (TAT) using Actinium-225 (Ac-225) could be beneficial in the treatment of pancreatic cancer. We recently developed a novel TAT agent, ^{225}Ac-DOTA-C595 designed to target cancer-specific mucin 1 epitopes (MUC1-CE) overexpressed on pancreatic cancer cells. The aim of this study was to

characterise ^{225}Ac-DOTA-C595 in terms of its cellular binding, internalisation and cytotoxicity to pancreatic cancer cells.
Methods Ac-225 was radiolabelled to DOTA-C595 using standard methods. Cell binding and internalisation assays were performed in four pancreatic cancer cells (PANC-1, CAPAN-1, BxPC-3 and AsPC-1) which had varying levels of MUC1-CE expression. Clonogenic assays and γH2AX assays were also performed in PANC-1 and AsPC-1 cell lines to evaluate the potential in vitro cytotoxicity of ^{225}Ac-DOTA-C595 compared to unlabelled Ac-225, cold DOTA-C595 and untreated controls.
Results At concentrations of 50 nM and greater, ^{225}Ac-DOTA-C595 had significantly higher binding to PANC-1 (strong MUC1-CE expression) compared to the other cell lines. All cell lines demonstrated rapid internalisation of ^{225}Ac-DOTA-C595 with at least 15% of activity internalised within 1 h. A maximum of 49% of internalised activity was noted at 48 h in the PANC-1 cell line. γH2AX assays showed ^{225}Ac-DOTA-C595 induced double strand DNA breaks in over 98% of pancreatic cancer cells within 1 h, indicating high potential cytotoxicity. This was supported by the results of the clonogenic assays.
Conclusion The results of the cellular binding, internalisation and cytotoxicity assays suggest ^{225}Ac-DOTA-C595 may be a feasible approach for TAT of pancreatic cancer. Further in vivo studies are needed to understand the therapeutic potential and side effects of ^{225}Ac-DOTA-C595 therapy.

O18. The search for the ideal synchrotron activated theranostic nanoparticle

Sarah Vogel[1,*], Michael Valceski[1], Abass Kochaiche[1], Carolyn Hollis[1], Jason Paino[1], Elette Engels[1,2], Micah Barnes[1,2], Alice O'Keefe[1], Matthew Cameron[2], Daniel Hausermann[2], Mitzi Klein[2], Michael de Veer[3], Michael Lerch[1], Stephanie Corde[4], Moeava Tehei[1]

[1]University of Wollongong, Wollongong, Australia, [2]Imaging and Medical Beam Line, ANSTO Australian Synchrotron, Clayton, Australia, [3]Monash Biomedical Imaging, Monash University, Clayton, Australia, [4]*Radiation Oncology Dept, Prince of Wales Hospital, Randwick, Australia.*

Introduction Nanoparticles as theranostic agents to enhance radiation therapies are a long-standing research area. Synchrotron modulated Microbeam Radiation Therapy (MRT) presents the ability to treat patients with extremely high dose rates, sparing normal tissue whilst delivering radio-surgical doses. The combination of nanoparticles and MRT presents a comprehensive treatment option, allowing for patient specific, tumour targeted radiation, delivered in a single dose. This study presents three high-Z nanoparticle options and evaluates their effectiveness in vitro and in vivo.
Method In vitro testing included clonogenic assays and DNA strand break quantification to determine the short- and long-term effects of 9L gliosarcoma cells (9LGS) treated with nanoparticles and synchrotron modulated MRT. In vivo experiments were performed to investigate rodent survival. Fischer 344 rats were inoculated with 9L gliosarcoma in the right caudate nucleus of the brain. 12 days later, thulium oxide, gadolinium oxide or gold nanoparticles were injected directly to the tumour. The rats were then aligned in-beam [1], and a bolus was placed over the irradiation site. One radiation fraction was given to different treatment groups at valley doses of either 8 or 15 Gy, with microbeams produced using the 4 T magnet and Al/Al filtration.
Results Through long-term in vitro and in vivo experiments, the biocompatibility, imaging functionality and therapeutic enhancement of nanoparticles coupled with synchrotron MRT was investigated. Both thulium and gadolinium oxide-based nanoparticles are more effective than gold at extending survival, with the combination of gadolinium oxide and 15 Gy valley dose MRT resulting in survival beyond 90 days (compared to a median survival of 44 days with 15 Gy MRT alone [2]).
Conclusion This study demonstrated the efficacy of nanoparticles, especially gadolinium oxide, as theranostic agents; they allow for effective tumour detection and when used in conjunction with synchrotron MRT, they successfully extend survival beyond MRT alone.
Disclosures
This study acknowledges the assistance from, and technical knowledge of, the Imaging and Medical Beamlime (IMBL) at the ANSTO Australian Synchrotron, the Illawarra Health and Medical Research Institute (IHMRI) at the University of Wollongong (UOW) and the Florescence Analysis Faculty at Molecular Horizons at UOW.
References

1. Paino J, Barnes M, Engels E, Davis J, Guatelli S, Veer M, Hall C, Häusermann D, Tehei, M, Corde S, Rosenfeld A, Lerch M (2021) Incorporating Clinical Imaging into the Delivery of Microbeam Radiation Therapy. Applied Sciences 11(19) 9101. https://doi.org/10.3390/app11199101
2. Engels E, Li N, Davis J, Paino J, Cameron M, Dipuglia A, Vogel S, Valceski M, Khochaiche A, O'Keefe A, Barnes M, Cullen A, Stevenson A, Guatelli S, Rosenfeld A, Lerch M, Corde S, Tehei M (2020). Toward personalized synchrotron microbeam radiation therapy. Scientific Reports. 10 8833. https://doi.org/10.1038/s41598-020-65729-z

O19. Unveiling the mechanisms and efficacy of radiosensitiser-enhanced synchrotron radiation therapies in vitro

Michael Valceski[1,*], Sarah Vogel[1], Elette Engels[1,4], Jason Paino[1], Dylan Potter[1], Carolyn Hollis[1], Abass Khochaiche[1], Micah Barnes[1,4], Alice O'Keefe[1], Matthew Cameron[4], Anatoly Rosenfeld[1,2], Michael Lerch[1,2], Stephanie Corde[1,2,3], Moeava Tehei[1,2]

[1]Centre for Medical Radiation Physics, University of Wollongong, Wollongong, Australia, [2]Illawarra Health and Medical Research Institute, University of Wollongong, Wollongong, Australia, [3]Prince of Wales Hospital, Randwick, Sydney, Australia, [4]Australian Synchrotron—Australia's Nuclear Science and Technology Organisation (ANSTO), Clayton, Victoria, Australia

Introduction The resistance of glioblastoma brain cancer can challenge the effectiveness of conventional radiotherapy. The use of high-dose-rate radiotherapies over conventional X-rays can allow for normal tissue protection whilst better controlling tumours [1]. The use of targeted radiosensitisers, such as cancer-selective nanoparticles or DNA-localised drugs, can deliver dose enhancement to cancer [2]. Combining these with high-dose-rate synchrotron broadbeams and microbeams can yield synergistic effects to enhance the efficacy of these multi-modal therapies compared to conventional treatments, and allow a deeper understanding of their underlying mechanisms.
Method 9L gliosarcoma (9LGS) cancer cells were exposed to combinations of thulium oxide nanoparticles (TmNPs), iododeoxyuridine (IUdR) and methotrexate (MTX) drugs. Cells were then irradiated with conventional X-rays, synchrotron broadbeams (> 40 Gy/s) or Microbeam Radiation Therapy (MRT), at optimal mean energy for radiosensitiser dose enhancement. Clonogenic assay was used to determine treatment efficacy. γH2AX immunofluorescence confocal

microscopy was used to assess double-strand DNA break (DSB) enhancement, and characterise the mechanisms and biological effects of broad and MRT beams.

Results TmNPs and IUdR resulted in 9LGS dose enhancement with all radiotherapy techniques. MTX provided enhancement greater than 500% for the most effective combination with 5 Gy synchrotron broadbeams compared to conventional X-rays. These results demonstrated dose-rate effects in cells treated with MTX, and further reduced 9LGS survival when used in synergistic combination with TmNPs or IUdR. γH2AX imaging and quantification unveiled DSB increases with synchrotron radiation (Fig. 1), and notable changes in DSB enhancements across MRT peaks and valleys.

Conclusion This study demonstrated the efficacy, and DSB mechanisms, of significantly radio-sensitising brain cancer with highly synergistic combinations of radiosensitisers, and high-dose-rate synchrotron radiation with chemotherapeutics.

Disclosures

We acknowledge the facilities, technical and scientific assistance of the Illawarra Health and Medical Research Institute, and the Florescence Analysis Faculty in Molecular Horizons, at the University of Wollongong, as well as Imaging and Medical Beamline (IMBL) at the ANSTO Australian Synchrotron.

References

1. Vozenin MC, Hendry JH, Limoli CL. Biological Benefits of Ultra-high Dose Rate FLASH Radiotherapy: Sleeping Beauty Awoken. Clin Oncol (R Coll Radiol). 2019 Jul;31(7):407–415. https://doi.org/10.1016/j.clon.2019.04.001. Epub 2019 Apr 19. PMID: 31,010,708; PMCID: PMC6850216.
2. Engels, E., Westlake, M., Li, N., Vogel, S., Gobert, Q., Thorpe, N., Rosenfeld, A., Lerch, M., Corde, S. & Tehei, M. (2018). Thulium Oxide Nanoparticles: A new candidate for image-guided radiotherapy. Biomedical Physics and Engineering Express, 4 (4), 044,001–1-044,001–11.

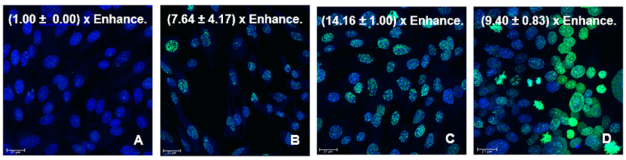

Fig. 1. 93 × γH2AX (DAPI counterstain) images showing 9LGS control without radiation or treatment (A); irradiated with 5 Gy conventional X-rays (B); 5 Gy synchrotron broadbeam after IUdR + MTX treatment (C); and 5 Gy (valley dose; PVDR 10.5) MRT after IUdR + MTX treatment (D). Green represents DSB foci while blue represents cell nuclei. Average foci/cell enhancement compared to the untreated control is shown for each image.

O20. Knowledge transfer for generating open-access auto-contouring tools

Robert Finnegan[1,2,3,*], Phillip Chlap[3,4,5], Daniel Al Mouiee[3,4,5], Vicky Chin[3,4,5], Lois Holloway[2,3,4,5]

[1]Northern Sydney Cancer Centre, Royal North Shore Hospital, St Leonards, Australia, [2]Institute of Medical Physics, University of Sydney, Camperdown, Australia, [3]Ingham Institute for Applied Medical Research, Liverpool, Australia, [4]Liverpool Cancer Therapy Centre, SWSLHD, Liverpool, Australia, [5]South Western Sydney Clinical School, University of New South Wales, Liverpool, Australia.

Introduction Sharing auto-contouring models enables external validation and inter-centre consistency. However, departmental policies often prevent distribution of locally-trained models. This study presents a novel approach called "knowledge transfer", a technique to create shareable models using publicly available data. The aims of this work were to demonstrate the feasibility of this approach and to characterise the performance of the resulting open-access auto-contouring model.

Methods The study design is illustrated in Fig. 1. Local data comprising 300 CT scans with manual whole heart contours and 10 CT scans with manual cardiac substructure contours were used to train deep learning and multi-atlas components of an auto-contouring model. This model was used to auto-contour 600 publicly available CT scans, which were screened for quality before 590/10 cases were used to train deep learning/multi-atlas components of a new open-access model. An independent validation set of 30 CT scans from lung cancer patients receiving radiotherapy had the heart and cardiac substructures contoured manually and automatically, using both local and open-access models. For each model, the Dice Similarity Coefficient (DSC) and Mean Distance to Agreement (MDA) was computed between manual and automatic contours. Differences in auto-contouring accuracy between the two models were assessed using Wilcoxon signed-rank tests. For each structure, relative differences in mean and maximum doses were calculated between the two auto-contours.

Results Results are presented in Fig. 2. Auto-contouring accuracy was consistent between the two models with no structures having statistically significant differences in both DSC and MDA. The median relative differences in the mean and maximum doses were below 1.57% and 0.97%, respectively.

Conclusion This study demonstrates the feasibility of creating an open-access auto-contouring model using knowledge transfer through publicly available data, with little to no loss in accuracy. Future research will investigate additional radiotherapy planning volumes and imaging modalities.

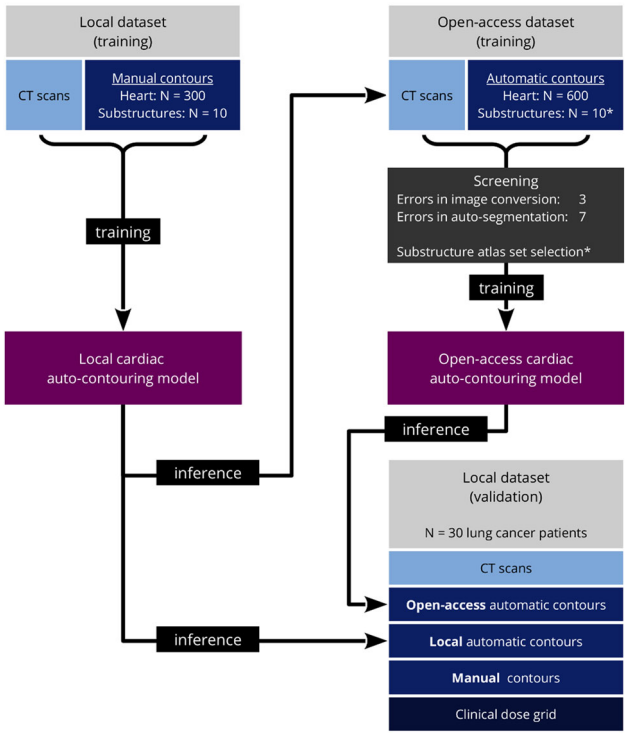

Fig. 1. Overview of study design.

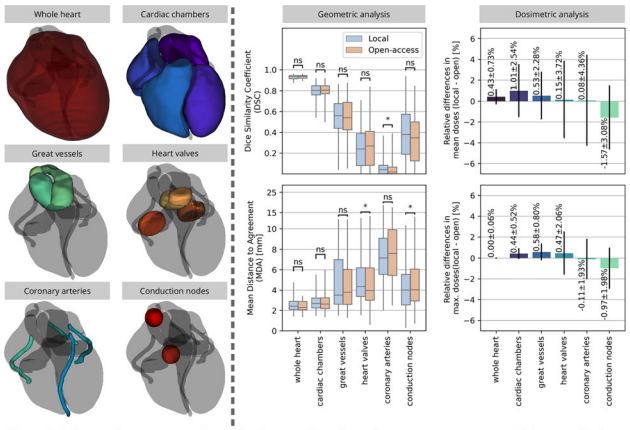

Figure 2. Left – surface representation of the heart and cardiac substructure auto-contours. Right – results from geometric and dosimetric analysis. In the geometric analysis, differences between contouring metrics were assessed using the Wilcoxon signed-rank test, where ns = not significant (p≥0.05) and * = significant (p<0.05). In the dosimetric analysis, the bars/lines represent the medians/median absolute deviations.

O21. Clinical utility of quantitative metrics for optimizing and assessing auto-segmentation model accuracy

Shrikant Deshpande[1,2,3,*], Phillip Chlap[1,2,3], Robert Finnegan[2,4,5], Dale Roach[1,2], Daniel Al-Mouiee[1,2], Anthony Espinoza[1,2], Alison Gray[1,2,3], Aitang Xing[1,2,3], Rebecca Bartlett[1], Roya Merie[1,2,3], Kim-Lin Chiew[1,3], Karen Lim[1,2,3], Mei Yap[1,2,3], Lois Holloway[1,2,3,4,6]

[1]South Western Sydney Cancer Services, NSW Health, Australia, Liverpool, Australia, [2]Ingham Institute for Applied Medical Research, Liverpool, Australia, [3]School of Clinical Medicine, UNSW Medicine & Health, South West Sydney Clinical Campus, Kensington, Australia, [4]School of Physics, Institute of Medical Physics, University of Sydney, Camperdown, Australia, [5]Northern Sydney Cancer Centre, Royal North Shore Hospital, St Leonards, Australia, [6]Centre for Medical Radiation Physics, University of Wollongong, Wollongong, Australia

Introduction Comprehensive evaluation using geometric agreement (quantitative) and physician-reported assessment (qualitative) is necessary to assess the clinical accuracy of auto-segmentation models [1]. However, the accuracy of an auto-segmentation model is dependent on an iterative optimisation process that compares the model output with ground-truth manual contours using quantitative metrics alone. Quantitative metrics are most useful for this but need to correlate well with clinical endpoints [1]. This work assesses the correlation between a number of quantitative metrics and a qualitative score for contour accuracy evaluation.

Methods Thirteen breast datasets with manually defined contours (13 organs-at-risk and 6 target volumes) reviewed previously were used. The structures were also segmented with two commercial atlas-based models. Contour generation and scoring was completed blinded from other methods. Qualitative score grading from 1–5 (1: no-modification required, 5: unusable) was performed by two independent observers following criteria outlined by Abadi et al. [2] Seven quantitative metrics including Mean Surface Distance(MSD), Hausdorff Distance(HD), 95thpercentile Hausdorff Distance($HD_{95\%}$), Dice Similarity Coefficient(DSC), Surface Dice Similarity Coefficient(sDSC), Relative Volume Difference(RVD) and Added Path Length(APL) were computed for each auto-segmented contour and compared against the manual contour. A Mann–Whitney-Wilcoxon test with two sided Bonferroni correction was performed to assess the correlation between the clinical score and each quantitative metric. The statistical significance was tested with $p > 0.05$(no correlation) and $p < 0.0001$(high correlation).

Results Correlations between clinical score and each quantitative metric are shown in Fig. 1. DSC, MSD, and HD_{95} showed statistically significant distinction between metric values and clinical score. DSC, while commonly utilised within the literature, was unable to distinguish between contours scored as 1 or 2. RVD, APL, and HD showed poor distinction between clinical scores.

Conclusion The quantitative metrics sDSC, MSD, $HD_{95\%}$ correlate with qualitative scores and are likely to be most useful for the purpose of optimizing and assessing auto-segmentation models.

References

1. Sherer, M. V., Lin, D., Elguindi, S., Duke, S., Tan, L–T., Cacicedo, J., Dahele, M., & Gillespie, E. F. (2021). Metrics to evaluate the performance of auto-segmentation for radiation treatment planning: A critical review. *Radiotherapy and Oncology*, *160*:185–191.
2. Abadi, S., Roguin, A., Engel, A., & Lessick, J. (2010). Feasibility of automatic assessment of four-chamber cardiac function with MDCT: Initial clinical application and validation. *European Journal of Radiology*, *74*(1):175–181.

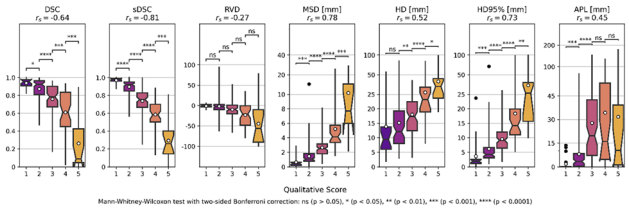

Fig. 1. Box plots displaying the correlation between various quantitative metrics and the qualitative clinical assessment score. The Mann–Whitney-Wilcoxon test with two sided Bonferroni correction was used to determine the correlation coefficient and statistical significance. The dot is mean and notch is median value.

O22. Automatic metastatic prostate cancer disease burden quantification in 68 Ga-PSMA PET/CT images

Jake Kendrick[1,*], Roslyn Francis[2,3], Ghulam Mubashar Hassan[1], Pejman Rowshanfarzad[1], Jeremy Ong[4], Martin Ebert[1,5,6]

[1]School of Physics, Mathematics and Computing, University of Western Australia, Perth, Australia, [2]Medical School, University of Western Australia, Perth, Australia, [3]Department of Nuclear Medicine, Sir Charles Gairdner Hospital, Perth, Australia, [4]Department of Nuclear Medicine, Fiona Stanley Hospital, Perth, Australia, [5]Department of Radiation Oncology, Sir Charles Gairdner Hospital, Perth, Australia, [6]5D Clinics, Claremont, Australia

Introduction The disease burden in metastatic prostate cancer (mPCa) patients has important implications for patient treatment decisions, however derivation of the total tumour burden through manual segmentation processes is laborious, time consuming, and subject to inter-observer variability. This work aims to develop an automatic mPCa lesion segmentation algorithm for ^{68} Ga-PSMA PET/CT scans using deep learning.

Methods A local dataset of 337 scans from biochemically recurrent PCa patients were included in this study. mPCa lesions were semi-automatically segmented by a clinical expert and used to train a 3D U-Net based on the nnU-Net framework [1]. A subset of scans

(n = 28) received delineations from a second observer. Segmentation performance was assessed using the Dice Similarity Coefficient (DSC) and the positive predictive value (PPV). Whole-body biomarkers were derived from the automated segmentations on a test set (n = 128) and evaluated for their prognostic potential.

Results Automated model DSC and PPV were found to be significantly greater than that of the second observer with respect to the first (DSC: median of 50.7% vs. 32%, p = 0.012. PPV: median of 64.9% vs. 25.7%, $p < 0.005$). Kaplan–Meier analysis of total lesional uptake (TLU_{auto}) and total lesional volume (TLV_{auto}) derived from the automated segmentations showed significant association with patient overall survival (OS) (both $p < 0.005$, Fig. 1).

Conclusion This novel research demonstrates the feasibility of automatically segmenting metastatic prostate lesions in whole body PET/CT images using deep learning techniques. Voxel-level DSC and PPV were found to be within inter-observer variability, and global biomarkers derived from the model segmentations were demonstrated to have significant univariate association with patient OS, indicating a potential for automated patient risk-stratification.

References

1. Isensee F, Jaeger PF, Kohl SAA, Petersen J, Maier-Hein KH (2021) nnU-Net: a self-configuring method for deep learning-based biomedical image segmentation. Nat Methods 18:203–11. https://doi.org/10.1038/s41592-020-01008-z.

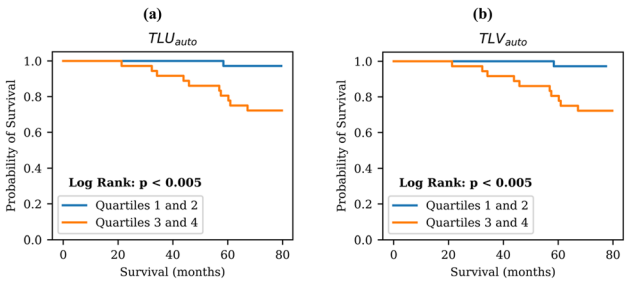

Fig. 1. Kaplan–Meier analyses on the TLU_{auto} (a) and TLV_{auto} (b) calculated on the dedicated test set segmentations.

O23. Automatic contouring of organs-at-risk in the head and neck on MR images using fully convolutional networks

Behzad Asadi[1], Peter Greer[1,2], Stephan Chalup[2], James Welsh[2], John Simpson[1,2,*]

[1]Calvary Mater Hospital, Waratah, Australia, [2]University of Newcastle, Callaghan, Australia

Introduction Manual contouring of organs-at-risk (OAR) in the head-and-neck is time-consuming and subjective due to the large number and complex anatomy of OAR. This work addresses the problem of auto-contouring of OAR in the head and neck on MR images. This is to facilitate an adaptive MRI-only radiotherapy workflow.

Method There are two main methods for auto-contouring [1]: atlas-based methods, and deep-learning methods. Deep-learning methods have shown to be superior to atlas-based methods. UNet [2] is employed as the deep-learning model for auto-contouring. UNet is trained and tested using a head-and-neck dataset consisting of images from 148 retrospective patients. For each patient, two MR T1 and T2 Dixon axial in-phase images, one CT scan, and one CT structure file are available. The CT structure file consists of manually-drawn clinical contours on CT images. CT scans are registered to MR images, and the resulting transformation is applied to CT contours to obtain MR reference contours.

Results UNet results in a test dice similarity coefficient (DSC) of 0.88 ± 0.03 for the brainstem, 0.81 ± 0.05 for the spinal cord, 0.89 ± 0.02 for the mandible, 0.88 ± 0.08 for the left orbit, 0.88 ± 0.05 for the right orbit, 0.84 ± 0.03 for the left parotid, 0.83 ± 0.04 for the right parotid, 0.76 ± 0.07 for the left sub-mandibular, and 0.70 ± 0.08 for the right sub-mandibular. Sample predicted and reference contours are shown in Fig. 1 for the left parotid, and in Fig. 2 for the right sub-mandibular.

Conclusion Deep learning methods have the potential to be successfully deployed as a method for auto-contouring on MR images in head-and-neck treatment planning where there is a consistent training dataset of a reasonable size.

Disclosures

This work is part of a grant supported by Varian Medical Systems.

References

1. Kosmin M, Ledsam J, Romera-Paredes B, Mendes R, Moinuddin S, de Souza D, Gunn L, Kelly C, Hughes CO, Karthikesalingam A, Nutting C, Sharma RA. Rapid advances in auto-segmentation of organs at risk and target volumes in head and neck cancer. Radiotherapy and Oncology. 2019 Jun;135:130–140.
2. Ronneberger O, Fischer P, Brox T. U-Net: Convolutional Networks for Biomedical Image Segmentation. Medical Image Computing and Computer-Assisted Intervention – MICCAI 2015 Nov.

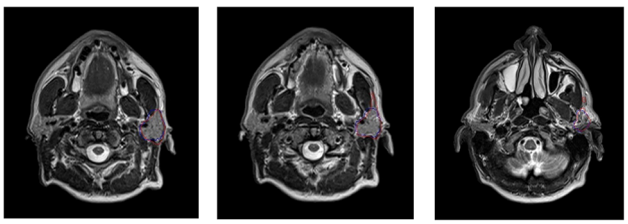

Fig. 1. Reference contours in blue, and predicted contours in red for the left parotid

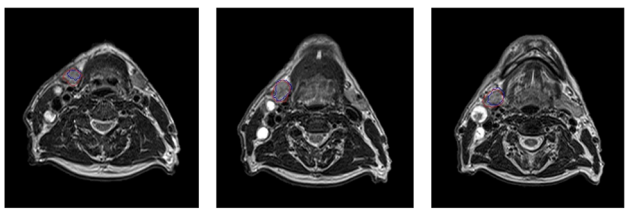

Fig. 2. Reference contours in blue, and predicted contours in red for the right submandibular

O24. Evaluating nnU-Net for bone metastases segmentation on computed tomography in metastatic lung cancer patients

Iromi Randika Paranavithana[1,2], Matthew Field[2,3,4], David Stirling[1], Montserrat Ros[1]

[1]Faculty of Engineering and Information Sciences, University of Wollongong, Wollongong, Australia, [2]Ingham Institute for Applied Medical Research, Liverpool, Australia, [3]South Western Sydney Cancer Services, NSW Health, Sydney, Australia, [4]South Western Sydney Clinical Campus, School of Clinical Medicine, UNSW, Sydney, Australia

Introduction Identifying the number of metastatic lesions, their locations, and prognostic radiomic biomarkers are important factors in selecting suitable treatment options for late-stage lung cancer patients with bone metastases [1, 2]. Manual segmentation is time-consuming [3] and prone to inter-observer variation. We investigated a nnU-Net [4], a self-adapting Convolutional Neural Network (CNN) technique that has become state-of-the-art in medical image segmentation for segmenting bone metastases in computed tomography(CT) of lung cancer patients, to develop an automated segmentation pipeline.
Method An nnU-net deep learning model was trained to identify the bone metastases in CT images of lung cancer patients. The local dataset consists of 6 patients. For each CT scan, a radiologist contoured the ground truth annotations, which were then used to train the nnU-net. The data was split into training and test sets using K-fold cross validation. The model was evaluated using Dice Similarity Coefficient (DSC) and Jaccard Index (JI) to measure the overlap between the model predictions and the ground truth annotations.
Results The preliminary results of the nnU-Net model achieved mean overlap accuracy, mean precision, and mean recall of 92.30%, 88.07% and 74.26%, respectively, compared with ground truth annotations. Regarding spatial overlap, mean DSC, and JI for the test set vs. ground truth annotations are 79.41% and 72.02%, respectively. Figure 1 shows a slice of a patient's CT scan segmented with nnU-net compared to ground truth annotation.
Conclusion Based on these results, we conclude that the nnU-net model is feasible to segment the metastatic bone lesions in CT images in small datasets. Further, studies are needed to evaluate how accurate the model performs in larger patient datasets to incorporate it to aid clinical decision-making.
References

1. S. T. H. Peeters, E. J. Van Limbergen, L. E. L. Hendriks, and D. De Ruysscher, "Radiation for Oligometastatic Lung Cancer in the Era of Immunotherapy: What Do We (Need to) Know?," (in eng), Cancers (Basel), vol. 13, no. 9, Apr 28 2021, https://doi.org/10.3390/cancers13092132.
2. D. De Ruysscher et al., "Radical treatment of non-small-cell lung cancer patients with synchronous oligometastases: long-term results of a prospective phase II trial (Nct01282450)," (in eng), J Thorac Oncol, vol. 7, no. 10, pp. 1547–55, Oct 2012, https://doi.org/10.1097/JTO.0b013e318262caf6.
3. T. Apiparakoon et al., "MaligNet: Semisupervised Learning for Bone Lesion Instance Segmentation Using Bone Scintigraphy," IEEE Access, vol. 8, pp. 27,047–27,066, 2020, https://doi.org/10.1109/ACCESS.2020.2971391.
4. F. Isensee, P. F. Jaeger, S. A. A. Kohl, J. Petersen, and K. H. Maier-Hein, "nnU-Net: a self-configuring method for deep learning-based biomedical image segmentation," Nature Methods, vol. 18, no. 2, pp. 203–211, 2021/02/01 2021, https://doi.org/10.1038/s41592-020-01008-z.

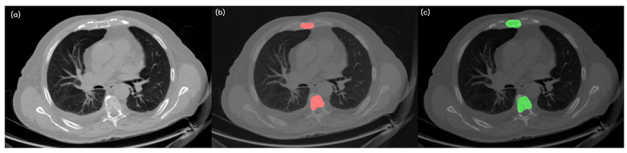

Fig. 1. Demonstration of the (a) CT image, (b) model prediction and (c) ground truth annotation.

O25. Automated scoring of American College of Radiology digital mammography phantom images

Zeyad Alawaji[1,2], Seyedamir Taba[1], Lucy Cartwright[4], William Rae[1,3]

[1]Discipline of Medical Imaging Science, Faculty of Medicine and Health, The University of Sydney, Sydney, Australia, [2]Department of Radiologic Technology, College of Applied Medical Sciences, Qassim University, Buraydah, Saudi Arabia, [3]Medical Imaging Department, Prince of Wales Hospital, Randwick, Australia, [4]Department of Medical Physics, Western Sydney Local Health District, Westmead, Australia

Introduction Mammography image quality control testing is usually carried out weekly by human observers using a physical phantom containing target objects that simulate breast pathologies such as: fibrous tissues, microcalcifications and tumours. This is done to ensure that mammography units produce optimal clinical images with minimum radiation dose. Human assessment is however subjective and influenced by other factors (e.g. level of expertise, viewing condition, etc.). An algorithm was developed and validated to automatically score of the American College of Radiology (ACR DM) phantom images and was compared to subjective assessments carried out by human observers.
Method A total of 22 ACR DM Phantom (Model 086) images were collected from a variety of units from different digital mammography manufacturers. The software was created to perform image quality analysis of the ACR DM phantom images and score them by first extracting 18 ROIs positioned around the embedded objects within the wax block (fibres, specks groups, masses) for individual evaluation (Fig. 1.). A template matching [1] algorithm was implemented to detect and score objects. A different supplemental method for each object (e.g., Gaussian fit for masses… etc.) was applied to validate the software. Eleven observers, including six Certified Mammography Testers and five researchers, evaluated the images.
Results The software and observers did not differ significantly when assessing low contrast objects (masses and fibres). However, they did differ significantly for the specks groups. The software was able to detect speck groups more effectively than human observers. Visibility thresholds for the automated scoring were established for the object types.
Conclusion The developed automated image quality analysis showed promising and consistent assessment results especially in detecting high contrast objects compared to human observers.
References

1. J. P. Lewis (1995) Fast Normalized Cross-Correlation, Industrial Light & Magic.

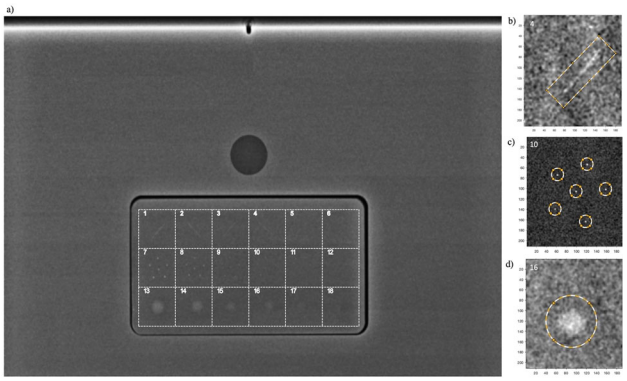

Fig. 2. (a) The ACR DM phantom highlighted 18 ROIs; (b), (c), and (d) example of the target objects detected by the software.

O26. Linac optimisation, part 1: Fast photon beam steering

Jacek Chojnowski[1,*], Jonathan Sykes[2,3], David Thwaites[2]

[1]North Coast Cancer Institute, Coffs Harbour, Australia, [2]University of Sydney, Sydney, Australia, [3]Western Sydney Local Health District, Sydney, Australia

Introduction One difficult problem during acceptance testing and commissioning of a linear accelerator is to tune photon beams to get them symmetric and centred i.e., aligned with the collimator axis of rotation. There are two main beam tuning parameters namely 'Position' and 'Angle' that can be adjusted to achieve this goal. Both of those parameters influence the beam symmetry and position and in general it is difficult to tell which one should be adjusted first and by how much.
Method A method of optimising photon beam parameters has been developed to adjust beam 'Position' and 'Angle' parameters in two orthogonal directions (radial and transverse) in-real time using the 2D array of ionisation chambers attached to the collimator [1]. For the beam to be symmetric and centred, the beam symmetry and position measured by the 2D detector should be the same at two opposing collimator angles. Additionally, a practical guidance is proposed recommending first to optimise the beam symmetry and then to adjust the beam position with the aid of the servo mechanism keeping the beam symmetry unchanged.
Results The whole procedure of beam steering for four energy beams on an Elekta Versa HD linac takes about an hour for an experience physicist. The achievable results of the beam symmetry and position (alignment) are below 1% and 0.1 mm, respectively [1]. Moreover, the procedure does not depend on the position and dosimetric calibration of the 2D detector and the utilisation of the beam servo mechanism significantly speeds up the overall beam tuning exercise. Photon flattening filter-free (FFF) beams need more attention during optimisation since a lateral shift of the symmetric beam is detected by the linac servo mechanism as a symmetry change (not a position change) and therefore the procedure might need to be repeated to achieve optimal results.
Conclusion The fast photon beam steering method has been developed and verified as an alternative approach to traditional time intensive and resource consuming procedures.
References

1. Chojnowski, J.M., Sykes, J.R. & Thwaites, D.I. Practical beam steering of X-ray beams on Elekta accelerators: The effect of focal spot alignment on beam (symmetry and position) and radiation isocentre (size and position). Phys Eng Sci Med 43, 1441–1450 (2020). https://doi.org/10.1007/s13246-020-00926-8

O27. Linac optimisation, part 2: Aligning linac isocentres

Jacek Chojnowski[1,*], Jonathan Sykes[2,3], David Thwaites[2]

[1]North Coast Cancer Institute, Coffs Harbour, Australia, [2]University of Sydney, Sydney, Australia, [3]Western Sydney Local Health District, Sydney, Australia

Introduction Linac isocentre is commonly determined by mechanical, radiation and imaging methods which are called as mechanical, radiation or imaging isocentres respectively. Since different determination methods give different results, it is difficult to decide which one should be considered as the reference linac (treatment) isocentre.
Method A novel method of localising the linac isocentre is presented, generally referred to as the mechanical isocentre (since the 'mechanical' collimator axis of rotation is used as a reference) but determined using radiation. The method is based on the localisation methodology of the radiation isocentre, as a centroid of the sphere comprising all the beams central axis at cardinal gantry angles but corrected for the beam focal spot offsets (misalignment) from the collimator axis of rotation. The beam focal spot offset at each gantry angle is measured using the image centre shift method [1] with a specially designed rigid phantom with two sets of ball-bearings attached to the collimator [2]. For optimal linac performance the radiation isocentres for all photon beams are adjusted to coincide with the mechanical isocentre and then the imaging isocentre is re-calibrated.
Results The linac mechanical isocentre, determined using radiation, does not depend on the beam setting parameters such as energy, MU or a beam limiting device [2]. The uncertainty of the localisation method is 0.1 mm (2sd) and is therefore recommended to be the reference treatment isocentre. Radiation and imaging isocentres can be aligned with the linac mechanical isocentre to within 0.1 mm.
Conclusion A novel method of localising linac isocentre has been developed and verified to be well defined and therefore all other isocentres, such as radiation and imaging should be aligned to it. The method is easy to use and accurate, thanks to customised automation and computer software.
References

1. Nyiri BJ, Smale JR, Gerig LH. Two self-referencing methods for the measurement of beam spot position. Med Phys. 2012;39: 7635–7643. https://doi.org/10.1118/1.4766270
2. Chojnowski JM, Sykes JR, Thwaites DI. A novel method to determine linac mechanical isocenter position and size and examples of specific QA applications. J Appl Clin Med Phys. 2021. https://doi.org/10.1002/acm2.13257

O28. Acceptance and commissioning of Australia's first Radixact™ radiation therapy system: initial experience

Ms. Nancy Yu[1,2], Ms. Sarah Maxwell[1], Mr. Craig M. Lancaster[1], Dr. Scott B. Crowe[1,2]

[1]Royal Brisbane and Women's Hospital, Brisbane, Australia, [2]Queensland University of Technology, Brisbane, Australia

Introduction Australia's first Radixact™ radiation therapy system has been installed at the Royal Brisbane and Women's Hospital in mid 2022 and replaced the legacy tomotherapy unit. The system arrived at the department in early May and went live in mid July. The post installation process including acceptance, commissioning, and onsite training took only four weeks. Our team was able to get the machine up and running in a relatively short time frame.
Method The main categories of the acceptance and commissioning tests performed include: beamline alignment tests, beam profiles, absolute dose calibration, and auxiliary system tests including ClearRT™ KV imaging system and Synchrony™ motion tracking system. Water tank scans were performed using the Standard Imaging™ water tank and A1SL ion chamber with Tomo Electrometer. Other tests were performed mainly using the Tomo-Phantom HE and Solid Water HE by made by Gammex.
Results All alignment tests show beamline alignment are well within the tolerance of ± 1 mm. Water tank scans of transverse profiles passed the gamma tolerance of 2%, 1 mm; longitudinal profiles passed the gamma tolerance of 2%, 0.5 mm; longitudinal asymmetric profiles passed the gamma tolerance of 3%, 0.5 mm; and PDD of all jaw widths passed the maximum deviation of ± 1%. Absolute dose calibration has the maximum difference of -0.69% and the average difference of -0.21%. The ClearRT™ KV imaging system shows superior image quality and the Synchrony™ motion tracking system was proven capable of both fiducial and respiratory lung tracking.
Conclusion The Radixact™ radiation therapy system has been installed and commissioned very swiftly at our department. The initial clinical release of the machine allows it to replace the legacy tomotherapy unit and perform similar treatment. New technologies such as Synchrony™ motion tracking system will be tested further and introduced to clinical use in the near future.

O29. Determination of representative reference and tolerance values for planar kV image quality for TrueBeams

Jeffrey Harwood[1,*], Deepak Basaula[2], Kimberley Legge[3]

[1]Barwon Health, Geelong, Australia, [2]Peter MacCallum Cancer Centre, Melbourne, Australia, [3]Canberra Health Services, Canberra, Australia

Introduction Image-guided radiation therapy (IGRT) is an essential component of modern radiotherapy. IGRT is used to verify patient position and monitor changes in patient anatomy. Protocols provide guidance on the quality assurance (QA) required to ensure IGRT systems are capable of providing clinically useful images [1–3]. It has also been reported that protocol-based QA tolerances are not reliable at predicting clinical image quality issues [4]. QA protocols instruct the user to compare to baseline data, but do not provide guidance on what variation from baseline is acceptable. The use of statistical process control charts (SPCC) to determine CBCT reference and tolerance values for a single treatment unit was the topic of a previous EPSM presentation [5]. This work extends that novel approach to determine generic representative reference and tolerance values for planar kV image quality for Varian TrueBeam linacs by looking at the variation in parameters across multiple treatment units.
Method We obtained 70 planar kV images of a LEEDS TOR.18FG phantom using the default acquisition parameters for a High Quality image across 5 TrueBeams from 3 centres. The data sets were analysed using pylinac (v2.5.1.7) [6]. We produced SPCCs to characterise the variation of image quality results and determine reference and tolerance values [7].
Results Representative reference and tolerance values for planar kV image quality for TrueBeams are presented in Table 1. An example SPCC is shown for the modulation transfer function (MTF80%) in Fig. 1. Combining data across TrueBeams leads to only a small variation in reference and tolerance values when compared to a machine by machine analysis.
Conclusion SPCCs were used to determine representative reference and tolerance values for planar kV image quality for 5 TrueBeams across 3 centres. This approach results in more specific tolerance limits when compared with published protocols, ensuring that scan quality and clinical utility can be more effectively monitored with routine QA.
References

1. Fontenot JD, Alkhatib H, Garrett JA, et al. (2014) AAPM Medical Physics Practice Guideline 2.a: Commissioning and quality assurance of X-ray-based image-guided radiotherapy systems. J Appl Clin Med Phys 15:3–13. https://doi.org/10.1120/jacmp.v15i1.4528
2. Bissonnette J-P (2018) COMP report: CPQR technical quality control guidelines for accelerator-integrated cone-beam systems for verification imaging. J Appl Clin Med Phys 19:9–12. https://doi.org/10.1002/acm2.12302
3. Varian TrueBeam Installation Product Acceptance IPA-HT-2X-ICP-H November 2018.
4. Manger RP, Pawlicki T, Hoisak J, Kim G (2019) Technical Note: Assessing the performance of monthly CBCT image quality QA. Med Phys 46:2575–2579. https://doi.org/10.1002/mp.13535
5. Harwood J, Legge, K (2020) Determination of cone beam computed tomography quality assurance tolerances using process control charts. EPSM 2020, Engineering and Physical Sciences in Medicine. Phys Eng Sci Med 44, 919–995 (2021). https://doi.org/10.1007/s13246-021-01024-z
6. Zaila A, Adili M, Bamajboor S (2016) Pylinac: A toolkit for performing TG-142 QA related tasks on linear accelerator. Phys Medica 32:292–293. https://doi.org/10.1016/j.ejmp.2016.07.122
7. Pawlicki T, Whitaker M, Boyer AL (2005) Statistical process control for radiotherapy quality assurance. Med Phys 32(9):2777–86. https://doi.org/10.1118/1.2001209

Table 1 Reference and tolerance values determined from SPCC analysis,

Parameter	Upper Limit	Centre Line	Lower Limit
MTF 80%	1.17	0.95	0.73
Median Contrast to noise ratio	8.57	6.70	4.83

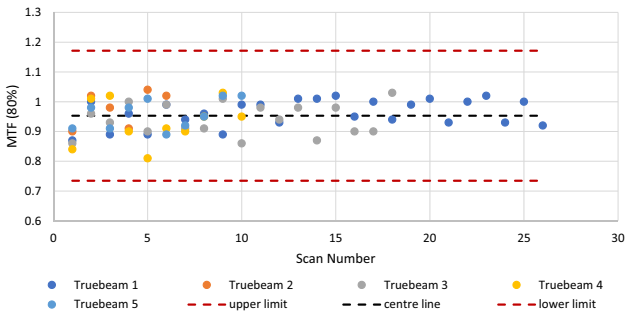

Fig. 3 SPCC for MTF 80%.

O30. End to end testing of the ExacTrac Dynamic Deep Inspiration Breath Hold (DIBH) workflow

Simon Goodall[1,2,*], Peter Rampant[1]

[1]GenesisCare, Perth, Australia, [2]School of Physics, Mathematics, and Computing, Faculty of Engineering and Mathematical Sciences, University of Western Australia, Crawley, Perth, Australia

Introduction The ExacTrac Dynamic system combines stereoscopic x-ray imaging with optical and thermal surface tracking. The recent release of the v 1.1 software included a Deep Inspiration Breath Hold (DIBH) workflow which is primarily designed for use with breast treatments. This work aimed to evaluate the ability of the workflow and imaging systems to position a breath hold phantom at a treatment location during end-to-end testing.

Method A breath hold phantom was developed with two different breath hold volumes in addition to an exhale position. A ball bearing (BB) was positioned within the breast tissue to allow MV imaging. The phantom was initially tested for positional reproducibility to verify its suitability for workflow evaluation. Following phantom validation, treatment plans were created for both breath hold positions comprising small fields centred on the BB. The end-to-end workflow was followed for both breath hold positions of the phantom. Workflow positioning of the phantom was verified using CBCT and MV imaging of the BB at isocentre.

Results The phantom was shown to have good reproducibility in positioning over repeat breath holds on both a given day, and set-ups on two separate days. The mean distance to agreement between inter-breath hold external phantom contours generated in MIM were $<$ 0.5 mm, the DICE similarity co-efficient values were $>$ 0.995. The final position of the phantom following the ExacTrac DIBH workflow showed mean errors, across all end-to-end tests, of $<$ 0.5 mm and $<$ 0.5° when evaluated by CBCT and $<$ 0.3 mm when evaluated by MV images.

Conclusion A phantom was successfully developed to allow testing of the ExacTrac DIBH workflow. The workflow positioned the phantom at the desired treatment location within an acceptable level of accuracy for DIBH breast treatments as evaluated by both CBCT and MV imaging.

O31. Medical Physics for sustainable healthcare- need for interdisciplinary approach

Arun Chougule[1,*]

[1]Sawai Man Singh (SMS) Medical College and Hospital, Jaipur, India

The theme of international day of medical Physics IDMP2022 is" ***Medical Physics for sustainable healthcare***". Clinically Qualified Medical Physicists [CQMP] working in healthcare are contributing immensely for safe and effective use of radiation for diagnosis and treatment. In addition, medical physicists are contributing to research, technology development, validation of technology and innovations in the medical physics. Medical physics is a bridge between medicine and physical sciences and therefore is responding to technological and scientific problems faced in the medical field. Developments in medical physics sometimes strongly overlap with developments in related disciplines like biomedical engineering, biophysics, and information technology. Medical physicists are good at interacting with physicians and other basic scientists, but it is essential to become much better at it with interdisciplinary approach. Medical physicists have knowledge and skills to attack the problems of modern medicine but should not be shy at embarking on new territories. Clinical medical physicists as health professionals require competency and therefore must undergo minimum of two years full time structured clinical training program and residency under experienced medical physicist in recognized institution after postgraduation in medical physics. Further medical physics is a fast-growing area needing high degree of knowledge and professional competency due to the rise in complexity of treatment procedures, increasing access to medical technology and the requirement of coordination between medicine, physics, and biomedical engineering areas. The unprecedented surge in medical physics competency in the last 2- 3 decades is due to implementation of specialized physics and technology intensive procedures such as particle therapy, image guided & intra operative radiotherapy, advanced imaging, and nuclear medicine techniques, artificial intelligence, large data mining, simulations of complex systems, translational research, molecular targeted therapies. Medical physics is facing significant changes, particularly with rapid development of biological sciences, more complex research requiring interdisciplinary teams and an urgent need for translational research. The changes towards personalized medicine are opening new avenues for medical physicists including molecular imaging and advanced adaptive radiation therapy.

In this scenario to handle this new technology era the quantity of qualified medical physicist needs to be in consonance with the competency needed. Rather than preparing medical physicists for the present, the programs should prepare them for the future. To prepare medical physicists for the future, education and training should be properly adjusted to include more basic non-physical sciences, particularly biology; more imaging, especially molecular imaging; and more interdisciplinary and translational research components. If we want to do justice to the theme of IDMP2022, a strong interaction between academic (medical) physics, biomedical engineer, computer/IT experts and clinical medical physics is essential to maximize both the scientific and the clinical output of research resources. Convergence of sciences and technologies needed to profoundly change health care by pushing the frontiers of technology to make the possible a reality. Focus on enabling technologies with broad applications to multiple diseases or biological processes with multi-disciplinary and collaborative research approach is needed.

The requirement for education and training of medical physicists lead to opening of numerous educational programs around the world and so in AFOMP region. However, in AFOMP countries we find huge diversity and therefore task of AFOMP to homogenise the medical Physics education and profession is quite challenging. AFOMP has formed a task group to draft a model curriculum for Master's in Medical Physics. Task group has drafted curriculum after number of meetings and deliberations and will be released soon.

O32. An Overview: Asia-Oceania Federation of Organizations for Medical Physics (AFOMP)

Hasin Anupama Azhari[1,*]

[1]Centre for Biomedical Science and Engineering, United International University (UIU)

Introduction The Asia-Oceania Federation of Organizations for Medical Physics was founded in 2000 to promote medical physics in the Asia and Oceania regions, through the advancement in status and standard of practice of the medical physics profession. It is one of the regional groups within the International Organization for Medical Physics. The main Aims & Objectives of AFOMP are promoting the co-operation and communication between medical physics organizations, promoting medical physics and related activities in the region, the advancement in status and standard of practice of the medical physics profession, organize and/or sponsor international conferences, regional and other meetings of courses and collaborate or affiliate with other scientific organizations.

Methods The AFOMP are striving to build a strong relationship between national organizations in the Asia-Oceania region and international bodies. AFOMP currently have 21-member national organizations and MEFOMP as members of the federation over 7000 medical physicists. If we look at socio-economic & educational status of AFOMP countries we find huge diversity and therefore task of AFOMP to homogenies the medical Physics education and profession is quite challenging. To cater to the needs of the medical physicists and their education, AFOMP has created five main committees to work on number of important tasks. Professional Relations Committee (PRC), Education and Training Committee (ETC), Science Committee (SC), Funding Committee and Award and honors Committee (AHC). These committees have drafted policy statements to deal with minimum level of education and training of medical physics, continuous professional development, funding, award for the person who contribute for medical physics promotion and development and career progression for clinical medical physicist in AFOMP countries.

Results AFOMP works in many areas to enhance medical physics by organizing various scientific activities, conferences and officially publishes & endorses various journals & newsletter. Also promotes students & young professional through various grants. One of the most important scientific events organized by AFOMP every year is Asia-Oceania congress of Medical Physics (AOCMP). This congress gives a strong platform to AFOMP region medical physics communities to unite, exchange their scientific research & expertise and discuss professional issues. AFOMP received responses from national medical physicist associations however from personal contacts and understanding then compiled the information and observed that only few countries have master level medical physics education Programme with proper residency and accreditation. The detail outcome of the survey and possible remedies to make it compatible with IAEA recommendations, teaching & education structural requirements are suggested. Official publication of AFOMP includes Physics and Engineering Sciences in Medicine, and Radiological Physics and Technology and Journal of Medical Physics. Besides this it publishes AFOMP newsletter twice a year. AFOMP is playing a lead role in scientific and professional development of medical physics communities in Asia-Oceania region.

Conclusion The tireless efforts exerted by the predecessors already has taken AFOMP to the height of the vibrant organization and regional leader in the development of medical physics in the Asia–Pacific region but still there is long way to go ahead to reach its goals. The lack of recognition of medical physics standards of practice is a common issue in many Asian countries. Most of the Asian countries do not have accreditation or certification systems for medical physicists. A well-prepared strategy and a strong action plan are crucial for the AFOMP to move forward.

O33. Science diplomacy in medical physics in the Asia-Oceania region

Chai Hong Yeong[1,*]

[1]School of Medicine, Faculty of Health and Medical Sciences, Taylor's University, 47,500 Subang Jaya, Malaysia

Asia-Oceania is the home for over 60 percent of the world's population (about 4.3 billion people) and it is popular for its vast diversity in demographic, socioeconomic, politics and cultural aspects. The Asia-Oceania Federation of Organizations for Medical Physics (AFOMP) was founded on 28 May 2000 with the important task of connecting and enhancing the medical physics profession in the region via science diplomacy. It consists of 19 national member organizations (NMOs) and 2 affiliate NMOs. The Federation works closely with the NMOs and other international organizations on matters such as development of professional status and standard, medical physics service and standard, education and training, scientific meetings and exchanges. AFOMP held the first congress (AOCMP) in 2001 in Thailand, and then annually at different member countries. In 2020, AFOMP celebrates its 20th anniversary with the theme of "Twenty Years of Teamwork". During this celebration, AFOMP launched the Monthly Webinar Series to provide free education and continuous professional development (CPD) to the medical physicists in the region. The webinars are accredited by the Australasian College of Physical Scientists and Engineers in Medicine (ACPSEM). In addition, AFOMP School was launched in June 2021 to provide free online courses to young medical physicists, trainees and students on a monthly basis. AFOMP publishes its Newsletter semi-annually. It also endorses three journals, namely Radiological Physics and Technology, Physical and Engineering Sciences in Medicine and Journal of Medical Physics as its official journals. Furthermore, AFOMP delivers several awards to inspire and acknowledge outstanding medical physicists from different categories. On 2 April 2022, a memorandum was signed between AFOMP and EFOMP to furthering collaboration between the two regional organizations in the area of education, training, scientific and research. This is an auspicious step towards global partnership for sustainable development of medical physics via science diplomacy.

O34. The Covid-19 International Survey of Medical Physicists and Biomedical Engineers: Are there any positives as a result of working from home during the pandemic?

Eva Bezak[1,*], [1,2]Loredana Marcu, [3]Magdalena Stoeva, [4]Lenka Lhotska, [5]Gilda Barabino, [6]Fatimah Ibrahim, [7]Eleni Kaldoudi, [8]Sierin Lim, [9]Ana Maria Marques da Silva, [10]Peck Ha Tan, [11]Virginia Tsapaki, [12]Monique Frize

[1]University of South Australia, Adelaide SA 5001, Australia, [2]Faculty of Science, University of Oradea, 1 Universitatii str, 410,087 Oradea, Romania, [3]Department of Diagnostic Imaging, Medical University of Plovdiv, Plovdiv, Bulgaria, [4]Faculty of Biomedical Engineering, Czech Technical University in Prague, Prague 6, Czech Republic, [5]Olin College of Engineering, Needham, MA 02,492, USA, [6]Department of Biomedical Engineering and Centre for Innovation in Medical Engineering, Faculty of Engineering, Universiti Malaya,

50,603 Kuala Lumpur, Malaysia, [7]School of Medicine, Democritus University of Thrace, Alexandroupoli, Greece, [8]School of Chemical and Biomedical Engineering, Nanyang Technological University, Singapore 637,457, [9]School of Technology, Pontifical Catholic University of Rio Grande do Sul, PUCRS, Porto Alegre, Brazil, [10]School of Engineering, Ngee Ann Polytechnic, Singapore, [11]Medical Physics Dpt, Konstantopoulio General Hospitals, Athens, Greece, [12]Dept of Systems and Computer Engineering, Carleton University, Ottawa, ON, Canada K1S 5B6

Introduction While there is considerable information published on the challenges that working from home has caused during the COVID-19 pandemic, the literature is scarcer on the emergence of any positives from this experience. As such, this paper aims to present and discuss the positive experiences and/or outcomes encountered by STEM professionals associated with remote working during the COVID-19 lockdowns.
Methods A survey was created by a committee of IUPESM (International Union for Physical and Engineering Sciences in Medicine); Ethic clearance was by Carleton University. It uses the SurveyMonkey platform and was distributed world-wide in late 2020. We performed a qualitative analysis of 921 responses from professionals from 76 countries to two open-ended questions: 1. What is the one positive that you have learnt/experienced as a result of working from home during this pandemic? 2. What advice would you have for others if you found ways to cope better as time went by? Cross-tabulation of gender with responses was also performed.
Results In regard to the first question (629 answers), the number one positive was the fast development of virtual communication and education (webinars, conferences, meetings,…), followed by mastering new software, saving time commuting, more flexibility with working hours and for some even having more time to spend with children. There were also indications of personal growth including learning how to look after one's health, developing assertiveness and positive frame of mind that challenges can be overcome. However there were no positives identified by many respondents. In regard to the second question (530 answers), the key message from respondents was around understanding how to schedule and balance the demands of work and family, plan breaks, have realistic expectations and have personal space for work.
Conclusions Online communication and education have emerged as positives of the pandemic.

O35. The ACPSEM Better Healthcare Technology Foundation– making tomorrow's technology today

Dale Bailey[1,2,*]

[1]Department of Nuclear Medicine, Royal North Shore Hospital, Sydney, [2]Faculty of Medicine & Health, University of Sydney, Sydney

O36. [Invited] Advances in quantitative liver MRI

Claudia Hillenbrand[1,*]

[1]University of New South Wales, Sydney, Australia

Chronic liver disease and hepatocellular carcinoma have become a global health burden. Liver function and disease severity are usually assessed clinically based on clinical symptoms, biopsy, and blood parameters. Recent technical advances in quantitative magnetic resonance imaging (MRI) provided new tools for diagnosis and monitoring of hepatic disease. This presentation aims to give an overview over emerging approaches for quantitative liver MRI, with a specific focus on iron siderosis, steatosis and fibrosis. In addition, future directions such as automated image analysis and machine learning approaches for liver function quantification will be discussed.

O37. ITV creation using MR exhale and cine motion assessment

Jessica Lye[1,*], Reza Alinaghi[1], Sandie Fisher[1], Nikki Shelton[1], Glenn Cahoon[1], Richard Khor[1], Sweet Ping Ng[1]

[1]ONJCWRC, Austin Health, Heidelberg, Australia

Introduction The improved ability to visualise soft tissue targets with onboard MR imaging can be compromised by respiratory motion artefacts. Serial motion artifact reduction technique (SMART) or the Navigator triggered on diaphragm motion can be used to produce a high-quality image in the exhale phase [1]. This work investigates two methods to generate an internal target volume (ITV) from a single breathing phase in combination with motion assessment from a sagittal-coronal pair of cine MR images.
Method Fig. 1 shows the two different approaches; (b)ITV generated from the GTV expanded from exhale with margin shift in superior and left direction and (c) ITV created by duplicating the exhale GTV and shifting to inhale and mid position, then combining with Boolean function. Figure 1(d) compares the PTV created from a 5 mm isotropic expansion of the ITV from the two methods—margin expansion (ME) or boolean combine (BC). The CIRS 0087Z MR-CT abdomen motion phantom was used to test the ITV generation on a complex rotating shape and a small target with large motion. Four patient case studies were investigated where the clinical PTV created from 4DCT was compared to the PTV generated from the exhale MR and cine motion information.
Results Fig. 2 shows the Dice Similarity Coefficient (DSE) and the mean distance to agreement (MDA) between the PTV generated from 4DCT compared to MR exhale and cine. The DSE and MDA were calculated using MIM Maestro v6.8.6. The BC method showed superior agreement with the 4DCT in all cases. MR exhale and cine with BC had a DSC $> 80\%$ for all cases except for phantom case 1 with large non-clinical rotation.
Conclusion An exhale MR combined with cine motion information can be used to create an ITV using either a non-isotropic margin expansion or boolean combine method.
References

1. Philips MRI manual Release 5 International.

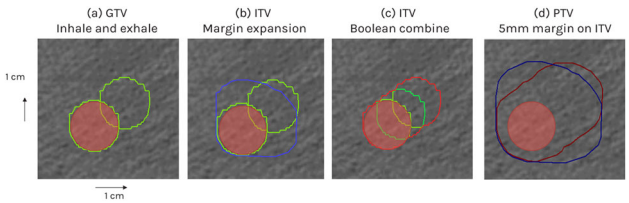

Fig. 4. The two methods for creating an ITV from an exhale image and known amplitude and direction of motion with (b) margin expansion and (c) Boolean Combine and (d) the resulting PTV from an exhale image and known amplitude and direction of motion.

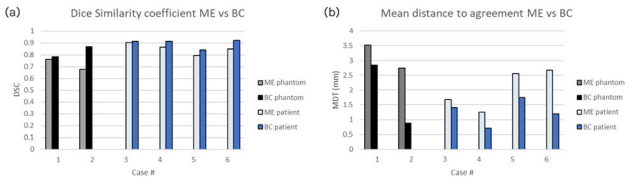

Fig. 5. (a) shows the DSE between the PTV generated from 4DCT compared to MR exhale and cine and (b) shows the MDA for two phantom and four patient case studies.

O38. PhoenixMR: A novel MRI simulation framework

Phillip Duncan-Gelder[1,*], Darin O'Keeffe[1,2], Phil Bones[1], Steven Marsh[1]

[1]University of Canterbury, Christchurch, New Zealand, [2]Christchurch Hospital, Health NZ, Christchurch, New Zealand

Introduction MRI simulation plays an important role in the ongoing development of MRI and needs to be fast, accurate, and flexible. Currently there are no existing general-purpose simulators which are able to satisfy all three of these requirements, rather there have been a number of unvalidated bespoke simulators designed for research. The PhoenixMR simulation framework has been developed to solve this problem. A general interface offers complete flexibility whereby specification of custom inputs can be easily user-defined by a Turing-complete programming model which runs directly on GPUs for maximum performance. Modelling real world MRI machines is one of the many use cases for this simulator. By measuring and characterizing a set of intrinsic MR parameters, specific machines can be modelled. This model can then be used for performing simulated MR experiments.
Method Using the HPD System 130 quantitative MRI phantom, a set of measurements were taken on a Siemens Skyra MRI system at St Georges Hospital (Christchurch, New Zealand) with various sequences and sequence parameters for a given coil and machine configuration. The k-space functions corresponding to these measurements were reconstructed to produce coil sensitivity and B0 inhomogeneity maps. These maps were then used as input parameters for the PhoenixMR simulator along with similar sequences and parameters. Acquired images were then compared to show agreement between simulation and experimental data.
Results Results are show in Fig. 1.
Conclusion Using PhoenixMR, real-world MRI experiments can be quickly, accurately, and flexibly modelled and executed. This has several applications in the ongoing development of MRI as both a standalone imaging modality and being used for on-board MR-guided radiotherapy treatments.

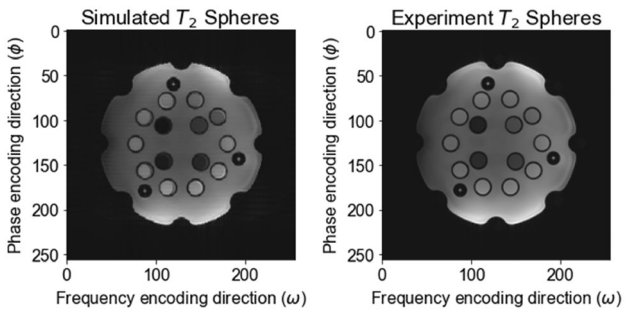

Fig. 1. A single reconstructed slice from simulated (left), experimental (right) with slice thickness of 6 mm. Volumetric linear regression was performed yielding r = 0.9747. Simulations were performed using a single GTX980Ti in 24 min.

O39. MRI pulse sequence simulator development

Catherine Jones[1,*]

[1]Princess Alexandra Hospital, Brisbane, Australia

Introduction Development of an MRI pulse sequence simulator is in progress. The purpose of the simulator is to trouble shoot during the development of new pulse sequences, and applications such as predicting geometric distortion following mapping of a scanner's field inhomogeneity, and gradient non-linearity. Currently the simulator can perform off-centre slice selection, chemical-based selection, inversion recovery saturation, and acquire a photon spectrum.
Method The initial stage of the simulator and the virtual phantom (proton density, T1, T2, chemical shift and B0-maps) is written in Python. Numerical simulation of the Bloch Eqs. [1] is written in C + + to improve computational efficiency. Free induction decays (FID) and corresponding spectra following FLAIR and STIR excitations from virtual water and fat pools were computed.
Results The FID and spectrum of the water/fat pool following a fat selective pulse is shown in Fig. 1.
Conclusion It is expected that simulations on small virtual phantoms for trouble shooting pulse sequence development can be performed in real-time. However, simulations on realistic 3 dimensional phantoms may require processing time similar to Monte Carlo simulations.
References

1. Bloch F (1946) Nuclear Induction. Physical Review 70:4604–40,731.

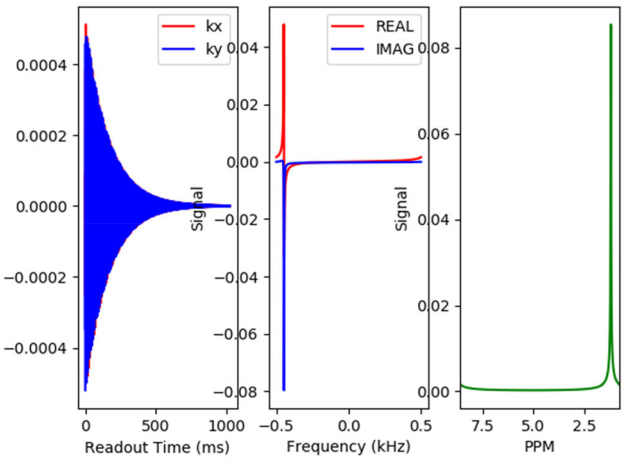

Fig. 1. Plots of FID and spectrum of a water/fat pool following a fat-selective pulse, where is clear that the water pool has not been excited.

O40. Real-time motion monitoring: An assessment of pre-release gating for prostate SBRT on the Elekta Unity MR-Linac

Madeline Carr[1,*], Jeremy de Leon[1], Vikneswary Batumalai[1], David Crawford[1], Maddison Picton[1], Gerard Perera[2], Tania Twentyman[1], Michael Jameson[1]

[1]GenesisCare, Sydney, Australia, [2]Elekta AB, Stockholm, Sweden

Introduction MR-Linacs provide a novel method of visualising and assessing organ motion in real-time during radiotherapy treatment [1]. At current, Elekta is developing gating for the 1.5 T Unity MR-Linac system using 2D balanced fast field echo (bFFE) orthogonal cine MRI [2]. The purpose of this study was to demonstrate the use of Elekta's updated pre-release gating motion monitoring research package (MMRP). This was completed by quantifying the motion of the clinical target volume (CTV) for prostate SBRT patients.

Method The data for five Unity SBRT prostate patients was retrospectively analysed using MMRP. The package algorithm creates a template using initial T1/T2-weighted bFFE images. This is registered to the corresponding T2-weighted 3D reference MRI image and incoming cine images for target tracking. The CTV was selected for tracking and the gating envelope thresholds were set to clinical PTV treatment margins (Fig. 1). The algorithm calculated the 'Beam on (%)' as the portion of acquisition time ($\geq$ 8 min for these patients) that the CTV displacement vector remained within the thresholds, and if the tracking quality was classified as successful.

Results Visually, MMRP successfully tracked all target structures. Quantitatively, the average (SD) target displacement found over the five patients was 0.25L (1.59), 0.92I (2.03) and 0.17P (1.08) mm in the Left(L)-Right, Superior-Inferior(I), and Anterior–Posterior(P) directions, respectively. Further, the proportion of Beam on time was 99.36%, suggesting minimal target motion outside of the set thresholds.

Conclusion MMRP was successful in tracking all target structures, which remained within thresholds for $>$ 99% of the time. Such treatment innovations may enable margins to be safely reduced in the future. Further investigations will involve validating these findings on larger patient datasets, over multiple fractions, and for different anatomical sites.

References

1. Keiper TD et al. (2020) Feasibility of real-time motion tracking using cine MRI during MR-guided radiation therapy for abdominal targets. Medical physics 47(8): 3554–3566
2. Hu P, et al. (2022) Dosimetry impact of gating latency in cine magnetic resonance image guided breath-hold pancreatic cancer radiotherapy. Physics in medicine and biology 67(5).

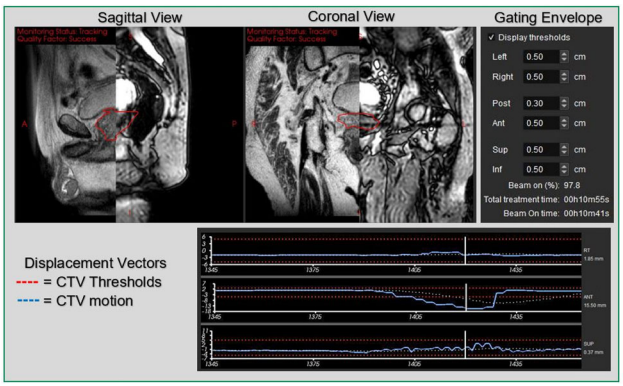

Fig. 1. Modified screenshot taken from MMRP capturing one patients CTV exiting the threshold limits when experiencing flatulence.

O41. [Invited] Medical physics and the metaverse: Optical scanning, 3D printing and deep learning techniques in radiation oncology

Michael Douglass[1,*], Corey Bridger, Paul Reich & Alexandre Santos

[1]Royal Adelaide Hospital, Adelaide, Australia, [2]Australian Bragg Centre for Proton Therapy and Research, Adelaide, Australia, [3]University of South Australia, Adelaide, Australia

The video game industry gave rise to the current innovations in deep learning research that we are seeing today, through the development of fast and affordable GPU technology. The next technological revolution, augmented/virtual reality and the Metaverse will benefit medical physics through accurate and affordable 3D scanning and 3D printing technologies which have seen widespread adoption for commercial applications. Such technologies include photogrammetry, Lidar and structured light scanning (SLS) [1,2] which are now available on some consumer smartphones. SLS is already used in radiation oncology for surface guided radiation therapy. Photogrammetry and Lidar scanning are two inexpensive technologies for 3D printing patient specific bolus [1,3] for external beam radiotherapy treatments or superficial brachytherapy applicators. In this horizon scanning presentation, we discuss recent developments in the field of optical 3D scanning technologies in radiation oncology which may compliment CT and MRI as a useful imaging modality in a radiation therapy treatment planning workflow.

References

1. Douglass, M.J.J. (2022), Can optical scanning technologies replace CT for 3D printed medical devices in radiation oncology?. J Med Radiat Sci, 69: 139–142. https://doi.org/10.1002/jmrs.579
2. Crowe S, Luscombe J, Maxwell S, et al. Evaluation of optical 3D scanning system for radiotherapy use. J Med Radiat Sci, 2022; 69: 218– 26. https://doi.org/10.1002/jmrs.562
3. Bridger CA, Reich PD, Caraça Santos AM, Douglass MJJ. A dosimetric comparison of CT- and photogrammetry- generated 3D printed HDR brachytherapy surface applicators. Phys Eng Sci Med 2022; 45: 125– 134. https://doi.org/10.1007/s13246-021-01092-1

Fig. 1. Comparison of 3D models of the Rando anthropomorphic phantom acquired using Left – CT, Middle – Lidar and Right – Photogrammetry.

O42. A federated machine learning framework for vertically partitioned health data

Amir Anees[1,*]

[1]University of New South Wales, Sydney, Australia

Introduction Federated machine learning trains a learning algorithm from data stored separately (distributed) without exchanging the data, preserving privacy [1,2]. Horizontal partitioning has been implemented previously in the Australian Computer Assisted Theragnostics (AusCAT) [3] network and refers to learning where data from an individual patient is only at one institution. Vertical partitioning refers to the scenario where data from an individual patient is split between institutions (e.g., hospitals and a registry). This work aims to develop a vertically partitioned federated machine learning algorithm.
Method The methodology employed, based on a neural network, labels the institution holding the input features along with the output feature as the hospital and the other institution(s) holding separate input features of the common patients as the registry. The registry first calculates the results of the first layer of the neural network and sends those results to the hospital. The hospital aggregates those results and performs the calculation for the rest of the layers of the neural network. Further, the hospital sends the derivative of the first layer results to each of the registries to update their model parameters locally. This methodology was tested on public datasets [4,5] and compared to a centralised neural network and privacy analysis was also undertaken.
Results Mathematically, the model developed in the vertical federated learning scenario is the same as when the data is centralized for this algorithm. This was demonstrated with the public datasets as shown in Fig. 1. Privacy analyses showed that these exchanges do not cause any leakage of sensitive data.
Conclusion A new federated learning algorithm was developed for vertically partitioned data. This could be extended in the future to incorporate horizontal partitioned data for an unbalanced number of patients, i.e., some hospitals have more data than others.
References

1. McMahan HB, Moore E, Ramage D, Hampson S, Arcas BAY (2016) Communication-Efficient Learning of Deep Networks from Decentralized Data. arXiv:1602.05629.
2. Li L, Fan Y, Tse M, Lin KY (2020) A review of applications in federated learning. Computers & Industrial Engineering 149:1–15.
3. Field M, Vinod S, Aherne N et al. (2021) Implementation of the Australian Computer-Assisted Theragnostics (AusCAT) network for radiation oncology data extraction, reporting and distributed learning. J Med Imaging Radiat Oncol 65(5):627–636.
4. Lohweg V (2012) Banknote authentication data set. UCI machine learning repository https://archive.ics.uci.edu/ml/datasets/banknote+authentication
5. Smith JW, Everhart JE, Dickson WC, Knowler WC, Johannes RS (1988) Using the ADAP learning algorithm to forecast the onset of diabetes mellitus. Proceedings of the Symposium on Computer Applications and Medical Care, IEEE Computer Society Press 261–265.

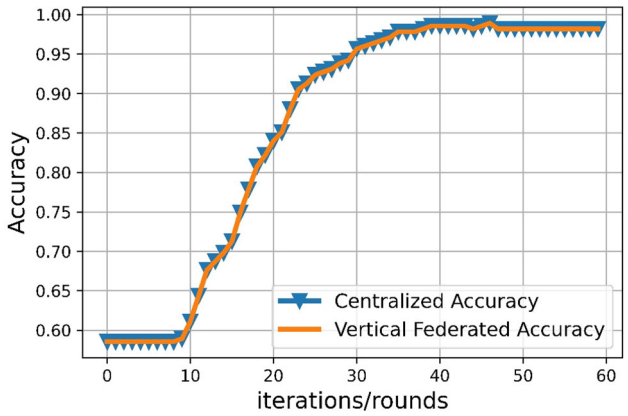

Fig. 1. Comparison of accuracy between centralized and distributed (proposed vertical federated framework) settings on banknote dataset [4]. The accuracy and the convergence rate in terms of required rounds/iterations remains the same in both cases demonstrating the effectiveness of the proposed work.

O43. A deep multimodal approach for standardising lung radiotherapy structure naming conventions

Fahim Alam[1,2,3,*], **Matthew Field**[1,2,3], **Ali Haidar**[1,2,3], **Daniel Al Mouiee**[1,2,3], **Lois Holloway**[1,2,3,4]

[1]South Western Sydney Clinical Campus, School of Clinical Medicine, University of New South Wales, Sydney, Australia, [2]South Western Sydney Cancer Services, NSW Health, Sydney, Australia, [3]Ingham Institute for Applied Medical Research, Sydney, Australia, [4]Institute of Medical Physics, University of Sydney, Sydney, Australia

Introduction In radiotherapy (RT) planning systems, standardised nomenclature of Organs-At-Risk (OARs) is essential to answer various clinical questions for improving patients' treatment. Manual standardisation approaches involve discussions between clinical staff and researchers to prepare the datasets, requiring considerable time and effort. To overcome this issue, machine learning-based automated processes have been investigated. Inspired by the standardisation approach in [1], we propose to include both text and image features in an integrated deep learning framework and evaluate this on a lung cancer dataset, standardising the nomenclature of six OARs.
Method A dataset of 422 non-small cell lung cancer (NSCLC) patients containing Computed Tomography (CT) and RT struct data was collected from the cancer imaging archive [2]. This dataset was standardised but OAR structure names commonly used in the clinic were assigned for this work. Naming inconsistencies were artificially added in the data by renaming various structures. After necessary preprocessing, 2D central slices containing the highest number of tumour pixels on the axial plane were extracted from the CT images and used to train a Convolutional Neural Network. Additionally, various patient structures were trained on a Gated recurrent unit to produce meaningful text features. These text and image features are combined and trained on an Artificial Neural Network to build a classification model which is used to predict the structure names on the test CT images. The proposed model (Fig. 1) was evaluated against several metrics by weighting each class by the number of samples from that class.
Results Table 1 shows the average classification results of the six OARs.

Conclusion A number of misclassifications were observed in cases of Esophagus and Spinal Cord which will be investigated to improve the model. Also, we plan to consider real historical data and more complicated clinical scenarios addressing important target volumes and control structures.

Disclosures
This work was supported by the Australian Research Data Commons (ARDC) and Cancer Institute, NSW.

References

1. Haidar, A., Field, Matthew., Batumalai, V., Cloak, K., Mouiee, D. A., Chlap, P., Huang, X., Chin, V., Carolan, M., Sykes, J., Vinod, S., Delaney, G., Holloway, L., PO-1618 Standardising Nomenclatures in Breast Radiotherapy Imaging Data using Machine Learning Algorithms, Radiotherapy and Oncology, Volume 170, Supplement 1, 2022, Pages S1406-S1407, ISSN 0167–8140, https://doi.org/10.1016/S0167-8140(22)03582-4
2. Aerts, H. J. W. L., Wee, L., Rios Velazquez, E., Leijenaar, R. T. H., Parmar, C., Grossmann, P., Carvalho, S., Bussink, J., Monshouwer, R., Haibe-Kains, B., Rietveld, D., Hoebers, F., Rietbergen, M. M., Leemans, C. R., Dekker, A., Quackenbush, J., Gillies, R. J., Lambin, P. (2019). Data From NSCLC-Radiomics [Data set]. The Cancer Imaging Archive. https://doi.org/10.7937/K9/TCIA.2015.PF0M9REI

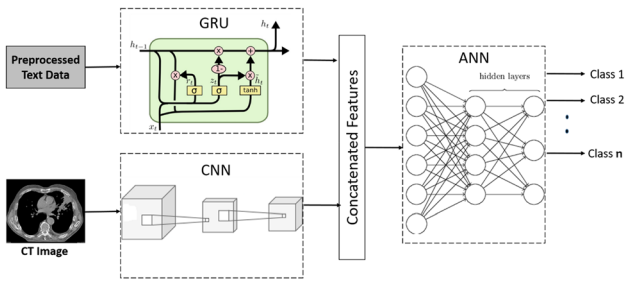

Fig. 1. An overview of the proposed framework.

Table 1. Classification Results (Training and Testing Stratified Splitting Ratio = 75:25).

Classification Results of Individual OARs

	Precision	Recall	F1-Score
Heart	100%	100%	100%
Left Lung	99.19%	99.35%	99.23%
Right Lung	98.79%	98.79%	98.79%
Combined Lung	99.27%	99.27%	99.27%
Esophagus	95.40%	96.78%	96.14%
Spinal Cord	94.59%	94.73%	94.65%
Average Score	97.87%	98.15%	98.01%

O44. Applying multi-modal federated deep learning in head and neck cancer survival outcome prediction

Daniel Al Mouiee[1,2,3,*], Ali Haidar[1,2], Phillip Chlap[1,2], Matthew Field[1,2], Fatemeh Vafaee[3], Lois Holloway[1,2]

[1]South Western Sydney Cancer Services, NSW Health and Ingham Institute, Liverpool, Australia, [2]South Western Sydney Clinical Campus, School of Clinical Medicine, UNSW, Sydney, Australia, [3]School of Biotechnology and Biomolecular Sciences, UNSW, Sydney, Australia

Introduction Artificial Intelligence, in particular deep learning (DL), has made much progress in radiation oncology [1]. Current implementations, however, are limited by its heavy reliance on data-driven approaches, as medical data is largely distributed across institutions, governed by complex legal and ethical regulations. As a result, DL generalizability is heavily affected when solving many medical classification tasks. To overcome such limitations, we propose and evaluate a multi-modal federated learning (FL) approach to train a DL model over distributed datasets.

Method A head and neck cancer dataset was collected from the cancer imaging archive [2]. A FL framework was implemented, with three clients representing clinics for training and one for testing. Datasets were kept isolated at each client. Three different input setups were used to train deep neural networks (NN); patient clinical features, their Computed Tomography treatment planning images and a combination of both using a multi-input NN. Experiments with the images included 2D central slices of the Gross Tumour Volume's (GTV) pixel data only and 2D Local-Z-Projected (LZP) [3] images of the entire volume. The experiments were repeated five times, where each client was used in turn for testing. Area Under the Curve (AUC) and Accuracy (ACC) were measured. This approach was compared to a centralised learning (CL) approach where the 3 training datasets would be combined into one.

Results Mean AUC values of 0.65 ± 0.05, 0.68 ± 0.04 were reported for FL and CL clinical-feature-only models, respectively (Fig. 1), while the image-dependent models showed low AUC and variable ACC (Fig. 2).

Conclusion Outcome survival prediction is a complex task in DL, taking into consideration the limited number of samples and data distribution across multiple centres. Next steps will be aimed at identifying complex patterns between patient data and survival outcomes by investigating various DL architectures, data augmentation techniques and other FL aggregation methods.

References

1. Huynh, E., Hosny, A., Guthier, C. et al. (2020). Artificial intelligence in radiation oncology. Nat Rev Clin Oncol 17, 771–781. https://doi.org/10.1038/s41571-020-0417-8
2. Vallières, M. et al. (2017). Radiomics strategies for risk assessment of tumour failure in head-and-neck cancer. Sci Rep 7, 10,117. https://doi.org/10.1038/s41598-017-10371-5
3. Herbert, S., Valon, L., Mancini, L. et al. (2021). LocalZProjector and DeProj: a toolbox for local 2D projection and accurate morphometrics of large 3D microscopy images. BMC Biol 19, 136. https://doi.org/10.1186/s12915-021-01037-w

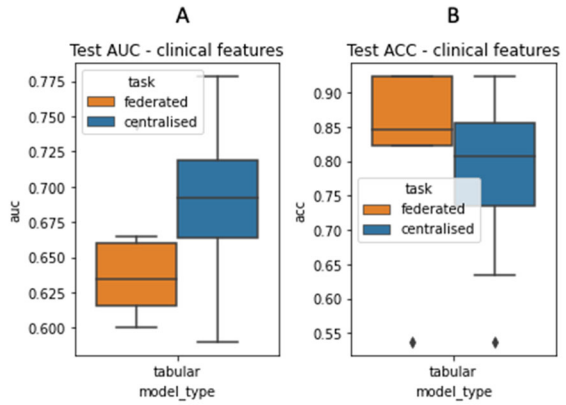

Fig 1: Boxplots of the mean test a) AUC and b) ACC for both FL and CL when training a DL model only using patient clinical features.

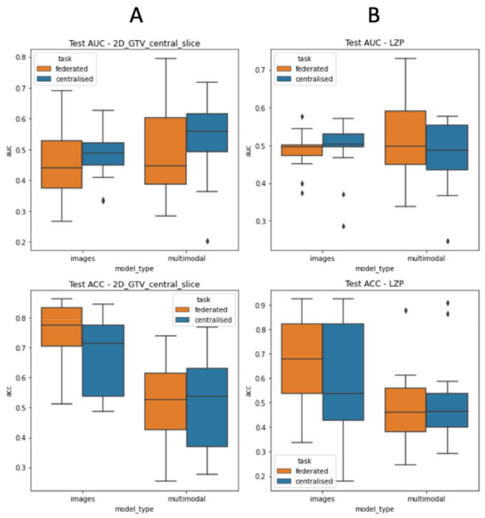

Fig 2: Boxplots of the mean test AUC and ACC for both FL and CL when training a images-only trained or multimodal DL model with (denoted columns) A) 2D GTV central slices or B) LZP protected images

O45. Assessing the benefit of training deep learning auto-segmentation models using in-house data over pre-trained vendor solutions

Phillip Chlap[1,2,3,*], Shrikant Deshpande[1,3], Daniel Al Mouiee[1,2,3], Robert Finnegan[2,4,5], Lois Holloway[1,2,3]

[1]South West Sydney Clinical Campuses, University of New South Wales, Liverpool, Australia, [2]Ingham Institute for Applied Medical Research, Liverpool, Australia, [3]Liverpool & Macarthur Cancer Therapy Centres, Liverpool, Australia, [4]The University of Sydney, Sydney, Australia, [5]Royal North Shore Hospital, Sydney, Australia

Introduction As utilisation of auto-segmentation becomes routine in clinical practice, many vendors are providing auto-segmentation solutions. Vendor deep-learning (DL) models are often trained using an external dataset while atlas-based models are usually built with in-house data. To assess the benefit of using in-house data, we trained our own DL models with the open-source nnUNet framework [1].

Method The nnUNet was trained with a Head & Neck (HN) dataset consisting of 28 cases to auto-segment 15 organs at risk using radiotherapy CT images. A 2D nnUNet model was trained which operates on each axial slice. In addition, a full- and low-resolution 3D nnUNet model was trained, where low first scales down the image. The composite output (ensemble) of these models provides a fourth model. Two vendor systems for HN auto-segmentation were also assessed with Vendor A providing an atlas- and DL-based auto-segmentation method and Vendor B an atlas-based method. Not all 15 structures were available on each vendor model. Inference was performed using all models on a separate validation set of 12 cases with the Dice Similarity Coefficient computed to compare the auto-segmented contour to the corresponding manual contour.

Results Best performing models differed for each structure (Table 1). The nnUNet models outperformed vendor solutions for 5 structures, although there was no clear best performing model. Vendor A's DL model achieved the highest DSC for 4 structures. While Vendor B's atlas appears to have performed better overall than other models (highest DSC for 7 structures), a significant bias exists since the manual contours being compared against were initially derived using that model.

Conclusion The nnUNet tool trained using a limited dataset can produce auto-segmentation models comparable to those supplied by radiotherapy software vendors. By increasing the size of the in-house dataset, it is expected that the nnUNet model can be improved.

References

1. F. Isensee, P. F. Jaeger, S. A. A. Kohl, J. Petersen, and K. H. Maier-Hein, "nnU-Net: a self-configuring method for deep learning-based biomedical image segmentation," *Nat. Methods*, vol. 18, no. 2, pp. 203–211, 2021, https://doi.org/10.1038/s41592-020-01008-z.

Table 1. Statistics (mean ± SD) of the DSC computed comparing each of the auto-segmentation models assessed against the manual contour in the validation set. Best performing model for each structure are indicated in bold.

Structure	In-house models (nnUNet)				Vendor A		Vendor B
	2D	3D Low	3D Full	Ensemble	Atlas	DL	Atlas
Brainstem	0.88 ± 0.04	**0.91 ± 0.03**	0.90 ± 0.03	**0.91 ± 0.03**	0.86 ± 0.05	0.83 ± 0.04	0.89 ± 0.07
Chiasm	0.00 ± 0.00	**0.56 ± 0.11**	**0.56 ± 0.16**	0.50 ± 0.13	0.37 ± 0.22	NA	0.28 ± 0.12
Larynx	0.79 ± 0.25	**0.86 ± 0.11**	0.81 ± 0.17	0.83 ± 0.18	0.79 ± 0.05	0.21 ± 0.07	0.70 ± 0.13
Lens (L)	0.00 ± 0.00	0.44 ± 0.34	0.18 ± 0.26	0.02 ± 0.07	0.39 ± 0.21	**0.69 ± 0.24**	0.43 ± 0.36
Lens (R)	0.00 ± 0.00	0.41 ± 0.32	0.20 ± 0.22	0.01 ± 0.03	0.49 ± 0.16	**0.72 ± 0.13**	0.45 ± 0.17
Mandible	0.94 ± 0.01	0.94 ± 0.01	0.94 ± 0.01	0.95 ± 0.01	0.93 ± 0.01	0.90 ± 0.03	**0.96 ± 0.03**
Optic nerve (L)	0.53 ± 0.27	0.48 ± 0.31	0.33 ± 0.36	0.50 ± 0.32	0.62 ± 0.10	0.59 ± 0.19	**0.72 ± 0.12**
Optic nerve (R)	0.42 ± 0.33	0.51 ± 0.31	0.32 ± 0.35	0.49 ± 0.31	0.63 ± 0.12	0.56 ± 0.10	**0.80 ± 0.08**
Oral Cavity	0.89 ± 0.02	0.90 ± 0.03	0.89 ± 0.04	**0.91 ± 0.02**	0.80 ± 0.06	0.72 ± 0.07	0.70 ± 0.10
Parotid (L)	0.74 ± 0.13	0.62 ± 0.35	0.25 ± 0.37	0.51 ± 0.39	0.78 ± 0.06	**0.79 ± 0.09**	0.78 ± 0.12
Parotid (R)	0.78 ± 0.11	0.53 ± 0.38	0.14 ± 0.33	0.46 ± 0.43	0.74 ± 0.11	**0.80 ± 0.11**	0.78 ± 0.13
Retina (L)	0.65 ± 0.12	0.51 ± 0.33	0.30 ± 0.34	0.48 ± 0.31	0.54 ± 0.12	NA	**0.77 ± 0.18**
Retina (R)	0.63 ± 0.12	0.48 ± 0.31	0.29 ± 0.33	0.47 ± 0.31	0.54 ± 0.14	NA	**0.73 ± 0.16**
Spinal Cord	0.82 ± 0.05	0.81 ± 0.05	0.82 ± 0.06	0.82 ± 0.05	0.78 ± 0.08	0.75 ± 0.09	**0.91 ± 0.18**
Trachea	0.85 ± 0.07	**0.87 ± 0.04**	0.86 ± 0.08	0.86 ± 0.07	0.83 ± 0.09	NA	**0.87 ± 0.10**

O46. [Invited] Overview of Geant4 for medical physics applications: Latest developments and future perspectives

Susanna Guatelli[1,*]

[1]University of Wollongong, Wollongong, Australia

Geant4, which is a Monte Carlo toolkit describing particle transport and interactions in matter, is widely used in medical physics in critical applications such as verification of radiotherapy treatment planning systems, and the design of equipment for radiotherapy and nuclear medicine. It is also used in medical imaging for dosimetry, to improve detectors and reconstruction algorithms, and for radiation protection assessments. In this talk, the speaker will provide an overview of the capability of Geant4 for medical physics applications, especially for medical imaging, detector development and radiation protection. The speaker will then provide information on how to start to use Geant4 for medical applications.

O47. Simulation study of over-the-barrier tertiary scatter of diagnostic x-rays

Mitchell Herrick[1,2,*], **Daniel Badger**[1], **Jake Forster**[1,2], **Kevin Hickson**[1,3]

[1]Medical Physics and Radiation Safety, SA Medical Imaging, Adelaide, Australia, [2]Department of Physics, The University of Adelaide, Adelaide, Australia, [3]Allied Health and Human Performance, University of South Australia, Adelaide, Australia

Introduction Radiation scattering over the primary barrier (tertiary scatter) can be significant when designing radiation shielding, particularly for high workload CT scanners. The model obtained using semi-empirical simulation by Martin and Sutton [1] is the current standard when estimating tertiary scatter. As the first step in expanding their work, a Monte Carlo simulation has been used to recreate their results.

Method Using the GEANT4 toolkit, a simulation was constructed to model and calculate tertiary scatter using the setup of Martin and Sutton. A 6 × 4x14 m 'room' consisting of a concrete ceiling and floor, and containing an impenetrable barrier, was simulated. An isotropic 85 kV X-ray scatter source was placed 3 m from the barrier. Two sensitive volumes (air, 10 cm diameter spheres) were created, one placed 2 m from the barrier on the source side, the other 1.5 m from the barrier on the other side. The energy, location and direction of all photons entering the spheres were recorded, and air kerma was calculated for each. The ratio of tertiary to direct scatter was plotted against varying barrier heights and compared to predictions using the semi-empirical model.

Results There is good agreement between predicted and simulated air kerma ratios when barriers are taller than 3 m. Below 3 m, there is a large difference in air kerma ratios. Martin and Sutton employed a simplifying assumption, ignoring scatter from part of the ceiling on the source side of the barrier, probably due to computational limitations. After removing contributions from the same part of the ceiling, excellent agreement is observed across all barrier heights.

Conclusion A Monte Carlo simulation has independently verified the semi-empirical model under the assumptions used by Martin and Sutton. The results obtained in this work highlight the need for further investigation outside those assumptions.

References

1. Martin CJ, Sutton DG, Magee J, McVey S, Williams JR, Peet D. Derivation of factors for estimating the scatter of diagnostic x-rays from walls and ceiling slabs. J Radiol Prot. 2012 Dec;32(4):373–96. https://doi.org/10.1088/0952-4746/32/4/373. Epub 2012 Sep 24. PMID: 23,006,642.

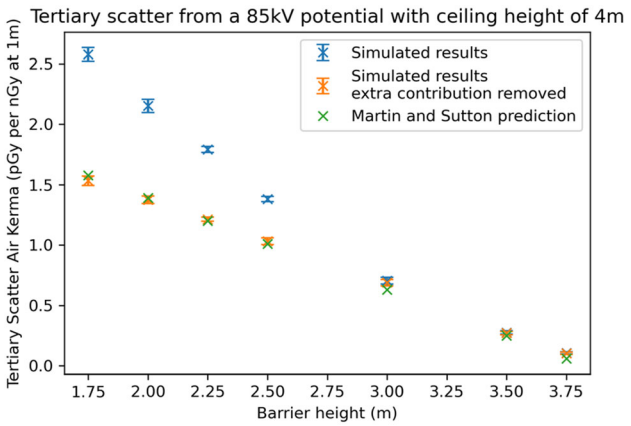

Fig. 1. Tertiary scatter air kerma calculations for various barrier heights using Martin and Suttons model (green), simulated results (blue) and simulation results removing contributions not considered by Martin and Sutton (orange).

O48. A method to estimate the effective dose to a bystander from a Nuclear Medicine patient using Monte Carlo simulation

Nelka Samaranayake[1], Erin Mckay[2,*]

[1]Prince of Wales Hospital, Randwick, Australia, [2]St George Hospital, Kogarah, Australia

Introduction The radiation dose from nuclear medicine patients is a safety concern for other health professionals. This work develops a method to estimate the dose to a bystander using the GATE Monte Carlo code and software phantoms representing the source and nearby targets.

Method A simulation was configured to estimate the dose to a target voxel phantom arising from an arbitrary distribution of radionuclide in a source voxel phantom. This was then validated for a realistic distribution of 18-F-FDG in a voxelised version of the Cristy & Eckerman adult voxel phantom. First, a single 2 mm voxel source of 18-F-FDG irradiating a 30 mm diameter sphere of ICRU tissue-equivalent material was simulated. The H*(10) operational dose quantity [1] was calculated from the simulation and compared to laboratory measurements. Next, a distributed source of 18-F-FDG in a Phillips ingenuity cylindrical PET SUV phantom of 9293 ml volume was simulated and the results were compared to laboratory measurements. Finally, dose rates near 18-F-FDG patients were measured. A voxelised Cristy & Eckerman adult phantom was used to represent the patient geometry. The activity distribution for the simulation was calculated using a biokinetic model for FDG from the ICRP [2].

Results Simulated H*(10) doses were found to be within 5% of point source measurements and 6% of distributed source measurements. The average discrepancy for patient measurements was 9% with a maximum of 37%.

Conclusion The GATE simulation successfully predicts H*(10) from a point source, a distributed source and from FDG patients, albeit with less accuracy. Similar simulations using an anthropomorphic phantom as a target should be useful to estimate effective dose for a variety of exposure situations.

Acknowledgement

We would like to thank Thomas Hennessy, Medical Physics specialist at nuclear medicine department of Prince of Wales Hospital and Nuclear Medicine technologists at St George Hospital for their valuable assistance to complete this work.

References

1. ICRP, 2007. Recommendations of the International Commission on Radiological Protection. ICRP Publication 103.
2. ICRP, 2015. Radiation Dose to Patients from Radiopharmaceuticals: A Compendium of Current Information Related to Frequently Used Substances. ICRP Publication 128. Ann. ICRP 44(2S).

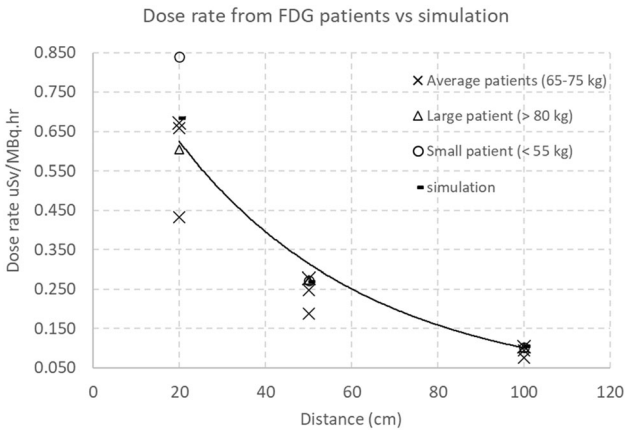

Fig. 1. Comparison of simulation vs measurement for H*(10) dose from 18-F-FDG patients at distance.

O49. Evaluation of the effectiveness of lead for shielding photoneutrons produced in medical linear accelerators: A Monte Carlo particle transport study

Christopher Colyer[1,*], Leyla Moghaddasi[2]

[1]Genesiscare, Kurralta Park, Australia, [2]The University of Adelaide, Adelaide, Australia

Introduction There is little information on the effectiveness of lead for shielding neutrons for radiotherapy rooms as neutrons historically were considered for photon energies greater than 10 MV; the use of high atomic number materials in this energy range is discouraged as photoneutron and neutron capture gamma ray production becomes significant but this may be too conservative [1]. Where the use of lead is necessary, a significant reduction in overall neutron dose is possible. This study aims to determine the TVLn for lead.

Method Monte Carlo (Geant4) was used to simulate the transport of photoneutrons through primary barriers containing layers of lead. The photoneutron spectrum generated in high-energy (18 MV) modern accelerator head components was simulated and projected to barriers of different thicknesses of lead including a control case of zero thickness. The contribution of photoneutron production within the barrier was explicitly included. To derive the TVL, absorbed dose was evaluated at 1 cm depth in a water phantom outside the barrier. The fluence and energy spectrum of neutron leakage outside the barrier was also calculated.

Results The first and second TVLs for the lead as a neutron shielding material were determined to be 11.5 cm and 20.4 cm respectively. The contribution of neutron dose produced by photoneutrons generated within the barrier was up to 3 orders of magnitude smaller than in the linac head. The lateral distribution of neutrons outside of the lead

barriers is shown to narrow with increasing thickness and the energy spectrum showed lead predominantly absorbs the fast neutron component, resulting in the production of thermal and epithermal neutrons, whose numbers increase with lead thickness up to approximately 25 cm.

Conclusion This paper demonstrates the inadequacy of simple empirical models, and we would advocate using the reported TVLs for linear accelerator bunker design where the maximum photon energy is 18 MV.

References

1. Rezende, G. F., Da Rosa, L. A., Facure, A. (2014). Production of neutrons in laminated barriers of radiotherapy rooms: comparison between the analytical methodology and Monte Carlo simulations. *J. Appl. Clin. Medical Phys. 15*(6), 5035. https://doi.org/10.1120/jacmp.v15i6.5035

O50. The energy independence of a cerium-doped silica scintillator

Joshua Southwell[1,*], Alexandre Santos[1,4], Ruth Shaw[1,2], Chris Kalnins[1,2], Nigel Spooner[1,2,3]

[1]School of Physical Sciences, The University of Adelaide, Adelaide, Australia, [2]Institute for Photonics and Advanced Sensing, The University of Adelaide, Adelaide, Australia, [3]Defence Science and Technology Group, Edinburgh, Australia, [4]The Australian Bragg Centre for Proton Therapy and Research, Adelaide, Australia

Introduction Rare earth-doped silica is a potential material for fibre-coupled luminescence dosimetry, possessing many desirable characteristics such as scintillation efficiency, mechanical strength, thermal resistance and radiation hardness [1–4]. The energy dependency over the superficial x-ray range of four Cerium-doped silica scintillators, fabricated through the novel reactive powder sintering of silica method (REPUSIL) is investigated before discussing the optimisation of Cerium concentration for improved energy independence over this range.

Method The REPUSIL scintillators were coupled to an optical fibre and irradiated for 20 s using a Gulmay D3150 superficial/orthovoltage X-ray unit with tube voltages between 30 and 150 kVp to obtain the overall energy dependence. The absorbed-dose energy dependence was then investigated via Monte-Carlo simulations with GEANT4 GATE before drawing conclusions on the intrinsic energy dependence. Finally, the Cerium concentration in the Monte-Carlo simulations was varied to investigate the detectors improved independence with varying levels of concentration.

Results While the lower Cerium concentrations showed significant energy dependence, the highest concentration was within 3% of the reference beam energy between 20 and 55 keV effective energies. This was supported by the absorbed dose and intrinsic energy dependencies which also exhibited constant energy dependence over this energy range. Additionally, the Monte-Carlo simulations of various Cerium concentrations suggest that it is possible to optimise the concentration and improve the absorbed-dose energy independence but the effect this will have on the overall energy dependence is unclear.

Conclusion The energy dependency of four Cerium doped scintillator was successfully investigated and at the highest concentration, was found to be largely independent on energy over the superficial X-ray range. Optimisation of the scintillator concentration also suggests that it is possible to improve this energy independence, but further research is needed to verify this behaviour.

References

1. Antunes P, Domingues F, Granada M, Andr P. Mechanical Properties of Optical Fibers. Selected Topics on Optical Fiber Technology. InTech; 2012.
2. Knight JC. Photonic crystal fibres. Nature. 2003;424(6950):847–51. https://doi.org/10.1038/nature01940.
3. Nguyen LV, Warren-Smith SC, Ebendorff-Heidepriem H, Monro TM. Interferometric high temperature sensor using suspended-core optical fibers. Opt Express. 2016;24(8):8967–77. https://doi.org/10.1364/Oe.24.008967.
4. Akchurin N, Kendir E, Yaltkaya S, Damgov J, De Guio F, Kunori S. Radiation-hardness studies with cerium-doped fused-silica fibers. J Instrum. 2019;14. doi: Artn P03020 https://doi.org/10.1088/1748–0221/14/03/P03020.

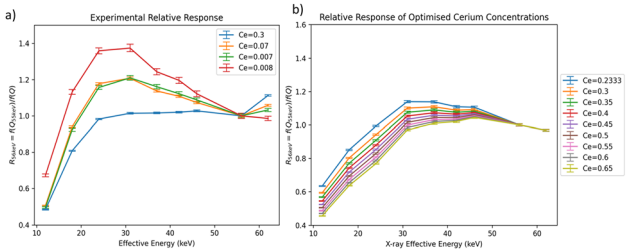

Fig. 6. a) Illustrates the experimental response of the four Cerium-doped silica fibres of the superficial X-ray range. b) Shows Monte-Carlo simulations of increasing Ce_2O_3 concentrations and the increasingly constant absorbed dose energy dependency.

O51. [Invited] Medical physics: How we can lead the way for EDI in STEM

Julianne Pollard-Larkin[1,*]

[1]University of Texas, MD Anderson Cancer Center, Houston, United States of America

Notably, Medical Physics has made great strides in increasing gender parity at the graduate school level when compared to Pure Physics programs and other STEM (science, technology, engineering and math) fields with nearly 42% of Medical PhD students classifying as women in 2017. However, the statistics on Medical Physics' other indicators (ie. Racial, ethnic, cultural, religious, etc.) of diversity are scant and leave room for improvement. This talk will help to explain the steps we should take to make Medical Physics a STEM leader for equity, diversity and inclusion in STEM and medicine.

O52. [Invited] Radiation oncology service delivery in the NT—success, failures, challenges and opportunities; special focus on Aboriginal cancer care in the NT

Julia Green[1,*]

[1]Alan Walker Cancer Care Centre, Darwin, Australia

O53. [Invited] Advanced particle accelerator technologies for radiotherapy and particle therapy

Suzie Sheehy[1,*]

[1]University of Melbourne, Parkville, Australia

In this talk I will give an update on current and emerging accelerator technologies for radiotherapy and particle therapy, in the context of new and emerging treatment modalities and trends. I will highlight the growing activity in this area in Australia, particularly at the University of Melbourne. Technologies to be discussed include: synchrotrons and linear accelerators for particle therapy, including considerations for compact superconducting synchrotrons and novel beam delivery systems. I will also discuss progress toward accelerators to deliver > 100 MeV electrons for 'Very High Energy Electron' therapy, conceptually based on compact 'X-band' high gradient accelerating technology. Finally, I will discuss the 'robustness frontier' of radiotherapy accelerators, including considerations related to equitable access to cancer treatment in Low and Middle-Income countries.

O54. A new dynamic collimator design: Delivering conformal radiotherapy fields with synchrotron radiation

Micah Barnes[1,2,3,*], Nader Afshar[3], Jonathan McKinlay[3], Callan Morey[3], Daniel Hausermann[3], Nicholas Hardcastle[1,2], Micahel Lerch[1]

[1]University of Wollongong, Wollongong, Australia, [2]Peter MacCallum Cancer Centre, Melbourne, Australia, [3]ANSTO Australian Synchrotron, Clayton, Australia

Introduction Research utilizing synchrotron radiation for radiotherapy applications is becoming increasingly complex as it pushes towards a human clinical trial [1–3]. Treatment planning and image guidance capabilities for synchrotron radiotherapy have been developed [4,5] and personalized treatments are possible [6]. However, conformal treatment fields are seldom employed as they require time-consuming fabrication of individualized masks per treatment field [7]. We present a proof-of-concept for a new dynamic collimator design aimed to solve the challenges of delivering conformal fields in synchrotron radiotherapy.

Method Our collimator consists of six linear motors and two circular collimator leaves (Fig. 1, left). Two motors are used for in-plane alignment of the system to the synchrotron beam and two motors are assigned per leaf allowing vertical and horizontal movement. The circular leaves are closed above and below the target, and as the patient is vertically scanned through the beam, they move to match the curvature of the target. A sample c-shape field was delivered to an imaging detector (CMOS detector with 28 micron pixels) to demonstrate the capabilities of the system (Fig. 1, right).

Results The c-shape produced in Fig. 1 demonstrates the system's capability to deliver a treatment field. Notably, the sharp field edges and curve-continuity are preserved on account of the curvature-matching slit design.

Conclusion We have demonstrated a proof-of-concept of this new collimator design. This design provides a way to achieve conformal treatment fields for dynamic radiotherapy treatments on synchrotron beamlines. With further work, the limitations of the system can be fully understood, and optimisation of fields given the systems capabilities will be possible.

References

1. Fernandez-Palomo, C. et al. Animal models in microbeam radiation therapy: A scoping review. Cancers (Basel). 12, 1–26 (2020).
2. Smyth, L., Donoghue, J. F., Crosbie, J., Senthi, S. & Rogers, P. Synchrotron radiotherapy: towards a human clinical trial. J. Med. Radiat. Sci. 64, 35–62 (2017).
3. Bartzsch, S. et al. Technical advances in x-ray microbeam radiation therapy. Phys. Med. Biol. 65, (2020).
4. Day, L. R. J. et al. A commercial treatment planning system with a hybrid dose calculation algorithm for synchrotron radiotherapy trials. Phys. Med. Biol. 66, 55,016 (2021).
5. Barnes, M. J. et al. SyncMRT: a solution to image-guided synchrotron radiotherapy for quality assurance and pre-clinical trials. J. Synchrotron Radiat. 29, (2022).
6. Engels, E. et al. Toward personalized synchrotron microbeam radiation therapy. Sci. Rep. 10, 1–13 (2020).
7. Barnes, M. A patient-positioning system for synchrotron microbeam radiotherapy (MRT). (RMIT University, 2018).

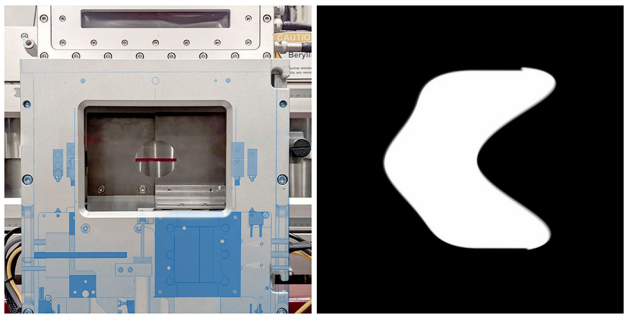

Fig. 1. (Left) the dynamic conformal slits are shown with the internal design overlayed in blue. (Right) a measured c-shape field delivered by the collimator to an imaging detector.

O55. Technology for Ultra Rapid Beam Operation (TURBO) – a new system to improve efficiency and efficacy for charged particle therapy

Jacinta Yap[1,*], Adam Steinberg[1,2,3], Hannah Norman[1,2,3], Robert Appleby[2,3], Suzie Sheehy[1,4]

[1]University of Melbourne, Melbourne, Australia, [2]University of Manchester, Manchester, United Kingdom, [3]Cockcroft Institute, Warrington, United Kingdom, [4]*ANSTO, Lucas Heights, Australia.*

Introduction Charged particle therapy (CPT) is a precise modality of radiotherapy which uses the physical advantages of hadrons for cancer treatment. The availability of CPT is growing worldwide but is still limited by high facility costs and technological challenges. These can be addressed by improvements to the beam delivery system (BDS), which determines the overall beam shaping and timing capabilities. As multiple beams are delivered and scanned across the tumour volume, the speed to change the depth of the beam: energy layer switching time (ELST) is a limiting constraint of the BDS, and a determinant of the overall treatment time. By increasing the energy acceptance of the BDS, it is possible to deliver and transport beams of varying energies [1] to minimise the dead time associated with changes to the magnetic and beamline components. A reduction in the ELST has the possibility of several benefits, improving delivery for better efficiency and effectiveness of CPT [2].

Method A proof-of-concept 'Technology for Ultra Rapid Beam Operation' (TURBO) demonstrator is currently in development for scaled-down conditions with the low energy ion Pelletron accelerator at the University of Melbourne [3]. The system will comprise several

interchangeable modules: matching, degrader, fixed field alternating gradient (FFA) arc, diagnostics, scanning and output sections. This novel prototype must be adapted firstly for the Pelletron, requiring experimental measurements with custom-built instrumentation and diagnostic components, and comprehensive design and simulation studies for full beam characterisation.

Results The TURBO project is overviewed, recent progress and measurements toward full characterisation are presented alongside simulated results. The capabilities and clinical benefits of TURBO as a fixed-beamline, fast ELST solution for CPT are discussed.

Conclusion Improvements in beam delivery technologies are necessary to provide faster, more effective, and advanced CPT treatments. TURBO explores the potential of a novel BDS with an increased energy acceptance for rapid depth scanning.

References

1. J. S.L. Yap, E. Higgins & S. L. Sheehy (2021). 'Preliminary Study of a Large Energy Acceptance FFA Beam Delivery System for Particle Therapy'. Proceedings of the 12th International Particle Accelerator Conference (IPAC'21).
2. J. Yap, A. De Franco & S. Sheehy (2021). 'Future Developments in Charged Particle Therapy: Improving Beam Delivery for Efficiency and Efficacy'. Front. Oncol., vol. 11, no. December, pp. 1–25.
3. J. S.L. Yap, A. F. Steinberg, H. X.Q. Norman, R. B. Appleby & S. L. Sheehy (2022). 'TURBO: A Novel Beam Delivery System Enabling Rapid Depth Scanning for Charged Particle Therapy'. Journal of Physics: Conference Series, 13th International Particle Accelerator Conference (in press).

O56. Commissioning of the SARRP Treatment Delivery System

Patrick Niemiec[1,3,*], Cameron Stanton[2], Kelly McKelvey[3,4], Jeremy Booth[2,3]

[1]St George Hospital, Sydney, Australia, [2]Northern Sydney Cancer Centre, Royal North Shore Hospital, Sydney, Australia, [3]University of Sydney, Sydney, Australia, [4]The Kolling Institute, Sydney, Australia

Introduction Preclinical radiotherapy systems are designed to mimic clinical radiotherapy machines. Featuring scaled down beam energies, sizes and geometries they facilitate preclinical radiotherapy studies on small animals like mice. However, scaling down the beam energy/geometry without degrading treatment dose accuracy is challenging, so the system must be validated to ensure efficacy of outcomes of preclinical animal radiobiological studies [1]. This work describes validation of the treatment planning system (TPS), MuriPlan® of the Small Animal Radiation Research Platform (SARRP, Xstrahl Inc.).

Method Commissioning of the SARRP followed ESTRO ACROP best practice [2]. Geometric tests included pinhole, Winston-Lutz and central-axis cone alignment, to validate mechanical stability of the system. Absolute dosimetry of the 220kVp beam (0.67 mm Cu) was performed under AAPM TG-61 guidelines to verify beam output calibration. Relative dosimetry was performed in water equivalent slab phantoms of similar thickness to a mouse (20 mm) and rat (55 mm) measured with Gafchromic EBT3 film, to validate the treatment delivery as calculated by the superposition-convolution algorithm in MuriPlan (using reference cone beam CT scans of each phantom). End-to-end testing was performed using 60° arc beams and film inserted into a mouse shaped plastic water phantom.

Results Beam profiles, PDDs and output factors were within 5% of MuriPlan for the smaller collimators (3×3, 3×9, 5×5, 10×10), but differences up to 10% were seen for the larger collimators. Mechanical alignments were within 0.3 mm.

Conclusion The Muriplan TPS was validated within 5% accuracy for the small collimators, degrading to $> 10\%$ for the large collimators, where an updated dose-conversion factor from the vendor is recommended. This work gives confidence that SARRP treatment delivery is within 10%, and suitable for preclinical investigations.

References

1. Lindsay, P. E., Granton, P. V., Gasparini, A., Jelveh, S., Clarkson, R., van Hoof, S., Hermans, J., Kaas, J., Wittkamper, F., Sonke, J. J., Verhaegen, F., & Jaffray, D. A. (2014). Multi-institutional dosimetric and geometric commissioning of image-guided small animal irradiators. Med Phys, 41(3), 031,714. https://doi.org/10.1118/1.4866215
2. Verhaegen, F., Dubois, L., Gianolini, S., Hill, M. A., Karger, C. P., Lauber, K., Prise, K. M., Sarrut, D., Thorwarth, D., Vanhove, C., Vojnovic, B., Weersink, R., Wilkens, J. J., & Georg, D. (2018). ESTRO ACROP: Technology for precision small animal radiotherapy research: Optimal use and challenges. Radiother Oncol., 126(3), 471–478. https://doi.org/10.1016/j.radonc.2017.11.016.

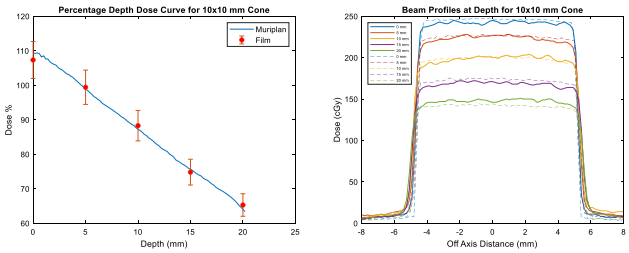

Fig. 7. PDD and beam profile for the 10×10 collimator in the water-equivalent mouse phantom (8% measurement error bars, MuriPlan dashed, film solid).

O57. Introducing the IAEA regional project RAS6101 "Improving the quality and safety of radiation medicine through medical physicist education and training"

Brendan Healy[1,*], Robin Hill[2,3,4]

[1]ACDS, Melbourne, Australia, [2]Department of Radiation Oncology, Chris O'Brien Lifehouse, Sydney, Australia, [3]Biomedical Innovation Hub, Chris O'Brien Lifehouse, Sydney, Australia, [4]Institute of Medical Physics, School of Physics, University of Sydney, Sydney, Australia

Introduction The project designated RAS6101 is a four-year regional initiative beginning in 2022 under the IAEA Regional Cooperative agreement (RCA) which takes in a range of countries in Asia and the Pacific (www.rcaro.org/states1) including Australia and New Zealand.

Method The project RAS6101 was devised and formed by regional medical physics leads including China as lead country coordinator, with input from various RCA Government Parties as well as IAEA technical officers. The project builds on previous regional RCA projects supporting the education and training of medical physicists in radiation medicine.

Results Project activities in 2022 have included an initial coordination meeting in April 2022 at which a workplan for the project was finalized. Also, a virtual regional training course on quality management and quality assurance in radiotherapy is planned for September 2022 with some lecturing support from ACDS, and participants from Australia joining the virtual training course. Future regional activities up to 2025 include training courses and workshops on quality management in nuclear medicine and radiology, and workshops on medical physics education and training including issues such as academic guidelines, training for clinical trainers, and certification practices.
Conclusion RAS6101 provides an opportunity to support the development of medical physics practice in radiation medicine in the Asia Pacific region. Professional issues in medical physics including quality management and clinical training will be emphasised in a regional approach.

O58. A report on virtual medical physics training within the IAEA RAS6096 project

Robin Hill[1,2,*], David Little[3], Elrick Inocencio[4], Muhammad Shahban[5], Athula Kumara[6], Iain Ward[3]

[1]Radiation Oncology, Chris O'Brien Lifehouse, Camperdown, Australia, [2]Biomedical Innovation, Chris O'Brien Lifehouse, Camperdown, 2050, [3]Department of Radiation Oncology, Christchurch Hospital, Christchurch, New Zealand, [4]University of the Philippines- Philippine General Hospital, Manila, Philippines, [5]AECH NORI Radiation Oncology, Islamabad, Pakistan, [6]National Cancer Hospital, Maharagama, Sri Lanka

Introduction The IAEA/RCA RAS6096 regional project was established with the aim of "Empowering Regional Collaboration among Radiotherapy Professionals through Online Clinical Networks". The first phase setup monthly virtual tumour board program to establish peer review of radiotherapy patient plans within Asia and the Pacific. The next phase, starting in September 2021, involved the development of virtual reviews and training for medical physics and radiation therapist professionals.
Methods The medical physics network was established by a combined meeting of the assigned physics leads within each of the representative countries. The decision of the team was to establish virtual training focussed on clinical aspects of radiation oncology medical physics and to build peer support across different centres. The virtual training occurs each month using the Microsoft Teams platform with one or two topics discussed in the one hour session. The lead physicist from each country is given responsibility for sharing meeting information to their colleagues via their established professional networks.
Results The topics presented in discussions to date have been on radiation shielding issues, beam matching results in commissioning a group of linear accelerators, independent brachytherapy audits, commissioning the Cyberknife system and a review of published IROC dosimetry data for use in quality assurance. The number of attendees for each session varies and estimated to be up to 40 people in some sessions. There is a broad range of experience for those attending including a number of medical physics students. Future activities will make use of the ProKnow software which has been purchased for use within the RAS6096 project.
Conclusions The RAS6096 has shown to be a useful virtual training program for medical physicists across the Asia Pacific region with collaborations being developed. Future training will continue to be focussed on clinical training needs across the region.

O59. Remote clinical training of PNG ROMP registrars

Emma Spelleken[1], Aitang Xing[2,3,4], Simon Downes[5]

[1]Kathleen Kilgour Centre, Tauranga, New Zealand, [2]Liverpool and Macarthur Cancer Therapy Centres, Sydney, Australia, [3]Ingham Institute for Applied Medical Research, Liverpool, Australia, [4]South Western Sydney Clinical School, Univeristy of NSW, Liverpool, Australia, [5]Nelune Comprehensive Cancer Centre, Prince of Wales Hospital, Randwick, Australia

Introduction In 2021, the Better Healthcare Technology Foundation received a Varian Global Education Grant for providing remote clinical training of three physicists for the new cancer centre being built at the Port Moresby General Hospital (PMGH) in Papua New Guinea. This training, recognized by the ACPSEM, will provide them with possible future placement on the ACPSEM Register and recognition as qualified Medical Physicists in PNG. The aim of this presentation is to report the current status of this project.
Method The training program (TEAP) of the ACPSEM has been used since 2004 for ROMP ceritification. The online COMET system allows access for internal and external assessment of training according to the Clinic Training Guide (CTG) syllabus. It was proposed COMET could be used via Zoom meetings to provide this remote clinical training. Two ACPSEM qualified medical physicists were recruited as remote supervisors for an initial two year period. Sessions are held weekly to provide CTG tutorials to the registrars and assess work. The CTG competencies are currently based on past practical experience (post graduate course work) and topics which could easily be covered via remote sessions. Further training opportunites will be to visit Australia/New Zealand clinicals to use equipment they will soon have at PMGH.
Results Challenges in this training are: (1) knowledge between registrars varies and it is difficult to cater to the different levels during a session. (2) The cancer centre is still under construction so training on treatment and physics equipment is limited and there's no other radiotherapy centre with functioning equipment in PNG. (3) Internet connection speed and availability.
Conclusion Clinical training is being successfully provided to the PNG registrars using the CTG syllabus via COMET. Training progress will quicken once they gain access to treatment and physics equipment within the next year.

O60. Applying adult learning theory to medical physics education

Emma Dyce[1,2,*]

[1]Genesiscare Victoria, East Albury, Australia, [2]Murdoch University, Perth, Australia

Introduction GenesisCare has a national physics training program for ROMP registrars involving weekly education sessions such as lectures, tutorials, and exam preparation sessions. Recently this program has expanded to include scientific officers and non-ACPSEM certified ROMPs intending to sit the Safe to Practice exam.
Method The author is undertaking a post graduate course in adult and tertiary education, and adult learning theory and teaching methods were applied to the online education of a group of medical physicists. The national education program was re-evaluated in the context of adult learning characteristics and addressing the needs and expectations of the learners. Key concepts such as creating a collaborative and informal learning environment, flexibility of attendance, problem-based learning scenarios and neuroscience of learning were examined. Current facilitation techniques such as lectures were

adapted to follow recommendations of education experts. For example, dividing content into 10–15 min blocks, providing ample discussion opportunities and multi-sensory stimulation as recommended by Bowman [1]. New learning practices were also implemented such as jigsaw learning exercises which required each learner to research a designated component, and presentations from each learner in the group built the complete picture.
Results Feedback was sought from learners after each new exercise and reflections were discussed by training coordinators. Responses received from learners were overwhelmingly positive and enthusiastic to continue with these new learning techniques. Reflection found the exercises and adaptions generated increased collaboration and responses rates, however time management was to be further refined. Comments from the post-graduate course convenor were also overwhelmingly positive and the author was encouraged to communicate *why* the changes were being implemented.
Conclusion Adult learning theory and new education practices have been implemented in the GenesisCare national training program with excellent feedback. Additional work is required to further develop the program and assess participation feedback and performance.
References

1. Bowman, S (2009). Training from the back of room! 65 ways to step aside and let them learn. Pfeiffer

O61. The impact of implementing Learning In Radiation ONcology (LIRON): In house electronic incident learning

Laura Adamson[1,2,*], Krystle Crouch[1], Rachael Beldham-Collins[1], Jonathan Sykes[1,2], David Thwaites[2]

[1]Crown Princess Mary Cancer Centre, Westmead, Australia, [2]School of Physics, University of Sydney, Camperdown, Australia

Introduction Robust incident learning systems (ILS) include a coordinated approach to reporting, analysis, data visualisation, feedback, and learning. ISLs with low-level reporting extends an ILSs capacity to identify quality improvement (QI) areas and strengthen quality assurance (QA) pathways. A QI project to develop an in-house radiation oncology (RO) ILS was undertaken, with success demonstrated in the first 12 months.
Method A needs assessment was performed in 2019, including a staff survey on knowledge and understanding of current incident reporting methods, ILS and the safety culture climate. A QI team designed and implemented an electronic reporting system called LIRON in the Varian Aria™ oncology information system to suit departmental needs and tested its impact at 12 months via a follow-up survey and audits.
Results Barriers to existing paper-based reporting system were perceived by 67% of respondents and most staff (75%) wanted an electronic RO-specific system. LIRON supports actual incident and lower-level reporting to increase capacity for learning and QA/QI guidance. LIRON works in parallel with the state-wide system to ensure clinical governance of higher-level reports. There is a dedicated triage team, ensuring accurate data capture and rapid coordination of further analysis/escalation when required. Increased data accuracy has been demonstrated in LIRON, with easy access for all staff to see reports. Monthly meetings to discuss learning opportunities and potential QI are open to all, rather than the previous separate cohort and senior staff meetings. Follow-up survey results showed: reduction in barriers to reporting (from 67 to 57%); increased participation (48% to 70% of staff reporting); increased perception of a no-blame culture (49% to 58%); and a large increased ability to learn from reported incidents (49% to 86%).
Conclusion LIRON addressed issues with the previous system and overall had a positive impact which adapted rapidly when COVID-19 impacted standard hospital workflow. The move to electronic an ILS has enabled easy access to data that highlight weaknesses in processes and protocols and has supported continuing QI initiatives.

O62. Radiation safety education and training in medical and allied disciplines

Madison Yeoh[1,*], William Rae[1,2]

[1]The University of Sydney, Camperdown, Australia, [2]Prince of Wales Hospital, Randwick, Australia

Introduction Current widespread adoption of ionising radiation applications has propelled x-ray imaging to the forefront of medical diagnosis. Annually, vast numbers of medical images are acquired worldwide, thus radiation safety measures must align with increased exposure risks to patients as well as staff from all involved professional craft groups.
Method Publicly available scientific articles, websites and literature were reviewed to determine what radiation safety training exists within Australian diagnostic imaging departments locally and nationally. Legislative frameworks and licensing requirements were also considered. Radiation safety education of relevant craft groups was assessed in light of guidelines from Australian Radiation Protection and Nuclear Safety Agency (ARPANSA) and gazetted legislation [1]. This education was evaluated against the content and quality of current training as implemented within some hospitals.
Results A lack of standardisation of training and knowledge was found in several craft groups, including limited training within nursing and administrative worker groups. In accordance with regulations, radiation safety training and protection must be strengthened in non-radiation worker occupations, such as amongst nurses. This has been shown to be effective amongst doctors [2]. Members of the public should be provided with adequate accessible information to allay unfounded fears based on misinformation.
Conclusion Ensuring consistent, good quality, radiation safety training as part of the curricula of all craft groups involved in x-ray imaging would be useful to bring about a safer working environment. Maybe this should be a registration requirement for relevant craft groups [3].
References

1. ARPANSA (2019) Radiation Protection Series C-5, Code for Radiation Protection in Medical Exposure. https://www.arpansa.gov.au/sites/default/files/medical-exposure-code-rps-c-5.pdf
2. Hankin RA, Jones, SP (2020) The impact of educational interventions on clinicians' knowledge of radiation protection; An integrative review. https://doi.org/10.1016/j.radi.2020.01.008
3. Ng KH, Brady, Z, Ng, AH, Soh, HS, Chou, YH, Varma, D (2021) The status of radiation protection in medicine in the Asia–Pacific region. J Med Imaging Radiat Oncol, 65(4)464–470. https://doi.org/10.1111/1754-9485.13165

O63. [Invited] Next generation treatment planning and delivery techniques in proton beam therapy

Scott Penfold[1,*]

[1]Australian Bragg Centre for Proton Therapy and Research, Adelaide, Australia

The transition from passive scattering to intensity modulated pencil beam scanning delivery systems has resulted in a major shift in proton therapy clinical practice akin to the transition from 3DCRT to IMRT in x-ray therapy. While x-ray therapy technology has continued to advance from IMRT, the equivalent evolution in proton beam therapy is only now appearing on the horizon. An overview of the next major developments in proton beam therapy treatment planning and delivery will be provided in this presentation. With the first Australian proton therapy centres under construction, it is an exciting time to embrace these soon-to-be-available technological advances.

O64. Update on the Australian Bragg Centre for Proton Therapy and Research

Scott Penfold[1,*]

[1]Australian Bragg Centre for Proton Therapy And Research, Adelaide, Australia

Introduction The Australian Bragg Centre for Proton Therapy and Research is currently under construction and is set to be Australia's first particle therapy centre. This presentation will provide an overview of the status of the project and summarize the project timeline through to first patient treatment.
Method The following key workstreams relevant to medical physicists will be discussed: building design and construction, EPA radiation facility licensing, SA Health private health facility licensing, establishing a national referral network including comparative planning, proton therapy MBS item numbers, medical physics staff training and credentialling, proton therapy equipment project management, and commissioning and clinical ramp-up.
Results A summary of the status of each of the above workstreams and future work to be conducted will be presented.
Conclusion Significant progress has been made with each of the workstreams listed above. Medical physicists across Australia will have the opportunity to play a role in particle therapy through the national referral network.

O65. Relevance of linear energy transfer spectra in models of biological effect for clinical proton beam therapy

Edward Smith[1,2,*], Dr Tracy Underwood[1,3], Dr Adam Aitkenhead[1,2], Dr Carla Winterhalter[1,3], Dr Jenny Richardson[1,2], Dr Michael Merchant[1,3], Prof. Norman Kirkby[1,3], Prof. Karen Kirkby[1,3], Prof. Ranald Mackay[1,2]

[1]Division of Cancer Sciences, School of Medical Sciences, Faculty of Biology, Medicine and Health, The University of Manchester, Manchester, United Kingdom, [2]Christie Medical Physics and Engineering, The Christie NHS Foundation Trust, Manchester, United Kingdom, [3]The Christie NHS Foundation Trust, Manchester Academic Health Science Centre, Manchester, United Kingdom

Introduction Variable Relative Biological Effectiveness (RBE) in Proton Beam Therapy (PBT) has received significant research, but is still not applied in routine clinical practice. Various issues need to be considered including a full understanding of RBE parameters such as Linear Energy Transfer (LET). We investigate averaged LET (dose-averaged LET (LET_d) and track-averaged LET (LET_t) and LET spectra present in both typical radiobiological experiments and patient plans.
Method MC simulations (GATE/GEANT4) were used to calculate LET_d, LET_t and LET spectra for a range of geometries relevant to radiobiological experiments and a clinical nasopharynx PBT plan.
Results When comparing across all geometries, voxels with similar LET_d or LET_t values were observed to have substantially different underlying spectra. This was particularly clear when comparing the LET spectra between the patient case, the pristine Bragg peak and the simple SOBP scenarios. Clear bi-modal distributions and greater LET spreads (within clinically relevant dose levels) were seen in the patient case, despite averaged LET values being similar for both the patient and simple cases.
Conclusion These results demonstrate that irregular LET distributions found in patient treatment plans can be masked by simple LET averaging. Usually, only simple geometries and averaged values of LET are considered in radiobiological irradiations. The authors suggest that the biological impact (or otherwise) of proton LET spectra should be further considered in radiobiological experiments.

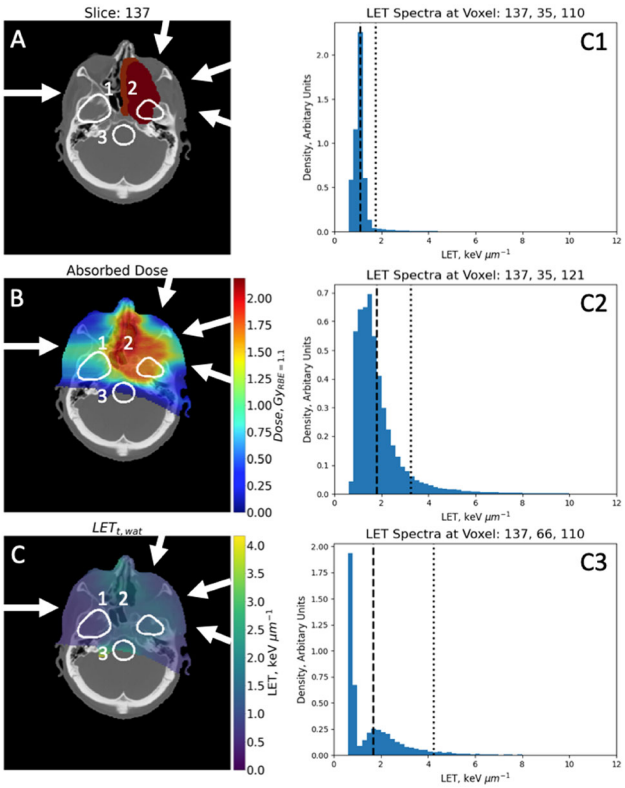

Fig. 1. Clinical proton beam therapy plan for a nasopharynx patient. (A) Contours. (B) Absorbed dose. (C) Track-averaged LET (LET_t). (C1-C3) LET spectra for selected voxels in (C). (A): High dose and low dose target volumes are shown in dark and light red, respectively. The brainstem and temporal lobe contours are outlined in white. (A), (B), (C): Field directions are shown by white arrows and positions of selected voxels for LET spectra analysis are shown by numbers.

O66. Towards the complete automated knowledge-based planning pipeline for photon-proton plan comparison in head and neck cancer adaptive radiotherapy

Adam Yeo[1,*], Lisa Hall[1], Gabrielle Drum[1], Emily Nigro[1], Tomas Kron[1]

[1]Peter Maccallum Cancer Centre, Melbourne, Australia

Introduction In Australia, a proton–photon comparative planning is required for medication treatment overseas program (MTOP) application and its federal funding needs to be justified by clinical recommendations based on predicted dosimetric assessment, which cab be often laborious and subjective. This work aims to demonstrate the automated photon-proton comparative planning pipeline including sensitivity analysis against given anatomy changes in H&N adaptive radiotherapy.

Method Photon and Proton specific Knowledge-Based-Planning (KBP) models are developed using RapidPlan™ (Eclipse v16.1, Varian Medical Systems, Palo Alto, USA). 30 Bilateral H&N patients were included to build both photon and proton KBP models. Another 20 datasets associated with re-scan CT due to anatomy change (e.g. weight loss and/or tumour response) were selected to recalculate dose to perform sensitivity analysis.

Results Both photons and protons showed comparable dosimetry for the vast majority of cases (CI95%) in terms of CTVs coverage while protons showed favourable dosimetry over photons in terms of intermediate- and low-dose levels as expected. DVH-estimates for both proton and photon KBP models showed good correlation between the predicted and achieved D_{mean} for OARs (Fig. 1). It's worth noting that protons predict slightly higher while photons slightly lower D_{mean} than what was actually achieved in its respective plans. As a rule of thumb, 2 cm separation reduction in bilateral necks in adaptive VMAT results in dose increase within a fraction size (2 Gy). Sensitivity of proton plans against such anatomy variation can be equivalent to that of VMAT due to the fact that four fixed beams are judiciously selected throughout 360 angles.

Conclusion This automated KBP pipeline allows effective and efficient photon-proton comparative planning, which enabled adaptive dosimetric assessment in a timely manner for H&N scenarios. This work has potential to play an important role as independent credentialing tools in context of MTOP as well as clinical trials.

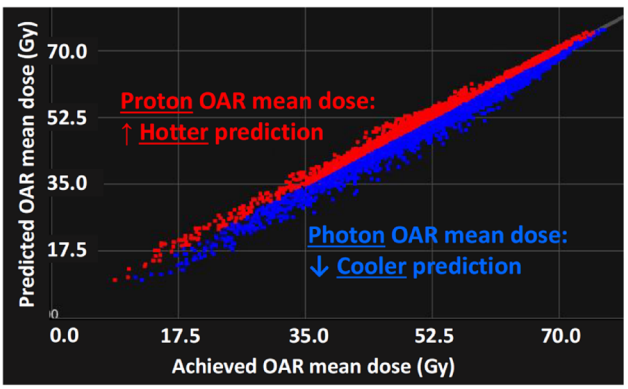

Fig. 1. Predicted vs achieved OARs D_{mean} for all cases.

O67. Comparative proton treatment planning at the Australian Bragg Centre for Proton Therapy and Research

Alexandre Santos[1,2,3,*], Scott Penfold[1,3]

[1]Australian Bragg Centre for Proton Therapy and Research, Adelaide, Australia, [2]Royal Adelaide Hospital, Adelaide, Australia, [3]The University of Adelaide, Adelaide, 5005

Comparative proton treatment planning is a service provided by the Australian Bragg Centre for Proton Therapy and Research (ABCPTR) which is required for any Medical Treatment Overseas Program application. This is where a proton treatment plan is generated and compared to the referring centres treatment plan. In this presentation, the process taken by the ABCPTR will be presented. Comparison of proton and x-ray treatment plans is not a straightforward task, complicated mainly by the difference in treatment planning approaches. Specifically, that the planning target volume is not as applicable in modern proton treatment planning, and hence utilising robust optimisation and evaluation in proton planning. This presentation will include what can be expected by the referring centre, the current treatment planning techniques used at the ABCPTR, and future plans to include radiobiological modelling into the comparisons. With many referring centres across Australasia and more expected before the ABCPTR is treating, this presentation will provide a much needed overview of the comparative planning process and future directions at the ABCPTR.

O68. Analysis of data from five years' clinical use of surface guidance in stereotactic radiation therapy

Sergei Zavgorodni[1,2,*], Lennon Wotzke[1,2]

[1]BC Cancer Agency, Victoria, Canada, [2]University of Victoria, Victoria, Canada

Introduction Surface guided radiotherapy (SGRT) allows intra-fraction patient motion monitoring and facilitates accurate delivery of stereotactic radiotherapy (SRT) and stereotactic radiosurgery (SRS) treatments with open face mask. SGRT is commonly used in conjunction with cone beam CT (CBCT), where CBCT image establishes initial reference position for SGRT monitoring. In our institution CBCT is also taken post SRS treatments to confirm correct treatment position. SGRT AlignRT system that was implemented in our institution in 2017, tracks patient motion and every 0.5 s records relative patient positions in six coordinates. It also records radiation beam status and interrupts beam if patient motion exceeds a set tolerance.

Method Data for the last 336 SRT and SRS patients were analyzed at the "patient population" level to confirm the absence of long term trends. Mean values and standard deviations of patent motion during beam-on time were calculated for each treatment fraction and for each treatment course. Intra-fraction motion and treatment interruptions were also recorded.

Results All SRT and SRS patient treatments were well within our tolerance of 1 mm translations and 1 degree rotations as monitored by AlignRT. In fact mean translations exceeded 0.3 mm for only 4 patients, and mean rotations exceeded 0.3 degrees for two patents. However, in 2020 we observed 5 patients with post-treatment CBCT patient shift exceeding 1 mm. This was attributed to the "dead-time" when patients were not monitored by AlignRT; this is the time between completion of CBCT and start of AlignRT monitoring. CBCT protocol was altered to minimize this "dead-time", and no patient shifts exceeding the tolerance were recorded after this change.

Conclusion AlignRT has been a useful tool to monitor and minimize intra-fraction motion in stereotactic therapy, however it is important to use it with CBCT protocol that minimizes "dead time" where the patient motion is not monitored.

O69. Incorporating patient-specific respiratory target motion into the pre-treatment verification measurement process

Ben Zwan[1,*], Cameron Stanton[1], Monica Le Mottee[1], Kankean Kandasamy[1], Christopher Lee[1], Peter Greer[2,3]

[1]Central Coast Cancer Centre, Gosford, Australia, [2]University of Newcastle, Newcastle, Australia, [3]Calvary Mater Hospital, Newcastle, Australia

Introduction Respiratory target motion can significantly affect the delivered dose during radiotherapy due to interplay and motion blurring.[1] The dosimetric impact of interplay is dependent on amplitude, breath-rate, MLC speed, dose rate and fractionation.[2] Despite this, pre-treatment verification measurements are routinely performed without consideration of patient-specific target motion. We have developed a novel method whereby the patient's target motion from CT-sim is incorporated into an EPID-based 3D-dose reconstruction for pre-treatment dose verification.

Method Cine EPID images were acquired during VMAT without a phantom present. Each cine image was translated to reflect 3D target motion during the delivery. The motion-encoded images were used to reconstruct the 3D-dose in a virtual cylindrical phantom [3] which was compared to planned dose within the gross-target-volume (GTV) using a 3%/2 mm 3D-gamma pass rate ($GPR_{3D,GTV}$). The method was tested using 20 SBRT plans generated on a CIRS Quasar phantom. Free-breathing (FB) motion was simulated for several amplitudes and breath-rates. Breath hold (BH) motion was simulated using 15 s BHs at random displacements within ± 3 mm and ± 5 mm range. The technique was then applied to both a clinical lung and a liver SBRT plan using 3D-motion derived from the respective patient's FB-4DCT and multiple-BH CTs.

Results GTV coverage reduces as amplitude increases, as breath-rate decreases and for larger BH gating window. For the clinical FB lung and BH liver plans the $GPR_{3D,GTV}$ reduced from 100% to 94.7% and 99.3% to 83.4% respectively due to motion.

Conclusion Interplay can significantly degrade dose accuracy and should be assessed per-patient prior to treatment. A novel method has been developed to incorporate patient-specific target motion into a 3D EPID-based dose reconstruction. This technique can be applied to any type of 3D motion, so that the impact of target motion can be quantified as part of pre-treatment quality assurance.

References

1. Stambaugh C, BE Nelms, T Dilling, C Stevens, K Latifi, G Zhang, E Moros, V Feygelman (2013) Experimentally studied dynamic dose interplay does not meaningfully affect target dose in VMAT SBRT lung treatments. Medical physics 40(9):091,710.
2. Ong CL, M Dahele, BJ Slotman, WF Verbakel (2013) Dosimetric impact of the interplay effect during stereotactic lung radiation therapy delivery using flattening filter-free beams and volumetric modulated arc therapy. International Journal of Radiation Oncology* Biology* Physics 86(4):743–8.
3. Ansbacher W (2006) Three-dimensional portal image-based dose reconstruction in a virtual phantom for rapid evaluation of IMRT plans. Medical physics 33(9):3369–82.

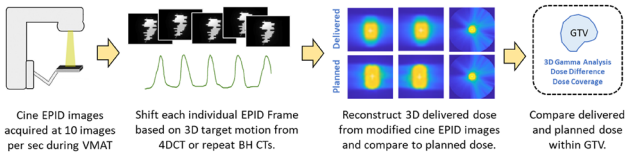

Fig. 1. Dose reconstruction methodology.

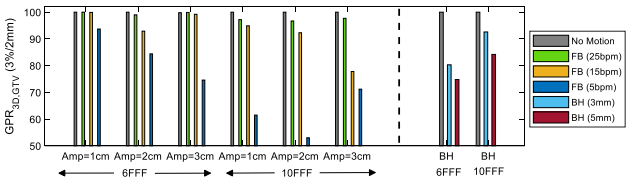

Fig. 2. Phantom test results per-fraction.

O70. Dosimetric impact of DIBH monitoring inaccuracies and the potential for real-time dose-led management

Natasha Gabay[1,2,*], Maegan Gargett[1], Jeremy Booth[1,2]

[1]Royal North Shore Hospital, St Leonards, Australia, [2]University of Sydney, Camperdown, Australia

Introduction Motion management in deep inspiration breath hold (DIBH) breast radiotherapy typically relies on external signals that place a geometric tolerance on recorded displacement (e.g. marker block) to infer accuracy of breath hold position; an assumption which can lead to dosimetric errors with a high degree of inter-patient variability [1]. Combining this approach with dose guidance, which reconstructs dosimetric errors in real time and relies directly on dosimetric tolerances, could enable a more accurate, patient-specific approach to DIBH monitoring. This research aimed to (i) simulate motion-induced dosimetric errors in DIBH breast VMAT treatments, and (ii) evaluate a real-time motion-including dose calculation software, DoseTracker [2], at detecting dosimetric errors for potential dose-guided treatment applications.

Method Deviations from planned DIBH position were simulated offline using five patient treatment plans. A range of systematic chest wall displacements d from the planned position (range -10 to + 10 mm), informed by previously measured intrafraction EPID imaging, were simulated in the Eclipse TPS via an isocentre shift method, and in DoseTracker using a motion encoded plan. Differences between planned and 'delivered' TPS doses for the breast CTV and PTV were reported.

Results In the TPS, simulated DIBH instabilities were found to introduce dosimetric uncertainties of up to 18.65%-pts (CTV) and 50.22%-pts (PTV). DoseTracker estimated the breast CTV with a root-mean square deviation to the TPS of 2.14%-pts and 0.51%-pts, respectively.

Conclusion The VMAT technique investigated was susceptible to large reductions in target dose coverage for the range of clinically observed chest wall displacements. DoseTracker accuracy at detecting such dosimetric errors deviated by more than 2% from the TPS; further development of the tool's dose engine is required in order for it to be suitable for real-time dose-error detection.

Acknowledgements
The authors would like to thank the developers of DoseTracker for access to this research software.

References

1. Lutz, C. M., Poulsen, P. R., Fledelius, W., Offersen, B. V., & Thomsen, M. S. (2016). Setup error and motion during deep inspiration breath-hold breast radiotherapy measured with continuous portal imaging. *Acta Oncologica*, *55*(2), 193–200.
2. Ravkilde, T., Keall, P. J., Grau, C., Høyer, M., & Poulsen, P. R. (2014). Fast motion-including dose error reconstruction for VMAT with and without MLC tracking. *Physics in Medicine & Biology*, *59*(23), 7279.

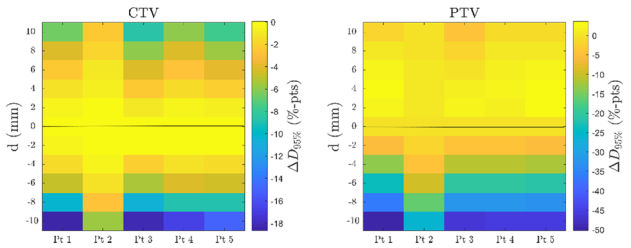

Fig. 1. TPS Dosimetric uncertainties in CTV and PTV associated with simulated chest wall displacements of d mm.

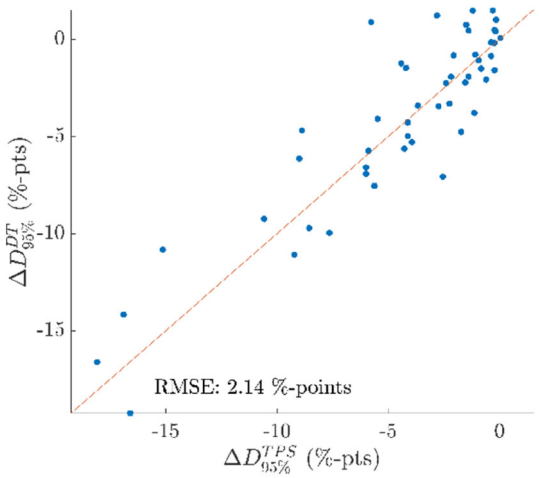

Fig. 2. DoseTracker and TPS dosimetric uncertainties in CTV for all patients and motions.

O71. Results from the AAPM Task Group 324 Respiratory Motion Management in Radiation Oncology Survey

Paul Keall[1,*], Helen Ball[1], Lakshmi Santanam[2], Suresh Senan[3], James Tanyi[4], Marcel van Herk[5]

[1]Image X Institute, University of Sydney, Eveleigh, Australia, [2]Medical Physics Department, Memorial Sloan-Kettering Cancer Center, New York, USA, [3]Amsterdam University Medical Center, Amsterdam, Netherlands, [4]Geisinger Cancer Institute, USA, [5]University of Manchester, Manchester, United Kingdom

Introduction Given the growth and changes in respiratory motion management since the 2006 publication of the existing American Association of Physicists in Medicine (AAPM) guidelines [1], the AAPM has formed Task Group 324, *The management of respiratory motion in radiation oncology: An update to Task Group 76*. Part of the approved Task Group plan was to conduct a survey of AAPM members. The primary purpose of this survey was to quantify the status, challenges, and future directions on the implementation of respiratory motion management on radiotherapy.
Method A respiratory motion management survey was designed and conducted based on clinician survey guidelines [2]. A cohort of NSW medical physicists performed pre-testing. The Task Group 324 members performed pilot testing. The survey was administered to AAPM members, including joint AAPM and ACPSEM members, on 17 August 2020. The survey was closed on 13 September 2020.
Results 527 respondents completed the entire survey and 651 respondents completed part of the survey. 84% of survey respondents used deep inspiration breath hold (DIBH) for left-sided breast cancer. 83% of respondents perceived respiratory motion management for thoracic and abdominal cancer radiotherapy patients to be either very important or required. 95% of respondents used respiratory motion management for thoracic and abdominal sites, with 36% of respondents using respiratory motion management for at least 90% of thoracic and abdominal patients. The majority (60%) of respondents used the internal target volume (ITV) method to treat thoracic and abdominal cancer patients, with 25% using breath hold or abdominal compression and 13% using gating or tracking.
Conclusion A respiratory motion management survey was completed by AAPM members. The survey results quantify the status, challenges, and future directions on the implementation of respiratory motion management in radiotherapy. The survey findings, primarily based on USA practice results, may be of interest to ACPSEM members to evaluate their motion management practices and advocate for different processes and additional motion management equipment.
References

1. Keall PJ, Mageras GS, Balter JM, Emery RS, Forster KM, Jiang SB, Kapatoes JM, Low DA, Murphy MJ, Murray BR, Ramsey CR, Van Herk MB, Vedam SS, Wong JW, Yorke E. The management of respiratory motion in radiation oncology report of AAPM Task Group 76. Med Phys. 2006;33(10):3874–3900.
2. Burns KE, Duffett M, Kho ME, Meade MO, Adhikari NK, Sinuff T, Cook DJ. A guide for the design and conduct of self-administered surveys of clinicians. Canadian Medical Association journal. 2008;179(3):245–252.

O72. A real-time dose guidance framework for motion management during pancreas SBRT

Maegan Gargett[1,2], Abdella Ahmed[1], Levi Madden[1], Ryan Brown[1], Jeremy Booth[1,3]

[1]Northern Sydney Cancer Centre, Royal North Shore Hospital, St Leonards, Australia, [2]School of Health Sciences, Faculty of Medicine and Health, University of Sydney, Sydney, Australia, [3]Institute of Medical Physics, School of Physics, University of Sydney, Sydney, Australia

Introduction Stereotactic body radiotherapy (SBRT) is playing an increasing role in the treatment of pancreatic cancer [1]. Accurate dose delivery is required for favourable clinical outcomes, but is compromised by motion. Online motion management protocols for SBRT standardly apply geometric tolerances to target motion in an indirect approach to ensure dose accuracy. This work assesses a real-time dose-guided motion management framework to compliment the use of geometric tolerances, utilising a fast motion-inclusive dose calculation software, DoseTracker [2].
Method Implanted fiducial marker positions were monitored during treatment using 2D kV imaging (@0.3 Hz) for 15 pancreas SBRT fractions (3 patients). Two 3D motion management protocols were

simulated offline for comparison, shown in Fig. 1. DoseTracker was used to reconstruct both time-resolved and fractional delivered doses, inclusive of motion indicated by marker position. Fractional dose errors, defined as the relative difference in dose-volume metrics (CTV D95%, PTV D90%) between motion-inclusive and planned distributions, were compared for each protocol.

Results Fig. 2 shows that dose errors were reduced for the 3D methods compared to the 2D method. Where the PTV D90% fractional dose error exceeded 5% for the 2D method (8/15), 3D image- and dose-guidance reduced the average dose error (± 1SD) by (5.3 ± 2.3)% and (4.9 ± 1.8)%, respectively. The reduction in number of couch shifts using dose-guidance compared to 3D-image-guidance was statistically significant ($p = 0.043$), on average 1 per-fraction.

Conclusion Dose-guided motion management improved delivered dose accuracy compared to a 2D image-guided approach, and demonstrated potential to improve treatment workflow by identifying and correcting motion events of dosimetric consequence.

Acknowledgements
The authors would like to thank the developers of DoseTracker for access to the research software. Data used for this study was collected under an ethically approved trial (ID: NCT03505229).

References

1. Petrelli F, Comito T, Ghidini A, Torri V, Scorsetti M, Barni S (2017) Stereotactic body radiation therapy for locally advanced pancreatic cancer: A systematic review and pooled analysis of 19 trials. Int J Rad Onc Biol Phys, 97(2): 313–322. https://doi.org/10.1016/j.ijrobp.2016.10.030
2. Skouboe S, Poulsen PR, Muurholm CG, Worm E, Hansen R, Hoyer M, Ravkilde T (2019) Simulated real-time dose reconstruction for moving tumors in stereotactic liver radiotherapy. Med Phys 46(11). https://doi.org/10.1002/mp.13792
3. Poulsen PR, Cho B, Langen K, Kupelian P, Keall PJ (2008) Three-dimensional prostate position estimation with a single x-ray imager utilizing the spatial probability density. Phys Med Biol 53(16):4331–4353. https://doi.org/10.1088/0031-9155/53/16/008

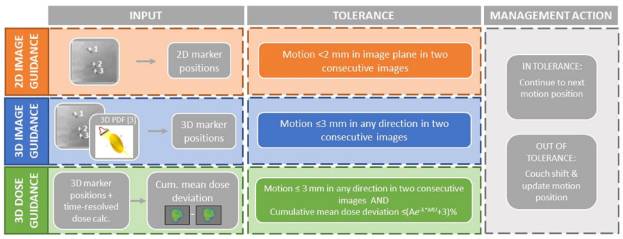

Fig. 1. Motion management protocols. "Cumulative mean dose deviation" refers to average point-dose deviations from planned dose within the CTV, accumulated to the current timepoint. A = 25, λ = 0.01, MU = cumulative monitor units.

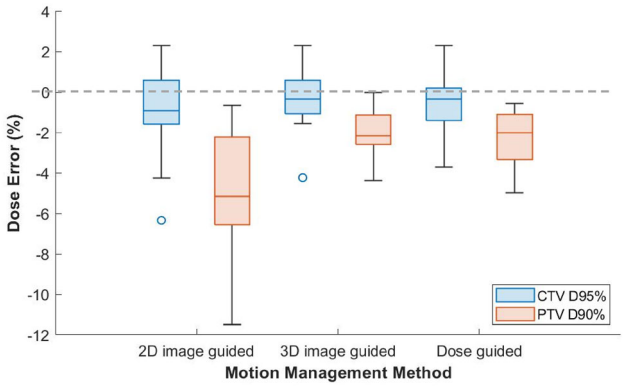

Fig. 2. Box and whisker distribution of fractional dose errors due to motion. Outliers shown as circles.

O73. The need for individualised breathing trace quality assurance for lung patients undergoing 4DCT simulation

James Rijken[1,*], Yunfei Hu[1], Kelvin Hiscoke[1]

[1]Icon Cancer Centre, Windsor Gardens, Australia

Introduction 4DCT simulation is a popular solution for scanning lung cancer patients for radiotherapy as it allows the clinician to gain an appreciation for movement of the target during the breathing cycle. Resultant binning of images and production of the 4DCT dataset relies heavily on the recorded breathing trace but quality assurance is not routinely performed on these and there lacks any substantial recommendations thereof.

Method An application was created for Windows in C# that was able to analyse the VXP breathing trace files from Varian RPM/RGSC and quantify various metrics associated with the patient breathing cycle. This data was then used to consider errors in voluming of targets for several example cases in order to justify recommendations on quality assurance.

Results For 291 real patient breathing traces from 4DCT simulation of lung targets, notable differences were found between RGSC and application calculations of phase data. For any new patient without individualised QA, the average marked phase calculation (which is used for 4DCT reconstruction) is only accurate to within 19% of the actual phases. The error in BPM within the scan due to breathing rate variation is 36%. The uncertainty in amplitude due to breathing variation is 34% in the mean. Phase uncertainty leads to misbinning which we have shown can lead to missing 66% of the target for phased based treatment. Variation in inhalation/exhalation level leads to voluming errors which, without individualised QA, can be assumed to be 11% (PTV is smaller than actual).

Conclusion Without individualised quality assurance of patient breathing traces, large uncertainties have to be assumed for metrics of both phase and amplitude, leading to clinically significant uncertainties in treatment. It is recommended to perform individualised quality assurance as this provides the clinician with an accurate quantification of uncertainty for their patient.

O74. [Invited] An overview of contrast-enhanced spectral mammography in a clinical environment

Jo Kim[1,*]

[1]Westmead Hospital, Westmead, Australia

Introduction Despite the successful outcomes of BreastScreen Australia with a standard two-view mammogram in reducing breast cancer mortality by around 45% [1], compromised detection sensitivity and diagnostic accuracy in dense breasts has been consistently identified as the area of improvement [2]. A relatively new, advanced breast imaging technique called contrast-enhanced mammography (CEM) has increasingly been reported to have superior diagnostic performance compared with standard mammography and ultrasound particularly for dense breast tissues [3,4] and comparable diagnostic accuracy to MRI [5]. The Breast Clinic at Royal Perth Hospital is one of the Australian pioneers in clinical implementation of this technique for breast cancer diagnosis since 2013 with CEM equipment from two different vendors. An audit of the clinical CEM images revealed some artefacts unique to CEM procedures [6] which led to further investigation of the CEM system. Although there is a scarcity of internationally-acknowledged standards and quality assurance or CEM units, several studies reported performance tests and results for their CEM systems [7–10]. We combined a number of these tests to form a comprehensive CEM Quality Assurance (QA) protocol and applied to our two CEM units to gain a greater insight into system performance. Our initial experience in this area is presented.

Method Important QA tests specific to CEM units were identified following a literature review. Performance tests unique to CEM mostly involve high energy exposure and recombined image assessment, as low energy images are analogous to conventional mammography. These include: (i) tube related tests for high energy exposure ($\geq$ 45 kVp) including kV accuracy, HVL, MGD and AEC repeatability and (ii) image quality tests on recombined images including background cancellation, linearity of iodine signal and image uniformity.

Results Results for all tube tests were well within the current compliance limit. Large deviations in background cancellation and differences in the linearity of the iodine signal were found between vendor systems.

Conclusion Our initial experiences in performance assessment of the CEM units highlight the importance of proper characterisation of the systems with regular performance tests specific to CEM and also indicate many aspects for further research in CEM.

Acknowledgements

This study was financially supported by Royal Perth Hospital Imaging Research Grants.

References

1. Australian Institute of Health and Welfare (aihw.gov.au).
2. Sung J et al. (2019) "Performance of dual-energy contrast-enhanced digital mammography for screening women at increased risk of breast cancer" Radiol. 293 81-8.
3. Lobbes M et al., (2014) "Contrast-enhanced spectral mammography in patients referred from the breast cancer screening programme" Eur. Radiol. 24 1668-76.
4. Luczynska E et al., (2016) "Comparison of the mammography, contrast-enhanced spectral mammography and ultrasonography in a group of 116 patients" AntiCancer Res 36 4359-66.
5. Phillips J et al., (2018) "Comparative dose of contrast enhanced spectral mammography (CESM), digital mammography and digital breast tomosynthesis" AJR 211 839-45.
6. Nappalli S et al., (2021) "Artifacts in contrast-enhanced mammography: are there differences between vendors?" Clin Imaging. 80 123-30.

O75. Impact of key algorithm parameters on the accuracy of CT ventilation imaging

Jeremy Lim[1,*], **Hilary Byrne**[1], **John Kipritidis**[2], **Jeremy Booth**[2], **Paul Keall**[1]

[1]ACRF Image X Institute, School of Health Sciences, The University of Sydney, Sydney, Australia, [2]Northern Sydney Cancer Centre, Royal North Shore Hospital, Sydney, Australia

Introduction Functional lung avoidance radiotherapy is anticipated to reduce treatment induced side effects such as radiation pneumonitis [1]. Computed Tomography Ventilation Imaging (CTVI) is an investigational technique for generating lung function (ventilation) maps from respiratory correlated CT scans, e.g. paired exhale/inhale breath hold CT (BHCT). The two main methods for calculating CTVI are the Hounsfield unit (HU)-based method and the Jacobian-based method [2]. This study performs a parameter sensitivity analysis and optimisation of CTVI.

Method Investigations were carried out using BHCT scans for CTVI evaluated against gold standard nuclear medicine ventilation scans, Galligas PET/CT. CTVI accuracy was characterised as the voxel-wise Spearman correlation with Galligas PET/CT. A clinically acceptable threshold of 0.4 was chosen from literature. Parameters investigated addressed different parts of the CTVI pipeline (Fig. 1) and included lung segmentation threshold, crop dimensions, DIR regularisation parameter, selection of DIR engine, and smoothing filter width.

Results The correlation between CTVI and Galligas PET/CT was demonstrated to be robust to changes in lung segmentation threshold, crop dimensions and DIR regularisation parameter between 1 and 5. The mean correlation fell below the threshold of 0.4 when using ANTsPy as the DIR engine for the Jacobian-based method and when no smoothing is performed for the HU-based method (Fig. 2).

Conclusion A parameter sensitivity analysis and optimisation of CTVI accuracy was successfully carried out. Future work should determine whether parameter selection or patient-specific differences is the driving factor for interpatient variability in CTVI accuracy.

Acknowledgements

The BHCT and Galligas PET dataset used in this study was acquired in a prior study by Eslick et al. [3] (ACTRN12612000775819).

References

1. Vinogradskiy Y, Castillo R, Castillo E et al. (2022) Results of a Multi-Institutional Phase 2 Clinical Trial for 4DCT-Ventilation Functional Avoidance Thoracic Radiation Therapy. *Int. J. Radiat. Oncol. Biol. Phys.* 112(4):986–995. https://doi.org/10.1016/j.ijrobp.2021.10.147
2. Kipritidis J, Woodruff HC, Eslick EM, Hegi-Johnson F, Keall PJ (2016) New pathways for end-to-end validation of CT ventilation imaging (CTVI) using deformable image registration. IEEE 13th International Symposium on Biomedical Imaging (ISBI) 939–942. https://doi.org/10.1109/ISBI.2016.7493419
3. Eslick EM, Kipritidis J, Gradinscak D, et al. (2018) CT ventilation imaging derived from breath hold CT exhibits good regional accuracy with Galligas PET. Radiother Oncol 127(2):267–273. https://doi.org/10.1016/j.radonc.2017.12.010

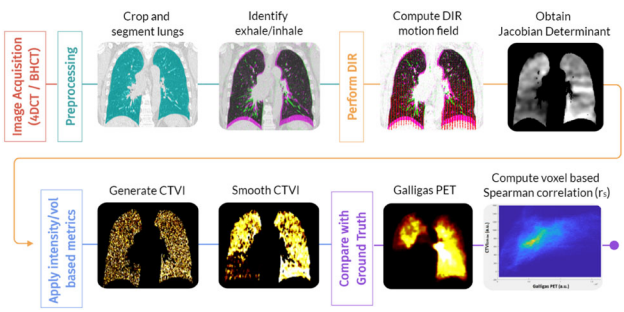

Fig. 1. Flowchart showing major stages in the CTVI pipeline.

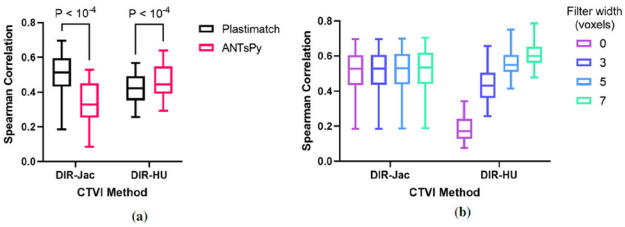

Fig. 2. Box plots of the correlations between each type of CTVI and the corresponding Galligas PET/CT for: (a) Plastimatch and ANTsPy (b) different median filter widths.

O76. Comparison of peak entrance skin dose estimation methods interventional radiology and cardiology

Leah Biffin[1,*]

[1]Western Health, Footscray, Melbourne, Australia

Introduction Accurate estimation of skin dose during angiographic procedures is important for patient radiation protection. Automated peak skin dose (PSD) tracking is incorporated into some modern angiography systems. While performance accuracy of such software has been typically carried out using phantom studies, few are done using real patient cases. For example, validation studies used phantoms to verify the Canon Dose Tracking System (DTS), show excellent visual agreement between DTS and film dose distributions where dose rate values agreed within 10% [1]. A limited study carried out locally in 2017 [2] using an anthropomorphic phantom demonstrated a wider variation of ± 30% between the DTS and film measurement. In 2020, Malchair et.al. explored literature on 12 software systems for correlation with phantom based simulations, finding many had acceptable (± 25%) correlation with film dose in phantom simulations. However only two studies reviewed used real patient cases and the agreement was poor (within ± 43% and ± 76%, respectively) [3]. This study reports a comparison of measured PSD using film in real world patient cases and PSD calculations performed by on-board software and other methods performed by Medical Physicists.

Method Radiochromic film (Gafchromic XR-RV3) is used to record the PSD in interventional radiology and cardiac cath lab cases.

The Radiation Structured Dose Report and other dose report data is used by blinded medical physicist experts to estimate PSD using various modelling methods. The PSD displayed by the laboratory on-board modelling systems; Canon DTS and Siemens CAREmonitor, is compared with that estimated by film and using computational methods by medical physicists.

Results The on-board software shows reasonable agreement with film (± 38%), with greater variation among desktop calculation methods utilized by Medical Physicists.

Conclusion The study outlines a comparison of peak skin dose estimation methods and real peak skin dose experienced by patients as indicated by film.

Acknowledgements

This study was supported by a grant from the Western Health Allied Health Science Scholarship, which was used to purchase the radiochromic film.

References

1. Bednarek D.R., Barbarits J., Rana V. K., Nagaraja S. P., Josan M.S. and Rudin S. (2011). Verification of the performance accuracy of a real-time-skin-dose tracking system for interventional fluoroscopic procedures. Proc. SPIE 7961, Medical Imaging 2011: Physics of Medical Imaging, 79,612, https://doi.org/10.1117/12.877677
2. Rajesh P, 2017. Comparison of peak entrance skin dose estimation techniques in interventional cardiology, MSc, RMIT University, Melbourne.
3. Malchair F, Dabin J, Deleu M, Sans Merce M, Ciraj Bjelac O, Gallagher A, Maccia C (2020). Review of skin dose calculation software in interventional cardiology. Physica Medica 80:75–83. https://doi.org/10.1016/j.ejmp.2020.09.023.

O77. Introduction of ARPAB expert certification

Cameron Jeffries[1,*], **Brent Rogers**[2], **Kent Gregory**[3], **Riaz Akber**[4]

[1]SA Medical Imaging, Adelaide, Australia, [2]South Eastern Sydney Local Health District, Sydney, Australia, [3]SA Radiation Pty Ltd, Kent Town, Australia, [4]Safe Radiation, Browns Plains, Australia

Introduction Professional accreditation in radiation protection had its official origin in Australia at the 1990 Conference, which was held jointly between ARPS and ACPSEM. Over the next decade a working group was empanelled to develop an accreditation scheme consisting of various practical examinations and a bank of questions so that a theoretical exam could be completed and graded. In 1997, ARPS and ACPSEM completed the "Candidates Kit" for a Radiation Protection Advisor level of certification, and were joined by the Australian Institute of Occupational Hygienists as a sponsoring organisation [1]. In 2000, the Australasian Radiation Protection Accreditation Board (ARPAB) was incorporated and began certifying Radiation Safety Advisors (CRSA). Since establishment, very little changed about ARPAB aside from the doubling from two to four representatives from each sponsoring society.

Method In 2018, during Kent Gregory's term as Chair, a new working group was empanelled to create an exam bank for an expert level of certification, along with designing the Candidates Kit for being a Certified Radiation Safety Expert (CRSE). This advanced level of certification is designed to comply with the 2016 IRPA Guidance on Certification of a Radiation Protection Expert [2]. The Working Group with Kent as convenor further consisted of Riaz Akber, Cameron Jeffries and Brent Rogers, and as with the original certification, the expert certification has been internally authenticated.

Conclusion At the 2021 ARPS Conference, March 2022, an advanced level of certification was introduced by ARPAB. The Working Group has now become the Panel of Examiners. The steps to achieving the Expert level of certification will be discussed in this presentation. Information about certification can be found on the ARPAB website [3].

References

1. https://www.arpab.org.au/how-to-get-accredited/
2. https://irpa.net/docs/IRPA%20Guidance%20on%20Certification%20of%20a%20RP%20Expert%20(2016).pdf
3. https://www.arpab.org.au/
4. Sun Nuclear Corporation. Mercury 4.0 Phantom. https://www.sunnuclear.com/uploads/documents/datasheets/Diagnostic/Mercury4Phantom_061720.pdf [Accessed 18 March 2022].

O78. Experiences and challenges with introducing a testing methodology of CT automatic exposure control

Raihan Rasheed[1,*], Laura Burberry[1], Ioannis Delakis[1]

[1]Department of Medical Imaging, Prince of Wales Hospital, Sydney, Australia

Introduction Automatic exposure control (AEC) is standard practice in CT imaging, designed to manage a balance between image quality and dose delivered across the patient. AEC operation can be complex with vendor specific parameters that dictate system behaviour affecting image quality and dose. Although appropriate functioning of AEC system is crucial, there is currently no professional guidance for AEC testing of CT systems although there are limited publications on proposed methodologies [1–3]. The aim of this work is to share our experiences and challenges faced when testing AEC performance of CT systems.

Method The Mercury 4.0 Phantom [4] was used for testing the AEC performance of a Siemens Symbia Intevo CT scanner. Performance metrics mA and image noise were studied against vendor-specific AEC parameters (modulation strength and quality reference mAs).

Results Fig. 1A, 1B demonstrate variation in mA and noise across the phantom for different modulation strengths (very weak to very strong) and different values of quality reference mAs (QRmAs), respectively. Results showed that increasing the QRmAs resulted in a proportionate increase in tube current and increases in modulation strength resulted in a greater mA variation. The testing also generated noise profiles that can be used as baselines to characterise and monitor scanner performance. A limitation of our current methodology was that the phantom was not elliptical, therefore not capable of testing in-plane AEC performance, and its diameter was not large enough to simulate AEC performance for bariatric imaging. Phantom design also presented practical limitations such heavy weight and potential air gaps between segments.

Conclusion Our methodology was successful in characterising the performance of AEC system across different phantom thicknesses when changing vendor-specific AEC variables (modulation strength and QRmAs). Future work will apply the proposed methodology on further CT scanner models/vendors and feedback will be provided to the phantom manufacturer on design improvements.

Acknowledgements: We would like to acknowledge the assistance and cooperation from Tom Hennessy and the department of Nuclear Medicine, Prince of Wales Hospital.

References

1. Diteko K, Duguid R, Hampson L. Computed Tomography (CT) Automatic Exposure Controls (AEC) Testing Protocol Using a CelT Phantom. Journal of Medical Physics and Applied Sciences. 2020; 5(14): https://doi.org/10.36648/2574-285X.5.1.4.
2. Iball GR, Moore AC, Crawford EJ. A routine quality assurance test for CT automatic exposure control systems. Journal of Applied Clinical Medical Physics. 2016; 17(4): 291–306. https://doi.org/10.1120/jacmp.v17i4.6165
3. Wilson JM, Christianson OI, Richard S, Samei E. A methodology for image quality evaluation of advanced CT systems. The International Journal of Medical Physics Research and Practice. 2013; 40(3): 031,908–1 – 03,908–9. https://doi.org/10.1118/1.4791645

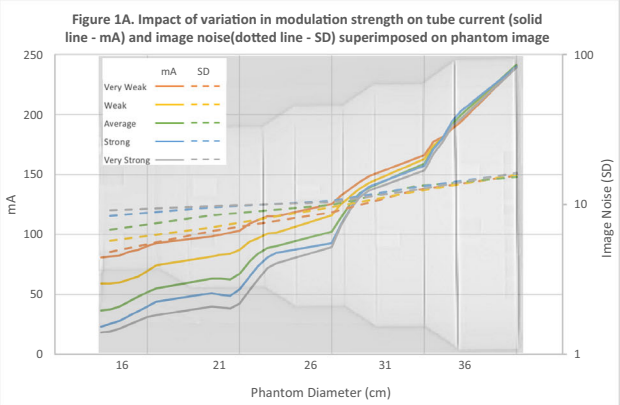

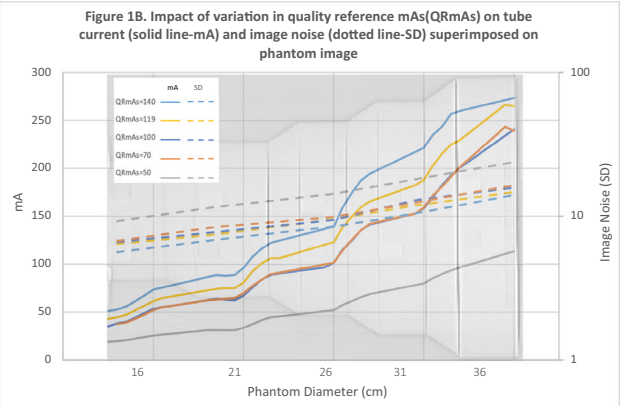

Fig. 1A and B.

O79. A quality program for MLC tracking

Jonathan Hindmarsh[1,*], Sonja Dieterich[2], Jeremy Booth[3], Paul Keall[1]

[1]Image X Institute, Faculty of Medicine and Health, University of Sydney, Eveleigh, Australia, [2]Department of Radiation Oncology, UC Davis Medical Center, Sacramento, USA, [3]Northern Sydney Cancer Center, Royal North Shore Hospital, St Leonards, Australia

Introduction Multi-leaf collimator (MLC) tracking, a real time adaptive treatment technique first proposed in 2001 [1], and now clinically available on the Accuray (Sunnyvale, CA) Radixact with Synchrony [2]. Thus, no longer confined to the research environment. In 2010, Sawant et al. [3] performed an FMEA on the system and proposed 7 specific monthly tests for MLC tracking. More recently AAPM TG264 [4] was published containing recommendations to determine the quality assurance (QA) needs of any clinical system based on results of a hazard analysis assessment. To reduce the impost of performing a system specific hazard analysis, this work

investigated the generation of generic guidelines for the creation of a quality program.

Method Following the recommendation of TG264, a recently developed hazard analysis technique built around complex theory, system theoretic process analysis (STPA), was applied to MLC Tracking. This was done according to the STPA Handbook [5]. Following the application of STPA on a generic MLC tracking treatment process, the results of the analysis were generalised and converted into questions for the users to consider when setting up a quality program.

Results STPA was successfully applied to a MLC tracking program and the results were generalised in order to create questions that can guide users in the creation of a suitable quality program covering quality control, assurance, and management. The questions range from treatment specific to considering the whole program including how MLC tracking should be prescribed.

Conclusion STPA was applied to MLC tracking and has facilitated the creation of questions to help guide users of MLC tracking in the creation of a quality program.

References

1. P. J. Keall, V. R. Kini, S. S. Vedam, and R. Mohan, Phys. Med. Biol. 46, 1 (2001).
2. G.-P. Chen, A. Tai, L. Puckett, E. Gore, S. Lim, T. Keiper, C. Johnstone, M. Shukla, C. Lawton, and X. A. Li, Pract. Radiat. Oncol. 11, e486 (2021).
3. A. Sawant, S. Dieterich, M. Svatos, and P. Keall, Med. Phys. 37, 6466 (2010).
4. P. J. Keall, A. Sawant, R. I. Berbeco, J. T. Booth, B. Cho, L. I. Cerviño, E. Cirino, S. Dieterich, M. F. Fast, P. B. Greer, P. M. af Rosenschöld, P. J. Parikh, P. R. Poulsen, L. Santanam, G. W. Sherouse, J. Shi, and S. Stathakis, Med. Phys. 48, e44 (2020).
5. N. G. Leveson and J. P. Thomas, STPA Handbook (MIT Press, Cambridge, UNITED STATES, 2018).

O80. Remote EPID-based dosimetric auditing using DVH patient dose analysis

Peter Greer[1,2,*], Therese Standen[1,3], Rajasekar David[2,4], Narges Miri[2], Kasia Bobrowski[5], Joerg Lehmann[1,2,3], Benjamin Zwan[4], Alisha Moore[2,6]

[1]Calvary Mater Newcastle Hospital, Newcastle, Australia, [2]University of Newcastle, Newcastle, Australia, [3]University of Sydney, Sydney, Australia, [4]Central Coast Cancer Centre, Gosford, Australia, [5]University of Wollongong, Wollongong, Australia, [6]TROG Cancer Research, Newcastle, Australia

Introduction The aim of this work was to develop and validate a method for remote dosimetric auditing that enables dose-volume histogram parameter comparisons of measured and planned dose in the patient CT volume.

Method The method is derived by adapting and combining a remote electronic portal imaging (EPID) based auditing method (Virtual Epid based Standard Phantom Audit—VESPA) and a method to estimate 3D in-patient dose distributions from planar dosimetric measurements [1,2]. EPID images of IMRT fields or VMAT subarcs are converted to planar dose in water phantom. These are compared to treatment planning system planar dose. The dose-ratios are backprojected to modify the dose in the patient CT volume for the beam or subarc to derive an estimated delivered dose distribution. The method was tested with a series of error-induced plans including monitor unit and multileaf collimator (MLC) positioning errors [3]. A pilot audit study was conducted with eleven radiotherapy centres for IMRT plans from two clinical trials, a post-prostatectomy (RAVES trial) plan and a head and neck (HPV trial) plan. Clinically relevant DVH parameters for the planned dose and estimated delivered dose were compared.

Results The method was found to reproduce the induced dose errors within 0.5% and was sensitive to MLC positioning errors as small as 0.5 mm. For 0.5 mm MLC errors the DVH dose errors were 2–3% which were not detectable by traditional gamma analysis. For the RAVES plan audit (Fig. 1) all DVH results except one were within 3% and for the HPV plan audit (Fig. 2) all DVH results were within 3% except three with a maximum difference of 3.2%.

Conclusion The new audit method produces clinically meaningful DVH metrics for the audited plan and could enable an improved understanding of a centre's radiotherapy quality.

References

1. Miri, N., et al., Virtual EPID standard phantom audit (VESPA) for remote IMRT and VMAT credentialing. Physics in Medicine and Biology, 2017. **62**(11): p. 4293–4299.
2. Zhen, H., Nelms, B. E., & Tome, W. A. (2011). Moving from gamma passing rates to patient DVH-based QA metrics in pretreatment dose QA. Medical Physics, 38 (10), 5477–5489.
3. Smith K et al., AAPM Medical Physics Practice Guideline 8.a.: Linear accelerator performance tests, J.Appl.Clin.Med.Phys., 2017;18:4:23–39.

O81. An open-source toolkit for independent, patient-specific DIR QA

Robert Finnegan[1,2,3,*], Phillip Chlap[3,4,5], Shrikant Deshpande[4,5], Lois Holloway[2,3,4,5]

[1]Northern Sydney Cancer Centre, Royal North Shore Hospital, St Leonards, Australia, [2]Institute of Medical Physics, University of Sydney, Camperdown, Australia, [3]Ingham Institute for Applied Medical Research, Liverpool, Australia, [4]Liverpool and Macarthur Cancer Therapy Centres, SWSLHD, Liverpool, Australia, [5]South Western Sydney Clinical School, University of New South Wales, Liverpool, Australia

Introduction Deformable image registration (DIR) is an integral component of modern radiotherapy. Safe and effective use of clinical DIR systems requires understanding the associated uncertainties, generally and in patient-specific scenarios. Ground-truth deformations between images enables quantitative assessment of DIR performance, however in practice this is not available and quality assurance (QA) of DIR systems remains limited. To address this, we developed and considered the use of a framework for QA of DIR software that provides reproducible, anatomically-feasible, and patient-specific ground-truth deformations.

Methods This proof-of-concept study included radiotherapy planning CT images and manually contoured volumes for six retrospective radiotherapy patients considering lung (N = 1), head and neck (2), pelvis (2), and abdomen (1) regions. A toolkit to model anatomical and positional changes was developed and released as part of the open-source software *platipy*. Simulated deformations can be based on specific structures, e.g. (asymmetric/symmetric) expansion, extension, contraction, and shifting, or based on changes in patient positioning, e.g. bending about a point (Fig. 1). Preservation of anatomical feasibility of structure-based deformations by fixing the location of bony anatomy is available. Using the toolkit, simulated deformations were applied to the CT images, which were imported into the RayStation treatment planning system. The clinical DIR system was used to register the original and deformed images, and the resulting DVF was compared to the ground-truth DVF.

Results An example report of simulated deformation to model neck flexion is shown in Fig. 2. RayStation DIR accurately recovered the DVF applied to the CT image, however significant differences to ground-truth were observed in some regions.
Conclusion This open-source software provides a toolkit for QA of clinical DIR systems by simulating realistic, patient-specific deformations. Continued research will expand the range of modelled scenarios and focus on streamlining QA processes.

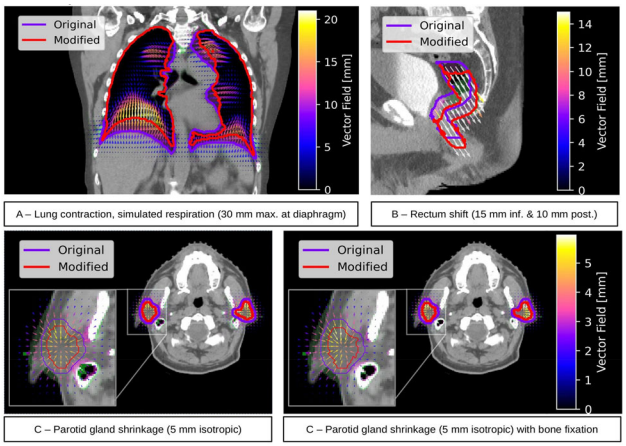

Figure 1. Examples of simulated deformations that can be generated using *platipy*.

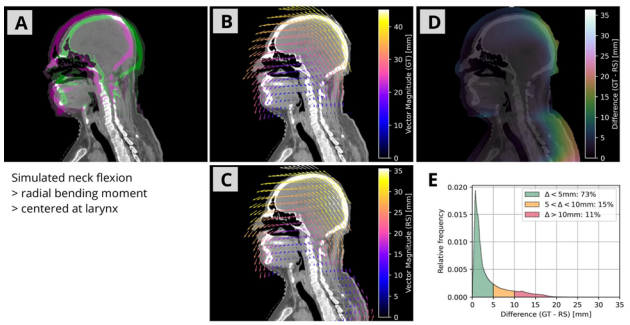

Figure 2. (A) comparison of original and deformed images, (B) ground-truth DVF, (C) RayStation DVF, (D) map and (E) histogram of the magnitude of deformation differences.

O82. Software development for pre-treatment QA to automate the virtual phantom EPID dose reconstruction method (autoVIPER)

Natalie Kong[1,*], Peter Greer[2]

[1]Calvary Mater Newcastle, Waratah, Australia, [2]University of Newcastle, Callaghan, Australia

Introduction The VIrtual Phantom EPID dose Reconstruction (VIPER) method is a tool used to reconstruct 3D dose distributions for pre-treatment IMRT/VMAT verification and generate PDF results of comparison to treatment planning calculations [1]. A software infrastructure was designed to automate this pre-treatment QA process.
Method VIPER is used to perform 2D field-by-field verification and/or 3D combined field verification. By summing the doses at the gantry angle and couch angle of each acquired image it gives the 3D dose distribution in the virtual phantom [1]. Images are acquired using frame-grabber PC's and in-house acquisition software (CDog) [2]. A CDog and DICOM Listener infrastructure was designed in the pre-treatment QA workflow to replace these manual processes and automate the entire workflow. DICOM Listener is a software written in C# running automatically in the background by Windows task scheduler. DICOM Listener monitors a verification plan folder where Eclipse verification plans are exported using a script. It then moves the plans to auto VIPER folder named by PatientMRN_PlanName by reading patient and plan information from the RP. file. CDog was modified to read available verification patients/plans to select for acquisition and save patient information to DICOM image headers. DICOM Listener triggers VIPER to run automatically once all acquired images automatically sent to VIPER folder for the patient from CDog software. It saves PDF results to patient folder when VIPER finalises all image analysis and archives the entire folder to research storage drive.
Results The automated workflow has been implemented successfully. It improves processing time and through reduced human input maximizes productivity, increases performance, easily manage tasks to be done and reduce human errors.
Conclusion Automation of the workflow of VIPER tool performed by ROMPs can handle multiple tasks simultaneously, thus speeding up processes to have higher productivity and help fulfil tedious tasks with minimal resources to increase efficiency and standardization.
References

1. Greer P, Zwan B 2020. *VIPER User Manual*, pp. 2–3.
2. Bhatia S, Greer P 2016. *CDog 3.10r4*, A software to acquire KV and/or MV images from Linacs.

O83. Using an application programming interface for automation of collimator optimization for single isocentre multi target intracranial radiotherapy

Luis Munoz[1,3,*], Peter McLoone[2], Peter Metcalfe[3], Anatoly Rosenfeld[3], Giordano Biasi[3,4]

[1]Genesiscare, Bedford Park, Australia, [2]Genesiscare, Alexandria, Australia, [3]University of Wollongong CMRP, Wollongong, Australia, [4]Peter MacCallum Cancer Centre, Melbourne, Australia

Introduction Linac based single isocentre multi target (SIMT) planning, provides an efficient and effective means of stereotactic treatment [1]. Plan generation can be an onerous task, and several solutions have been presented for autonomation that use algorithms divorced from the treatment planning system (TPS) [2–4].
Method This study explored the use of an Application Programming Interface (API) to select optimal collimator angles for automation of SIMT planning in Monaco V6.0.1. Three patients with 2, 5, and 11 lesions were generated using planning templates created via the API driven script. The algorithm finds the angle that exposes targets to the most MLCs for solution. Target coverage, conformity index and gradient index were assessed. All plans were optimized with 98% of each PTV covered by the prescription dose, so 100% of each GTV volume is covered by the prescription dose. Normal tissue was assessed using the V12Gy, V10Gy and mean dose to the brain. Plan complexity was assessed using MU/cGy and quality assurance (QA) of generated plans was completed using a CIRS Multi lesion M037 and Gafchromic XD film.
Results All plans generated with the script met clinical dosimetric criterion used to assess plan quality, marginal improvement to dose to normal tissue was found for a limited number of mets. Table 1 denotes the median target coverage along with the range and MU/cGy. A qualitative assessment of the MLC travel noted a reduction in the amount of intra-target dose bridging. QA results from delivery to film yielded clinically acceptable pass rates for gamma criterion of 5%/1 mm at 10% threshold.

Conclusion A simple API driven script was successful at automating SIMT planning in Monaco. This yielded a clinically acceptable solution, and for a limited number of lesions provided a benefit to reducing the volume of irradiated normal tissue.

Acknowledgements: Genesiscare would like to acknowledge Elekta for an alpha agreement for scripting in Monaco 6.0.1.

References

1. Li, J., et al., Stereotactic radiosurgery versus whole-brain radiation therapy for patients with 4–15 brain metastases: a phase III randomized controlled trial. International Journal of Radiation Oncology, Biology, Physics, 2020. 108(3): p. S21-S22.
2. Pudsey, L.M., et al., The use of collimator angle optimization and jaw tracking for VMAT-based single-isocenter multiple-target stereotactic radiosurgery for up to six targets in the Varian Eclipse treatment planning system. Journal of applied clinical medical physics, 2021. 22(9): p. 171–182.
3. Mann, T.D., K.S. Thind, and N.P. Ploquin, Fast stereotactic radiosurgery planning using patient-specific beam angle optimization and automation. Physics and Imaging in Radiation Oncology, 2022. 21: p. 90–95.
4. Kang, J., et al., A method for optimizing LINAC treatment geometry for volumetric modulated arc therapy of multiple brain metastases. Medical physics, 2010. 37(8): p. 4146–4154.

Table 1. Summary of dosimetric parameters, median coverage, and range in parenthesis.

Patient	Number of targets	Median target coverage		MU/cGy	
		Clinical plan	Scripted plan	Clinical Plan	Scripted plan
1	2	98.4% (98.8%–98.0%)	99.03% (99.5%–98.5%)	1.9	2.3
3	5	98.4% (99.2%–98.1%)	99.8% (100.0%–98.1%)	6.1	3.5
5	11	98.4% (100.0%–98.4%)	99.0% (100.0%–99.3%)	7.0	7.6

O84. Abstract withdrawn

O85. [Invited] Uncertainties in theranostics—what value is knowing what we don't know?

George McGill[1,*]

[1]Queensland Health, Brisbane, Australia

O86. Modelling the effect of daughter migration on dosimetry estimates for Ac-225 in targeted alpha therapy

Stephen Tronchin[1,*], Jake Forster[1,2], Kevin Hickson[2,3], Eva Bezak[1,4]

[1]Department of Physics, University of Adelaide, Adelaide, Australia, [2]Medical Physics & Radiation Safety, South Australia Medical Imaging, Adelaide, Australia, [3]Allied Health & Human Performance, University of South Australia, Adelaide, Australia, [4]Cancer Research Institute, University of South Australia, Adelaide, Australia

Introduction Targeted Alpha Therapy (TAT) is a form of cancer treatment that delivers a highly localised dose to tumour cells while sparing the surrounding healthy tissue. In TAT, an alpha-emitting radionuclide is bound to a targeting vehicle, forming a radioimmunoconjugate (RIC). However, the decay energy of the alpha-emissions is sufficient to break the bond to the RIC, resulting in the release of free daughter radionuclides in the body. This is especially concerning for parent isotopes that produce multiple unstable daughters, such as actinium-225. In nuclear medicine dosimetry, daughter migration is generally not considered and the daughters are assumed to decay at the site of the parent. This can produce inaccurate dose estimates.

Method A complex multilevel compartment model for actinium-225 and its daughters was developed in Python, where we account for unique biokinetics by assigning each daughter unique transfer rates between compartments. Using this model, time-activity curves of each isotope were obtained for the different compartments. We determined organ doses for two scenarios: 1) assuming the daughters decay at the site of actinium, and 2) assigning the daughters unique biokinetics. Simulations were performed for 1 MBq of free actinium-225 placed in the plasma. The kidney dose was determined. We also performed a sensitivity study to see how changing the transfer rates between compartments impacts kidney dose.

Results When the daughters of actinium-225 have their own unique biokinetics, there is a 7.5% increase in kidney dose compared to assuming the daughters decay at the site of actinium-225. The sensitivity study revealed a 40% increase in kidney dose when the kidney clearance rate is reduced by a factor of 4.

Conclusion These results highlight that accurate absorbed dose estimates require accurate modelling of daughter biokinetics. Next, we plan to study doses to other organs and include tumour uptake/retention into the model.

O87. Evaluation of the performance parameters on the Biograph Vision PET/CT scanner using the NU2-2012

Subhash Kheruka[1,*], Naema Al Maymani[1], Noura Al Makhmari[1], Tasnim Al Rahii[1], Huoda Al Saidi[1], Khulood Al Riyami[1], Rashid Al Sukaiti[1]

[1]Department of Radiology and Nuclear Medicine, Sultan Qaboos Comprehensive Cancer Care and Research Centre, Muscat, Oman

Introduction To evaluate the performance of the Biograph Vision (Siemens Healthineers) PET/CT system. This new system is based on the Siemens Biograph Vision 600, using the same silicon photomultiplier-based detectors with 3.2 × 3.2 × 20-mm lutetium-oxoorthosilicate crystals. The Vision 8 detector rings provide the axial field of view (AFOV) of 26 cm, enabling imaging of major organs in a one-bed position.

Methods The new digital PET/CT features silicon photomultiplier (SiPM)based detectors with 3.2 mm lutetium oxyorthosilicate (LSO) crystals and full coverage of the scintillator area. The PET components incorporate eight rings of 38 detector blocks and each block contains 4 × 2 mini blocks. Each miniblock consists of a 5 × 5 LSOarray of 3.2 × 3.2x20 mm crystals coupled to a SiPM array of 16 × 16 mm, resulting in an axial field of view (FOV) of 26.1 cm. In this study, PET/CT system performance will be evaluated to conform

to the NEMA NU 2 2012 standard. The Spatial resolution, sensitivity, count rate performance, scatter correction, Time-of-Flight (TOF) performance, and image quality will be determined. Measurements will be directly compared to results from their predecessor.
Results The Biograph Vision shows a NEMA sensitivity of 15.1 kcps/MBq, an axial spatial resolution at Full Width Half Maximum (FWHM) of 3.5 mm at 1 cm offset of the center of the FOV, a NEMA peak NECR of 259 kcps at 32 kBq/mL and TOF timing resolution was 213.7 ps. The overall image contrast seen with the NEMA image quality phantom ranged from 80.79% to 90.86%.
Conclusions: The Biograph Vision is able to meet NEMA standards.

O88. Feasibility of 3D printed hollow spheres for quality assurance of Siemens quantitative reconstruction algorithm xSPECT bone

Tuyet Oanh Lam[1,*]

[1]Department of Medical Imaging and Nuclear Medicine, Gosford Hospital, Gosford, Australia

Introduction Quantitative accuracy and constancy of Siemens xSPECT Bone quantitative reconstruction algorithm (xBone) can be monitored using activity-filled hollow spheres, which could be 3D printed. 3D prints can have air gaps in the walls which may pose issues for attenuation correction and xBone tissue zone mapping. This study assesses the feasibility of using 3DP-S with materials PLA + , PETG and SL1-Resin as substitutes for commercially available hollow spheres (C-S) using xBone.
Method Phantom preparation and acquisition parameters were chosen based on the white paper [1]. A Jaszczak phantom was fitted with six ^{99m}Tc- and contrast-filled 3DP-S (0.5–17 mL) with a 1:5 background-to-sphere ratio (80:400 kBq/mL). SPECT/CT acquisitions were performed on the Siemens Intevo T6 (64 and 120 projections, 12-s/projection, contour orbit), and reconstructed with xBone. Region-of-interests for activity concentration measurements were drawn to the internal diameter of the spheres.
Results PLA + and PETG printed via filament freeform fabrication resulted in air gaps mainly at steep overhang. SL1-Resin printed via stereolithography experienced resin pooling and increased wall thickness due to viscosity and surface tension – the smallest sphere was not usable. Activity concentration recovery coefficients of the 3DP-S were compared to C-S.
Conclusion Elimination of air bubbles at filling were difficult due to material opacity and filling hole design. The air gaps from manufacturing the prints were not detected by the zone map and did not seem to impact quantitation. Excessive resin within the smaller SL1-Resin prints is suspected to cause PVE-related issues. 3DP-S may potentially be used for QA of xSPECT quantitative accuracy due to comparable recovery performance to C-S for volumes > 2 mL. Further experiments using redesigned 3DP-S are in progress investigating reproducibility and relationship between PVE and wall thickness amongst smaller spheres.
References

1. Vija AH (2017) Characteristics of the xSPECT reconstruction method. Siemens Medical Solutions USA, Inc., Molecular Imaging, White Paper. https://www.siemens-healthineers.com/molecular-imaging/mi-clinical-corner/whitepapers/xspect-reconstruction-method.html. Accessed 1 September 2021.

O89. [Invited] Mimicking motion and getting adaptation right in radiotherapy

Adam Yeo[1,*]

[1]Peter MacCallum Cancer Centre, Melbourne, Australia

Radiation therapy relies on accurate conformal delivery of radiation and one of the major challenges is the fact that organs move, squash and stretch in the abdomen regularly during breathing and due to organ filling and tumour response to treatment. The precision of modern radiotherapy techniques is limited by such anatomy changes along radiotherapy journey from CT simulation to treatment, resulting in different spatial components of tumours and surrounding organs 'seeing' different radiation doses than that planned. Such discrepancies between planned and delivered doses need to be thoroughly examined, to ensure tumours receive the correct radiation dose and surrounding organs are not overdosed.

Though there are now various commercial solutions available for offline and online adaptive radiotherapy (ART), there are still lack of tools to validate ART tools in terms of imaging, treatment planning and delivery verification. In this context, this Boyce Worthley Award talk overviews what the awardee achieved in the past and what is currently being studied in this ART domain. This talk is mainly consist of three parts: i) development of physical phantoms that can mimic patient motion and deformation to various extents, ii) validation of ART simulations for various RT applications (imaging, treatment planning and delivery), and iii) patient data evaluation of various ART scenarios that can affect outcome in standard of care radiotherapy as well as clinical trials.

Addressing anatomical changes throughout patient journey for radiotherapy has been one of the main challenges and it will be so in future. Therefore, it's guaranteed to see active research and development activities in this domain, and the author looks forward to contributing further to enhance clinical outcome in precision adaptive radiotherapy.

O90. First in-human use of real-time tumour tracking for liver SBRT on a standard Elekta linear accelerator

Chandrima Sengupta[1,*], Doan Trang Nguyen[1], Catherine Jones[2], Ben Perrett[2], Sau Fan Liu[2], Elizabeth Brown[2], Daniel Mason[3], Trent Causer[3], Jianjie Luo[3], Ricky O'Brien[1], Jeremy Booth[4], Yoo Young Lee[2], Tim Wang[5], Paul Keall[1]

[1]ACRF Image X Institute, Sydney, Australia, [2]Princess Alexandra Hospital, Brisbane, Australia, [3]Nepean Cancer Care Centre, Sydney, Australia, [4]Royal North Shore Hospital, Sydney, Australia, [5]Crown Princess Mary Cancer Centre, Sydney, Australia

Introduction We developed and clinically implemented a cancer targeting technology named Kilovoltage Intrafraction Monitoring (KIM) [1] for liver tumour motion tracking during stereotactic body radiation therapy (SBRT) on a standard Elekta linear accelerator (linac) in the TROG LARK trial [2]. We report on the first in-human prospective use of KIM for liver SBRT patients on Elekta linacs.
Methods The KIM system was adapted to meet the requirements of liver SBRT. A quality assurance program was developed using a 6 degrees-of-freedom robotic phantom. A clinical workflow was developed to treat liver cancer patients with KIM. Three patients were enrolled in the trial at two centres with Elekta linacs. The patients were treated either at end-exhale breath-hold (EEBH) or deep-inspiration breath-hold (DIBH) using 6FFF plans. Three gold markers were implanted near the tumour for internal motion tracking with KIM. During treatment, Active Breathing Control (ABC) was used to

control patient's breath-hold. A gating threshold of 3 mm (EEBH patients) and 5 mm (DIBH patients) was set in KIM. Motion outside this gating threshold was corrected by applying an equivalent couch shift triggered by KIM (Fig. 1). Triangulation method was used to evaluate KIM accuracy during treatment. Motion-included dose reconstruction method was developed to evaluate the dosimetric accuracy achieved with KIM-guidance.

Results KIM was successfully clinically implemented on Elekta linacs with tracking accuracy and precision being < 2 mm. A total of 7 intrafraction couch shifts was triggered by KIM when ABC was insensitive to this motion. $1.2 \pm 0.2\%$ better dosimetric accuracy was achieved with KIM-guidance for PTV D95 compared to standard-of-care treatment.

Conclusions The treatments demonstrated the importance of real-time internal tumour motion tracking with KIM. Motion outside the treatment tolerance was detected with KIM, however not detected by ABC. This achievement paves the way for broader adoption of KIM to improve cancer targeting and dosimetric accuracy.

References

1. Hewson EA, Nguyen DT, O'Brien R et al., The accuracy and precision of the KIM motion monitoring system used in the multi-institutional TROG 15.01 Stereotactic Prostate Ablative Radiotherapy with KIM (SPARK) trial. Med Phys. 2019;46(11):4725–4737. https://doi.org/10.1002/mp.13784.
2. Lee YYD, Nguyen DT, Moodie T et al., Study protocol of the LARK (TROG 17.03) clinical trial: a phase II trial investigating the dosimetric impact of Liver Ablative Radiotherapy using Kilovoltage intrafraction monitoring. BMC Cancer. 2021 May 3;21(1):494.

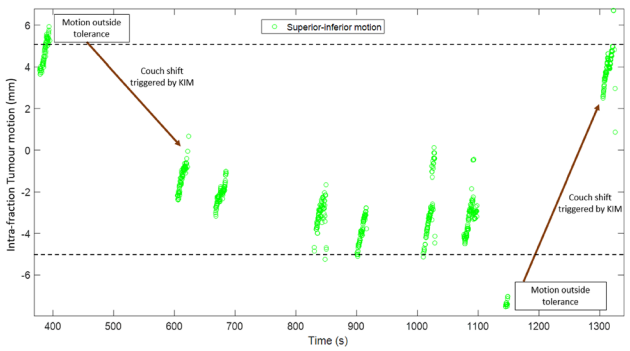

Fig. 1. Intra-fraction tumour motion in one of the fractions where large superior-inferior motion was detected by KIM, triggering couch shifts.

O91. Free breathing SBRT for moving tumors-basics of 4-dimensional patient specific quality assurance

Jaysree Ukath[1,2], Prabhakar Ramachandran[1], Annette Haworth[2]

[1]Princess Alexandra Hospital, MSH, QLD HEALTH, Woolloongabba, Australia, [2]School of Physics, University of Sydney, Camperdown, Australia

Introduction To implement a novel robotic arm and motion control software to drive a dosimetric phantom and perform preliminary measurements with and without motion traces, to verify breathing motion incorporated in the patient specific quality assurance (PSQA) for free breathing stereotactic body radiation therapy (SBRT) of thoracic tumors.

Method A commercially available robotic arm system (Universal Robots, Odense, Denmark) and robotic motion control software (GitHub; University of Sydney) [1, 2] were used to drive an acrylic phantom (dimensions of $20 \times 20 \times 4$ cm) with provision to hold EBT3 Gafchromic film. The robotic motion system was evaluated in terms of set-up, motion trace repeatability, static localization accuracy and dynamic localization accuracy. Two motion amplitudes of 5 mm and 8 mm in the sup- inf and the ant- post directions were studied for 5, 12 and 20 breath per minute (BPM) respiration groups. In-house film dosimetry software was used for dose map creation, and commercial software was used for gamma analysis at a set pass criterion of 95% points to be within 2% or 2 mm of predicted values above a 10% threshold.

Results The phantom localization accuracy was found within 0.5 mm. Comparisons with and without motion indicated that the gamma pass rates reduced with motion depending on amplitude and breath rate. For lower amplitudes in sup-inf direction, a breathing rate effect was visible only beyond 12 BPM. Higher amplitudes of sup-inf motions affected dosimetry in both sup-inf and lateral directions. For ant-post motions, coronal pass rates were higher compared to sup-inf motions of the same amplitude, but the higher the amplitude the lower the pass rate.

Conclusion Preliminary results indicate that this system may be more suitable for pre-treatment patient-specific quality assurance compared with currently available commercial systems to better understand the validity of margins used in treatment planning.

References

1. Shiinoki, Fujii, F., Fujimoto, K., Yuasa, Y., & Sera, T. (2020). A novel dynamic robotic moving phantom system for patient-specific quality assurance in real-time tumor-tracking radiotherapy. Journal of Applied Clinical Medical Physics, 21(7), 16–28. https://doi.org/10.1002/acm2.12876
2. Alnaghi, Kyme, A., Caillet, V., Nguyen, D. T., O'Brien, R., Booth, J. T., & Keall, P. J. (2019). A six-degree-of-freedom robotic motion system for quality assurance of real-time image-guided radiotherapy. Physics in Medicine & Biology, 64(10), 105,021–105,021. https://doi.org/10.1088/1361-6560/ab1935

O92. Respiratory motion management using three breath-hold planning CTs for lung and liver stereotactic ablative body radiotherapy (SABR)

Erin Seymour[1,*], Benjamin Zwan[1], Benjamin Tacon[1], Rebecca Cone[1], Simon Tang[1]

[1]Central Coast Cancer Centre, Gosford, Australia

Introduction Treating stereotactic lung and liver patients in breath-hold (BH) is a popular technique used to mitigate the internal target motion experienced by patients due to respiration [1]. Standard planning margins are typically applied in practice even though the reproducibility of internal anatomy during BH can be highly variable between patients. Acquiring three BH (3BH) CTs at simulation can account for intrafraction motion in patients with poor BH reproducibility [2]. This study aims to assess whether collecting 3BH simulation scans to produce a combined gross tumour volume (iGTV) is superior to using the single BH approach.

Method Ten lung and ten liver SABR patients who had iGTVs comprised from 3BHCTs had retrospective data collected to examine the differences in planning target volumes (PTVs) when using a single or 3BH approach with standardised margins (3BH: 5 mm

symmetric, single BH: 5 mm symmetric, 10 mm craniocaudal). The 3BH margins were also reviewed to ensure they account for patient specific intrafraction motion variability as measured with mid- and post-CBCTs during each treatment fraction.

Results 8/10 lung patients and 5/10 liver patients had reduced PTVs using the 3BH approach. For all patients, the BH reproducibility (defined by the standard deviation of all measured CBCT shifts) was less than the specified 5 mm PTV margin in all directions. The craniocaudal direction measured the largest uncertainty, with an average of 3.1 mm and 2.4 mm for lung and liver respectively.

Conclusion Assessment of patient-specific BH reproducibility during simulation, in conjunction with intrafraction monitoring, allows treatment margin reduction and healthy tissue sparing for a substantial proportion of lung and liver SABR patients. Conversely, it highlights when an increase in volume is required to account for poor BH reproducibility so that target coverage is not compromised during treatment.

References

1. Kimura T, Hirokawa Y, Murakami Y, Tsujimura M, Nakashima T, Ohno Y, Kenjo M, Kaneyasu Y, Wadasaki K, Ito K (2004) Reproducibility of organ position using voluntary breath-hold method with spirometer for extracranial stereotactic radiotherapy. Int J Radiat Oncol, Biol, Phys 60(4):1307–1313.
2. Lu L, Ouyang Z, Lin S, Mastroianni A, Stephans K, Xia P (2020) Dosimetric assessment of patient-specific breath-hold reproducibility on liver motion for SBRT planning. J Appl Clin Med Phys 21(7):77–83. https://doi.org/10.1002/acm2.12887

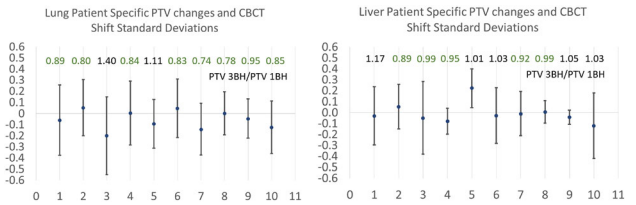

Figs. 1 and 2. PTV ratios and measured standard deviations from all CBCT treatment shifts.

O93. Evaluation of set-up accuracy for a large cohort of radiotherapy patients positioned with SGRT-only without the aid of skin-marks at a single institution

Mantaj Sekhon[1,2,*], Catherine Russell[2], Rick Franich[1], Vanessa Panettieri[2,3,4]

[1]School Of Science, RMIT University, Melbourne, Australia, [2]Alfred Health Radiation Oncology, Alfred Hospital, Melbourne, Australia, [3]Central Clinical School, Monash University, Melbourne, Australia, [4]Medical Imaging and Radiation Sciences, Monash University, Clayton, Australia

Introduction Surface-Guided Radiotherapy (SGRT) is increasingly being used for patient set-up and intrafraction motion monitoring. Traditionally skin-marks with room-mounted lasers were used [1,2] but a shift to SGRT-only workflows is occurring globally due to potentially reduced set-up times and improved psychosocial impact. There has been hesitancy by clinics in adopting this technique, particularly for abdomen/pelvic regions due to possible poor correlation between patient surface and deep internal targets. This study focusses on evaluating set-up accuracy of SGRT-only positioning for abdomen/pelvic anatomical sites in a large cohort of patients treated at a single institution.

Method A total of 316 patients (n = 4883 fractions) positioned with SGRT-only between 2018–2021 at our institution were studied. After positioning, Cone-Beam-CT (CBCT with either soft or bony-match) or kV-kV paired pre-treatment verification images were acquired. Setup accuracy was evaluated based on the pre-treatment translational corrections applied. Statistical differences in the mean set-up error of two group means was tested using an independent two-tailed t-test at a significance level of $\alpha = 0.05$ (Python). Comparison with published skin-mark based methods was also performed.

Results SGRT-only mean set-up errors obtained by either CBCT with both matching techniques or kV-kV pairs (Table 1) were equivalent to skin-mark based positioning for both anatomies [3,4]. SGRT-only positioning sorted by CBCT-match type showed that soft tissue match was significantly more accurate in the longitudinal (-1.1 mm vs 3.1 mm- $p = 0.025$) direction than CBCT-bony match in the abdomen. Differently, CBCT-bony tissue match was more accurate in the pelvis in the vertical direction (-1.3 mm vs -2.2 mm-$p < 0.001$), proving no clear trend of one of the other matching method after SGRT-only setup (Fig. 1).

Conclusion SGRT-only patient positioning for the abdomen and pelvis was found to perform similarly or superiorly to traditional skin-mark-based set-up, reinforcing its usefulness in clinical practice.

References

1. Probst, H., Dodwell, D., Gray, J. C., & Holmes, M. (2006). An evaluation of the accuracy of semi-permanent skin marks for breast cancer irradiation. Radiography, 12(3): 186–188.
2. Rathod, S., Munshi, A., & Agarwal, J. (2012). Skin markings methods and guidelines: A reality in image guidance radiotherapy era. South Asian J Cancer, 1(1): 27–29.
3. Carl, G., Reitz, D., Schönecker, S., Pazos, M., Freislederer, P., Reiner, M., Alongi, F., Niyazi, M., Ganswindt, U., Belka, C., & Corradini, S. (2018). Optical Surface Scanning for Patient Positioning in Radiation Therapy: A Prospective Analysis of 1902 Fractions. Technol Cancer Res Treat, 17:1,533,033,818,806,002.
4. Walter, F., Freislederer, P., Belka, C., Heinz, C., Söhn, M., & Roeder, F. (2016). Evaluation of daily patient positioning for radiotherapy with a commercial 3D surface-imaging system (Catalyst^{TM}). Radiat Oncol, 11(1): 154.

Table 1. The mean setofup accuracy and standard deviation (in brackets) of SGRT-only positioning compared to skin-marks based positioning provided in the literature (for CBCT all matches and kV-kV pair images).

Anatomical site	Direction	Mean signed error of SGRT-only positioning	Mean error of skin mark-based positioning (Carl et al [3])	Mean error of skin mark-based positioning (Walter et al [4])
Abdomen CBCT	Vertical (mm)	-1.5 (3.3)	0.68 (3.9)	2.1 (2.7)
	Longitudinal (mm)	-2.0 (6.5)	1.56 (4.2)	-0.4 (1.2)
	Lateral (mm)	-0.1 (6.2)	-0.06 (4.0)	2.2 (1.3)
Pelvis CBCT	Vertical (mm)	-1.3 (3.6)	-	1.0 (1.1)
	Longitudinal (mm)	-1.8 (4.8)	-	0.4 (1.4)
	Lateral (mm)	0.2 (1.8)	-	-0.9 (1.4)
Abdomen kV-kV pair	Vertical (mm)	-0.7 (4.4)	0.68 (3.9)	2.1 (2.7)
	Longitudinal (mm)	-0.9 (5.3)	1.56 (4.2)	-0.4 (1.2)
	Lateral (mm)	0.9 (3.1)	-0.06 (4.0)	2.2 (1.3)
Pelvis kV-kV pair	Vertical (mm)	-1.1 (3.2)	-	1.0 (1.1)
	Longitudinal (mm)	-1.8 (5.4)	-	0.4 (1.4)
	Lateral (mm)	0.1 (2.9)	-	-0.9 (1.4)

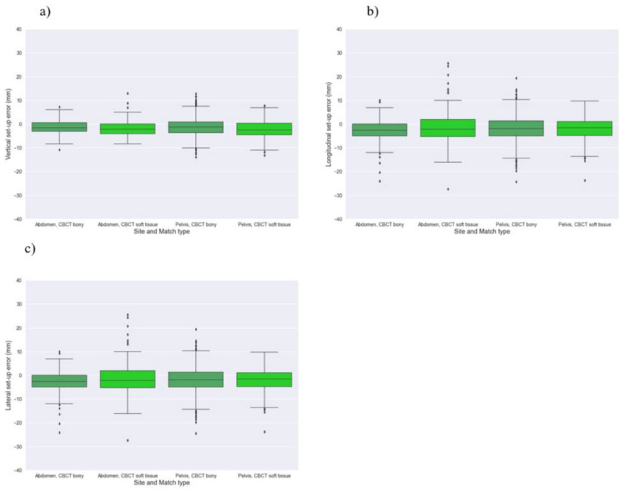

Fig. 1. Boxplots of the set-up error in the a) vertical b) longitudinal c) lateral and d) rotation directions sorted by anatomical sites and imaging types. The middle line represents the mean signed error in Table1.

O94. [Invited] The magic of photon-counting CT

Magdalena Bazlova-Carter[1,*]

[1]University of Victoria, Victoria BC, Canada

O95. Phase marker—a novel method of verifying phase accuracy of 4D CT/CBCT

Roger Li[1,*], Chris Low[1], Jidi Sun[1,2]

[1]Genesiscare Victoria, Melbourne, Australia, [2]Peter Mac Cancer Centre, Melbourne, Australia

Introduction 4D CT/CBCT is a technique of acquiring patient's tomographic images that are affected by breathing motion. The images of moving target are sorted and grouped into phases of breathing cycle during the 4D CT/CBCT post processing called binning. The accuracy or the correctness of the (often ten) phases is critical for target positioning and treatment delivery if gated technique is employed. We have developed a method to verify the accuracy of phases and the performance of 4D CT/CBCT.

Methods A strip of water equivalent material was attached onto a motion phantom that simulates breathing cycles, in a way that the strip coincides with the peak of inhalation. This design establishes a link between temporal phases to the physical location of this stripe. When imaged by CT or CBCT, the orientation of the strip resembles a hand in a clock and indicates the phase of that image. It is named as phase marker (see Fig. 1.)

Results Fig. 2 are the images of the phaser marker scanned on GE CT and Varian CBCT. The top images are ten separate phase images on GE CT. The orientation of the strip indicates the phase. When played in a movie mode, it rotates clockwise from phase one to phase ten. The middle image in Fig. 2 shows a MIP image of all phases on Varian Truebeam 4D CBCT. The fan shape of the images is intra-phase artefact manifested differently in 4D CBCT comparing to 4D CT. The bottom images in Fig. 2 show a gated CBCT verification for the phase 4, 5 and 6, that is widely used in liver and pancreatic cancer treatment where the end of exhalation is treated. It has confirmed that the gated CT was performed correctly.

Conclusion The phase marker provides a direct measure of the phase accuracy and correctness of 4D CT/CBCT and gives medical physicists a high level of confidence of the performance of the equipment, therefore, it can be widely used for commissioning and ongoing QA of gated CBCT, 4D CT/CBCT.

References

1. Varian Medical System, 2017, TrueBeam Technical Reference Volume 2: Imaging.
2. Varian Medical System, 2012, RPM Respiratory Gating System Reference Guide,
3. Keall PJ and et al., The management of respiratory motion in radiation oncology report of AAPM Task Group 76, Med Phys, 2006, 33(10):3874–900.
4. Low D, Clinical use of 4DCT, presentation, AAPM summer school, 2006.
5. Jiang SB, Management of moving targets in radiotherapy, presentation, AAPM summer school, 2006.

Fig. 1. A phantom illustrates the concept of phase marker.

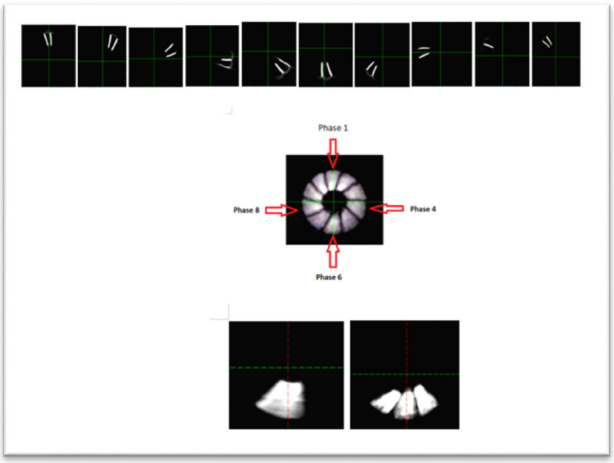

Fig. 2. Phase marker imaged by CT and CBCT.

O96. A benchtop prototype Eu-155 dual-energy CBCT system for adaptive proton therapy applications

Mitchell Herrick[1,2,*], Scott Penfold[1,3], Kevin Hickson[2], Alexandre Santos[1,3,4]

[1]University of Adelaide, Adelaide, Australia, [2]SA Medical Imaging, SA Health, Adelaide, Australia, [3]Australian Bragg Centre for Proton Therapy and Research, Adelaide, Australia, [4]Department of Radiation Oncology, RAH, Adelaide, Australia

Introduction Inter-fractional anatomical changes can impact the quality of proton therapy treatment plans. Online adaptive proton therapy (APT) requires quantitatively accurate 3D images acquired immediately before treatment to adapt the planned dose delivery to these changes. Helical single-energy or dual-energy computed tomography (CT) images are the current standard for accurate quantitative tissue measurements, yet they currently cannot be acquired at treatment isocentre. Conventional cone beam CT (CBCT) systems can acquire images at treatment isocentre, however, are not appropriate for accurate quantitative tissue measurements due to increased scatter. Here we present preliminary results from a benchtop prototype Eu-155 based dual-energy CBCT system, which ultimately aims to provide a solution for accurate relative stopping power (RSP) measurements at treatment isocentre.
Method The benchtop prototype consists of a radioactive Eu-155 source opposing a pixelated spectroscopic CZT detector panel. An in-house phantom containing tissue equivalent inserts of known composition was scanned. A simulation of the physical setup was constructed using Geant4. Low and high energy images using both the physical and simulation data were reconstructed using the 86.5 keV and 105.3 keV gamma emissions of Europium-155. Measured attenuation coefficients were compared to theory and a modified RSP parameterisation method was used to extract RSP information.
Results Measured attenuation coefficients were systematically lower than the expected value due to coherent scatter and artefacts present in the image reconstruction. Simulated results, with coherent scatter turned off, agreed well with theory with a RMSE of 0.46% for attenuation coefficient measurements and a RMSE of 0.63% for RSP measurements.
Conclusion We have demonstrated the feasibility of this prototype under geometric conditions that reduce the influence of coherent scatter. Further work is needed to improve the image quality of our prototype for RSP measurements.

O97. Real-time optically stimulated luminescence (rtOSL) fibre-coupled dosimetry with beryllium oxide

Erin Lukas[1], Levi Madden[2,3], Alexandre Santos[1,4], Miftar Ganija[1,5], Peter Veitch[1], Anatoly Rosenfeld[2], Enbang Li[2]

[1]School of Physical Sciences, University of Adelaide, Adelaide, Australia, [2]Centre for Medical Radiation Physics, University of Wollongong, Wollongong, Australia, [3]Northern Sydney Cancer Centre, Royal North Shore Hospital, St Leonards, Australia, [4]Department of Medical Physics, Royal Adelaide Hospital, Adelaide, Australia, [5]Defence Science and Technology, Edinburgh, Australia

Introduction Beryllium oxide (BeO) coupled fibre-optic dosimeters possess many desirable characteristics for radiation dosimetry, including high sensitivity, compact size, simple design, and a flat energy response across therapeutic energy ranges. However, light produced in the optical fibre during irradiation can significantly perturb dose measurements. This "stem" signal must be removed to ensure accurate dose measurement. Furthermore, BeO's luminescence signal is non-linear with absorbed dose and must also be corrected. The purpose of this work is to quantify the dose–response uncertainties of the BeO coupled fibre-optic dosimetry system using a novel stem correction method.
Method In this work, we apply the real-time optically stimulated luminescence (rtOSL) method [1] to produce stem-free dose measurements with a BeO fibre-optic dosimeter; an example of the measured signals and stem-corrected rtOSL signal are shown in Fig. 1. Deconvolution analysis was applied to correct the non-linearity in the rtOSL signal. Measurements were performed using a clinical linear accelerator (Varian TrueBeam, Palo Alto, CA, USA). Dose rate response was assessed by varying the repetition rate and SSD. Dose–response uncertainty was determined through the deconvolution analysis method.
Results The processed rtOSL measurements are observed to be linear with dose rate and are free of the stem effect. However, the rtOSL signal begins to saturate with accumulated dose. Deconvolution analysis proved to be the most effective signal correction method of those tested, with a mean difference of 1.5% from corresponding known doses.
Conclusion The rtOSL method was successful in removing stem luminescence from the detector signal. However, saturation effects reduce the effectiveness of the detector system. Though computational modelling has been implemented to correct this nonlinearity, we intend to further optimise the hardware to improve its dosimetric accuracy.

References

1. Polf JC et al. (2004) Real-time luminescence from Al_2O_3 fiber dosimeters. Radiat Meas 38:227–240

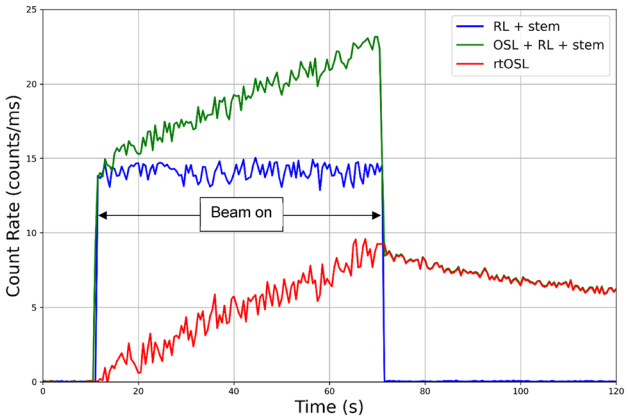

Fig. 1. Sample of the measured and derived signals using the rtOSL method.

O98. Response of ruby based optic dosimetry system to flourine-18

Shalee Birajdar[1,*], Wen Qi Zhang[1], Alexandre Santos[2,3], Kevin Hickson[4], Shahraam Afshar[1]

[1]Laser Physics and Photonic Devices Laboratories, UNISA STEM, The University of South Australia, Mawson Lakes, SA 5095, Adelaide, Australia, [2]Department of Medical Physics, Royal Adelaide Hospital, Adelaide, SA 5000, Adelaide, Australia, [3]School of Physical Sciences, The University of Adelaide, Adelaide, SA 5005, Adelaide, Australia, [4]Medical Physics & Radiation Safety, SA Medical Imaging, Adelaide, SA 5000, Adelaide, Australia

Introduction Selective internal radiation therapy (SIRT) with yttrium-90 (Y-90) is a commonly used liver cancer treatment. The dose delivered to a patient is verified from the Y-90 distribution obtained by post-treatment images. In vivo dosimetry (IVD) refers to techniques that measure the dose delivered to the patient during the treatment and help to ensure the accurate dose delivery of radionuclide therapy. To date, there has been no report of any IVD technique during SIRT. The goal of our study is to investigate the concept of fibre optic dosimetry (FOD) as an IVD technique for the real-time dose rate measurement during SIRT. Here, we investigate the response of a ruby FOD to a readily available fluorine-18.
Method The ruby FOD system consists of a fibre optic probe fabricated by attaching a half-sphere ruby of 1 mm diameter to a silica fibre of 600 μm core diameter, and a reader. The ruby emits light via radioluminescence (RL), with the intensity ideally proportional to the exposure dose rate, i.e. time decaying activity of F-18. The reader detects RL light and displays the RL counts/sec in response to time decaying activity.
Results The RL count rate response of ruby FOD to the time decaying activity of F-18 showed a strong positive linear relationship. The estimated half-life of F-18 from the RL count rate data, 109 ± 1 min, was in good agreement with the actual half-life,109.77 min.
Conclusion The ruby FOD has demonstrated linear RL response with varying dose rates, a desirable characteristic of an ideal dosimeter. Further studies include the dosimetric characteristics of ruby FOD and validating the image-based dosimetry used in SIRT.

O99. CPAP in SABR: clinical worth for centrally located lung tumours

Suzanne Lydiard[1,2,*], Uta Machold[2], Gareth Le Grice[2], Clair King[3], S. Hussain[3], Louis Lao[2]

[1]Kathleen Kilgour Centre, Tauranga, New Zealand, [2]Cancer & Blood, Radiation Oncology, Auckland City Hospital, Auckland, New Zealand, [3]Respiratory & Sleep laboratory, Auckland City Hospital, Auckland, New Zealand

Introduction Continuous positive airway pressure (CPAP), commonly used for sleep apnoea, can reduce lung tumour motion and increase lung and heart dose sparing in lung radiotherapy [1,2]. This work aims to explore the clinical worth of CPAP in SABR treatments of centrally located lung tumours by evaluating patient tolerability, tumour displacement to critical structures and plan dosimetry.
Method Fourteen study participants practiced breathing with CPAP at a pressure of 15 cmH_20. 3D and 4D CT simulation was then performed twice for each participant: (i) free-breathing and (ii) with CPAP. Participants ranked their CPAP experience from 1 (very good) to 10 (very bad). A 3DCRT plan prescribed to 60 Gy in 8 fractions was created for each dataset and plan dosimetry was compared. Participants were treated with CPAP if the Radiation Oncologist deemed the CPAP plan superior. Retrospective analysis compared minimum 3D tumour displacements to critical structures.
Results Participants generally tolerated CPAP well, on average scoring CPAP tolerability, pressure comfort and mask comfort all 3 at simulation. However, two participants withdrew from the study during CT simulation due to CPAP discomfort. Of the twelve participants who underwent double simulation, CPAP provided superior overall plan dosimetry in eight participants (67%). Compared to free-breathing, on average CPAP displaced tumours further away from the heart by 5 mm, oesophagus by 0.5 mm, trachea by 2 mm and great vessels by 2 mm. As seen in Fig. 1, this resulted in the CPAP plan having on average lower maximum heart and great vessels doses, but higher maximum esophagus and trachea doses.
Conclusion CPAP was well tolerated, displaced many critical structures away from centrally located lung tumours and provided superior overall plan dosimetry in 67% of analysed participants compared to free-breathing.
Acknowledgements: Thank you to all of the clinical Radiation Oncology and respiratory staff who helped support this trial.
References

1. Goldstein JD, Lawrence YR, Appel S, et al. (2015) Continuous positive airway pressure for motion management in stereotactic body radiation therapy to the lung: A controlled pilot study. Int J Radiat Oncol Biol Phys 93, 391–399 doi: 0.1016/j.ijrobp.2015.06.011.
2. Jacobson G, Lawrence YR, Appel S, et al. (2021) Benefits of Continuous Positive Airway Pressure (CPAP) During Radiation Therapy: A Prospective Trial. Int J Radiat Oncol Biol Phys 1;110(5):1466–1472. https://doi.org/10.1016/j.ijrobp.2021.03.044

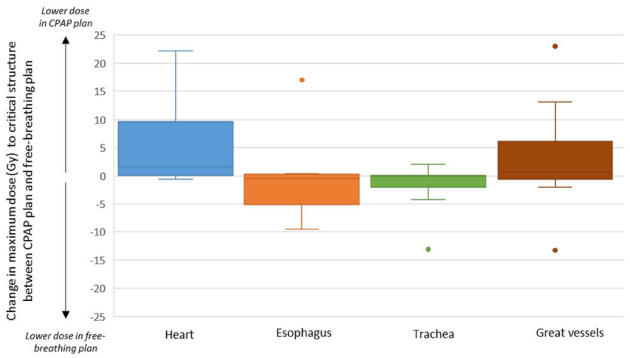

Fig. 1. Box and whisker plot illustrating the differences in maximum doses to critical structures between CPAP and free-breathing treatment plans.

O100. T-spine SABR, should 4DCTs be used for dose calculation?

Phil Tai[1,*], Nick Hardcastle[1,2,3], Tomas Kron[1]

[1]Physical Sciences, Peter MacCallum Cancer Centre, Melbourne, Australia, [2]Sir Peter MacCallum Department of Oncology, University of Melbourne, Melbourne, Australia, [3]Centre for Medical Radiation Physics, University of Wollongong, Wollongong, Australia

Introduction In patients receiving SABR to T7-T12 vertebra, doses to adjacent organs may vary with the path length through a diaphragm moving with respiratory motion [1]. A 3DCT planning image could represent one extreme, either inhale/exhale. In our institution, we use 4DCTs to account for varying radiological pathways through the diaphragm. We aimed to quantify the differences in dose to the spinal cord as the diaphragm moves with respiratory motion.
Method In 30 patients receiving SABR to T7-T12 planned on the average of a 4DCT (AVG), the plan and structures were copied from the AVG to the inhale/exhale phases and the dose recalculated. Plans consisted of a two-arc VMAT plan using AcurosXB reporting dose to medium. The spinal cord planning target volume (PRV) is defined by bony canal or 2 mm margin from an MRI-determined true cord. The near maximum dose (D0.03 cc) to the cord PRV was extracted and normalised to the value from the plan calculated on the AVG. The results were categorised based on approximate proximity to diaphragm.
Results The D0.03 cc calculated on the inhale image was on average 1.3% higher than on the AVG (range -0.1 – 5.8%), and 0.5% higher when calculated on the exhale (range -3.2 – 3.9%) (Fig. 1). The largest difference between the inhale/exhale cord doses, up to 3.2%, occurs for vertebra above and at the level of diaphragm (Fig. 2) as expected due to the movement of the diaphragm in field.
Conclusion Differences in dose to the spinal cord due to the variation in path length as the diaphragm moves are modest. In some patients the near maximum cord PRV dose was up to 5.8% higher, however this would represent the extreme and the true difference would likely be lower as the diaphragm continuously moves during treatment.
References

1. Wang X, Ghia A, Zhao Z et al. "Prospective evaluation of target and spinal cord motion and dosimetric changes with respiration in spinal stereotactic body radiation therapy utilizing 4-D CT" Jour. Of Radiosurgery and SBRT Vol 4 pp191-201 (2016).

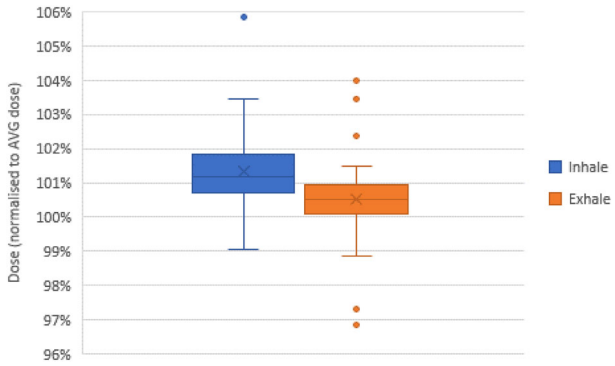

Fig. 1. Normalised spinal cord dose organised by breathing phase. The median dose is displayed as the horizontal bar within each box. The mean dose is shown as the cross inside each box.

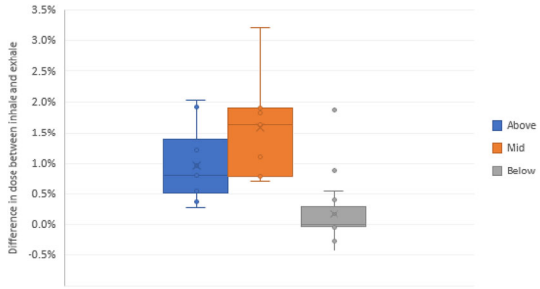

Fig. 2. Difference between normalised inhale and exhale cord doses depending on proximity to diaphragm. Difference was calculated as inhale dose – exhale dose.

O101. Impact of camera occlusion on surface guided radiation therapy for SRS treatments

Joerg Lehmann[1,2,3,*]

[1]Calvary Mater Newcastle, Newcastle, Australia, [2]University of Newcastle, Newcastle, Australia, [3]University of Sydney, Sydney, Australia

Introduction Surface guided radiation therapy (SGRT) systems generally use multiple camera pods one or two of which can be occluded with gantry rotation on C-arm linac treatment systems (Fig. 1). Guideline documents [1,2] recommend checking the max impact of camera occlusion during commissioning. For clinical practice in the context of stereotactic (SRS) treatments it is desirable to understand the gantry angle specific deviations to be expected. This work reports on measurements addressing this need and the clinical recommendations formed on their basis.
Method The response of the C-Rad Catalyst + HD system in treatment mode (cMotion) was recorded with stationary phantoms positioned in realistic treatment positions for relevant gantry angles. Using the exported cMotion trace, average deviations per gantry angle were calculated. Data recorded while the gantry was moving between measurement points was excluded. Measurements were performed with different phantoms, including two head phantoms, and for different isocentre positions within the phantom.
Results Observing a stationary phantom Catalyst should report zero position deviations. However, for gantry angles at which one camera pod is blocked from view of the phantom, the system reported erroneous deviations. For the SRS setups these deviations exceeded 1 mm

when the isocentre depths was 0 and 15 cm, and 0.3 mm for 5 cm (Fig. 2). These findings surpass literature values of < 0.2 mm[3] and ≤ 0.4 mm[4], but match our clinical experience. Smaller deviations were seen in breast and prostate setups where larger regions of interest are used with the SGRT system.

Conclusions Camera occlusion can cause erroneous deviation reporting of > 1 mm for SRS treatments. The magnitude of the error depends on isocentre position. Gantry angles between -90° and -5° are most affected, indicating a stronger impact on the left than the right camera for the current system. Individual assessments need to be made for each system and after relevant software upgrades.

References

1. Al-Hallaq HA, Cerviño L, Gutierrez AN, Havnen-Smith A, Higgins SA, Kügele M, Padilla L, Pawlicki T, Remmes N, Smith K, Tang X,Tomé WA (2022) AAPM task group report 302: Surface-guided radiotherapy. Med Phys. https://doi.org/10.1002/mp.15532
2. Freislederer P, Batista V, Öllers M, Buschmann M, Steiner E, Kügele M, Fracchiolla F, Corradini S, de Smet M, Moura F, Perryck S, Dionisi F, Nguyen D, Bert C, Lehmann J (2022) ESTRO-ACROP guideline on surface guided radiation therapy. Radiother Oncol. https://doi.org/10.1016/j.radonc.2022.05.026
3. Wiant DB, Liu H, Hayes TL, Shang Q, Mutic S, Sintay B (2019) Direct comparison between surface imaging and orthogonal radiographic imaging for SRS localization in phantom. J Appl Clin Med Phys. https://doi.org/10.1002/acm2.12498
4. Peng L, Kahler D, Li JG, Smaant S, Yan G, Amdur R, Liu C (2010) Characterization of a real-time surface image-guided stereotactic positioning system. Med Phys. https://doi.org/10.1118/1.3483783

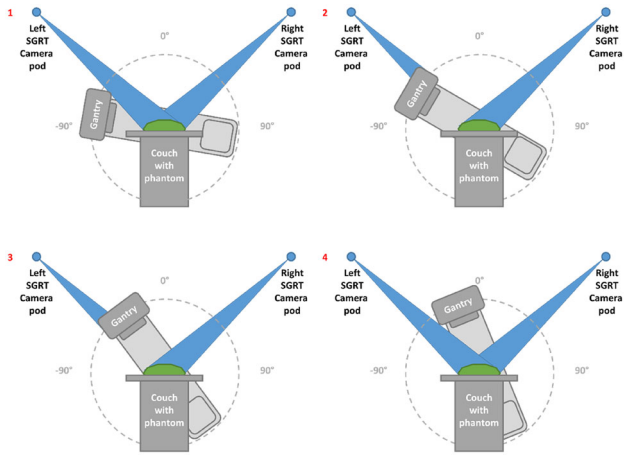

Fig. 1. Illustration of the occlusion of the left SGRT camera pod with clockwise rotating gantry. Total occlusion occurs between positions 2 and 4, partial occlusion between 1 and 2, and 3 and 4. Not shown: central SGRT camera pod above the foot of the couch.

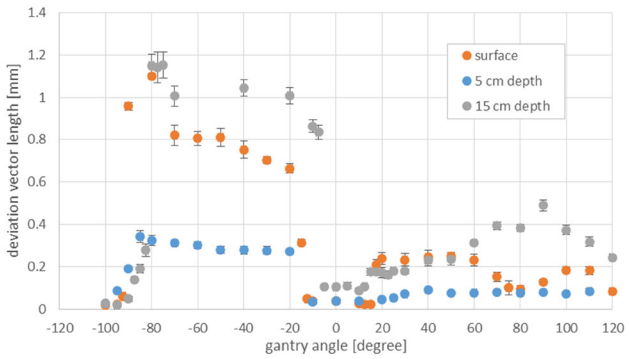

Fig. 2. Erroneous deviations for a stationary head phantom with a midline isocentre at the anterior phantom surface and at 5 and 15 cm depths.

O102. An anthropomorphic 3D printed inhomogeneity thorax phantom slab for SABR commissioning and quality assurance

Stephen How[1,*], Dilli Banjade[1], Scott Crowe[2], Greg Dillon[1], Andrew Skimmings[3]

[1]Central West Cancer Care Centre, Orange, Australia, [2]Royal Brisbane and Women's Hospital, Herston, Australia, [3]North West Cancer Care Centre, North Tamworth, Australia

Introduction Anthropomorphic phantoms with tissue equivalency are required in radiotherapy for quality assurance of imaging and dosimetric processes used in radiotherapy treatments. An example is stereotactic body radiotherapy (SBRT) treatments which typically treats small targets located within inhomogeneous tissues such as lung and bone [1]. A cost-effective anthropomorphic 3D printed phantom can be 3D printed in clinical departments to accurately simulate inhomogeneity for robust commissioning and quality assurance in SBRT [2].

Method An anthropomorphic thoracic slab phantom was designed and 3D printed from a CT dataset ([O102] **Fig. 9**). It was manufactured from polylactic acid with an in-fill density of 80% to simulate tissue equivalency and 26% to simulate lung equivalency. A readily available radio-opacifier, barium sulfate ($BaSO_4$), was added 6% w/w to an epoxy resin mixture to simulate similar HU numbers for bone equivalency. A half-cylinder was cropped away from the spine region to allow the insertion of a bone equivalent mixture. Two Gafchromic^{TM} EBT3 film strips were inserted into the 3D printed phantom for dosimetric measurement of two stereotactic radiotherapy plans targeting lung and bone lesions respectively.

Results The average HU number on the 3D printed phantom for tissue was 0 HU (= 0.99), lung was -650 HU (= 0.35) and bone was + 700 HU (= 1.40). The film results were analysed using SNC Patient with a low dose threshold of 10% and a gamma criterion of 3%/2 mm and 5%/1 mm. The resulting gamma pass rate across both criterions for lung and bone were $\geq$ 95% and approximately 85% respectively.

Conclusion The results shows that a cost-effective anthropomorphic 3D printed phantom with realistic heterogeneity simulation may be fabricated at clinical departments with access to a suitable 3D printer. A similar 3D printed phantom can be fabricated for performing commissioning and quality assurance measurements for stereotactic type radiotherapy in the presence of heterogeneity.

Acknowledgements: This study has received support from the Health Education Training Institute Rural Research Capacity Building Program (HETI RRCBP). The author would also like to thank David

Schmidt, Kerith Duncanson and Claire Dempsey for their support and contributions throughout the course of this project.

References

1. S. H. Benedict et al., "Stereotactic body radiation therapy: The report of AAPM Task Group 101," Med. Phys., vol. 37, no. 8, pp. 4078–4101, 2010, https://doi.org/10.1118/1.3438081.
2. R. B. Tino, A. U. Yeo, M. Brandt, M. Leary, and T. Kron, "A customizable anthropomorphic phantom for dosimetric verification of 3D-printed lung, tissue, and bone density materials," Med. Phys., vol. 49, no. 1, pp. 52–69, Jan. 2022, https://doi.org/10.1002/mp.15364.

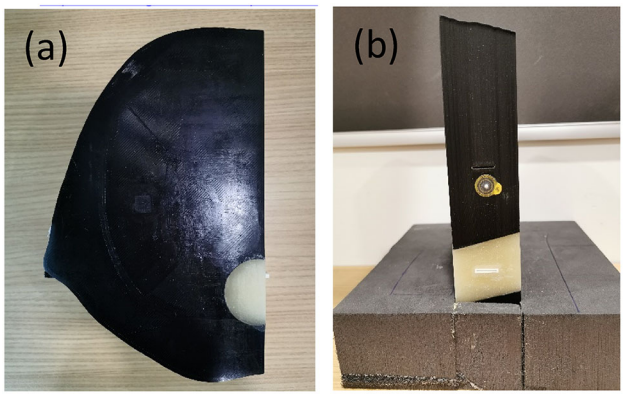

Fig. 9. The anthropomorphic 3D printed inhomogeneity thorax phantom slab a) axial view and b) sagittal view.

O103. The Neutactic Stereotactic System: A novel solution for image-guided stereotactic surgery

Elette Engels[1,2,3,*], Ashish Mitra[4], Allan Reji[4], Stéphanie Corde[1,3,5], Moeava Tehei[1,3], Michael Lerch[1,3]

[1]University of Wollongong, Wollongong, Australia, [2]Australian Synchrotron, ANSTO, Clayton, Australia, [3]Illawarra Heath and Medical Research Institute, Wollongong, Australia, [4]Neutactic Pvt Ltd,, India, [5]Prince of Wales Hospital, Randwick, Australia

Introduction Stereotactic systems are used in many intracranial surgical procedures such as laser ablation, neurostimulation, deep brain stimulation for Parkinson's disease treatment, brain biopsy, and brain cyst aspiration. Traditionally, the intracranial stereotactic procedure involves fixing a large metal frame to the patient's skull with large screws or pins (Fig. 1A). The Neutactic™ device is palm sized (Fig. 1B), both CT and MRI compatible, light weight, far less invasive and much simpler to use. This work evaluates the accuracy and compatibility of the Neutactic™ system with CT and MRI.
Method Accuracy and compatibility of the Neutactic™ device was assessed using a specially designed multi-target phantom and imaged using a Siemens Skyra 3 T MRI and Toshiba Asteion CT scanner at 1 mm resolution. Gelatine rats incorporating BluTack® or silicone targets were used as subjects. The device has CT and MRI visible fiducial markers and a dedicated software to determine positioning of its parts for needle insertion into the desired target location.
Results The device produced no imaging artefacts in 80–120 kV CT scans and T1- and T2-weighted MRI scans. The Neutactic™ system achieved the needle tip placement 100% of the time for 40 targets within average tolerance limits of 2.2 mm for MRI and 1.8 mm for CT ($p = 0.00001$), (Fig. 1B).
Conclusion The Neutactic™ device is a novel miniature stereotactic frame which is compatible with CT and MRI and can be used with near 100% accuracy for targets larger than 5 mm. The Neutactic™ system could reduce the time required for patient setup and thereby the stereotactic procedure. We are now ready for preclinical and subsequent clinical testing of the device.

Disclosures
We acknowledge the funding and support of the Australia-India Council Grants Program (https://www.dfat.gov.au/people-to-people/foundations-councils-institutes/australia-india-council/grants/australia-india-council-grant-recipients-2020-21

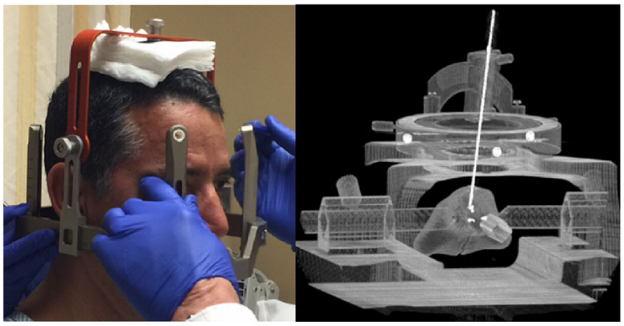

Fig. 1. Traditional stetereotactic frame (A). The Neutactic™ device (B) used to guide a needle to Blutack® targets in a gelatine rat phantom using CT scan imaging

O104. Feasibility of using PLA-based 3D printed phantoms for small-field high-energy photon beam dosimetry

Nicholas Arico[1,*], Kankean Kandasamy[2], Benjamin Zwan[2], Cameron Stanton[2], Emily Searle[2], Ashley Cullen[2], Christopher Lee[2]

[1]Institute Of Medical Physics, School Of Physics, University of Sydney, Sydney, Australia, [2]Central Coast LHD, Gosford, Australia

Introduction Previous studies have reported on the use of 3D printed dosimetric phantoms [1, 2], however water-equivalence for small-field applications has not been investigated. Herein we outline a methodology for optimising a 3D-printed phantom for small-field dosimetry and demonstrate its suitability for the pre-treatment verification of single isocentre, multi-target (SIMT) SRS treatment plans.
Method 3D printed Polylactic Acid (PLA) slab phantoms were optimised for water equivalency by iteratively adjusting the infill density until absolute dose, PDDs, profiles and output factors agreed with measurements in water. 6X, 6FFF and 10FFF MV photon beams from a Varian TrueBeam Edge linac were tested with field sizes ranging from 0.5×0.5 cm^2 to 10×10 cm^2. Measurements were made using the CC01 small volume ionisation chamber (IBA) and EBT3 GafChromic film (Ashland). A 20 cm diameter spherical phantom was printed using the optimised infill density. The phantom design has an interchangeable ion chamber cavity or film holder at the centre enabling point-dose and 2D planar measurements to be acquired. All measurements were compared to the Varian Eclipse

Treatment Planning System (TPS) using the Anisotropic Analytical Algorithm (Version 15.6.06).

Results PDDs, absolute dose and output factor measurements agreed to within 2% of water measurements at the optimised infill density of 90% for all field sizes measured and photon energies tested. Point-dose measurements at the centre of the sphere for SIMT SRS plans agreed to within 3% the TPS. Film measurements resulted in gamma pass rates of 99% (3%, 2 mm, 10% dose threshold).

Conclusion PLA can be optimised for water equivalence in small fields. Future work will include the validation of multiple off-axis measurement locations as well as the characterisation of anthropomorphic phantoms.

References

1. Sun, H., J. Li, and N. Wang, Research on Individualized Phantom Based on 3D Printing for Radiotherapy Dose Verification. Zhongguo Yi Liao Qi Xie Za Zhi, 2021. 45(4): p. 454–458. https://doi.org/10.3969/j.issn.1671-7104.2021.04.023
2. Kamomae, T., et al., Three-dimensional printer-generated patient-specific phantom for artificial in vivo dosimetry in radiotherapy quality assurance. Phys Med, 2017. 44: p. 205–211. https://doi.org/10.1016/j.ejmp.2017.10.005

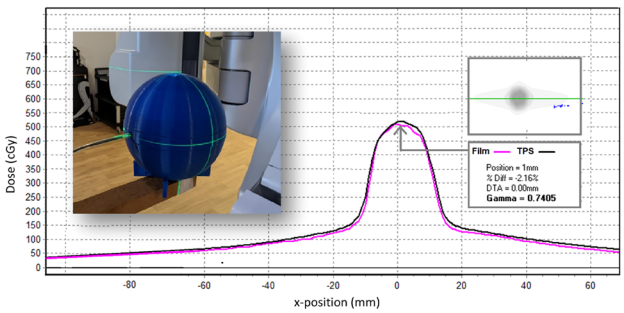

Fig. 1. Film verification of SIMT SRS delivery in the PLA Spherical Phantom.

O105. [Invited] Adaptive RT—what's all the hype about?

Michael Jameson[1,*]

[1]Genesis Care

Adaptive radiation therapy (ART) whereby the treatment plan is modified during the treatment course, is a natural extension of image guided radiation therapy (IGRT). ART was first introduced in 1997 by Yan et al.before the hardware and software was available to make it practical [1]. There are broadly three different types of ART. Anatomic ART where the treatment plan is adapted to changes in size, shape and location of visible anatomy [2]. Dose ART where delivered dose is accounted for when adapting via some form of dose accumulation [3]. Response or functional ART considers physiological changes in tumours or normal anatomy when adapting via imaging or other biomarkers [4]. The timescales in which ART may be applied include inline, online and offline (Fig. 1). Dedicated ART machines have been available for clinical use since 2014. There has been uptake in the application of online anatomic ART, but much less dose and response ART. Also, we are yet to see routine ART widely available in radiotherapy departments globally. There are a number of possible reasons for this including, resource requirements, lack of clinical evidence, lack of funding and the treatment tools available [5]. In this presentation ART will be briefly introduced and a summary of available and ideal technology described. The current clinical trial landscape and challenges will be detailed along with opportunities to progress ART.

References

1. Yan, D., F. Vicini, J. Wong, and A. Martinez, *Adaptive radiation therapy.* Phys Med Biol, 1997. **42**(1): p. 123.
2. Sonke, J.-J., M. Aznar, and C. Rasch. Adaptive radiotherapy for anatomical changes. in Seminars in radiation oncology. 2019. Elsevier.
3. Bohoudi, O., A.M. Bruynzeel, S. Tetar, B.J. Slotman, M.A. Palacios, and F.J. Lagerwaard, *Dose accumulation for personalized stereotactic MR-guided adaptive radiation therapy in prostate cancer.* Radiotherapy and Oncology, 2021. **157**: p. 197–202.
4. Matuszak, M.M., R. Kashani, M. Green, C. Lee, Y. Cao, D. Owen, S. Jolly, and M. Mierzwa. *Functional adaptation in radiation therapy*. in *Seminars in radiation oncology*. 2019. Elsevier.
5. Glide-Hurst, C.K., P. Lee, A.D. Yock, J.R. Olsen, M. Cao, F. Siddiqui, W. Parker, A. Doemer, Y. Rong, and A.U. Kishan, *Adaptive radiation therapy (ART) strategies and technical considerations: a state of the ART review from NRG oncology.* Int J Rad Oncol Biol Phys, 2021. **109**(4): p. 1054–1075.

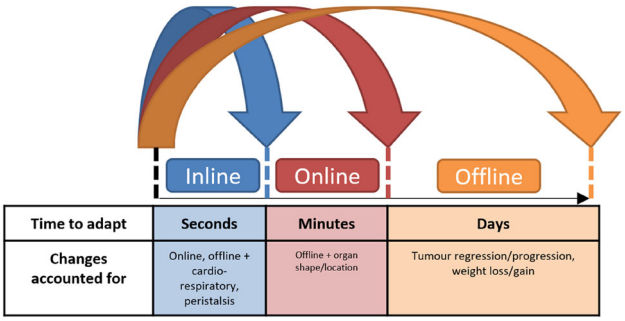

Fig. 1. The timescales of application and changes accounted for in ART.

O106. Automated or supervised online adaptive radiation therapy for rectal cancer: A geometric and dosimetric comparison

Adam Briggs[1], **Isabelle Fent**[2], **Ryan Brown**[3], **Alexandra Turk**[3], **Leigh Ambrose**[3], **George Hruby**[3,4], **Andrew Kneebone**[3,4], **Jeremy Booth**[3,5]

[1]Shoalhaven Cancer Care Centre, Shoalhaven District Memorial Hospital, Nowra, Australia, [2]Peter MacCallum Cancer Centre, Parkville, Melbourne, Australia, [3]Northern Sydney Cancer Centre, Royal North Shore Hospital, St Leonards, Australia, [4]Northern Clinical School, Sydney Medical School | University of Sydney, Sydney, Australia, [5]School of Physics, University of Sydney, Sydney, Australia

Introduction The Varian Ethos online adaptive radiation therapy (ART) platform is a system leveraging use of computing technology such as automatic segmentation, artificial intelligence (AI), deformable image registration (DIR), automated plan optimisation and dose

calculation. The performance of these technologies influences the accuracy and required level of supervision throughout the ART workflow. In this study, we compare anatomical contours and subsequent dose distributions generated from an automated-ART (a-ART) workflow and a standard of care, supervised-ART (s-ART) workflow.

Method Ten patients with locally advanced rectal adenocarcinoma (5 fractions per patient), were included in a retrospective study using an offline ART emulator. A two-arm study was formed for evaluation, requiring ART simulation of the cohort twice (n = 100 simulations): a-ART, automated contouring based on refined DIR-guidance AI contours (bladder, rectum) with automated planning; and s-ART, where all contours were reviewed and corrected by radiation oncologists and radiation therapists prior to automated plan generation. Geometric contour comparisons for six target and organ-at-risk (OAR) were completed, evaluating dice similarity coefficient and mean distance-to-agreement (MDA). Dose-volume metrics were compared using contours from both a-ART and s-ART arms.

Results Key geometric and dosimetric differences of a-ART and s-ART are evaluated across the cohort and shown in Figs. 1 and 2.

Conclusion This study shows a small reduction in target coverage for the a-ART workflow. This reduction corresponds to increased MDA. The geometric comparisons evaluated can be used to inform implementation of a-ART workflows e.g. setting thresholds for contour modification or provision of population margins to account for uncertainties introduced by a-ART.

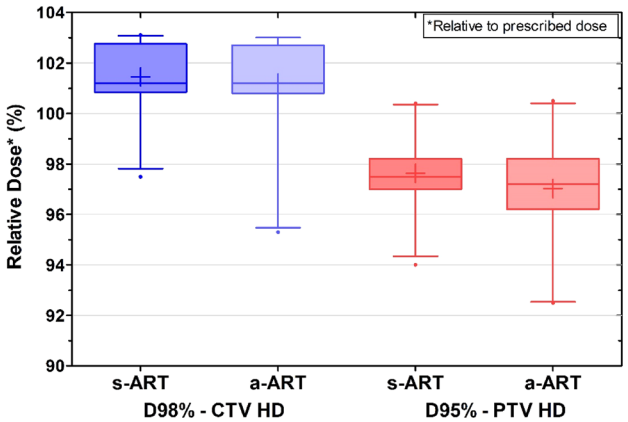

Fig. 1. Boxplot comparison of target coverage metrics for CTV HD and PTV HD for the s-ART and a-ART cohorts.

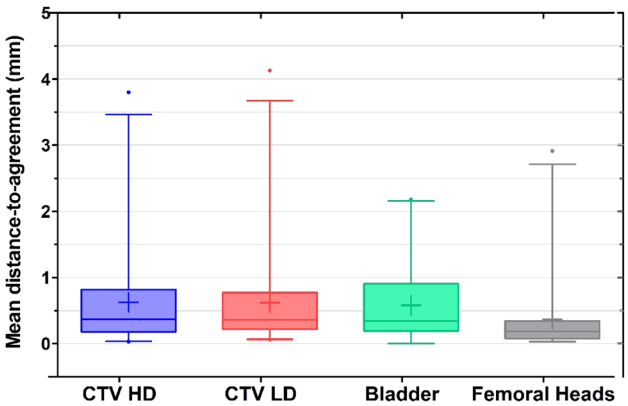

Fig. 2. Geometric comparison of target and OAR contours between s-ART and a-ART workflows.

O107. Chasing the pendulum: Online adaptive radiotherapy for extra-mobile lymphoma, a case study

Alannah Kejda[1,*], Susan Carroll[1,2], Toby Lowe[1], Alexandra Quinn[1], Maegan Gargett[1], Jeremy Booth[1,3]

[1]Northern Sydney Cancer Centre, St Leonards, Australia, [2]Northern Clinical School, University of Sydney, St Leonards, Australia, [3]Institute of Medical Physics, University of Sydney, Camperdown, Asutralia

Introduction A 52-year-old man was referred for radiotherapy to treat an isolated, bulky mesenteric mass following a relapsed follicular non-Hodgkins lymphoma diagnosis, after chemotherapy alone. The patient was prescribed 24 Gy in 12 fractions, VMAT-planned using Varian Eclipse and scheduled for IGRT soft-tissue matching using Varian Truebeam CBCT. Day 1 treatment did not proceed, as the GTV mass laterally moved approximately 8 cm within the habitus. The patient was subsequently IMRT-planned for online adaptive radiotherapy and treated using the Varian Ethos system.

Method Retrospective dosimetric analysis was conducted for each fraction, comparing three planning and treatment scenarios: 1. Ethos online adaption utilising CBCT for anatomy-of–the-day, 2. Original VMAT plan, CBCT soft-tissue matched to reference, 3. A conformal RT (CRT) plan, CBCT bone matched to reference. For each scenario, the plan was mapped to each fraction's CBCT and calculated. The GTV V95%, Body V105%, and the Remaining Volume at Risk (RVR) mean dose were compared. Interfraction target motion was recorded using the GTV centroid position.

Results All adaptive and VMAT fractions passed the primary plan metric of V95% > 95%, while 5/12 CRT fractions failed. The mean GTV V95% for adaptive, VMAT and CRT scenarios were 100 ± 0.0%, 99.8 ± 0.1%, and 87.5 ± 31.9% (k = 2), respectively. The RVR mean dose measured 23.8 ± 2.3%, 28.1 ± 4.3 Gy and 33.4 ± 8.3% (k = 2) for adapted, VMAT and CRT scenarios, while the Body V105% measured 117.4 ± 133.2 cc, 326.3 ± 562.7 cc, and 8.3 ± 16.8 cc (k = 2), respectively. GTV motion ranged between 0.5–9.2 cm.

Conclusion Ethos AI-driven adaptive fractions were shown to account for substantial GTV motion to reproducibly achieve excellent target coverage and normal tissue sparing. VMAT fractions were uniform in GTV coverage, but resulted in large volumes of 105% dose, while CRT plans often resulted in low GTV dose coverage. This case demonstrated the potential online adaption can improve treatment accuracy, potentially reduce margins and improve treatment efficacy for abdominal lymphoma patients.

O108. Determining internal anatomy replan triggers for plan adaptation of cervix external beam radiotherapy using MRI

Rhianna Brown[1,2,3,*], Lois Holloway[1,2,3,4,5], Peter Metcalfe[1,2], Annie Lau[6], Pereshin Moodaley[6], Karen Lim[4,6], Viet Do[4,6], Dean Cutajar[1,7], Amy Walker[1,2,3,4]

[1]Centre for Medical and Radiation Physics, University of Wollongong, Wollongong, Australia, [2]Ingham Institute for Applied Medical Research, Liverpool, Australia, [3]Department of Medical Physics, Liverpool and Macarthur Cancer Therapy Centre, Liverpool, Australia, [4]South Western Sydney Clinical School, University of New South Wales, Liverpool, Australia, [5]Institute of Medical Physics, University of Sydney, Camperdown, Australia, [6]South Western Sydney Local Health District, Liverpool Cancer Therapy Centre,

Liverpool Hospital, Liverpool, Australia, [7]St George Cancer Care Centre, St George Hospital, Kogarah, Australia

Introduction During the course of treatment of cervical cancer with external beam radiotherapy, anatomical changes can occur [1, 2]. These changes can affect the dose to the organs at risk (OARs) or coverage of the target volumes (TVs) [3]. By investigating the relationship between the anatomical and dosimetric changes, we can determine potential triggers for plan adaptation for offline adaptive radiotherapy.
Method OARs and TVs were delineated retrospectively on the pre-treatment and mid-treatment MRIs from 10 cervical cancer patients. The anatomical change assessed was volumetric change. A treatment plan was generated from the pre-treatment contours and applied to the mid-treatment contours. Dosimetric changes assessed included V30Gy and V40Gy for the OARs, and V95% and V100% for TVs. We compared these changes between the initial and mid-treatment contours. A statistically significant change was determined using a paired t-test and $p < 0.05$.
Results A statistically significant change in volume was observed for the bowel, increasing by 8.6 ± 1.8%, whilst the parametrium volume decreased by 31.2 ± 50.4%. TVs decreased significantly, with average changes ranging between 7.5% and 35.8%. The changes in dose to the OARs and TVs can be seen in table 1 and table 2, respectively. The increase in dose to the bowel in terms of the V30Gy and V40Gy was statistically significant. The decrease in target coverage for the ITV45 and PTV45 in terms of V95% and V100% was statistically significant.
Conclusion Anatomical changes during treatment have an impact on bowel dose and the coverage of the ITV45 and PTV45, reflecting a potential application for offline plan adaptation to account for these changes. This work is ongoing, with future analysis investigating the clinical significance of the changes, and the relationship between different anatomical changes and their specific dosimetric impact.
Disclosures
This project had support from the SWSLHD Radiation Oncology department through SWSLHD Medical Physics top-up scholarship, as well as support from the Australian Government Research Training Program Scholarship.
References

1. Jadon R, Pembroke CA, Hanna CL, Palanippan N, Evans M, Cleves AE, Staffurth J (2014) A Systematic Review of Organ Motion and Image-guided Strategies in External Beam Radiotherapy for Cervical Cancer. Clin. Oncol. 26: 185–196. https://doi.org.10.1016/j.clon.2013.11.031
2. van de Bunt L, Jürgenliemk-Schulz IM, de Kort GAP, Roesink JM, Tersteeg RJHA, van der Heide UA (2008) Motion and deformation of the target volumes during IMRT for cervical cancer: What margins do we need?. Radiother. Oncol. 88: 233–240. https://doi.org/10.1016/j.radonc.2007.12.017
3. Stewart J, Lim K, Kelly V et al. (2010) Automated Weekly Replanning for Intensity-Modulated Radiotherapy of Cervix Cancer. Radiat. Oncol. 78: 350–358. https://doi.org/10.1016/j.ijrobp.2009.07.1699

Table 2. Dosimetric changes to the OARs.

Organs at Risk	Change in V30 (%)	Change in V40 (%)
Bladder	-1.7 ± 6.4	-2.3 ± 15.0
Bowel	+ 6.8 ± 4.5	+ 7.5 ± 5.7
Rectum	-4.9 ± 12.0	-2.0 ± 18.8

Table 3. Dosimetric changes to the TVs.

Target Volume	Change in V95% (%)	Change in V100% (%)
Tumour GTV	0.0 ± 0.0	-0.9 ± 2.6
High Risk Tumour CTV	-0.9 ± 2.8	-2.3 ± 6.7
Low Risk Tumour CTV	-0.5 ± 0.8	-2.0 ± 4.4
Low Risk Tumour ITV	-1.4 ± 2.2	-2.6 ± 6.2
ITV45	-0.8 ± 1.4	-2.1 ± 3.1
PTV45	-1.7 ± 2.1	-3.2 ± 4.3

O109. CBCT based synthetic CT generation for adaptive radiotherapy

Brani Rusanov[1,*]

[1]The University of Western Australia, Duncraig, Australia

Introduction Cone-beam CT (CBCT) devices are commonly used for patient positioning prior to radiation therapy. They are cheap and ubiquitously found on linear accelerator gantries, however, they suffer from poor image quality owing to increased X-ray scatter conditions. The use of generative adversarial networks to convert CBCT images to diagnostic level CT images can enable pre-treatment dose verification, and facilitate an adaptive radiotherapy protocol.
Method 50 CBCT and paired CT images were collected. A highly modified version of the unpaired image translation architecture CycleGan is utilized in conjunction with several novel loss functions to generate synthetic CT images. Synthetic CTs are evaluated against ground truth CT images using image quality and dosimetric criteria. Furthermore, anatomic preservation is verified using phantom data.
Results Several model configurations and loss functions are evaluated. Synthetic CT images were converted from noisy and artefact ridden CBCT data, with image quality and dosimetric metrics indicating clinically viable endpoints were reached. Cycle-GAN showed robust anatomic preservation.
Conclusion CBCT based synthetic CT images can be rapidly produced prior to patient irradiation to help facilitate dose monitoring and online adaptive radiotherapy protocols. Specifically, downstream autosegmentation tasks could benefit enormously from the improved image quality of synthetic CT data.

O110. [Invited] Fetal neuroprotection by prenatal maternal choline supplementation by heavy drinking women

Ernesta Meintjes[1,*]

[1]University of Cape Town, Cape Town, South Africa

O111. Quantitative MRI: quality assurance for a longitudinal multi-center clinical trial for prostate cancer treatment response

Yu-Feng Wang[1,2,*], Sirisha Tadimalla[1], Robba Rai[2,3,4], Jonathan Goodwin[5], Sheryl Foster[6,7], Gary Liney[2,3,4], Lois Holloway[2,3,4], Annette Haworth[1]

[1]Institute of Medical Physics, School of Physics, Faculty of Science, The University of Sydney, Camperdown, Australia, [2]Ingham Institute for Applied Medical Research, Liverpool, Australia, [3]Liverpool and Macarthur Cancer Therapy Centre, Liverpool Hospital, Liverpool, Australia, [4]South Western Sydney Clinical School, University of New South Wales, Liverpool, Australia, [5]Department of Radiation Oncology, Calvary Mater Hospital, Waratah, Australia, [6]Discipline of Medical Imaging Science, Faculty of Medicine and Health, University of Sydney, Sydney, Australia, [7]Radiology Department, Westmead Hospital, Westmead, Australia

Introduction Quantitative imaging using multiparametric MRI has shown potential for providing non-invasive biomarkers for diagnosis, post-treatment monitoring and response prediction [1, 2]. Uncertainties in quantitative (qMRI) parameters can arise from differences between scanners and drifts within the same scanner [3]. We report the results of the quality assurance (QA) program that aimed to determine robust parameters for treatment response monitoring in the Sequential Imaging – Biofocussed Radiotherapy (SI-BiRT) clinical trial for post-radiation therapy response monitoring for prostate cancer [3].

Method Longitudinal measurements were made over a period of 12 months using two commercial phantoms, an inhouse developed phantom and three 3 T MRI scanners (two Skyra and one Prisma, Siemens Healthineers, Erlangen, Germany). The apparent diffusion coefficient (ADC), longitudinal relaxation time T1 and transverse relaxation rate R2* were the focus of the study. Considering mean parametric values from defined regions of interest, the coefficient of variance (%CV) was calculated to evaluate the variability within (repeatability) and across (reproducibility) the scanners.

Results The repeatability and reproducibility of the qMRI parameter measurements were comparable across all timepoints, with differences in median %CV between subsequent QA scans of $\leq 1\%$ and $\leq 4\%$ in the commercial and inhouse developed phantoms, respectively. ADC had highest repeatability and reproducibility compared to T1 and R2*.

Conclusion Scanner-related uncertainty of qMRI parameters measurements were intended to inform the analysis of the SI-BiRT trial data. The stability of qMRI parameter repeatability indicated that no intra-scanner corrections are required and similarly, a comparable magnitude of repeatability and reproducibility indicated that no significant inter-scanner differences need to be accounted for in the analysis of the combined multi-centre data. Inter-scanner variability in absolute values of parameters were measured, but not considered relevant, as the trial is concerned with only relative changes in parameters over time. Future studies will report inter and intra-patient variability in qMRI.

Acknowledgements: This project was supported by NHMRC grant APP1126955 and Sydney West TCRC – Partner Program 2019.

References

1. Sun, Y, Reynolds, HM, Parameswaran, B, Wraith, D, Finnegan, ME, Williams, S,Haworth, A (2019) Multiparametric MRI and radiomics in prostate cancer: a review. Australas. Phys. Eng. Sci. Med. 42(1):3–25.
2. Wang, YF, Tadimalla, S, Hayden, AJ, Holloway, L,Haworth, A (2021) Artificial intelligence and imaging biomarkers for prostate radiation therapy during and after treatment. J. Med. Imaging Radiat. Oncol. 65(5):612–26.
3. Wang, Y, Tadimalla, S, Rai, R, Goodwin, J, Foster, S, Liney, G, Holloway, L,Haworth, A (2021) Quantitative MRI: Defining repeatability, reproducibility and accuracy for prostate cancer imaging biomarker development. Magn. Reson. Imaging 77:169–79.

O112. A machine learning-based prediction pipeline for MRI radiomic feature extraction and survival analysis of glioma patients treated with radiotherapy

Adrian Remigio[1], Alessia Tamboriello[2], Sashendra Senthi[3,4], Rick Franich[5], Vanessa Panettieri[3,4,6,*]

[1]Advanced Science and Technology Institute, Diliman, Philippines, [2]Medical Oncology, GenesisCare, Frankston, Australia, [3]Alfred Heath Radiation Oncology, Alfred Hospital, Melbourne, Australia, [4]Central Clinical School, Monash University, Melbourne, Australia, [5]School of Science, RMIT University, Melbourne, Australia, [6]Medical Imaging and Radiation Sciences, Monash University, Clayton, Australia

Introduction Several studies found correlation between MRI-derived radiomic features and pathophysiology, including clinical outcomes, of patients with glioma. Our goal was to determine if radiomic features extracted with the aid of machine learning from the tumor plus peritumoral brain zone (PBZ) provides clinically relevant information for survival analysis of glioma patients treated with radiotherapy.

Methods A 2D U-Net neural network model[1] was trained and optimized to automatically segment the tumor plus PBZ on 540 2D-contrast-enhanced T1-weighted and T2-FLAIR MRIs from 45 patients available in the BraTS dataset[2]. First-order statistics, shape, and texture radiomic features were calculated from these regions. Using the 159 patients MR data from BraTS, correlated radiomic profiles were selected from Pearson and Spearman correlations. The same analysis was also carried out on 120 independent patient MRIs from Alfred Health Radiation Oncology (AHRO) with available outcome data. The DeepSurv model was applied to perform survival analysis based on the correlated radiomic profiles for both cohorts using the PyCox python package[3,4]. The developed DeepSurv models were evaluated using the integrated Brier score (IBS) and concordance index (C-index).

Results Our developed U-Net segmentation algorithm obtained a mean dice similarity coefficient (DSC) of 0.79 ± 0.12 for the BraTS validation set. For the survival probability prediction task, our best performing DeepSurv model achieved an IBS (at 1050 days) of 0.1403 and a C-index of 0.654 (Fig. 1). Superior predictive performance in terms of IBS was obtained compared to some published results for the survival analysis model (Table 1).

Conclusion This study pioneers the integration of the DeepSurv model to a radiomic analysis pipeline that focuses on whole tumor plus PBZ of glioma patients treated with radiotherapy. Our results show that such approach can provide clinically informative predictions for the tumor segmentation and prognosis of glioma patients treated with radiotherapy.

References

1. Ayalew YA, Fante KA, Mohammed M (2021) Modified U-Net for liver cancer segmentation from computed tomography images with a new class balancing method. BMC Biomed Eng 3. https://doi.org/10.1186/s42490-021-00050-y

2. Menze BH, Jakab A, Bauer S et al. (2015) The Multimodal Brain Tumor Image Segmentation Benchmark (BRATS). IEEE Trans Med Imaging 34(10): 1993–2024
3. Katzman JL, Shaham U, Cloninger A et al. (2018) DeepSurv: personalized treatment recommender system using a Cox proportional hazards deep neural network. BMC Medical Res Methodol 18. https://doi.org/10.1186/s12874-018-0482-1
4. Kvamme H, Borgan Ø, Scheel I (2019) Time-to-Event Prediction with Neural Networks and Cox Regression. J Mach Learning Res 20: 1–30.
5. Kickingereder P, Burth S,Wick A et al. (2016) Radiomic Profiling of Glioblastoma: Identifying an Imaging Predictor of Patient Survival with Improved Performance over Established Clinical and Radiologic Risk Models. Radiology 280(3): 880–889.

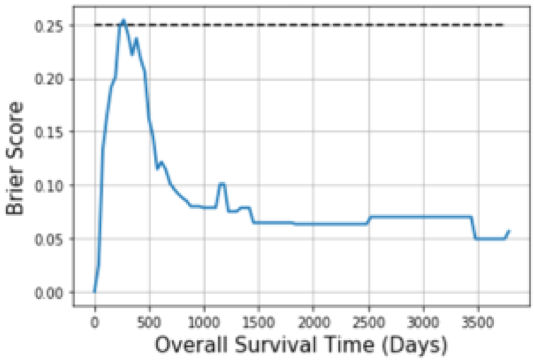

Fig. 1. The Brier score as a function of overall survival time for the best performing DeepSurv model.

Table 1. C-index and IBS scores of the developed DeepSurv models in this study. Survival analysis models from other studies were also included for comparison.

Survival Analysis Model	Input Features of the Model	Integrated Brier score (3780 days)	Integrated Brier score (1050 days)	C-index
A	Features with significant Spearman coefficient in the AHRO dataset	0.118	0.176	0.611
B	Features with significant Spearman coefficient in the BRATS dataset	0.105	0.161	0.633
C	Features with significant Pearson coefficient in the BRATS dataset	0.087	0.140	0.656
Kickingereder et al. [5]	Cox model with supervised principal component analysis (SPCA)	-	0.149	0.654
Kickingereder et al. [5]	SPCA + clinical features in Cox model	-	0.142	0.696

O113. Acceptance and commissioning of the 1.5 Tesla Marlin MRI scanner

Rob Behan[1,*], Reza Alinaghi Zadeh[1], Sarah Elliot[1], Glen Cahoon[1], Nikki Shelton[1], Sandra Fisher[1]

[1]Olivia Newton John Cancer and Wellness Centre, Melbourne, Australia

Introduction The benefits of MRI within radiotherapy are being increasingly realized with the clinical introduction of the Elekta Unity 1.5 Tesla MRI Linac. Vendor training/commissioning support focuses on the linac component of the system while international guidance on MRI acceptance and commissioning focuses on diagnostic rather than therapeutic QA requirements. The aim of this work was to implement evidence-based practice for the acceptance and commissioning of the Unity 1.5 Tesla MRI scanner (Marlin).

Method Commissioning and acceptance tests were carried out with vendor supplied and in-house QA solutions, in line with international guidelines [1] [2] and peer reviewed literature [3]. At installation, B0 survey measurements were performed, and quality assurance tests were carried out to verify that magnet ramp up did not adversely affect the adjacent linacs. Device inventory was conducted, and network connectivity was tested at acceptance. Vendor supplied and ACR QA phantoms were used for testing a range of image quality metrics, based on the ACR and NEMA MRI standards [4] [5] [6]. This included tests for uniformity, signal to noise ratio, slice thickness, linearity and resolution. In addition, geometric distortion was assessed with the vendor phantom and the Modus QUASER MRI-3D phantom. Spurious noise tests were carried out and the accuracy and constancy of the MR to MV isocenter offset was characterized. The impact of linac state as well as gantry position and movement on MR image quality were assessed. The geometric fidelity of clinical exam cards was measured, and beam profile measurements demonstrated that the TPS correctly modeled the 1.5 Tesla B field direction.

Results The results demonstrated successful connectivity, artefact-free images with image quality within the vendor QA tolerances, ACR recommendations and acceptable geometric distortion as per AAPM report 284 [2].

Conclusion In-house developed guidelines were necessary to commission the MRI for radiotherapy adaptive treatments.

References

1. AAPM, "Acceptance Testing and Quality Assurance Procedures for Magnetic Resonance Facilities," American Association of Physicists in Medicine, Maryland, 2010.
2. C. Glide-Hurst, E. Paulson, K. McGee, N. Tyagi, Y. Hu, J. Balter and J. Bayouth, "Task group 284 report: magnetic resonance imaging simulation in radiotherapy: considerations for clinical implementation, optimization, and quality assurance," Med Phys, vol. 48, no. 7, pp. e636-e670, 2021.
3. R. Tijssen, M. Philippens, E. Paulson, M. Glitzner, B. Chugh, A. Wetscherek, M. Dubec, J. Wang and U. van der Heide, "MRI commissioning of 1.5 T MR-linac systems – a multi-insitutional study," Radiother Oncol, vol. 132, pp. 114–120, 2019.
4. ACR, "Magnetic Resonance Imaging: Quality Control Manual," American College of Radiology, 2015.
5. NEMA, "NEMA MS 9-2008: Characterization of Phased Array Coils for Diagnostic Magnetic Resonance Images," National Electrical manufacturers Association, Rosslyn, 2021.
6. NEMA, "NEMA Standards Publication MS 5–2018: Determination of Slice Thickness in Diagnostic Magnetic Resonance Imaging," National Electrical Manufacturers Association, Rosslyn, 2018.

O114. Hazard ahead, proceed with caution: Clinically implementing artificial intelligence (AI) for object detection

Chris Boyd[1,2,*], Wolfgang Mayer[3], Timothy Kleinig[4,5], Greg Brown[2], Joseph Dawson[6,7], Mark Jenkinson[8,9,10], Eva Bezak[11,12]

[1]Medical Physics & Radiation Safety, South Australia Medical Imaging, Adelaide, Australia, [2]Allied Health and Human Performance, University of South Australia, Adelaide, Australia, [3]Artificial Intelligence and Software Engineering Lab, UniSA STEM, Adelaide, Australia, [4]Department of Neurology, Royal Adelaide Hospital, Adelaide, Australia, [5]Adelaide Medical School, The University of Adelaide, Adelaide, Australia, [6]Discipline of Surgery, University of Adelaide, Adelaide, Australia, [7]Department of Vascular & Endovascular Surgery, Royal Adelaide Hospital, Adelaide, Australia, [8]Australian Institute for Machine Learning (AIML), School of Computer Science, University of Adelaide, Adelaide, Australia, [9]South Australian Health and Medical Research Institute (SAHMRI), Adelaide, Australia, [10]Oxford Centre for Functional MRI of the Brain (FMRIB), University of Oxford, Oxford, UK, [11]Cancer Research Institute, University of South Australia, Adelaide, Australia, [12]Department of Physics, University of Adelaide, Adelaide, Australia

Introduction A niche that medical physicists have been filling for some time is assisting the implementation of emerging and complex technologies [1], the integration of AI is a current opportunity for this. With most medical physicists having some programming proficiency and AI design tools being relatively simple, the development of AI image analysis tools can appear straightforward. To those new to the field, three basic things are all that is required to make functional tools: 1. basic familiarity in domain specific terminology; 2. understanding of common development issues; and 3. access to internet guides for troubleshooting.
Method A case study in model development was undertaken by designing a liver and bone segmentation tool using publicly available CT images. A pre-existing 'U-net' model was modified using TensorFlow™ 2.1.0, to perform multi-patient, multi-class semantic segmentation. Performance was evaluated using statistical metrics, including accuracy, recall, precision, Dice and F1-score. Seven hyperparameters (sample size, image patch size, U-net filters, dropout, optimiser, loss function, U-net depth) were systematically altered across two to five different values, covering ranges used in similar "large-scale" recent optimisation works. This examined the relative impact of 450 hyperparameter combinations on model performance metrics.
Results Through this process, five recommendations for developing or implementing AI medical imaging tools were identified: 1. Question published metrics or images. They may be 'cherry-picked' results. 2. Use multiple combinations of parameters during model development. 3. Choose parameters carefully and test regularly. Stray from convention when required by your dataset and model. 4. Presenting information on model performance with different parameters improves transparency. 5. Extreme caution is needed when adopting published small scale 'in-house' models.
Conclusion Medical physicists can and should engage with the development and/or implementation of AI into the clinic. Familiarity with model biases and limitations introduced during training is needed, to ensure rigorous development and implementation.
References

1. E. Samei et al., "Redefining and reinvigorating the role of physics in clinical medicine: A Report from the AAPM Medical Physics 3.0 Ad Hoc Committee," Med Phys, Jul 10 2018, https://doi.org/10.1002/mp.13087.

O115. 'Oops, I did it again': Inappropriate referrals in medical imaging

Samuel Lilli[1,*], Victoria Earl[2], Amanda Perdomo[1]

[1]The Royal Children's Hospital, Parkville, Australia, [2]The Royal Melbourne Hospital, Parkville, Australia

Introduction Mandatory reporting of radiation incidents has been established by the Victorian Department of Health (DOH). Any unplanned exposure to a person under the age of 18 must be reported to DOH [1]. These incidents, as well as inappropriate referrals received, are collected and logged at our institution. This study aims to determine the rate of inappropriate referrals and identify potential areas for referrer education.
Method Radiographers collected the inappropriate referrals they received and justified the reason it was deemed inappropriate. The reportable incidents are centrally logged by the medical physicists. The rate of incidents and inappropriate referrals were investigated by the medical physicists. Trends were identified including the referring department with the highest rate of inappropriate imaging referrals which highlights areas where further education would be beneficial.
Results From January 2018—December 2021 there were 488 inappropriate referrals collected by the radiographers and 65 reportable radiation incidents at our institution. Incidents and inappropriate referrals make up 0.17% of the 331,231 total exams conducted during the same time period. The orthopaedic unit issued 34,359 referrals with 240 being deemed as inappropriate, resulting in an inappropriate referral rate of 0.7%. In comparison, 59 of the over 35,000 referrals received from the emergency department were deemed as inappropriate, resulting in a 0.17% inappropriate referral rate. See Fig. 1.
Conclusion Incidents and inappropriate referrals make up a small percentage of total exams conducted at our institution, 0.02% and 0.15%, respectively. By collating and reviewing the source of inappropriate referrals, we can identify areas where education of referrers may help reduce the number of incidents and unnecessary patient radiation exposure. There is also an opportunity to optimise workflow by minimising the inappropriate referral rate as radiographers do not need to clarify referrals with referrers.
References

1. Department of Health Victoria (2022) Mandatory reporting of radiation incidents. Department of Health. https://content.health.vic.gov.au/sites/default/files/2022-01/mandatory-reporting-of-radiation-incidents-ml-holder-obligation-doc.docx. Accessed 1 June 2022.

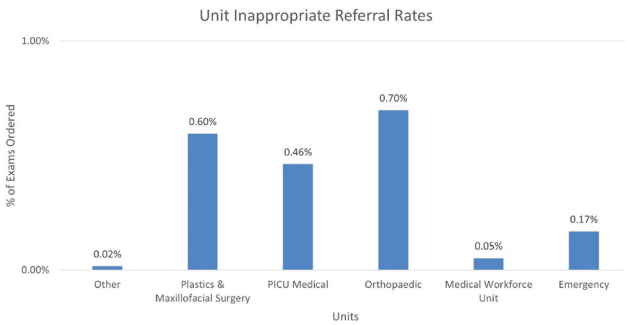

Fig. 1. Unit inappropriate referral rates.

O116. Fetal and maternal risk from imaging for pulmonary embolism: Survey results

Donald McLean[1,*]

[1]Canberra Health Services, Canberra, Australia

Introduction A meta study of the recent literature indicates that both CTPA and VQ examinations to rule out pulmonary embolism gave a similar diagnostic efficiency, however similar comparisons for dose and risk were not possible due to a lack of high quality data [1].
Method An analysis of 36 CTPA and 32 VQ scan reported pregnant patient cases over 4 years was undertaken. Data was taken from PACS records along with size and gestational age status. Size and gender specific effective dose and breast dose for the patient as well fetal dose was calculated using Impactdose software [2] for CTPA cases. Effective, breast and fetal doses were calculated with activity to dose conversion factors [3,4] for VQ scan cases. The risk of cancer detriment was determined by applying factors of 5% Sv^{-1} and 15% Sv^{-1} to effective maternal dose and fetal dose respectively.
Results The median CTPA fetal dose was 0.04 mGy with a maternal effective dose of 2.1 mSv giving a combined cancer detriment risk of 0.11 per 1000 cases. Changes, particularly in maternal effective dose, were associated strongly with patient size but also with radiographic technique. Median VQ scans doses of 0.25 mGy and 1.29 mSv for the fetal and effective maternal doses respectively gave a combined cancer risk also of 0.11 per 1000 cases. The application of conversion coefficients based on new fetal phantoms utilised by RADAR [4] generally saw a reduction in fetal dose compared to that from ICRP, except in the first trimester when the fetal dose increased by a factor of 3.
Conclusion Combined fetal and maternal cancer risk for the two examination types appears remarkably similar, noting however that fetal doses for VQ scans in the first trimester may exceed 1 mGy. Attention to radiographic technique can give significant reductions to CTPA doses.
Acknowledgements: I would like to acknowledge the encouragement and helpful discussions with Jason Tse.
References

1. Tromeur C, van der Pol LM, Le Roux PY, et al. (2019) Computed tomography pulmonary angiography versus ventilation-perfusion lung scanning for diagnosing pulmonary embolism during pregnancy: a systematic review and meta-analysis. Haematologica. 104(1):176–88.
2. Deak P, van Straten M, Shrimpton PC, Zankl M, Kalender WA. (2008) Validation of a Monte Carlo tool for patient-specific dose simulations in multi-slice computed tomography. Eur Radiol. 18(4):759–72.
3. International Commission on Radiological Protection. Radiation Dose to Patients from Radiopharmaceuticals: a Compendium of Current Information Related to Frequently Used Substances: Elsevier 2015.
4. Society of Nuclear Medicine and Molecular Imaging 2018. Nuclear Medicine Radiation Dose Tool VERSION: 4.10 http://www.snmmi.org/clinicalpractice/dosetool.aspx?itemnumber=1

O117. Management of patients with cardiac implantable electronic devices during intraoperative electron radiotherapy (IOERT)

Hossein Aslian[1,*], Mara Severgnini[2], Sara Savatović[3], Nikki Shelton[1], Francesco Longo[4]

[1]Olivia Newton-john Cancer Wellness & Research Centre, Austin Hospital, Heidelberg, Australia, [2]Department of Medical Physics, Azienda Sanitaria Universitaria Integrata di Trieste, Trieste, Italy, [3]Department of Physics, University of Trieste, Trieste, Italy, [4]Department of Physics, University of Trieste & Istituto Nazionale di Fisica Nucleare, Sezione di Trieste, Trieste, Italy

Introduction Management of patients with cardiac implantable electronic devices (CIEDs) during intraoperative electron radiotherapy (IOERT) might be challenging, especially when the device is in the vicinity of the PTV. In this study, the effect of IOERT on CIED patients was investigated.
Method The influence of some of the damaging effects on CIED function during IOERT such as cumulative dose effect, neutron-induced upsets, dose rate effect and electromagnetic interference was investigated. This was done by gathering and analysing the clinical data from patients receiving accelerated partial breast irradiation (APBI) using the Mobetron® (IntraOp Medical, Inc. Santa Clara, CA). The Mobetron is a dedicated electron beam accelerator that produces electrons with nominal energies of 6, 9, and 12 MeV at dose rates up to approximately 10 Gy/min. The results of dosimetry studies using MOSFETs and GAFCHROMIC film during IOERT, and our ongoing Monte-Carlo studies focusing on neutron and photon out-of-field doses at CIED depths were also analysed [1–4].
Results Results show that neutrons produced by electron beams $<$ 15 MeV are negligible and thus IOERT with nominal energy up to 12 MeV is considered as a non-neutron producing radiotherapy. Given the necessity of real-time treatment monitoring, real-time in vivo dosimetry using micro-MOSFET and at least two patient monitoring methods (i.e. ECG, ear or finger pulse oximetry) are recommended. In the out-of-field regions ($>$ 3 cm) and at CIED depths, the average estimated dose rate in CIED was $<$ 10 cGy/min and the dose-rate effect is not significant. Using bipolar electrocautery system or electrosurgical with electromagnetic compatibility (EMC) characterization would reduce the potential risk of EMI to CIED.
Conclusion Our studies showed that IOERT could presents a manageable risk for CIED patients due to minimal neutron contamination, EMI, dose-rate effect, and insignificant out-of-field dose (CIED-to-PTV $>$ 3 cm). However, precautions should be taken to minimize a possible device malfunction.
References

1. Aslian H, Kron T, Longo F, et al. (2019) A review and analysis of stereotactic body radiotherapy and radiosurgery of patients with cardiac implantable electronic devices. Australasian Physical and Engineering Sciences in Medicine 42:415–425.
2. Aslian H, Kron T, Watts T, et al. (2020) The effect of stereotactic body radiotherapy (SBRT) using flattening filter-free beams on cardiac implantable electronic devices (CIEDs) in clinical situations. Journal of Applied Clinical Medical Physics 21:121–131. https://doi.org/10.1002/acm2.12873
3. Aslian H, Severgnini M, Khaledi N, et al. (2021) Neutron and photon out-of-field doses at cardiac implantable electronic device (CIED) depths. Applied Radiation and Isotopes 176:109,895. https://doi.org/10.1016/J.APRADISO.2021.109895
4. Savatović S, Severgnini M, Longo F (2021) A IOERT Geant4 Monte Carlo simulation for the computation of field output factors and 3D dosimetry. Physica Medica 92:S181. https://doi.org/10.1016/S1120-1797(22)00387-8

O118. Paediatric whole body and organ effective doses and risks from planar imaging, including repeat examinations

Amanda Fenton[1,*], Elaine Ryan[1]

[1]Biomedical Technology Services, Coopers Plains, Australia

Introduction Paediatric patients are especially vulnerable to radiation detriment, and some inpatients can be imaged multiple times a month resulting in a higher accumulated risk. However, there is little data on effective dose estimates or patient risk due to planar imaging examinations. This study aims to provide clinicians with up-to-date information on doses and risk to paediatric patients from common planar imaging exams, including organ doses and organ risk factors. This will particularly help with informed decision making in the referral of planar x-ray procedures and frequent examinations.
Methods Four years of exposure data from a major paediatric x-ray department was used to determine Dose-Area Product (DAP) values for common head and body planar imaging protocols for 6 age groups. These values were then used to determine estimates of organ and whole-body effective dose ranges for patients, as well as associated cancer risks. Data from the hospital Radiology Information System (RIS) was used to find the upper percentiles of patients receiving multiple head and body planar images, due to follow-ups. Risk was then determined using the frequency of examinations and median effective dose per patient age group.
Results Effective doses from planar images were found to be between 0.01 – 0.05 mSv and the organs most at risk for head, chest, abdomen and pelvis images found to be the thyroid, lungs and colon for males and thyroid, breast, lungs and bladder for females. The upper first percentile of patients receiving head or body planar imaging (subject to between 25 and 211 examinations) were still found to only have a risk $< 5\%$ of natural cancer incidence rates.
Conclusion Organ and whole-body effective doses have been determined, along with organs most at risk from common head and body planar examinations for paediatric patients. The frequency of repeat imaging has also been investigated.

O119. Effective doses and radiation risks in paediatric medical imaging

Amanda Perdomo[1,*]

[1]The Royal Children's Hospital Melbourne, Parkville, Australia

Introduction Healthcare Professionals (HCP) working in medical imaging are routinely required to communicate radiation risks. Effective dose alone cannot be used to specify and communicate the radiation risk for an individual as risks are dependent on many factors including age and patient sex. We estimated the typical effective doses for common general radiography (GXR), nuclear medicine (NM) and positron emission tomography (PET) paediatric studies. Effective doses were used to estimate and categorise radiation risks with commonly used risk terminology.
Methods Protocols for common GXR, NM and PET studies with the World Health Organisation (WHO) 50th percentile weight-for-age data up to 18 years were used to estimate typical organ and effective doses for paediatric patients at our institution [1]. The lifetime risk of cancer incidence using BEIR VII report data was calculated and the results were used to determine standardised levels of risk using the Calman risk model [2–3]. Information posters including the typical effective dose, background equivalent radiation time (BERT), risk of cancer incidence, and the Calman risk model category were developed.
Results Paediatric effective doses, risk of cancer incidence and level of risk category from 20 GXR examinations, four NM, and two PET studies were calculated. Doses ranged from < 0.001 mSv (negligible risk) to 6 mSv (moderate risk). As the effective dose did not vary meaningfully for different patient weights in some protocols the data was able to be summarised into a simple poster (Fig. 1 for NM and PET). This provides the HCP a resource to convey radiation risks in an easy manner.
Conclusion Typical effective doses and the associated risk from common GXR, NM and PET studies were calculated and presented in posters. These posters can be used to convey radiation risks in ways that are easy to understand and compare with other everyday risks.
References

1. World Health Organisation (WHO). The WHO Child Growth Standards. Available from https://www.who.int/childgrowth/standards/en/; Accessed 09 August 2019.
2. Committee to Assess Health Risks from Exposure to Low Levels of Ionizing Radiation, National Research Council. Health Risks from Exposure to Low Levels of Ionizing Radiation: BEIR VII Phase 2. Available from http://nap.edu/11340. 2006.
3. Calman KC. Cancer: science and society and the communication of risk. British Medical Journal. 1996;313(7060):799–802. https://doi.org/10.1136/bmj.313.7060.799

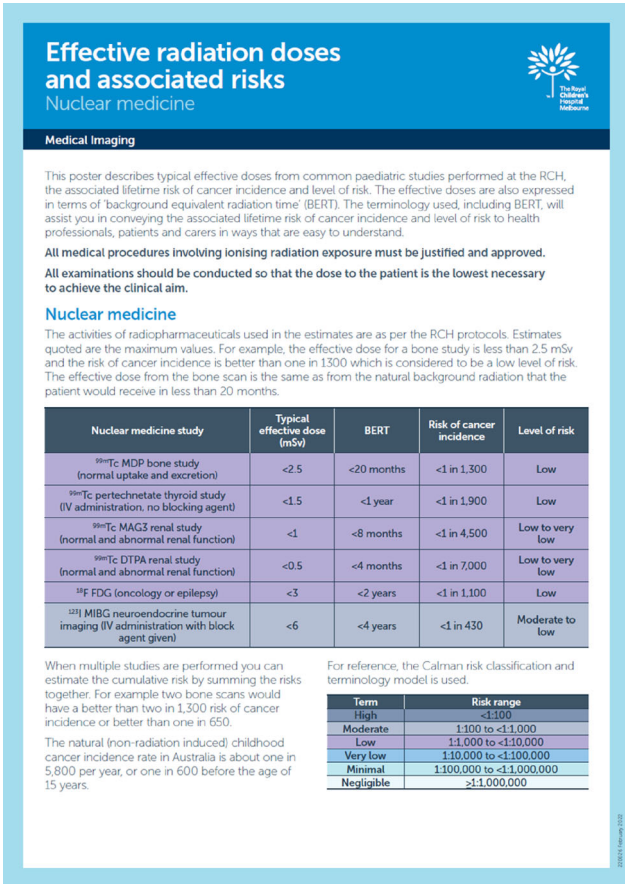

Effective radiation doses and associated risks
Nuclear medicine

The Royal Children's Hospital Melbourne

Medical Imaging

This poster describes typical effective doses from common paediatric studies performed at the RCH, the associated lifetime risk of cancer incidence and level of risk. The effective doses are also expressed in terms of 'background equivalent radiation time' (BERT). The terminology used, including BERT, will assist you in conveying the associated lifetime risk of cancer incidence and level of risk to health professionals, patients and carers in ways that are easy to understand.

All medical procedures involving ionising radiation exposure must be justified and approved.

All examinations should be conducted so that the dose to the patient is the lowest necessary to achieve the clinical aim.

Nuclear medicine

The activities of radiopharmaceuticals used in the estimates are as per the RCH protocols. Estimates quoted are the maximum values. For example, the effective dose for a bone study is less than 2.5 mSv and the risk of cancer incidence is better than one in 1300 which is considered to be a low level of risk. The effective dose from the bone scan is the same as from the natural background radiation that the patient would receive in less than 20 months.

Nuclear medicine study	Typical effective dose (mSv)	BERT	Risk of cancer incidence	Level of risk
^{99m}Tc MDP bone study (normal uptake and excretion)	<2.5	<20 months	<1 in 1,300	Low
^{99m}Tc pertechnetate thyroid study (IV administration, no blocking agent)	<1.5	<1 year	<1 in 1,900	Low
^{99m}Tc MAG3 renal study (normal and abnormal renal function)	<1	<8 months	<1 in 4,500	Low to very low
^{99m}Tc DTPA renal study (normal and abnormal renal function)	<0.5	<4 months	<1 in 7,000	Low to very low
^{18}F FDG (oncology or epilepsy)	<3	<2 years	<1 in 1,100	Low
^{123}I MIBG neuroendocrine tumour imaging (IV administration with block agent given)	<6	<4 years	<1 in 430	Moderate to low

When multiple studies are performed you can estimate the cumulative risk by summing the risks together. For example two bone scans would have a better than two in 1,300 risk of cancer incidence or better than one in 650.

The natural (non-radiation induced) childhood cancer incidence rate in Australia is about one in 5,800 per year, or one in 600 before the age of 15 years.

For reference, the Calman risk classification and terminology model is used.

Term	Risk range
High	<1:100
Moderate	1:100 to <1:1,000
Low	1:1,000 to <1:10,000
Very low	1:10,000 to <1:100,000
Minimal	1:100,000 to <1:1,000,000
Negligible	>1:1,000,000

Fig. 1. Radiation doses and risks for NM and PET examinations.

O120. "Who's the more foolish: the fool or the fool who follows him?" Audit of radiation dose and risk assessments against RPS-8 requirements

Daniel Badger[1,*]

[1]SA Medical Imaging, Woodville South, Australia

Introduction In most jurisdictions in Australia, clinical research that involves the exposure of humans to ionising radiation must comply with RPS-8 [1]. The code puts obligations on researchers, requiring the submission of a radiation dose and risk assessment (RDRA), written by an approved medical physicist, and giving specific information for use by the Human Research Ethics Committee (HREC). This work audits RDRAs against the requirements of the code.
Method As part of his radiation safety officer role, the author sits on an HREC to advise on radiation safety and scientific issues, attending up to 24 meetings per year. Under National Mutual Acceptance, the HREC regularly reviews submissions on research studies being conducted at multiple sites, including RDRAs from across Australia. The author assessed RDRAs on a convenience sampling basis (ie the first RDRA by each author seen after being submitted to the HREC during 2018–2022). Each RDRA was reviewed against 14 explicitly stated and 12 implied requirements in RPS-8, with each requirement being scored as either "met" or "not met". In some circumstances, specific requirements do not apply, so these were scored as "not applicable".
Results 37 unique author RDRAs were reviewed, from VIC, NSW, SA, QLD, WA, and ACT. 97% (36) did not meet every applicable requirement, with 89% (33) not meeting all explicit, applicable requirements. The average RDRA had 5.27 "not met" requirements and 4.95 "not applicable". One state (9 authors) scored significantly ($p = 0.0001$) better than the other states, averaging 2.0 "not met". Six reports failed to meet 10 or more of the requirements. Six authors were on neither the ACPSEM register nor regulatory authority approved lists.
Conclusion RDRAs show poor adherence to requirements in RPS8. TEAP doesn't require training/competencies in this area, but RPS8 specifically requires medical physicists to be ACPSEM certified (or an approved equivalent).
References

1. ARPANSA "Code of Practice for the Exposure of Humans to Ionizing Radiation for Research Purposes" (2005), Radiation Protection Series No. 8

O121. Postal audit for all high dose-rate brachytherapy centers in Australia & New Zealand: lessons learned

Emily Simpson-Page[1], Rachael Wilks[1,2,3], Tanya Kairn[1,2,3,4], Scott Crowe[1,2,3,4,*]

[1]Royal Brisbane & Women's Hospital, Herston, Australia, [2]Herston Biofabrication Institute, Herston, Australia, [3]University of Queensland, St. Lucia, Australia, [4]Queensland University of Technology, Brisbane, Australia

Introduction In Australia and New Zealand, high dose-rate (HDR) brachytherapy sources can be calibrated with an in-air method when a well chamber is not readily available. The ability to use a cylindrical chamber relies on a robust, reproducible set up, a calibrated Farmer chamber and knowledge of the IAEA calibration requirements. 3D printed jigs can provide a cheap, easy way to set up in air measurements for HDR sources. In 2021–22, a small 3D printed jig was sent to all brachytherapy centres in Australia and New Zealand as a postal audit exercise. This presentation outlines the methods used for the audit, overall results and lessons learned.
Method The jig was created in 2020 [1] and successfully tested across multiple local HDR departments. Over 2021–22, all 24 radiation oncology departments that provided HDR brachytherapy across Australia and New Zealand were invited to participate in a reference air-kerma rate (RAKR) audit using the 3D printed jig. An audit spreadsheet was developed with detailed instructions, customisable to the calibrated cylindrical chamber that would be used for measurements.
Results The success rate of involvement was 100%, with all centres that were approached about the audit agreed to participate. The RAKR values measured using calibrated cylindrical chambers and the 3D printed jig were all within 5% of calibration certificate values. An open text box in the audit spreadsheet provided valuable feedback that was used to improve the audit process.
Conclusion The audit successfully allowed an intercomparison between all HDR centres in Australia and New Zealand. The results provided interesting summaries of different methods used for a well chamber calibration as well as a useful summary of chamber calibration information and RAKR measurement accuracy with a cylindrical chamber across Australasia.
Acknowledgements: The authors would like to extend the warmest thanks to all HDR brachytherapy centres and physicists around Australia and New Zealand who so generously gave up time to participate in the audit and who provided thoughtful, constructive feedback throughout the project.
References

1. Simpson-Page E, Hamlett L, Lew D, Stephens H, Wilks R, Kairn T, Crowe SB (2021) 3D printed brachytherapy jig for Reference Air Kerma Rate calibration. *Physical and Engineering Sciences in Medicine*, *44*(4), 1141–1150. https://doi.org/10.1007/s13246-021-01050-x

O122. Investigating action thresholds for in vivo source tracking in interstitial and intracavitary HDR cervical brachytherapy

Yashiv Dookie[1,2,*], Joel Poder[1,2], Simon Downes[4], Dean Cutajar[2], Anatoly Rosenfeld[2]

[1]Shoalhaven Cancer Care Centre, Nowra, Australia, [2]Centre for Medical Radiation Physics, University of Wollongong, Wollongong, Australia, [3]Department of Radiation Oncology, St George Cancer Care Centre, Kogarah, Australia, [4]Nelune Comprehensive Cancer Centre, Prince of Wales Hospital, Randwick, Australia

Introduction The purpose of this study was to determine a comprehensive in-vivo source tracking error threshold (ISTET) in high dose rate (HDR) brachytherapy for cervical cancer. ISTET enables a source positioning error threshold for imminent real-time in-vivo source tracking technologies and treatment monitoring devices, possibly preventing clinically relevant changes to the applied dose.
Method Retrospective HDR interstitial (n = 10) and intracavitary (n = 20) cervical brachytherapy patients were randomly selected to determine the feasibility of implementing an ISTET. A script was developed to generate a dwell position displacement of treatment plans along each major axis from their original position. Dose-volume histogram (DVH) indices were calculated without re-optimisation to determine appropriate ISTETs in each direction. A relative decrease of 10% in HR-CTV coverage or a 10% increase in organ-at-risk (OAR) dose to 25% of the patient population was set as the limit used to determine the ISTET.
Results ISTETs were directionally dependent for OARs, the smallest found to be 2 mm in the anterior, posterior directions for interstitial and intracavitary treatments. The HR-CTV D_{90} met the action level with displacements of 4 and 5 mm along each axis. Critically, variation in DVH metric increases with displacement. Differences in dwell weighting and patient anatomy demonstrates a diversity in plan robustness which needs to be considered if selecting an ISTET.

Conclusion Determining the dosimetric impact of dwell position displacement provides a clinical benchmark for the development of verification devices and an action level for real-time treatment monitoring. It has been established that an ISTET needs to be patient specific and can be determined with the script based method established in this work.

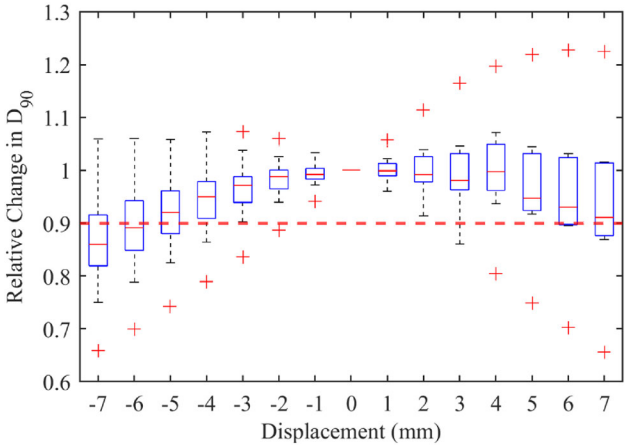

Fig. 1. Distribution of relative change in HR-CTV D_{90} with Superior-Inferior displacement of interstitial treatments. Outliers are denoted by a red ' + ' symbol.

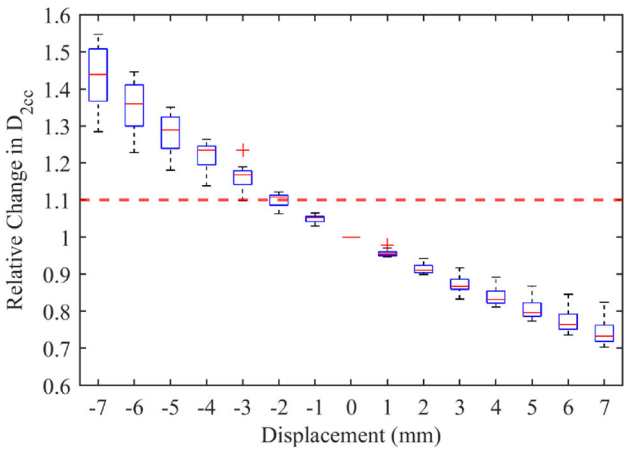

Fig. 2. Distribution of relative change in bladder D_{2cc} with Anterior–Posterior displacement of intracavitary treatments.

O123. Quantifying uncertainties in high-dose-rate prostate brachytherapy using robust evaluation

Andrew Kennedy[1,*]

[1]University of Adelaide, Adelaide, Australia

Introduction Uncertainties are well quantified for high-dose-rate prostate brachytherapy in the literature; however, their impact on the dosimetric quality of an individual patient's treatment plan (TP) in combination has not been explored in detail. Uncertainties are generally accounted for by increasing the margin around the prostate target and/or organs at risk, but this may lead to some healthy tissue being un-necessarily irradiated or compromising dose coverage in more critical areas.

Method In this study, uncertainties are considered during the treatment planning procedure by calculating worst-case and probabilistic scenarios for the prostate target, urethra, and rectum. One patient's TP was selected retrospectively to demonstrate a robust evaluation method, involving 2944 uncertainty scenarios. For each uncertainty scenario, the combination of TP parameter variables (five structural and one temporal) was adjusted from their nominal values and the new dose distribution calculated.

Results The variation in dose-volume metrics were used to quantify the robustness of the nominal plan to uncertainties. The standard deviation for D_{90} (objective > 16 Gy) of the prostate target was 0.75 Gy, and in the worst case 11.87 Gy (nominal = 16.4 Gy). For the urethra, D_{10} (objective < 18.4 Gy) had a standard deviation of 1.1 Gy and a worst-case dose of 23.8 Gy (nominal = 17.2 Gy). The V_{75} constraint for the rectum (objective < 1 cc) was not normally distributed and had first and third quartile values of 0.03 cc and 0.49 cc respectively; and worst-case scenario of 5.33 cc (nominal = 0.12 cc).

Conclusion A method of robust evaluation was demonstrated for one patient, which allows assessment of the combined impact of uncertainties on the nominal dose distribution. A larger retrospective study of dose-volume metrics is required to assess the significance of the deviations found for the patient in this work.

O124. Single-institution dosimetric review of a decade of MRI-guided brachytherapy for cervical cancer

Emily Flower[1,2], **Gemma Busuttil**[1], **Niluja Thiruthaneeswaran**[1,2], **Salman Zanjani**[1], **Eireann Cosgriff**[1], **Alison Salkeld**[1,2,3], **David Thwaites**[2], **Jennifer Chard**[1]

[1]Crown Princess Mary Cancer Centre, Westmead, Australia, [2]School of Physics, University of Sydney, Camperdown, Australia, [3]School of Medicine, University of Sydney, Westmead, Australia.

Introduction Radiochemotherapy with MRI-guided brachytherapy boosts are gold standard care for locally advanced cervical cancer. Since the GEC-ESTRO guidelines [1,2] for standardized contouring and reporting were published, further recommendations have also been published. Newer applicators have also become available with interstitial components. In this study, dosimetric plan quality is reviewed over the decade since the implementation of MRI-guided brachytherapy for locally advanced cervical cancer.

Methods Patients received MRI-guided brachytherapy according to the local protocol at the time. Changes to practice were identified and the dose-volume histogram parameters tested to identify changes to dosimetry.

Results 118 consecutively treated patients were included, with brachytherapy delivered between 2012 and 2022. Major changes in practice were identified and included implementation of full MR adaptive planning and moving from the Varisource to Flexitron afterloader. The median dose to 90% of the high-risk clinical target volume (CTV_HR D90) increased from 7.8 Gy to 9.7 Gy as treatment evolved over the 10 years from using a Fletcher-Suit-Delclos intracavitary applicator only to the Venezia intracavity + interstitial applicator. Plan conformity evaluated using the Paddick index increased from 0.27 to 0.57. Organ-at-risk doses either remained stable or decreased slightly. Doses to the intermediate-risk clinical target volume decreased with the Venezia applicator until all doses stabilised under the current applicator and dose protocol.

Conclusion Implementing best-practice brachytherapy increases dosimetric plan quality.

References

1. Haie-Meder C, Pötter R, Van Limbergen E et al. (2005) Gynaecological (GYN) GEC-ESTRO Working Group. Recommendations from Gynaecological (GYN) GEC-ESTRO Working Group (I): concepts and terms in 3D image-based 3D treatment planning in cervix cancer brachytherapy with emphasis on MRI assessment of GTV and CTV. Radiother Oncol 74:235–45. https://doi.org/10.1016/j.radonc.2004.12.015.
2. Pötter R, Haie-Meder C, Van Limbergen E et al. (2006) GEC ESTRO Working Group. Recommendations from gynaecological (GYN) GEC ESTRO working group (II): concepts and terms in 3D image-based treatment planning in cervix cancer brachytherapy-3D dose volume parameters and aspects of 3D image-based anatomy, radiation physics, radiobiology. Radiother Oncol 78:67–77. https://doi.org/10.1016/j.radonc.2005.11.014.

O125. Survey of brachytherapy training experience among radiation oncology medical physics registrars in Australia and New Zealand: where to from here?

Joel Poder[1,2,*], Annette Haworth[3]

[1]St George Hospital Cancer Care Centre, Kogarah, Australia, [2]Centre for Medical Radiation Physics, University of Wollongong, Wollongong, Australia, [3]School of Physics, University of Sydney, Camperdown, Australia

Introduction To evaluate the current status of brachytherapy training among radiation oncology medical physics (ROMP) registrars in Australia and New Zealand (Aus/NZ) trained through the Australasian College of Physical Scientists and Engineers in Medicine (ACPSEM) syllabus.

Method All current ROMP registrars in Aus/NZ enrolled in the ACPSEM training and accreditation (TEAP) program, and registrars within 2 years of completing the program were sent an online anonymous questionnaire on aspects of their brachytherapy training including; number of cases observed/performed, methods used to teach in their department, personal confidence in performing brachytherapy tasks, and opinions on the future of ROMP brachytherapy training in Aus/NZ.

Results The survey response rate was 44% (43/97). Two-thirds of respondents (28/43) had high dose rate (HDR) brachytherapy treatments performed in their department, and only 23% (10/43) had low dose rate (LDR) brachytherapy performed in their department. Of the respondents, 81% (35/43) had some or all of their brachytherapy training performed at another department. Most respondents had exposure to gynaecological brachytherapy, followed by HDR prostate. Sixty percent (26/43) of respondents believe they gained enough training to confidently practice brachytherapy for the sites treated in their department. Most common barriers to achieving desired confidence in practicing brachytherapy were time constraints and low caseload in department. The majority of respondent's level of interest in performing brachytherapy procedures increased after completing their brachytherapy training and 62% (27/43) would like to perform brachytherapy procedures after completing TEAP. Finally, 70% (30/43) respondents would be open to pursuing some form of brachytherapy fellowship post-training.

Conclusion The survey revealed the disparity in brachytherapy training across ROMP registrars in ACPSEMs TEAP program and highlights the need to improve access to practical brachytherapy training in the ROMP TEAP syllabus. Despite barriers in receiving adequate training in brachytherapy, respondent interest in continuing to practice the technique was positive.

O126. Effect of using single-energy metal artifact reduction algorithm corrected CT scans on the accuracy of external beam radiotherapy treatment planning in spine and pelvis regions

Daliya Ignatius[1,2,*], Zaid Alkhatib[3], Pejman Rowshanfarzad[2], Simon Goodall[4], Mounir Ibrahim[3], Andrew Hirst[2], Riley Croxford[2], Mahsheed Sabet[2,3]

[1]Mid North Coast Cancer Institute, Port Macquarie, Australia, [2]School of Physics, Mathematics and Computing, The University of Western Australia, Crawley, Australia, [3]Department of Radiation Oncology, Sir Charles Gairdner Hospital, Nedlands, Australia, [4]GenesisCare Cancer Center, Wembley, Australia

Introduction Artefacts from metal implants on computed tomography (CT) images result in incorrect CT numbers, which can impact the accuracy of patient treatment. Traditional method of manual overriding of artefacts using surrounding soft tissue density may not be accurate if true CT numbers are unknown. This work aimed to evaluate the clinical suitability of single-energy metal artefact reduction (SEMAR) algorithm for external beam radiation therapy treatment planning.

Method Two spine phantoms and two hip phantoms were 3D printed in-house. For each type of phantom, one was constructed with metal and the other without metal. Phantoms were CT scanned generating three datasets for each type: 1) without metal (CT_{ref}), 2) with metal (CT_{No_SEMAR}), 3) and with metal reconstructed with SEMAR filter (CT_{SEMAR}). For each case, including two patients' data, clinical VMAT plan was calculated under two artefact correction conditions: artefacts on CT_{No_SEMAR} manually overridden using RED of water, and artefacts on CT_{SEMAR} corrected using SEMAR. The effect of SEMAR was studied on 1) CT number accuracy using paired student *t* test, 2) dose volume histogram (DVH) analysis between CT_{SEMAR} and CT_{No_SEMAR}, 3) and dose measurements using film and ionization chamber.

Results Mean CT number difference between CT_{Spine_Ref} compared to CT_{Spine_SEMAR} and $CT_{Spine\_No\_SEMAR}$ were 12.8 ± 50.2 HU and 36.3 ± 77.7 HU, respectively. Similarly, mean CT number difference between CT_{Hip_Ref} compared to CT_{Hip_SEMAR} and $CT_{Hip\_No\_SEMAR}$ were 3.1 ± 174.7 HU and 23.7 ± 255.4 HU, respectively. All DVHs showed clinically negligible dose difference with values in the range of a percent or less. Gamma passing rate was higher for CT_{Spine_SEMAR} by 2% for 2%/2 mm. Point dose measured was closer to planned dose for CT_{Hip_SEMAR} by 0.5%.

Conclusion SEMAR accurately predicts CT numbers and improves accuracy of plan and resultant dose. SEMAR assisted CT reconstruction is effective for treatment planning in spinal and pelvic regions.

Acknowledgments: Thanks to the medical physics team in Perth, WA, at Sir Charles Gardiner Hospital, Genesis Cancer Care, University of Western Australia, and ICON Cancer Center for their guidance, support and resources during this study. Special thanks to Brendan James Chick, Mahesh Mundayadan Chandroth, and Anthony James Venning for their insightful review and critique in the drafting of this manuscript. Thanks to Gabore Neveri for advice and help with CT scanning the phantoms, and Nathaniel Barry for advice on statistical evaluations.

O127. Towards simulation-free MR-linac treatment planning

Urszula Jelen[1,*], Madeline Carr[1], Maddison Picton[1], Vikneswary Batumalai[1], David Crawford[1], Valery Peng[1], Tania Twentyman[1], Jeremy de Leon[1], Michael Jameson[1]

[1]Genesis Care, Sydney, Australia

Introduction In the current Elekta Unity MR-Linac (MRL) radiotherapy workflow, a simulation-CT provides reference anatomical and voxelised electron density (ED) information for treatment planning. Each contoured organ is then assigned an average bulk-density value, which is later used to assign densities to structures contoured on the daily MR scans. An MRL provides opportunities to explore novel MR-only workflows [1] and accurate ED estimates are required without simulation-CT [2–4]. This MRL-based study investigates the dosimetric impact of using an individual- and population-based bulk-density override.

Method Datasets of 74 male-pelvis patients treated on the St Vincent's Unity MRL were analysed retrospectively. Their individual-EDs were extracted and the population value was calculated for several organs (rectum, sigmoid, bladder, GTV, patient outline, bone, femurs). 10 patients with outlying organ ED values had their reference plans recalculated to find an individual-ED dose (IndD) and population-ED dose (PopD). Percentage differences in mean dose were calculated between these plans and the voxelised simulation-CT dose (sCTD).

Results The individual-EDs of all selected patients remained within 5% of the population average for solid soft tissue organs, and within 8% for bony structures. The largest residual variation was observed for hollow organs (rectum, sigmoid) due to variable amounts of gas included in the contour. The differences in maximum doses, mean doses and minimum doses (recorded for target structures only) between sCTD and IndD/PopD plans remained $\leq \pm 1.9\%$, $\pm 2.9\%$ and $\pm 3.7\%$ for soft tissue organs, target organs, and bony structures, respectively. No clear correlation was observed between structures with larger differences in their individual-ED values compared to the population, and %differences in dose indices between the 3 calculated plans.

Conclusion Given the comparable dose differences observed between PopD and IndD (current clinical method), using a population-based ED was deemed feasible in an MRL workflow.

References

1. Liu C et al. (2022) Advances in MRI-guided precision radiotherapy. Precision Radiation Oncology 6: 75– 84.
2. Karotki A, Mah K, Meijer G and Meltsner M (2011) Comparison of bulk electron density and voxel-based electron density treatment planning. Journal of Applied Clinical Medical Physics 12: 97–104.
3. Hsu SH, Zawisza I, O'Grady K, Peng Q, and Tomé WA (2018) Towards abdominal MRI-based treatment planning using population-based Hounsfield units for bulk density assignment. Physics in medicine and biology 63(15): 155,003.
4. Prior P et al. (2016) MRI-based IMRT planning for MR-linac: comparison between CT- and MRI-based plans for pancreatic and prostate cancers. Physics in medicine and biology 61(10): 3819–3842.

O128. Voxel level dose prescription in precision prostate cancer radiotherapy

Yutong Zhao[1], Hayley Reynolds[2], Robert Finnegan[3,4], Annette Haworth[4,*], Martin Ebert[1,5]

[1]University of Western Australia, School of Physics, Mathematics and Computing, Crawley, Australia, [2]University of Auckland, Bioengineering Institute, Aukland, New Zealand, [3]Royal North Shore Hospital, St Leonards, Australia, [4]University of Sydney, School of Physics, Camperdown, Australia, [5]Sir Charles Gairdner Hospital, Radiation Oncology, Nedlands, Australia

Introduction The conventional practice of prescribing a uniform dose in prostate cancer radiotherapy fails to accommodate the heterogeneous nature of the disease. Approaches based on voxel level tumour characteristics have been developed.

Method Using patient histological information, tumour maps were developed for 62 study participants. The maps provide voxel-level information at 0.22 mm in-plane resolution/2.5 mm slice thickness regarding tumour probability, cell density and tumour grade. A tumour control probability (TCP) model was used to guide the optimal redistribution of a boost dose allocated according to previously reported protocols. The optimisation was constrained requiring integral dose (energy) in the prostate volume to remain fixed. Evaluation was via the potential increase in TCP using conventional uniform-dose prescription as the comparator. Inter-voxel variations in grade were considered via a population distribution of radiosensitivity as well as via derivation of grade-dependent sensitivity parameters.

Results Prescription based on a dose redistribution consistently improved predicted TCP. The relative improvement tends to reduce as boost dose is increased with the largest improvement seen for the most hypofractionated schedules. Use of population-based radiosensitivity distributions led to consistent results across the studied patients, whereas use of a grade-dependent sensitivity led to large variations in results across the studied patients.

Conclusion There is considerable scope for providing judicious redistribution of dose in order to optimise prostate cancer radiotherapy prescription and reduce normal tissue toxicity. The most benefit for redistribution occurs for hypofractionated schedules. The impact of local tumour grade suggests that the accuracy of the utilised model may require more precise grade information. A full assessment of the voxel-based approach will require consideration of the multiple uncertainties in the treatment process including motion at treatment.

Acknowledgements: The authors gratefully acknowledge the support of NHMRC grant 1,126,955.

O129. Dosimetric impact on plan-quality with variable air cavity dimension and density override within the PTV for rectum patients

Eujin Chan[1,*], Simon Goodall[2], Leon Dunn[1], Paul Moorfoot[1]

[1]Genesiscare, Footscray, Australia, [2]Genesiscare, Wembley, Australia

Introduction The aim of this study is to determine the impact of rectal air volume changes on treatment plan quality, and subsequently inform daily cone-beam computed tomography (CBCT) evaluation constraints, in terms of acceptable rectal air volume during treatment.

Method Reference plans were generated for twelve patients using the same optimization objectives. Two studies were performed: 1) An evaluation of plan quality degradation with expanding air volume. Plans were recalculated with the clinically observed air volume expanded uniformly by 0.3 cm, 0.6 cm, 0.8 cm, 1.0 cm, and 1.5 cm,

respectively. 2) An investigation of the impact on plan quality from overriding rectal air. Plans were generated for all twelve patients by reoptimizing the reference plan with the existing air cavity overridden to tissue density. All calculations were compared to their reference for both studies.

Results An average air cavity volume increase from 8.7 ± 5.3 cc to 139.6 ± 24.4 cc corresponded to uniform expansions from 0 cm to 1.5 cm respectively. Volume increases from 0.3 cm to 1.5 cm, resulted in D98% coverage decreasing by up to 7.8 ± 1.6% and D2% increasing by up to 1.6 ± 0.3%. Plan quality following override of rectal air had minimal impact to the OARs whilst maintaining PTV coverage when compared to the reference plan. For the reoptimized, air overridden plans, the total MU decreased on average by 2.7 ± 1.4%.

Conclusion Air cavity volumes above 20 cc are seen to degrade the high-dose PTV coverage while increasing the 102% and 105% isodose coverage. By reoptimizing plans without the air cavity, a similar plan quality was achieved when compared to the reference plan. A reduction in total MU were seen thus reducing the total plan complexity. Clinical CBCT guidelines on acceptable rectal air volume and position during fractions could be deduced.

O130. Feasibility of automated CBCT-based online adaptive radiotherapy in cervical cancer: A comparison study of supervised and automated workflows

Ryan Brown[1,*], Alex Turk[1], Adam Briggs[2], Isabelle Fent[3], Leigh Ambrose[1], Marita Morgia[1], Mark Stevens[1,4], Jeremy Booth[1,5]

[1]Northern Sydney Cancer Centre, Royal North Shore Hospital, St Leonards, Australia, [2]Shoalhaven Cancer Centre, Shoalhaven District Memorial Hospital, Nowra, Australia, [3]Peter MacCallum Cancer Centre, Parkville, Melbourne, Australia, [4]Northern Clinical School, Sydney Medical School, University of Sydney, Sydney, Australia, [5]School of Physics, University of Sydney, Sydney, Australia

Introduction Conventional radiotherapy techniques for cervical cancer utilise large margins to account for interfraction anatomical variations, such as cervical-uterine motion [1,2]. Online adaptive radiotherapy (oART) can account for interfraction changes and may facilitate margin reduction [3]. Current daily oART processes require user input for contour modification, which can be time-consuming and result in larger intrafraction uncertainties [4]. This study evaluates the geometric and dosimetric differences between the standard of care supervised oART (S-ART) workflow and an autonomous oART (A-ART) workflow.

Method Five previously treated locally advanced cervical cancer patients were planned in the Ethos (Varian) research emulator environment. All patients underwent simulated treatment with 2 methods, A-ART and S-ART (n = 50 simulations). The methods were defined as: A-ART- key influencer contours affecting target propagation (bladder, rectum and uterus) were manually modified by the radiation therapist (RT), while all other target and organ-at-risk (OAR) contours were not modified; S-ART- all OAR and target contours were manually modified by the radiation oncologist (RO). A-ART and S-ART contours were compared using volume/surface-distance metrics, such as mean-distance-to-agreement (MDA). For dosimetric analyses, key dose-volume-histogram (DVH) metrics were quantified for all A-ART and S-ART contours.

Results Geometric comparison of A-ART and S-ART contours is shown in Fig. 1. Dosimetric analysis of A-ART and S-ART contours (Fig. 2) showed D95% for all targets and D2cc for all OARs to be on average less than 1% different across the population.

Conclusion Geometric and dosimetric differences between A-ART and S-ART in the setting of cervical cancer are within the current margins and accepted uncertainties for treatment. Daily A-ART is feasible with minimal user interaction required. This work may help to identify outlier patients prospectively and inform margins required for A-ART workflows.

References

1. Pötter, R., Tanderup, K., Kirisits, C., de Leeuw, A., Kirchheiner, K., et al. (2018). The EMBRACE II study: The outcome and prospect of two decades of evolution within the GEC-ESTRO GYN working group and the EMBRACE studies. *Clinical and translational radiation oncology*, *9*, 48–60.
2. Taylor, A., Powell, M. E. (2008). An assessment of interfractional uterine and cervical motion: implications for radiotherapy target volume definition in gynaecological cancer. *Radiotherapy and oncology*, *88*(2), 250–257.
3. Heijkoop, S. T., Langerak, T. R., Quint, S., Mens, J. W. M., Zolnay, A. G., et al. (2015). Quantification of intra-fraction changes during radiotherapy of cervical cancer assessed with pre- and post-fraction Cone Beam CT scans. *Radiotherapy and Oncology*, *117*(3), 536–541.
4. Brown, R., Yock, A., Moore, K., Briggs, A., Turk, A., et al. (2021). Best practices white paper: Cervix adaptive radiotherapy with Ethos. Varian: A Siemens Healthineers Company. https://medicalaffairs.varian.com/Clinical-Notes-Technical-Notes-and-White-Papers. Accessed 15/07/2022.

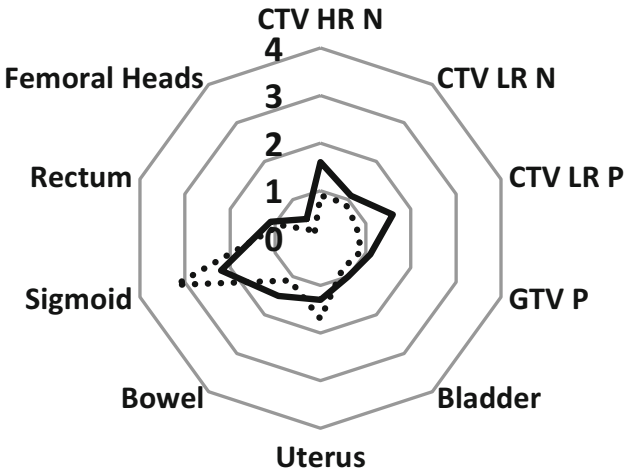

Fig. 13. Radar plot of MDA and stdev for all structures.

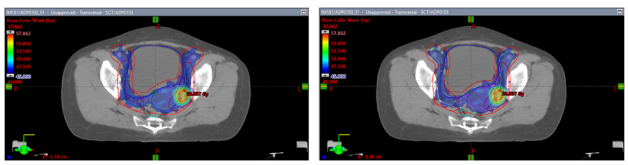

Fig. 2. Planned dose distributions for S-ART (left) and A-ART (right) contours.

O131. Comparison of synthetic CTs derived from 2D versus 3D convolutional neural networks via Head and Neck MRIs for RT planning

Jacob Antunes[1], Dane Pittock[1], Paul Jacobs[1], Kanak Chatterjee[1], Aaron Nelson[1], Jonathan Piper[1], Tony Young[2,3,4], Shrikant Desphande[3,4,*]

[1]Mim Software, Inc, Cleveland, United States, [2]Institute of Medical Physics, School of Physics, University of Sydney, Sydney, Australia, [3]South Western Sydney Cancer Services, NSW Health, Sydney, Australia, [4]Ingham Institute, Sydney, Australia

Introduction MR-only guided Radiation Therapy (RT) requires electron density information, usually acquired from a planning CT (pCT). Several works propose utilizing deep-learning to generate synthetic CT (sCT) from MR. However, most have focused on 2D implementations. We present in this work the efficacy of a 3D-convolutional neural network (CNN) for sCT generation from MR for head and neck cancers and compare its output to its 2D-CNN implementation.

Methods 54 head and neck cancer patients who were scanned simultaneously with Dixon-MR sequences and pCT using fixed immobilization were included. A UNet-based CNN was constructed with residual blocks. 2D and 3D implementations were trained on 46 patients to generate sCT from Dixon-MR phases, iteratively reducing pixel-wise error between the sCT and pCT. For 3D experiments, varying patch sizes were assessed. Dose was calculated on the sCTs and pCTs using a Monte-Carlo algorithm. Performance was evaluated on 8 patients using mean absolute error (MAE), global gamma analysis (3%/3 mm), and qualitative assessment.

Results All 3D-CNN experiments yielded similar or better MAE compared to 2D-CNN (Table 1). Noticeable improvement in bone reconstruction was observed with 3D-CNN outputs compared to 2D-CNN, primarily in sagittal and coronal planes (Fig. 1). A 3D patch of 96 row-pixels yielded significantly lower MAE than 2D-CNN (73.4 ± 6.5 HU versus 79.5 ± 8.4, $p < 0.05$). Minimal differences were measured in terms of Gamma pass rate ($99.5 \pm 0.4\%$ versus $99.4 \pm 0.7\%$, $p \geq 0.05$).

Conclusion Generating sCTs for MR-only guided RT planning may benefit from 3D-CNNs over 2D-CNNs due to lower MAE, better bone reconstruction and limited impact on calculated dose.

Table 1. Quantitative comparison of sCTs derived from 2D- versus 3D-CNN.

Experiment	Patch (row-pixels)	MAE (HU)	Global Gamma Pass Rate (%)
2D-CNN	256	79.5 ± 8.4	99.4 ± 0.7
3D-CNN	32	81.7 ± 6.4	98.7 ± 0.9
	64	74.5 ± 5.6	99.0 ± 0.9
	96	73.4 ± 6.5*	99.5 ± 0.4
	128	73.6 ± 6.1	99.4 ± 0.4

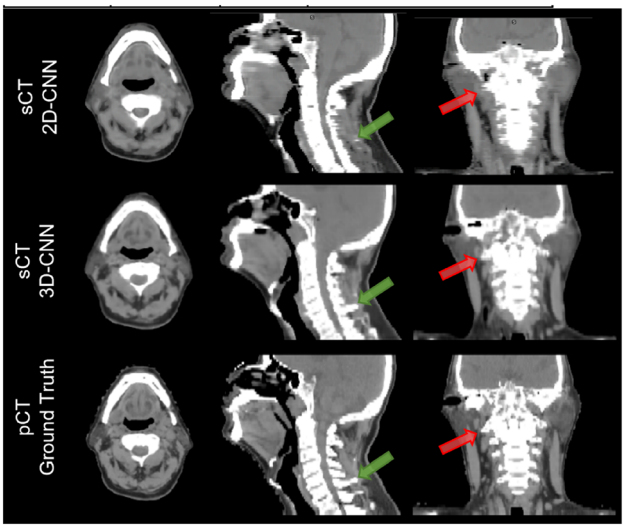

Fig. 1. Qualitative comparison of sCTs derived from 2D-versus 3D-CNN.

O132. [Invited] Learning from every patient

Marcel van Herk[1,*]

[1]University of Manchester, Manchester, UK

O133. Integrating radiation treatment planning data into virtual surgical planning for the surgical management of radiation osteonecrosis

Ashley Cullen[1,2,*], Robin Hill[1,3], Kai Cheng[1,4], Jonathan Clark[1,3], Dale Howes[1,3]

[1]Chris O'Brien Lifehouse, Camperdown, Australia, [2]University of Wollongong, Wollongong, Australia, [3]University of Sydney, Camperdown, Australia, [4]Royal Prince Alfred Hospital, Camperdown, Australia.

Introduction Radiotherapy is a highly effective modality for the treatment of head and neck (H&N) malignancies. Whilst toxicities have largely decreased with the widespread introduction of modulated treatment delivery, one toxicity that remains an issue for a subset of patients is mandibular radiation osteonecrosis (ORN). [1] One common treatment for this is mandibular free-flap reconstruction of the affected bone, however despite the advanced of technology in both radiotherapy and surgery, there is for the most part a disconnect between the radiation doses which have resulted in the ORN, and the surgical planning for its subsequent treatment. [2].

Method A custom application was written in C# utilising the Varian Eclipse Scripting API, which segments regions of H&N radiotherapy plans in which doses to the mandible and facial bones exceed dose thresholds deemed radiobiologically significant for the induction of

ORN. The application then exports all segmented volumes in a format compatible with the virtual surgical planning (VSP) software, which are coregistered to the planning CT coordinate system. The exported structures and planning CT are then imported in the VSP software so the dose regions of concern are able to be overlaid over the high-resolution surgical CT scans, and used for the pre-operative planning and manufacture of 3D-printed surgical guides.

Results This approach resulted in a high degree of confidence in the decision making for resection margins in challenging mandibular reconstruction cases by the surgeon, where radiation dosimetry data directly guided the surgical approach.

Conclusion The incorporation of radiation dosimetry data in the planning of ORN reconstruction surgery can improve reconstruction accuracy, enhance dental rehabilitation, as well as reduce intraoperative and postoperative complications. [3].

References

1. Aarup-Kristensen, S et al. Osteoradionecrosis of the Mandible after Radiotherapy for Head and Neck Cancer: Risk Factors and Dose-Volume Correlations. Acta oncologica 58.10 (2019): 1373–1377.
2. O'Dell, Karla, and Uttam Sinha. Osteoradionecrosis. Oral and maxillofacial surgery clinics of North America 23.3 (2011): 455–464.
3. Jenkins, Glyndwr W et al. Dosimetry-Guided Virtual Surgical Planning in the Reconstruction of Mandibular Osteoradionecrosis. British journal of oral & maxillofacial surgery 59.8 (2021): 947–951.

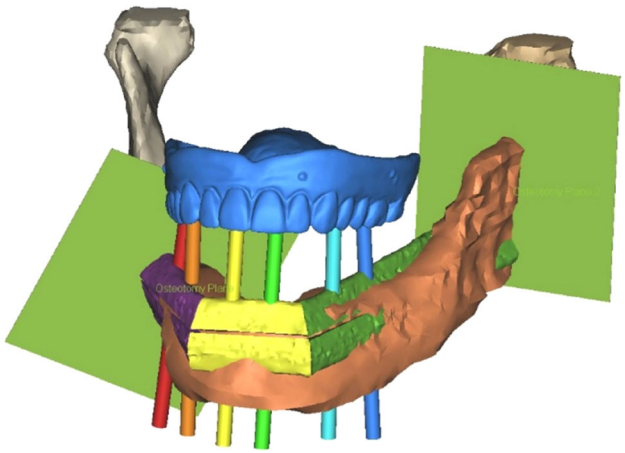

Fig. 1. With the use of radiation dosimetry data, two resection planes (green) are placed. The virtual mandible is reconstructed utilising multiple fibula segments (purple, yellow, and green).

O134. Insufficiencies in ray tracing dose calculation relative to Monte Carlo in CyberKnife multiple brain targets treatment

Godfrey Mukwada[1,2], Malgorzata Skorska[1], Pejman Rowshawfarzad[2], Martin Ebert[1,2]

[1]Sir Charles Gairdner Hospital, Nedlands, Australia, [2]The University of Western Australia, Nedlands, Australia

Introduction Monte Carlo (MC) and Ray Tracing (RT) calculated dose differences is scarce for single plan multiple brain targets stereotactic radiosurgery (SRS). This study investigates factors leading to the differences between MC and RT calculated doses through retrospective study and measurements.

Method CyberKnife commissioning beam data including the detectors used were queried for integrity. RT and MC calculated Off-Centre-Ratios (OCRs) and Tissue-Phantom-Ratios (TPRs) were exported from Precision TPS and compared with measured. Following the review, a retrospective study was undertaken of 53 patients with a total of 209 brain metastases that were treated using the CyberKnife M6 system between 2018 and 2020. Patients were treated with treatment plans generated using RT algorithm and fixed cones. The number of gross tumour volumes (GTVs) per plan ranged from 1 to 18. Treatment plans were then recalculated using MC keeping the beam parameters unchanged. Plan parameters for MC and RT were extracted and dose differences were normalised to MC calculated doses. Relationships were investigated between GTV mean dose and plan parameters. Plans with 5 GTVs were created on a phantom and dose was measured and compared with MC and RT calculated dose.

Results MC and RT calculated TPR agreed with measured data within ± 1% beyond depth of maximum dose and OCR showed up to 4.3% difference in the penumbra and out-off-field regions. MC and RT calculated GTV mean dose differences were up to -5.7%. More GTVs per plan and reduction in their geometric separation were associated with increased differences between RT and MC. Measured doses were more consistent with MC calculated doses.

Conclusion RT and MC calculated dose disagreement in multiple cranial targets depends on the number of GTVs per plan, number of GTVs in proximity and plan complexity. MC dose calculation is recommended for complex CyberKnife SRS of multiple brain metastases.

O135. SEAFARER Australia – Is our patient specific quality assurance effective?

Joerg Lehmann[1,2,3,*], Mohammad Hussein[4], Catharine Helen Clark[4,5,6], Peter Greer[1,2]

[1]Calvary Mater Newcastle, Newcastle, Australia, [2]University of Newcastle, Newcastle, Australia, [3]University of Sydney, Sydney, Australia, [4]National Physical Laboratory, Teddington, UK, [5]University College Hospital London, London, UK, [6]*University College London, London, UK.*

Introduction The success of radiotherapy, including patient survival, has been shown to be impacted by its quality [1]. Patient-Specific Quality Assurance (PSQA) is generally performed to assess whether the planned dose distribution of an intensity modulated treatment can be delivered to the patient. However, PSQA has been found to be unreliable at times [2] and hence warrants closer inspection. This work builds on the international "Sensitivity of Patient Specific Quality Assurance" (SEAFARER) study [3] and introduces a broader follow-on study for Australia.

Method In the original SEAFARER study, known delivery errors were introduced into SABR spine plans created by 17 participating institutions producing 12 variations of each plan. Institutions, blinded to the errors introduced, performed PSQA and reported outcome. For clinical impact assessment the dose distributions of the error plans were also calculated. Change in two DVH parameters relative to the original plan were used to assess impact of errors.

Results While the results showed problems with sensitivity, as well as with specificity, of the clinical PSQA procedures [3], they also demonstrated a large variation of the impact the errors had on the plans [4]. These were not related to the planning system used (Fig. 1). To avoid variation in the impact of the errors introduced and to

standardise the plan used such that different systems can be more directly compared, the SEAFARER Australia project will use the same plan for each treatment site. It will also expand the scope to include lung, and head and neck body sites. The project will investigate factors that influence sensitivity and specificity including dosimetry equipment, software, assessment metrics and tolerances.
Conclusion SEAFARER Australia will perform PSQA assessments for Australian radiotherapy institutions for spine, lung, and head and neck body sites and quantify the sensitivity and specificity of the PSQA process to clinically relevant errors.
References

1. Peters LJ, O'Sullivan B, Giralt J, Fitzgerald TJ, Trotti A, Bernier J, Bourhis J, Yuen K, Fisher R, Rischin D (2010) Critical impact of radiotherapy protocol compliance and quality in the treatment of advanced head and neck cancer: results from TROG 02.02. J Clin Oncol. https://doi.org/10.1200/jco.2009.27.4498
2. Kry SF, Molineu A, Kerns JR, Faught AM, Huang JY, Pulliam KB, Tonigan J, Alvarez P, Stingo F, Followill DS. (2014) Institutional patient-specific IMRT QA does not predict unacceptable plan delivery. Int J Radiat Oncol Biol Phys. https://doi.org/10.1016/j.ijrobp.2014.08.334
3. Lehmann J, Hussein M, Barry MA, Siva S, Moore A, Chu M, Díez P, Eaton DJ, Harwood J, Lonski P, Claridge Mackonis E, Meehan C, Patel R, Ray X, Shaw M, Shepherd J, Smyth G, Standen TS, Subramanian B, Greer PB, Clark CH. (2022) SEAFARER – A new concept for validating radiotherapy patient specific QA for clinical trials and clinical practice. Radiother Oncol https://doi.org/10.1016/j.radonc.2022.04.019
4. Hussein M, Lehmann J, Clark CH (2022) Robustness of spine SABR plans to delivery errors within machine tolerance: multicentre analysis ESTRO 2022.

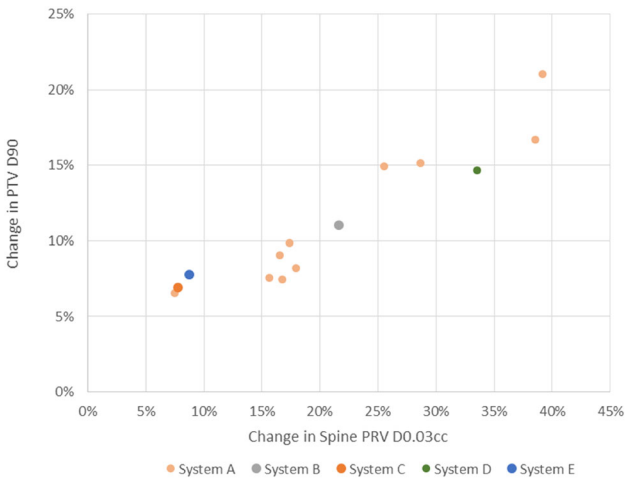

Fig. 1. Impact of the same combination of delivery errors (within machine specifications) on selected DVH parameters for various treatment planning systems.

O136. Advancing the quality of patient pre-treatment verification

Andrew Kovendy[1,*]

[1]North Coast Cancer Institute NSW, Coffs Harbour, Australia

Introduction The verification of patient treatment plans has evolved significantly over the past 20 years along with sophistication of instrumentation and methods used to ensure that patients undergoing radiation therapy are treated to within acceptable tolerances. However patient–specific QA (PSQA) still largely involves surrogate measurements and/or calculated fluence and assessment usually in the form of a gamma pass rate which provides limited information. Such verification methods are essential in identifying potential treatment errors but may not address the quality of treatment of interest to clinicians.
Method As part of the process of moving towards newer PSQA methods our institution is trialing the clinical pre-treatment assessment of treatment quality using the ArcCheck® and 3DVH® in addition to Suncheck® Patient PerFraction and EPID dosimetry as the first stage towards developing an automated reporting system that can provide more detailed treatment analysis. Following validation of the methodology clinical plans were measured and assessed using multiple methods to compare treatment quality results.
Results While all plans measured using current methods typically showed high pass rates (> 95% for 3%/3 mm and > 90% 2%/2 mm gamma criteria) detailed assessment including measured Dose Volume Histogram (DVH) analysis revealed variability with target coverage and dose to organs at risk. This has been of significant value with the assessment of coverage of small targets (below 10 mm) and high-risk regions such as spinal vertebra treated with Stereotactic Radiation Therapy (SRT).
Conclusion Multiple independent pre-treatment measurements and heuristic automated analysis can report on areas where clear improvements can be made in areas of linac performance, plan quality and beam modelling and provide clinical assessment information to Radiation Oncologists, and provide a potential role expansion for medical physicists.

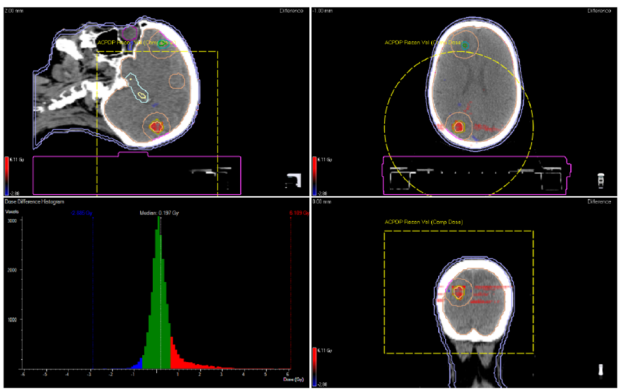

Fig. 14. A 3D measured vs plan calculation for a brain SRT treatment.

O137. [Invited] Neutron capture enhanced particle therapy (NCEPT): A series of fortunate events

Mitra Safavi-Naeini[1,*]

[1]Australian Nuclear Science and Technology Organisation, Sydney, Australia

Neutron Capture Enhanced Particle Therapy (NCEPT) is an augmentation of charged particle therapy which exploits thermal neutrons generated internally via nuclear fragmentation within the treatment site to deliver a biochemically, spatially and temporally-targeted radiation dose boost directly to cancer cells1. This is achieved by

using biochemically-targeted agents to capture thermal neutrons inside the cancer cells. The dose delivered to the target thus consists of two principal components: the ion dose and the neutron capture dose; exploitation of the latter enables the reduction of the former, reducing the dose to non-malignant tissue and facilitating hypofractionation1. Furthermore, NCEPT enables delivery of a therapeutic neutron capture dose to micro-infiltrates that have spread beyond the primary target volume. Our in vitro results demonstrate that following proton, helium or carbon ion irradiation, the proliferative capacity of tumour cells pre-treated with 10B or 157Gd-based neutron capture agents is reduced by a factor of 2 to 3; furthermore, tumour cell viability outside of the primary target volume is also substantially reduced. These results demonstrate the potential for NCEPT to provide an effective dose to tumour tissue with a reduced collateral radiation dose to off target tissues when compared to current heavy-ion therapy protocols. More importantly, NCEPT introduces the concept of biochemically targeting this dose to micro-infiltrates outside the margins of a conventionally image-targeted irradiation volume. In this talk, I will take the audience through the history of NCEPT, from its discovery to the preliminary in vivo results and our plans for the clinical translation of NCEPT.

O138. [Invited] Radiosensitising strategy for peptide receptor radionuclide therapy with 177Lu-DOTATATE

Zena Wimana[1,*]

[1]Institut Jules Bordet, Bruxelles, Belgium

O139. Characterization of a 0.8 mm3 Medscint plastic scintillator detector system for small field dosimetry

Elena Timakova[1,2,*], Sergei Zavgorodni[1,2], Magdalena Bazalova-Carter[1]

[1]University of Victoria, Victoria, Canada, [2]BC Cancer Agency, Victoria, Canada

Introduction Plastic scintillator detectors (PSDs) have demonstrated ability to meet requirements of small field dosimetry, and recently Medscint developed a 1 mm long, 1 mm diameter cylindrical PSD with effective volume of 0.8 mm^3. Clinically relevant, small field dosimetric properties of this detector, combined with a novel scintillation dosimetry system—HYPSERSCINT RP-200, and HYPERDOSE analysis software were evaluated in this study.
Methods This novel scintillator-based dosimetry system was dosimetrically characterized with 6MV and 10MV-FFF x-ray beams delivered by a Varian TrueBeam STx. The detector was characterized for leakage, short-term repeatability, dose response linearity, angular response, dose rate dependence, and field size dependence for fields of 0.25×0.25 to 10×10 cm^2. Measured output factors were compared with published data to determine Kq.
Results The dosimetry system showed excellent short-term repeatability with standard deviation of only 0.044 0.007%. It demonstrated good dose linearity with variations less than 1.0% for 25 MU and above. The dosimetry system was found to be independent of dose rate and angle of irradiation, with deviations for both below 0.5%. Leakage was found to be minimal—within measurement uncertainty. The output factors for field sizes 2×2 cm^2 and larger agreed within 1.4% with those reported in literature. However, for 10MV-FFF field size of 0.6×0.6 cm^2 differences up to 3.8% were seen. Kq factors for this PSD for fields of 0.6×0.6 cm^2 and up were determined to be within 4.0% of unity. For fields smaller than 0.5×0.5 cm^2 no comparable data were found in the literature.
Conclusions The HYPERSCINT RP-200 dosimetry system coupled with a 0.8 mm^3 plastic scintillator detector and HYPERDOSE analysis software showed excellent dosimetric properties demonstrating to be clinically relevant for relative dosimetry down to fields sizes of 0.6×0.6 cm^2 and potentially smaller.

O140. Containerisation in the Australian Computer-Assisted Theragnostics network (AusCAT)

Janet Cui[1,2,*], Matthew Field[1,2], Phillip Chlap[1,2], Daniel Al Mouiee[1,2], Robert Finnegan[1,3], Vicky Chin[1,2], Lois Holloway[1,2,3]

[1]South Western Sydney Cancer Services, NSW Health and Ingham Institute, Sydney, Australia, [2]South Western Sydney Clinical Campus, School of Clinical Medicine, University of New South Wales, Sydney, Australia, [3]Institute of Medical Physics, School of Physics, University of Sydney, Sydney, Australia

Introduction In recent years, healthcare's technological dependence has been revolutionised.This change, however, must be adaptive to the various software infrastructures within oncology information networks, as technical barriers emerge when installing and updating software over time. In the Australian Computer-Assisted Theragnostics (AusCAT) [1] federated learning network for radiation oncology, we have utilised Docker as a tool to containerise the required software into flexible submodules that are isolated from a host machine's operating system.
Methods An automated pipeline was constructed, using Docker [2], to run a multi-service network of AusCAT tools at a single node. This included databases and structured query language (SQL) extraction tools (PostgreSQL[3], pgAdmin[4], Pentaho Data Integration [5]), DICOM-RT anonymisation and PACS (Clinical Trials Processor (CTP)[6], Orthanc[7]), data harmonisation (D2RQ Platform[8]), and the AusCAT federated learning platform (Apache Tomcat[1, 9]). A Docker compose script orchestrates the tools and additional scripts were implemented to configure each environment as well as an automated testing pipeline for each component. Figure 1 shows the overview of Docker architecture in AusCAT. Artificial data modelled on AusCAT's clinical and imaging databases was used to test the docker pipeline.
Results On average, the docker pipeline took 100 s to deploy the containers. This runtime was also dependent on the network speed, configuration, and hardware specifications of the host machine. Figure 2 shows that the Docker container consumes around 810 MiB of memory in total, and the Docker operation is dynamic.
Conclusion The utilisation of Docker is expected to save time and reduce infrastructure cost when deploying and maintaining AusCAT client software. New nodes joining the AusCAT collaborations can setup the pipeline on their servers, with little-to-no manual intervention The next step is to optimise the Docker image such as reducing image hard disk utilisation whilst preserving all containerisation features.

Disclosures

Acknowledgement of Australian Research Data Commons for a platforms grants and Cancer Institute NSW for an early career grant which made this work possible.

References

1. Field M, et al. Implementation of the Australian Computer-Assisted Theragnostics (AusCAT) network for radiation oncology data extraction, reporting and distributed learning. J Med

Imaging Radiat Oncol. 2021;65(5):627–636. https://doi.org/10.1111/1754-9485.13287.—DOI—PubMed.
2. Docker Inc. 2022, "Developers Love Docker. Businesses Trust It.", accessed 09 July 2022, < https://www.docker.com/ > .
3. The PostgreSQL Global Development Group 2022, "PostgreSQL: The World's Most Advanced Open Source Relational Database", accessed 09 July 2022, < https://www.postgresql.org/ > .
4. pgAdmin—PostgreSQL Tools, accessed 09 July 2022, < https://www.pgadmin.org/ > .
5. Hitachi Vantara Corporation LLC 2022, Hitachi Vantara Lumada and Pentaho Documentation, accessed 09 July 2022, < https://help.hitachivantara.com/Documentation/Pentaho/9.3 > .
6. MIRC Medical Imaging Resource Center 2021, MIRC CTP, accessed 09 July 2022, < https://mircwiki.rsna.org/index.php?title=MIRC_CTP > .
7. Sébastien Jodogne, ICTEAM UCLouvain, "Orthanc, Open-source, lightweight DICOM server", accessed 09 July 2022, < https://www.orthanc-server.com/ > .
8. D2RQ, Accessing Relational Databases as Virtual RDF Graphs, accessed 09 July 2022, < http://d2rq.org/ > .
9. The Apache Software Foundation 2022, Apache Tomcat, accessed 09 July 2022, < https://tomcat.apache.org/ >

.

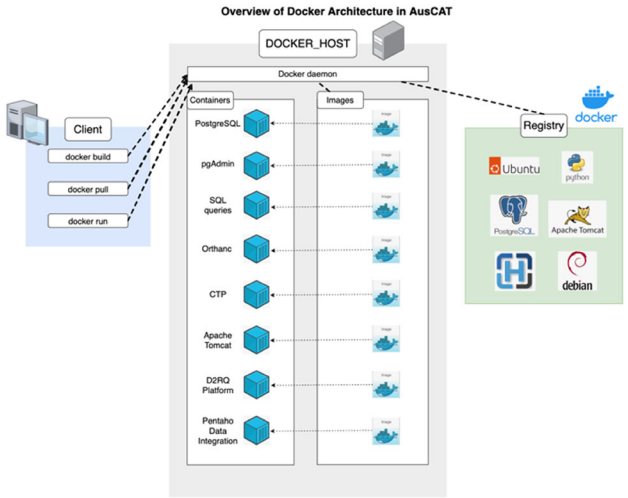

Fig. 1. Overview of Docker architecture in AusCAT.

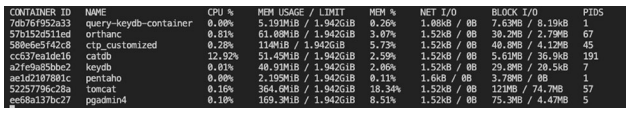

Fig. 2. The docker stats command returns a live data stream for running containers.

O141. Trend in off-axis beam modelling observed for AcurosXB in ANZ audit data

Jeremy Supple[1,*], Andrew Alves[1]

[1]Australian Clinical Dosimetry Service, Yallambie, Australia

Introduction IAEA TRS-430 [1] recommends that off-axis beam modelling for homogenous geometries should be within ± 3%. The ACDS dataset has identified a mean difference of more than 3% in off-axis beam modelling with AcurosXB models in the ANZ data for 10 × 10 cm^2 field sizes. This trend was not present in the other treatment planning beam models.

Method The ACDS Level II audit is a test of treatment planning system performance utilising the PTW Octavius® 1500^{MR} ionisation chamber arrays in rectilinear solid water and lung phantoms. A planar matrix of dose measurement points, at 10 cm depth, is obtained during audits for comparison against the planned dose. The audit data was normalized to the central axis (CAX) value in the 10 × 10 cm^2 field.

Results The AcurosXB algorithm overestimates dose towards the corners of 10 × 10 cm^2 fields. The range between the most positive and most negative local dose variations within the scored region is used as a metric to quantify this observation. See Fig. 1. There were 320 Case 2 (20 × 20 cm^2) measurements analysed and 394 Case 3 (10 × 10 cm^2) measurements analysed. The mean dose variation range for AcurosXB 20 × 20 cm^2 plans was 2.0% and the mean range for non-AcurosXB plans was 2.2%. The mean range for AcurosXB 10 × 10 cm^2 plans was 3.1% and the mean range for non-AcurosXB plans was 2.3%.

Conclusion The ACDS is investigating this issue and has launched a nationwide experimental program to corroborate these findings.

References

1. International Atomic Energy Agency (2004) Commissioning and Quality Assurance of Computerized Planning Systems for Radiation Treatment of Cancer, Technical Reports Series No. 430, IAEA, Vienna.

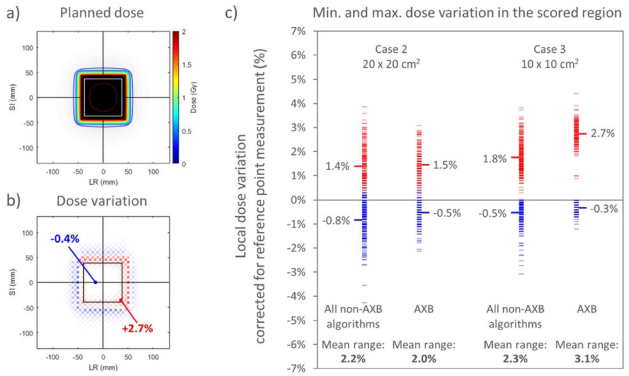

Fig. 1. Beam flatness is assessed within 80% of the field width (a) shown as the white square and (b) shows an example of the minimum and maximum dose variation between the planned dose and measurement within the assessed region. The minimum (blue) and maximum (red) dose variations have been plotted in (c) for non-AXB algorithms and AXB algorithms for two field sizes.

O142. Future dose festival: Implementing a radiation dose structured report program

Amanda Perdomo[1,*]

[1]The Royal Children's Hospital Melbourne, Parkville, Australia

Introduction The application of radiation dose structured report (RDSR) software automates the collation, analysis, and reporting of patient radiation dose. The comprehensive information provided by RDSRs allows for more meaningful assessment of a clinic's radiation

dose as well as image quality (IQ) if images are imported and assessed by the software.

Methods Our clinic implemented a commercial image quality and dose management software, MyXrayDose, in 2019. MyXrayDose imports both images and RDSR files and stores the information after performing IQ assessments. It has comprehensive dashboards with search and alert functionalities. MyXrayDose has been utilised to track IQ and dose over time as well as set alerts for when an individual examination's dose or IQ does not meet pre-set criteria.

Results The implementation of MyXrayDose has allowed the physics team to oversee thousands of examinations and identify trends as well as outliers. One example is shown in Fig. 1 where the dose area product (DAP) for a 12-year-old chest X-ray was 1124 mGy.cm^2 while the average for a 12-year-old is 50 mGy.cm^2 at our clinic. A follow-up on this examination found that the radiographer was inexperienced which allowed our clinic to provide further education to the radiographer to assist in optimising our doses.

Conclusion MyXrayDose is a patient radiation dose and IQ monitoring software that collates information for all patients for all exams involving ionising radiation at our clinic. This allows physicists to identify areas and protocols of concern where the dose and IQ can be optimised as well as identify any trends in increasing dose or decreasing IQ over time.

Acknowledgements: Brian Lunt, MyXrayDose. Funding from The Royal Children's Hospital Foundation.

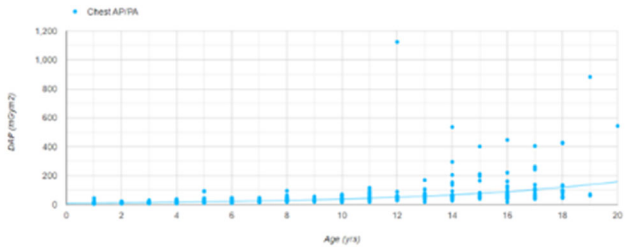

Fig. 1. DAP vs. age for chest X-rays performed at our institution.

O143. Update of the national nuclear medicine diagnostic reference levels

Peter Thomas[1,*], Toby Beveridge[1]

[1]Australian Radiation Protection and Nuclear Safety Agency, Yallambie, Australia

Introduction Australian national diagnostic reference levels (DRLs) for nuclear medicine, including positron emission tomography (PET) and hybrid studies, were last published by ARPANSA in 2017. The levels were based on survey data collected in 2014/15 and also on earlier survey data for rarer procedures. Since 2015, there have been technological developments (particularly in PET) and the way the modalities are utilised has changed. It is therefore appropriate to update the national DRLs for nuclear medicine.

Method A survey of general nuclear medicine and PET facilities was conducted between September 2021 and March 2022. Participants were asked to provide details relating to the doses prescribed for all protocols offered at their facility and to record the doses delivered to patients over a two-week period for both administered radionuclides and CT scans conducted as part of a hybrid imaging study.

Results There were 137 survey spreadsheets submitted to ARPANSA. The data was presented to a liaison panel consisting of representatives from relevant professional and government bodies. The data has informed recommendations made by the panel for updated DRLs for general nuclear medicine, PET and hybrid radiopharmaceutical imaging. The proposed DRLs for the CT portion of hybrid studies include both DLP and $CTDI_{vol}$ metrics, which should provide facilities comparing their doses against the DRLs a better indication of their imaging performance relative to their peers.

Conclusion Data submitted to ARPANSA as part of the nuclear medicine DRL survey has informed recommendations for updated DRLs for nuclear medicine (including PET and hybrid imaging). The new DRLs should provide a better reflection of current practice and should therefore be of greater use to the imaging community.

O144. A generalised approach for estimating patient-like cone beam computed tomography doses

Aaron Fetin[1,*], Lucy Cartwright[2], Jonathan Sykes [3], Alicja Wach[2]

[1]GenesisCare, Lake Macquarie, Australia, [2]Westmead Public Hospital, Westmead, Australia, [3]Blacktown Public Hospital, Blacktown, Australia.

Introduction Cone beam computed tomography (CBCT) is amongst the most utilised image guidance modalities [1]. However, imaging doses are often neglected and vary with patient size [2]. Building upon previous methods, an approach using PCXMC (a diagnostic Monte Carlo simulator) and MATLAB was developed for simulating any CBCT protocol to patients of any size [3]. Investigations were performed for Varian OBI pelvis protocols, using 94 anthropomorphic mathematical phantoms representing 6 ages with size variations. The approach enables tabulation of imaging doses with patient size, across vendors and protocols, for guiding routine use, clinical trials and optimisation.

Method Spatial variance of beam quality and air kerma from Varian OBI 1.6 CBCT protocols were characterized by measurement across the bowtie filters using the Unfors R/F detector. MATLAB was used to automate input of field and patient data to PCXMC. The field is divided into a subset of constant fields, each simulated at a limited number of gantry angles and added. The number of sub-fields and projections for accurate representation was established and used for estimating effective and absorbed doses for pelvis spotlight examinations.

Results Adult absorbed prostate doses ranged from 5.9 ± 0.7 to 36.8 ± 3.9 mGy. Organ dose variations with patient size were location dependent, and hence formulation of effective dose is difficult. However, doses (can be tabulated and adjusted for various air kerma (and beam quality), through a simple relationship:

$$D = \frac{K}{K_0} D_0 \left[a \bullet \ln\left(\frac{Q}{Q_0}\right) + 1 \right]$$

where K_0 and Q_0 are the reference air kerma and beam quality, respectively, and a is a protocol and age dependent constant determined through simulation.

Conclusion A method allowing patient-like CBCT doses to be estimated with factors accounting for variations in tube output and beam quality was developed. The method was used to estimate effective and absorbed doses for 94 phantoms undergoing pelvis spotlight examinations.

References

1. V. Batumalai et al., "Survey of image-guided radiotherapy use in Australia," *J Med Imaging Radiat Oncol,* vol. 61, no. 3, pp. 394–401, 2016, https://doi.org/10.1111/1754-9485.12556.
2. G. X. Ding et al., "Image guidance doses delivered during radiotherapy: Quantification, management, and reduction: Report

of the AAPM Therapy Physics Committee Task Group 180," *Med Phys,* vol. 45, no. 5, pp. 84–99, 2018, https://doi.org/10.1002/mp.12824.
3. T. J. Wood, C. S. Moore, J. R. Saunderson, and A. W. Beavis, "Validation of a technique for estimating organ doses for kilovoltage cone-beam CT of the prostate using the PCXMC 2.0 patient dose calculator," *J Radiol Prot,* vol. 35, no. 1, pp. 153–63, 2015, https://doi.org/10.1088/0952-4746/35/1/153.

O145. [jedi hand wave] These are not the sieverts you are looking for—researchers don't know about or ignore RPS-8 and no-one reads the reports…

Daniel Badger[1,*]

[1]SA Medical Imaging, Woodville South, Australia

Introduction In many jurisdictions in Australia, clinical research that involves the exposure of humans to ionising radiation must comply with RPS-8[1], including a radiation dose and risk assessment (RDRA) of radiation exposure due to the research that are above the participant's Normal Clinical Management (NCM). In some cases, radiation procedures required by the protocol will be done in NCM. There is considerable confusion about this, and researchers often claim that some or all procedures are "Standard of Care"; even those used in screening for the study or that not all participants would have had outside the study. Care is rarely standardised in actual medical practice, and evidence for these claims is scarce. This study tries to determine the extent of this issue.
Method As a radiation safety officer, the author sits on a Human Research Ethics Committee (HREC) to advise on radiation safety and scientific issues, attending up to 24 meetings per year. 22 meetings in 2021 and 2022 were analysed in this study.
Results Of the 187 studies reviewed, 20% (37) required radiation exposure above the normal clinical management of the participants. Of these, 38% (14) neglected to inform the HREC of the radiation exposure, or incorrectly stated it was part of NCM, and 57% (21) had not provided a RDRA to the HREC as part of their application.
Conclusion The exclusion of NCM radiation exposure makes sense but is confusing for researchers, who may not be aware of their RPS-8 obligations. Sometimes radiation exposure that is not part of NCM for all participants is stated to be NCM for all, and some applicants do not even know that procedures are required by the protocol or that they involve radiation exposure. Failure of researchers to correctly address the requirements of RPS-8 results in delays to the ethical approval process.
References

1. ARPANSA "Code of Practice for the Exposure of Humans to Ionizing Radiation for Research Purposes" (2005), Radiation Protection Series No. 8.

P01. A novel bolus for reconstructed breast radiotherapy

Kasia Bobrowski[1,*]

[1]Canberra Health Services, Canberra, Australia

Introduction Bolus for reconstructed breast radiotherapy is indicated for close/positive margins or cases of skin involvement [1]. We developed an in-house alternative mouldable and reusable bolus, "ThermoBolus", incorporating thermoplastic sheets [2] and silicone [3], resulting in a mouldable, reshapeable sheet that can be made to any thickness. We assessed its suitability for clinical use in the treatment of patients undergoing radiotherapy following a breast reconstruction.
Method A 0.5 cm ThermoBolus was created to fit RANDO [4]. A dart was made and excess bolus removed, then rejoined with tape (Fig. 1(a)). To compare with traditionally used bolus (wet combine) two VMAT plans were created, one for each bolus. 2 Gy per fraction was prescribed with 100% of the dose to be delivered to the entire breast. Three fractions were delivered, with wax added to simulate swelling for two fractions (Fig. 1(b)). TLDs and film were placed beneath the bolus for each fraction.
Results Five out of the six TLD measurements had a dose difference within 3.5% of the calculated dose. A single dose difference of 10% was due to perturbation of the dose from the added wax. Wet combine TLD dose differences were -13.5% – 13.1%. Film measurement gave an average surface dose of 2.02 Gy in both cases. Figure 2 shows the flexibility of ThermoBolus when a contour change is introduced.
Conclusion Measurements with TLDs and film confirmed a homogenous and reproducible surface dose when using ThermoBolus when compared to wet combine. The flexibility of ThermoBolus meant that introduced contour change did not significantly affect the fit of the bolus.
References

1. Chen SA, Hiley C, Nickleach D, Petsuksiri J, Andic F, Riesterer O, Switchenko JM, Torres MA (2013) Breast reconstruction and post-mastectomy radiation practice. Radiat Oncol 8:45. https://doi.org/10.1186/1748-717X-8-45.
2. Klarity Medical, Guangzhou, China.
3. SynTec, Netherlands.
4. Radiology Support Devices Inc, Long Beach, CA.

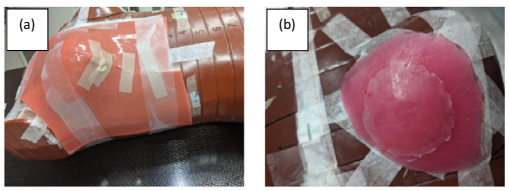

[P01] Figure 1. (a) ThermoBolus on RANDO. (b) wax for contour change.

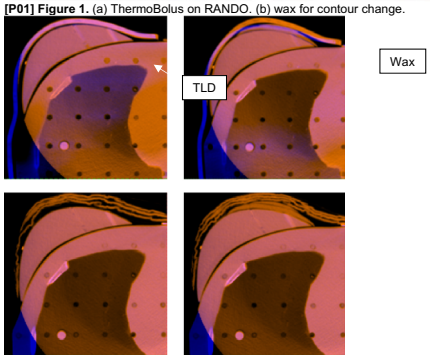

[P01] Figure 2. CBCTs obtained during measurement (orange) and planning CT (blue). Virtual bolus is used for wet combine plan.

P02. Clinical use of 3D printed intra-oral stents: opportunities and obstacles

Tanya Kairn[1,*], **Tania Poroa**[1], **Susannah Cleland**[2], **Jodi Dawes**[1], **Lizbeth Kenny**[1], **Craig Lancaster**[1], **Charles Lin**[1], **Scott Crowe**[1]

[1]Royal Brisbane and Women's Hospital, Herston, Australia, [2]Radiation Oncology Princess Alexandra Raymond Terrace (ROPART), South Brisbane, Australia

Introduction 3D printed intra-oral stents can provide a safe and robust option for achieving reproducible oral positioning to maximise organ-at-risk and normal tissue sparing during head-and-neck radiotherapy [1,2,3]. Previous investigations of 3D printed stents using rigid polylactic acid (PLA) [1] and modular stents printed with slightly flexible thermoplastic polyurethane (TPU) [2,3] have suggested a potential benefit for using flexible filaments to replicate customised wax stents with patient- and treatment-specific detail, without the deterioration of wax or reported jaw strain associated with rigid 3D printed replicas of wax stents [3,4].
Method A 3D printed replica of a personalised wax intra-oral stent was fabricated from food-safe PLA-flex, a flexible PLA filament, at the same density as the wax. VMAT treatments for the tongue and tongue plus jugular nodes were calculated for a modified head phantom with the wax stent in situ and then measured for each of the two stents using radiochromic film. A healthy participant also evaluated the comfort of both stents.
Results Film measurements showed the 3D printed stent to be a suitable replacement for the wax stent, achieving equivalent or improved sparing of tissues lateral and superior to the treated tongue (Fig. 1). The healthy participant reported that although the flexibility of the 3D printed stent was only slightly apparent when placed between the teeth, this stent generally felt more stable in the mouth, and therefore more comfortable, than either the wax stent or the rigid 3D prints tested previously [3,4]. Routine clinical adoption of these patient-specific 3D printed stents was impeded by the challenge of infection control compliance for these 'channelled' devices that 'contact mucous membranes'. Difficulty sourcing flexible filaments that printed with consistent quality across batches also became a substantial obstacle in 2020–2021.
Conclusion Although this work demonstrated a straightforward method for flexible 3D printed oral stents to replace unstable wax stents, further work is needed to ensure 3D stents can comply with infection control requirements and to identify suitably consistent materials, to produce 3D printed stents for routine clinical use.
References

1. Cleland S, Chan P, Chua B, Crowe SB, Dawes J, Kenny L, Lin C, Obereigner E, Peet SC, Trapp JV, Poroa T, Kairn T (2021) Dosimetric evaluation of a patient-specific 3D-printed oral positioning stent for head-and-neck radiotherapy. Phys Eng Sci Med 44:887–899. https://doi.org/10.1007/s13246-021-01025-y
2. Cleland S, Crowe S B, Chan P, Chua B, Dawes J, Kenny L, Lin CY, McDowall WR, Obereigner E, Poroa T, Stewart K, Kairn T (2022) Development of a customisable 3D-printed intra-oral stent for head-and-neck radiotherapy. Tech Innov Patient Support Radiat Oncol 23:1–7. https://doi.org/10.1016/j.tipsro.2022.06.001
3. Kairn T, Chan P, Chua B, et al. (2022) Magnetic resonance imaging assessment of the suitability and consistency of radiotherapy treatment positioning achieved using intra-oral stents, IFMBE Proc **In press.**
4. Kairn T, Cleland S, Dawes J, et al. (2022) Patient-specific and modular oral positioning stents for potential use during head-and-neck radiotherapy treatments. Phys Eng Sci Med 45:355. https://doi.org/10.1007/s13246-021-01094-z

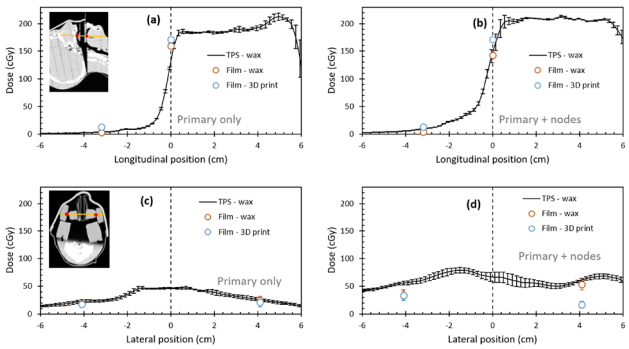

Fig. 1: Single fraction dose calculated by TPS for phantom with wax stent and measured using film for phantom with wax stent and 3D printed replica. Insets in (a) and (c) show locations of film dose profiles (yellow lines) and film dose points (red dots).

P03. An evaluation of 3D printed bolus in radiotherapy MV x-ray beams

Chunsu Zhang[1,*], Robin Hill[2], Will Lewin[3], Ashley Cullen[2]

[1]University of Sydney, Sydney, Australia, [2]Department of Radiation Oncology, Chris O'Brien Lifehouse, Sydney, Australia, [3]Biomedical Innovation Hub, Chris O'Brien Lifehouse, Sydney, Australia

Introduction Superficial tumours treated with megavoltage x-ray beams are located in regions of high dose gradients due to the build-up effect. In these situations, bolus is commonly used to increase skin dose and dose uniformity. This study evaluated and compared the dosimetric characteristics of conventional bolus with customized 3D printed bolus fabricated from a patient conforming material.
Method The bolus materials compared in this study were RMI457 Solid Water (reference material), dental wax, SuperFlab and 3D printed TPU. The TPU bolus slabs were printed using a Pro2 Plus 3D printer (RAISE3D, Irvine, CA) with print settings optimized for radiotherapy applications. An advanced Markus parallel-plate ionization chamber was used to measure the surface and percentage depth doses of a 6 MV x-ray beam in all bolus materials. Dose measurements were performed on a Varian Clinac 6EX (Varian Medical Systems, USA) with a 10×10 cm^2 field. Boluses of different materials with different thicknesses were placed on top of the ionization chamber, adjusting the distance from the source to the surface to 100 cm.
Results All measured PDD results were normalized to D_{max} point (depth = 1.5 cm). The PDD increased from 15% to approximately 40% for all materials to within 1 mm of the built-up area. The dosimetric agreement with the RMI457 Solid Water was better for the 3D printed TPU (< 3%) as compared to the conventional materials wax and SuperFlab (< 5%), as shown in Fig. 1.
Conclusion Compared to conventional bolus, PDD measurements show that 3D printed boluses have dosimetric properties closer to those of Solid Water. The obtained results show that the 3D printed TPU bolus has better dosimetric characteristics for use in 6 MV x-ray beams.

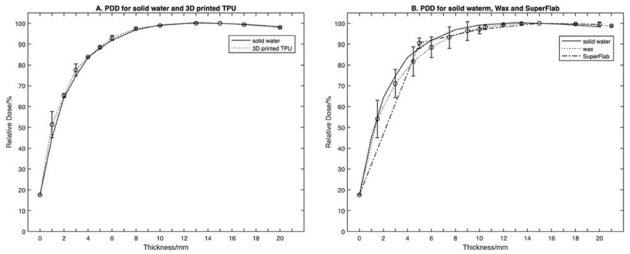

Fig. 1. PDD was compared among different materials and solid water. A. 3D printed TPU. B. Wax and Superflab.

P04. Evaluating 3D printing materials for intracavitary gynaecological brachytherapy

Rachael Wilks[1,2,3], Jacob Skewes[2], David Forrestal[2,3], Tanya Kairn[1,2,3,4], Scott Crowe[1,2,3,4,*]

[1]Royal Brisbane & Women's Hospital, Herston, Australia, [2]Herston Biofabrication Institute, Herston, Australia, [3]University of Queensland, St. Lucia, Australia, [4]Queensland University of Technology, Brisbane, Australia

Introduction Additive manufacturing (or 3D printing) allows the production of bespoke brachytherapy applicators for patients with gynaecological cancers that cannot be treated with conventional dome applicators due to scarring or irregular vaginal vaults. This study characterised the robustness and radiological properties of materials that might be used to manufacture such applicators.
Method Seven test devices were designed: a rod containing a single catheter channel, a small mould with 5 blind-ended catheter channels, a large mould with 3 open-ended catheter channels, three 3×3 cm^2 slabs of variable height (0.5, 1, 2 cm) for transmission measurements, a dog bone for tensile testing. These devices were 3D printed using four biocompatible materials: KeyGuide, Biomed Clear, MED610, and Nylon 12. Tests performed on these samples included visual inspection, catheter insertion, quantification of radiological properties by CT and transmission measurements, and comparison of CT-derived 3D model of printed device against the initial design. Tests were performed before and after sterilisation by autoclave.
Results For some prints, catheter channels were blocked, due to poor drainage of uncured resin or build-up of powdered material. Following post-processing there was good agreement between most points in the CT-derived 3D models of the devices and initial designs, within the CT scanning resolution of 0.5 mm slice width. The materials were approximately water equivalent (within $\pm$ 0.1 RED), with the largest deviation in dose beyond of a 2 cm slab being 1% when compared against dose beyond a water-equivalent plastic. The sterilisation process resulted in damage to some applicators, particularly at channel openings or where resin had not adequately cured. The catheter could still be inserted in all channels of test devices printed with the Biomed material.
Conclusion The materials were approximately water equivalent, but some devices were damaged by the sterilisation process.

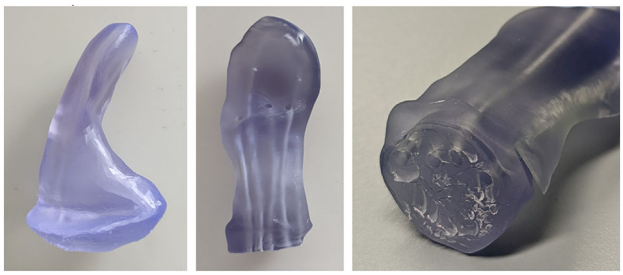

Fig. 1. Test applicators (left-centre) and sterilisation damage (right).

P05. Radiation dose reduction strategy for SPECT/CT bone scan

Manal Alezzi[1,2,*]

[1]King Abdullah Medical City, Saudi Arabia, [2]Umm Al-Qura University, Saudi Arabia

Introduction This study aimed to introduce the optimization method of CT parameters to reduce patient radiation exposure in bone SPECT/CT while maintaining image quality. The results of the new protocol were then compared to the results of the standard protocol.
Method First part: Using Deluxe Jaszczak Phantom. The cylindrical phantom consisted of six bottles in a pie arrangement. These bottles were placed in the source tank. SPECT/CT scans were carried out with different x-ray tube current values and three different slice thicknesses. The (CR) and (COV) in the SPECT images as well as the (SNR) and were measured. An optimal acquisition protocol that obtained SPECT/CT images with no artifacts on both CT and SPECT images, acceptable CR, COV, and SNR values. Second part: The study was done on patients who required a SPECT/CT bone scan of the spine area. Different parameters that were obtained from the new reduced protocol were compared to old historical data saved in the system for patients who did the same image using the old standard protocol. The difference between the two systems was only by the X-ray tube current (the old 60 mA versus the new 40 mA).
Results The optimal set of parameters for bone SPECT/CT was determined based on a phantom part. It has been implemented in clinical practice. Two groups of patients were examined according to the baseline and optimized protocols, respectively. The new SPECT/CT protocol substantially reduced patients' radiation exposure compared to the old protocol while maintaining the required diagnostic quality of SPECT and CT images.
Conclusion The new bone scan SPECT/CT protocol established was implemented into clinical practice. It has significantly reduced patient exposure dose compared to the old protocol while maintaining the required diagnostic quality of SPECT and CT images.

P06. Abstract withdrawn

P07. Evaluation of Siemens Healthineers Biograph Vision Quadra (the 'Quadra') extended axial field-of-view (EAFOV) PET-CT scanner

Irena Janevska Pejoska[1,*], Jordan Verschuer[1], Stefan Eberl[1,2], Angela Brewer[1], Michael Fulham[1,2]

[1]Department of Molecular Imaging, Royal Prince Alfred Hospital, Sydney, Camperdown, Australia, [2]School of Computer Science, University of Sydney, Sydney, Australia

Introduction The Quadra has an extended axial field of view (EAFOV) of 106 cm that allows the head and torso to be imaged in single bed position [1]; its performance was evaluated.
Method Full NEMA NU 2–2018 tests were performed. A realistic thorax phantom (16 lesions: diameters 7–37 mm) was acquired in list mode for 30 min with a lesion / background of 3.7 to 1. Data were reconstructed (recons) into 30 × 1, 15 × 2, 10 × 3, 6 × 5 and 3 × 10 min frames as follows: i) Recon 1 (R1): 16 iterations 5 subsets (16i5s); 3.3 × 3.3 × 3 mm voxel; 4 mm FWHM filter; (ii) R2: same as R1 except with 2 mm FWHM filter; iii) R3: 12i5s; 1.65 × 1.65 × 2 mm voxel; 2 mm FWHM filter and, iv) R4: same as R3 except will an all pass filter. All reconstructions used TOF and resolution recovery.
Results Quadra NEMA sensitivity was 82.2 cps/kBq (70 cm line source; maximum ring difference [MRD] 85) and 201.0 cps/kBq (140 cm line source, MRD 322) compared to 15.5 cps/kBq for Biograph Vision 600 (AFOV = 26.5 cm), while maintaining the same spatial resolution. For the 7 mm lesion: a) for R4, Recovery Coefficient (RC) = 0.88 but high noise required > 10 min frames for a lesion estimation coefficient of variation (CoV) of ≤ 5%; b) for R1, RC = 0.52 and > 2 min acquisitions were acceptable; c) for R2, RC = 0.72; d) for R3, RC = 0.76. and e) for R2 and R3, frames ≥ 5 min were required.
Conclusion The markedly increased Quadra sensitivity allows dose and scan times to be reduced while maintaining low noise and high resolution. The realistic phantom allowed systematic analyses of the trade-off between imaging time, resolution and noise for various reconstruction parameter sets and is informing the optimisation of scanning protocols.
References

1. Alberts I, Hünermund JN, Prenosil G, Mingels C, Bohn KP, Viscione M, Sari H, Vollnberg B, Shi K, Afshar-Oromieh A, Rominger A (2021) Clinical performance of long axial field of view PET/CT: a head-to-head intra-individual comparison of the Biograph Vision Quadra with the Biograph Vision PET/CT. Eur J Nucl Med Mol Imaging. 48:2395–2404. https://doi.org/10.1007/s00259-021-05282-7.

P08. Automated analysis of NEMA tomographic contrast and absolute quantification accuracy

Anthony Baker[1,*], Isabelle Smith[1], Irena Janevska Pejoska[2], Stefan Eberl[2], Alessandra Malaroda[1], William Ryder[1]

[1]Nepean Hospital, Kingswood, Australia, [2]Royal Prince Alfred Hospital, Camperdown, Australia

Introduction Assessment of NEMA tomographic contrast and absolute quantification accuracy (image quality) is part of routine performance tests of SPECT/CT systems. The test evaluates quantitative metrics such as lesion contrast and background variability of the NEMA/IEC body phantom. ROI position accuracy of ≤ 1 mm and information accounting for pixel fractions makes analysis of the test with conventional software challenging. A robust and efficient Python tool has been developed for automated processing of NEMA/IEC phantom image quality.
Method Python (ver3.9) software was developed to automatically evaluate information from the SPECT/CT scans of the NEMA/IEC body phantom. Segmentation of the co-registered CT scan is carried out by a spherical median filter proportional to the known ROI diameters, followed by image thresholding. Centroids are identified by centre-of-mass and peak-analysis, utilised also for the evaluation of the phantom's orientation (Fig. 1). Background ROIs are positioned by translation and rotation from predefined coordinates (Fig. 2). ROIs are then transferred to the SPECT image for the evaluation of NEMA image quality parameters. An automated report, including segmentation information for user verification, is generated. Software was validated against 7 reconstructions of 3 NEMA/IEC phantom acquisitions analysed with A Medical Imaging Data Examiner (AMIDE) tool.
Results The execution time for the estimation of NEMA image quality is < 5 min. Good agreement was shown against the manual analysis (AMIDE) with differences ≤ 5% on 2D and 3D ROI mean counts. A high-statistic CT acquired for one of the acquisitions showed no significant improvement in image segmentation.
Conclusion A robust and time-efficient code to automatically estimate NEMA tomographic contrast and absolute quantification accuracy has been developed and validated. The code requires minimal user-input making analysis of NEMA/IEC phantoms for optimisation of imaging protocols more efficient.

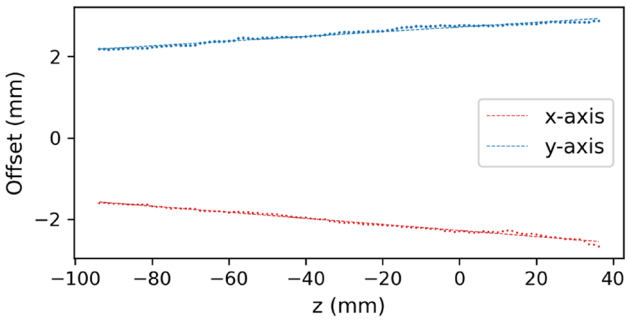

Fig. 1. Phantom axial offset.

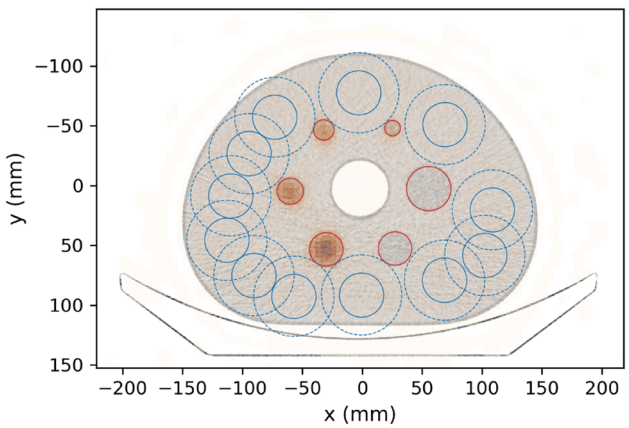

Fig. 2. ROI positioning on fused image (dotted lines: 15 mm buffer region).

P09. Anatomically Guided Contour Augmentation for Validation of an Automated Contour Quality Assurance Tool for Radiotherapy of Gastric Cancer

Phillip Chlap[1,2,3,*], Robert Finnegan[2,4,5], Hang Min[1,2,6], Jason Dowling[2,6], Matthew Field[1,2,3], Kirrily Cloak[1,2,3], Mark Lee[3],

Trevor Leong[7], Julie Chu[7], Jennifer Tan[7,9], Philip Tran[7], Annette Haworth[4], Martin Ebert[8], Shalini Vinod[1,2,3], Lois Holloway[1,2,3]

[1]South West Sydney Clinical Campuses, University of New South Wales, Liverpool, Australia, [2]Ingham Institute for Applied Medical Research, Liverpool, Australia, [3]Liverpool & Macarthur Cancer Therapy Centres, Liverpool, Australia, [4]The University of Sydney, Sydney, Australia, [5]Royal North Shore Hospital, Sydney, Australia, [6]Australian e-Health Research Centre, CSIRO, Royal Brisbane Hospital, Brisbane, Australia, [7]Peter MacCallum Cancer Centre, Melbourne, Australia, [8]Sir Charles Gairdner Hospital and University of Western Australia, Perth, Australia, [9]Sir Peter MacCallum Department of Oncology, The University of Melbourne,, Melbourne, Australia

Introduction The TOPGEAR clinical trial, which investigates the effects of chemoradiation over chemotherapy prior to surgery for gastric cancer patients, defines a relatively complex Clinical Target Volume (CTV) [1]. A set of cases were manually reviewed throughout the trial and was used to assess an automated contour QA tool developed for TOPGEAR. Since the proportion of contours failing QA is low, we investigated the augmentation of additional fail (and pass) contours to reduce bias in the model.

Method The contour QA tool consists of a model to auto-segment the CTV, trained on a set of 10 cases using the nnUNet [2]. The Dice Similarity Coefficient (DSC) is computed between the manual and the auto contour. By varying the threshold value of the DSC pass/fail cases are distinguished and the area under the receiver operating characteristic curve (AUC) is calculated to assess model performance. The validation set contained 49 cases passing and 7 cases failing QA. Additional CTV failures were augmented by generating synthetic deformation fields expanding/contracting the CTV towards/away from surrounding structures (Fig. 1). Ten fail augmentations were generated per case, increasing the number of fail cases in the dataset to 490. To rebalance the dataset, random expansions, contractions and shifts of structures generated an additional deformation and was applied to the images and CTVs to produce a passing case for each failing case.

Results An AUC of 0.79 is achieved when assessing the model with the original validation set. This drops to 0.77 after adding augmented fail cases with improved sensitivity at the cost of increased false positives. With the augmented pass cases added to balance the validation set the AUC drops again to 0.71, better indicating the actual performance (Fig. 2).

Conclusion The proposed method shows promise in providing a fairer assessment of an automated contour QA tool.

References

1. T. Leong et al., (2015) TOPGEAR: A randomised phase III trial of perioperative ECF chemotherapy versus preoperative chemoradiation plus perioperative ECF chemotherapy for resectable gastric cancer (an international, intergroup trial of the AGITG/TROG/EORTC/NCIC CTG)," BMC Cancer, 15:1–, https://doi.org/10.1186/s12885-015-1529-x.
2. Isensee F, Jaeger PF, Kohl SAA, Petersen J, Maier-Hein KH (2021) nnU-Net: a self-configuring method for deep learning-based biomedical image segmentation Nat Methods 18:203–211 https://doi.org/10.1038/s41592-020–01,008-z.x

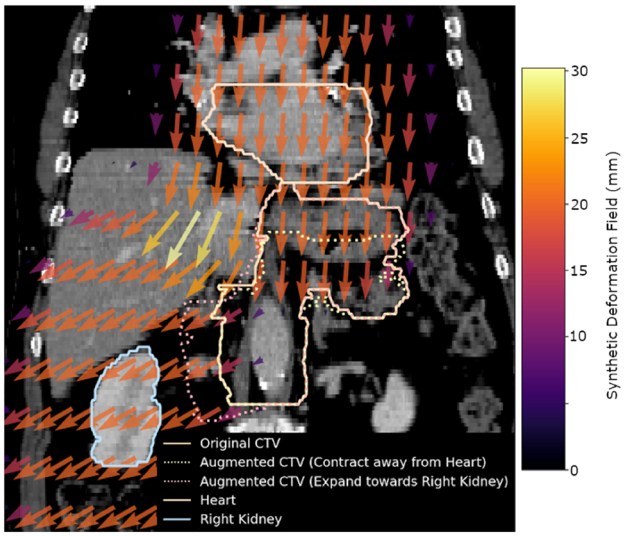

Fig. 1. Example of augmented fail contour contracted away from the Heart and expanded towards the Right Kidney. The deformation vector fields applied to the original CTV to produce these augmented CTVs has been summed and overlaid for illustration purposes.

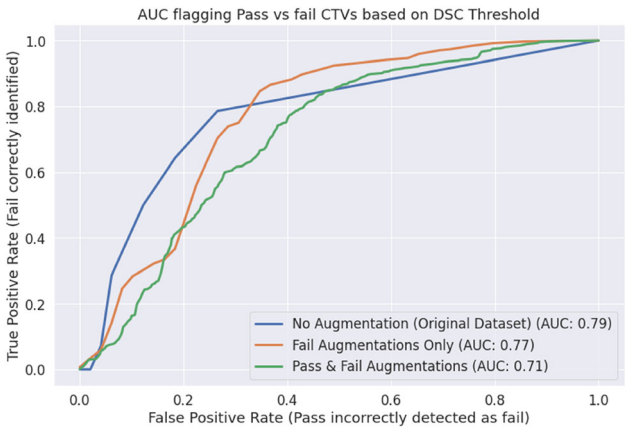

Fig. 2. AUC when assessing the QA model performance with the original dataset (blue), with only fail augmentations (red) and with both pass and fail augmentations (green).

P10. Machine learning based model for recurrence prediction in radiotherapy of head- and-neck cancer

Jothy Selvaraj[1,2,*], Amit Bahl[3]

[1]Canberra Health Services, Canberra, Australia, [2]University of New South Wales, Sydney, Australia, [3]Postgraduate Institute of Medical Education and Research, Chandigarh, India

Introduction Outcomes in nasopharyngeal carcinoma has improved over the years mainly due to improvements in radiotherapy and chemotherapy. However, significant proportion of patients experience recurrent disease. It will be prudential to have a prediction model to better stratify and manage recurrent disease in head-and-neck cancers. Due to multitude of parameters involved in the development of recurrence, use of machine learning (ML) models is robust. In this

study, several ML models are compared utilizing data collected from a clinical trial approved by the institutional review board.
Method Total of 119 patients with 105 variables each were available for the analysis including dose-volume metrics, confounding factors such as smoking, alcohol intake and tobacco chewing. 36 patients had recurrence out of 119 with one censored. In addition, it also included clinical characteristics of the patients such as TNM status, co-morbidities, weight loss, adjuvant chemotherapy and adaptive radiotherapy statuses. Missing values were imputed by average/most frequent methods for numerical and categorical variables respectively. Methods employed were Logistic Regression, SVM, KNN, Neural Networks, Naive Bayes, Random Forest, Gradient Boosting, AdaBoost and ensemble of these models was also used. K-fold cross-validation is used to evaluate the models with ROC analysis.
Results AdaBoost and Gradient Boosting methods had the highest AUC = 1, classification accuracy (CA), F1, precision and recall values compared to all other models. Ensemble model had the same AUC as AdaBoost and Gradient Boosting methods, but the rest of the parameters were reduced due to averaging of the inferior models (CA, F1, precision and recall = 0.992). The worst model was KNN with AUC, CA, F1, precision and recall values of 0.761,0.739,0.671,0.770 and 00.739 respectively. The AUC plots of several model are shown in Fig. 1.
Conclusion An ML model was developed to predict recurrent cancers in patient undergoing adjuvant chemoradiotherapy.

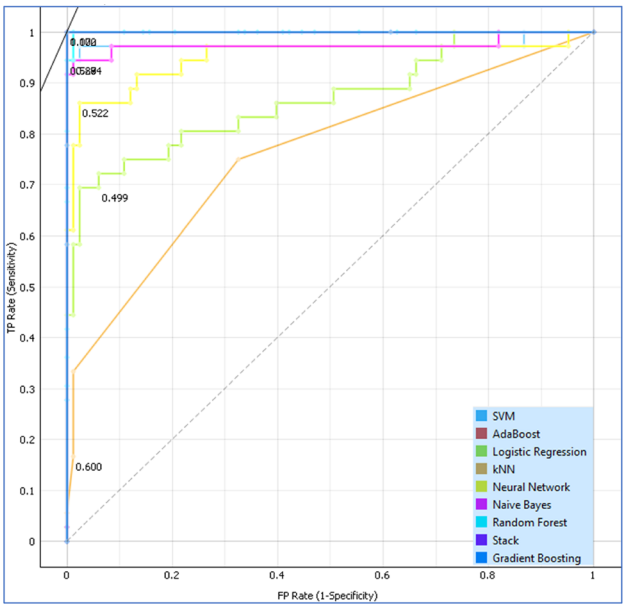

Figure 1.

P11. Automating the RapidPlan model validation phase

Bradley Beeksma[1], Andrew Dipuglia[1], Rebecca Artschan[1,*], Joshua Sams[1]

[1]Calvary Mater Newcastle, Warratah, Australia

Introduction Validating a RapidPlan model involves re-planning patient plans and comparing plan quality against the delivered clinical plan (CP). This process is undertaken with multiple patient datasets (N), across numerous permutations of model versions (M), resulting in NxM number of plans. Consequently, validation quickly becomes resource extensive, laborious and time consuming. To reduce the burden, the process has been automated via the development of a custom automated planning script utilising Eclipse Scripting Application Programming Interface (ESAPI) and an automated analysis tool, Estimation Statistics1 via a custom python script.
Method A standalone executable script was written in C# to loop through a patients list to batch plan and export DVH metrics. For each patient, the script generates a new plan, then copies the patient CT, structure set, technique, prescription dose, and beam setup of the CP. It generates the required optimisation structures, applies the RapidPlan model, then optimises and calculates the plan. Once dose is calculated, the plan is normalised to the prescribed coverage of the CP, and dose volume histogram (DVH) metrics are exported to a.CSV file for both the automatically generated plan (AP) and CP. Once the APs are generated for all patients, a Python script populates comparison plots for each DVH metric of the population data.
Results APs were generated in approximately 10 min per patient with no user input, where manual methods took ~ 1 h. Efficiency gains thus permit fine tuning of modelling parameters at a level not previously feasible. Variable inputs are called from an external configuration file, allowing it be run by end users with no coding experience. Utilising this script 256 plans (N = 12, M = 22) were generated during model validation for a local RP model.
Conclusion RapidPlan model validation process was able to be automated, turning a time consuming, tedious task into a streamlined efficient process.
References

1. Ho J, Tumkaya T, Aryal S, Choi H, Claridge-Chang A (2019) Moving beyond P values: Everyday data analysis with estimation plots. Nature Methods, 1548–7105. https://doi.org/10.1038/s41592-019-0470-3
2. Simon L, Arnaud F-X, Beeksma B (2022) Dose Hunter Repository.

P12. Abstract withdrawn

P13. Commissioning the 2.5 MV imaging X-ray beam on a Varian TrueBeam

Julie-anne Miller[1,*]

[1]Qhealth, South Brisbane, Australia

Introduction The Varian TrueBeam v 2.7 2.5 MV FFF portal imaging beam was characterised and absolute dose calibrated. As the 2.5 MV beam will be used in place of the 6 MV beam for portal imaging, this was the energy used for comparison of the Winston Lutz and output factor trends. The 2.5 MV will be used for mid treatment position verification for patients undergoing Brain SRT treatment with noncoplanar beam arrangements.
Method A SemiFlex 3D chamber in a PTW BeamScan water tank was used to measure the PDD and symmetry. A profiler was used to measure symmetry with rotation at 45° increments. The output factors were measured in Plastic Water at 5 and 10 cm depth for field sizes 5 × 5 to 20 × 20 cm^2. A farmer type chamber in a jig was used to measure the output linearity and variation with gantry angle. An absolute calibration was carried out using IAEA TRS 398[1], with an extrapolated k_{Q,Q_o} of 1.002 for a $TPR_{20,10}$ of 0.481. Daily MPC and fortnightly chamber measurements were used to track outputs. The Winston-Lutz (WL) test was performed at the cardinal angles to determine the isocentre size and coincidence with the treatment 6 MV beam. The contrast resolution was measured with the MV Las Vegas phantom.

Results The 2.5 MV imaging beam showed a nonlinearity and output variation of less than 0.5%. The WL isocentre size was comparable to 6MV and shifts were 1 mm or less. The output factor variation with field size was larger than 6MV, but as 3 MU per beam was used, it was still a small absolute overall dose variation.
Conclusion The 2.5 MV beam has successfully been implemented for Brain patients on a TrueBeam platform.
References

1. International Atomic Energy Agency TRS398 Absorbed Dose Determination in External Beam Radiotherapy: An International Code of Practice for Dosimetry based on Standards of Absorbed Dose to Water (2006).
2. Varian TrueBeam Technical Reference Guide—Volume 2: Imaging, TrueBeam Platform for Physicists 2.7, TrueBeam Platform On-Demand Imaging and Iterative CBCT notables documents (2018).
3. Varian TrueBeam Platform for Physicists course notes (2021).
4. Rajamanickam T, Muthu S, Murugan P, Dinesan C, Mekala C, Senthilnathan K, Raj NAN, Babu PR (2019) An assessment of dosimetric characteristics of inline 2.5 mega voltage unflattened imaging X-ray beam. Asian Pac J Cancer Prev 20:2531–2539.

Table 1. Results of 2.5 MV tests.

Test	Quantities tested	Result
Linearity	1,2,3, 5 MU and normalisation point 100 MU	max difference -0.4%
Output with Gantry Angle	0, 90, 270, 180 degrees	± 0.2%
Symmetry with Gantry Angle	Every 45 degrees	± 1%
WL isocentre size	0, 90, 270, 180 degrees	0.85 mm (6 MV was 0.7 mm)
Max WL isocentre shifts WRT 6 MV		X shift = 0.2 mm and Y shift = 1 mm
Contrast resolution		Column "F" visible (Column "E" for 6 MV)

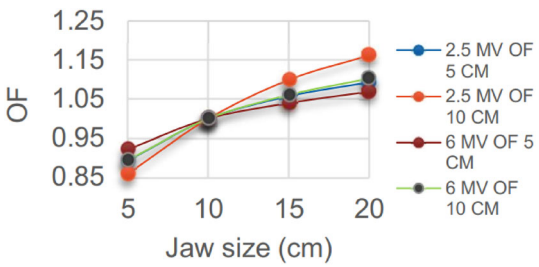

Fig. 1. Output Factor (OF) Variation with depth.

P14. A multi-department analysis of traditional Winston Lutz measurements vs MPC on a Varian Truebeam linac

Dean Wallace[1,*]

[1]Icon Cancer Centre Mulgrave, Mulgrave, Australia

Introduction The current, standard process for stereotactic radiation therapy treatments quality assurance (QA) requires a day of treatment Winston Lutz (W-L) test to ensure accurate imaging and radiation isocentre congruence. By analysing a large subsection of Varian Machine Performance Check (MPC) & traditional W-L measurements, a correlation was established between the two and allowed the substitution of the traditional W-L method with daily MPC at our institutions.
Method To analyse the MPC & W-L results, 2 years of MPC data was evaluated for 9 Truebeam linear accelerators (linacs) within a multi-department environment. This data was then compared to the W-L results, taken using the traditional ball bearing method [4], across the corresponding linacs. The radiation isocentre position and size W-L method, involving multiple gantry, collimator and couch angles to determine a maximum total delta, was analysed using SNC machine [Sun Nuclear Corporation, Melbourne, Fl, USA].
Results The results in Fig. 1 show that all 9 linacs have a similar distribution of results, with the averages having minor differences due to inter-linac and inter-user variations. An evaluation of the averages of MPC and W-L results & analysis methods is given in Fig. 1 below. This highlights machine variation, as well as comparison to W-L results, and includes some custom results created from the MPC data to correlate more closely to W-L measurements. It was found that the closest surrogate in MPC for the W-L results is the Iso-Size and the Rotation Induced Couch Shift (Full range).
Conclusion MPC was found to be an accurate and time-saving surrogate for daily W-L tests on Truebeam linacs used for stereotactic radiation therapy.
References

1. Halvorsen PH, Cirino E, Das IJ, Garrett JA, Yang J, Yin FF, Fairobent LA (2017) AAPM-RSS Medical Physics Practice Guideline 9.a. for SRS-SBRT. J Appl Clin Med Phys18:10–21. https://doi.org/10.1002/acm2.12146. Epub 2017 Aug 8. PMID: 28,786,239; PMCID: PMC5874865.
2. Denton TR, Shields LB, Howe JN, Spalding AC (2015) Quantifying isocenter measurements to establish clinically meaningful thresholds. J Appl Clin Med Phys 16:5183. https://doi.org/10.1120/jacmp.v16i2.5183. PMID: 26,103,187; PMCID: PMC5690087.
3. Galvin JM, Bednarz G (2008) Quality assurance procedures for stereotactic body radiation therapy. Int J Radia Oncol Biol Phys 71:S122–125. https://doi.org/10.1016/j.ijrobp.2007.10.002. PMID: 18,406,909.
4. Lutz W, Winston KR, Maleki N (1988) A system for stereotactic radiosurgery with a linear accelerator. Int J Radiat Oncol Biol Phys 14:373–381. https://doi.org/10.1016/0360-3016(88)90446-4 . PMID: 3,276,655.

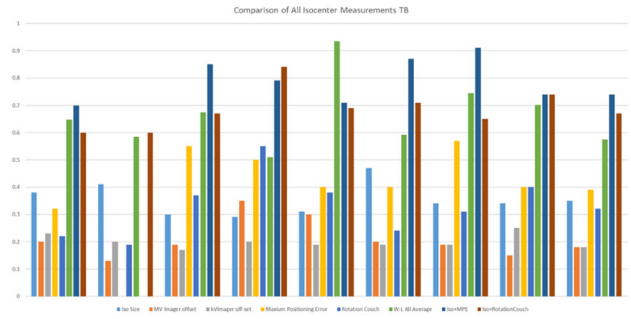

Fig. 1. Comparison of average MPC parameters & Winston Lutz measurements.

P15. Beam output variations indicative of target degradation in a Varian Truebeam

Godfrey Mukwada[1,*], Jonny Thompson[1]

[1]Sir Charles Gairdner Hospital, Nedlands, Australia

Introduction A linear accelerator generates a high energy x-ray beam by bombarding a 'target' with electrons and producing x-rays via 'bremsstrahlung' radiation. Damage to the target can have an impact on beam characteristics and is here examined.

Method Linear accelerator output and $TPR_{20,10}$ energy measurements were performed using an IBA FC65-G 0.6 cc ionisation chamber as part of monthly quality assurance (QA) over a period of $\sim$ 20 months. A gradual and consistent decrease in machine output for 6MV FFF was observed, whilst the 6 and 10MV FF beams maintained a normal upward trend [1–4]. In this period, two annual QAs were also performed but did not show any anomalies in beam characteristics. Although the 6MV FFF output and energy were checked every month, it was not used clinically. Through remote machine performance monitoring, the vendor independently noticed the decrease in output and requested further measurements to be performed which confirmed target degradation. IC Profiler diagonal measurements were also performed before and after target replacement (40 $\times$ 40 cm field, 1.5 cm depth) to check if there was any observable change to the beam profiles.

Results The change in beam quality was less than 0.5% from baseline for both 6MV FF and 6MV FFF beams. The output variation without correction deviated from baseline by -18% for 6MV FFF and 4% for 6MV FF (see Fig. 1). The diagonal profiles were within 1% of each other at both $\pm$ 6 cm and $\pm$ 18 cm.

Conclusion Monthly $TPR_{20,10}$ and IC profiler flatness and symmetry measurements were not predictors of target degradation. The continuous decrease in output for 6MV FFF can be used as predictor of target degradation.

Acknowledgements: Authors acknowledge the Physicists involved in monthly and annual QA and the engineers involved in trouble shooting.

References

1. Barnes MP, Greer PB (2017) Evaluation of the TrueBeam machine performance check (MPC) beam constancy checks for flattened and flattening filter-free (FFF) photon beams. J Appl Clin Med Phys 18:139–150.
2. McCaw TJ, et al. (2020) Diagnosing atmospheric communication of a sealed monitor chamber. J Appl Clin Med Phys 21:309–314.
3. Binny D, et al. (2019) A multi-institutional evaluation of machine performance check system on treatment beam output and symmetry using statistical process control. J Appl Clin Med Phys 20:71–80.
4. Milan T, Mukwada G (2019) Long-term evaluation of TrueBeam MPC and Checkmate2 photon and electron beam output presented at EPSM 2019, Perth.

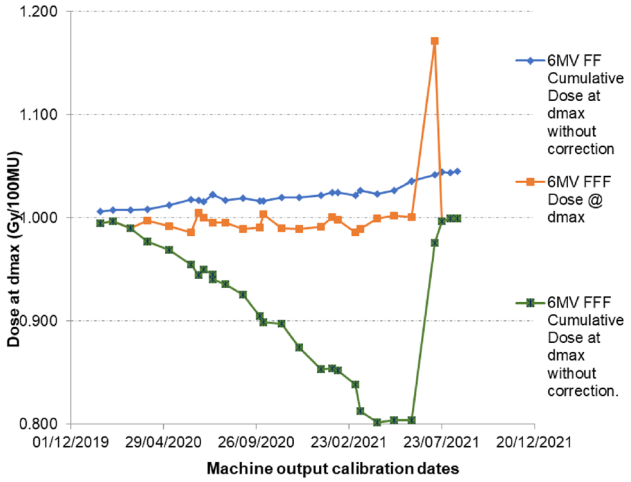

Fig. 1. Output change with time for 6MV FF (blue) and 6MV FFF (orange, green) beams.

P16. Optimisation of dose and image quality of CBCT protocols on Varian TrueBeam™ linear accelerators in a multi-campus environment

Deloar Hossain[1,*], Joby Mathew[1], Adam Yeo[2], Chris Fox[2], Alan Turner[1], Lisa Hall[2], Karen McGoldrick[3], Kenton Thompson[2], Tomas Kron[2]

[1]Peter MacCallum Cancer Centre, Bendigo, Australia, [2]Peter MacCallum Cancer Centre, Melbourne, Australia, [3]Peter MacCallum Cancer Centre, Moorabbin, Australia

Introduction Varian TrueBeam™ (TB,) Linear Accelerators (Linacs) have default CBCT protocols pre-installed on delivery. Optimisation of these CBCT protocols can help to reduce the patients' imaging dose [1]. In this work, we investigated a methodology to optimize five default CBCT protocols of TB, which are head, thorax, pelvis, large pelvis and spotlight.

Method We have investigated the dose reduction and image quality (IQ) for four different combinations of each of five default protocols by changing the kVp, mA or both. For each combination, in-air dose was measured using a RaySafe™ (Billdal, SE) device and CBCT of the anthropomorphic-phantom was acquired. Three experienced radiation therapists examined the anthropomorphic-phantom CBCT images and ranked them as high or moderate or inadequate IQ. The protocols with the lowest dose and high IQ were considered as optimized protocols and made available on Linacs across five campuses as part of clinical trial. A total of 117 CBCT datasets were acquired for different body sites with at least 13 dataset for each protocol. A team of experienced radiation therapists ranked the images based on the five points criteria; excellent, good-for-the-job, adequate-for-the-job, could-benefit-from-improvement and not usable. The images ranked as "adequate-for-the-job and above" were considered for the clinical roll out. Finally, the CatPhan CBCT

images of the five optimised protocols were acquired for the HU linearity, geometry, uniformity and MTF and to use them for future reference.

Results We have optimised the five CBCT protocols in terms of dose and IQ. Doses for the optimised protocols for head, thorax, spotlight, pelvis, large pelvis have been reduced by 1.4, 2.7, 1.8, 1.9 and 2.4 times, respectively compared to the default protocols.

Conclusion With current clinical IGRT practices, use of the optimised protocols will reduce the patient-imaging dose significantly and frequency of CBCT imaging can be increased depending on the clinical needs.

References

1. Ding GX, Alaei P, Curran B, Flynn R, et al. (2018) Image guidance doses delivered during radiotherapy: Quantification, management, and reduction: Report of the AAPM Therapy Physics Committee Task Group 180. Med Phys 45:

Acknowledgements: Thanks to Hayley Maggs, Luu Steven, Raeburn Tegan, De Silva Anouk, Glenn Christy, Tan Kelvin, Roxanne Hendricks and Miras Chris for ranking the images from clinical trial.

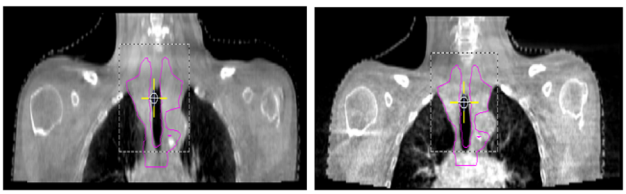

Fig. 1. A pair of CBCT images with the default (on the left) and the modified (on the right) to reduce dose by a factor of 2.7 for comparison in H&N clinical scenario.

P17. Abstract withdrawn

P18. Measuring treatment and imaging beam-on/off latency in gated treatments on Varian TrueBeam linacs

Alex Burton[1,*], Jenny Lydon[1]

[1]Peter MacCallum Cancer Centre, Melbourne, Australia

Introduction Quantifying the temporal accuracy of gating events is recommended as part of ongoing linear accelerator quality assurance (QA)[1,2]. In this work, we present a method for quantifying kV imaging and MV treatment beam-on and beam-off latency.

Method The method was developed based on the technique published by Woods et al[3], using a CIRS 008A Thorax Motion Phantom with implanted gold fiducial markers, programmed to move with a sawtooth waveform with fixed amplitude of 30 mm peak-to-peak. One marker was aligned to the treatment isocentre halfway between inhale and exhale (mid-position). Triggered (kV) and continuous imaging (MV) was performed, with gating window start and end coinciding with marker mid-position. Each test was conducted by gating during both the inhale and exhale phases (see Fig. 1), and measuring the positional offset of the marker from isocentre in the acquired images. The testing was performed with amplitude- and phase-gating treatment modes with velocities from 6-15 mm/s (period 4-10 s). Latency was determined using two Methods 1. Dividing the average positional offset by the marker velocity for each configuration, and then taking the average of all values (beam-on and beam-off). 2. Plotting the average offset as a function of marker velocity for both the inhale and exhale series, and finding the average slope of linear fits to these plots (beam-on only).

Results Both methods yielded beam-on latencies of approximately 100 ms for all treatment modes and beam types (see Table 1). kV imaging beam-off latency was approximately 100 ms whereas MV beam-off latency was < 30 ms. Contrary to Woods et al., we did not observe a difference between MV and kV beam-on latency, or latency variation with marker velocity.

Conclusion In image-based latency measurements, it is essential to perform measurements in both the inhale and exhale phases using to ensure accurate results, however testing at more than one object velocity is not required. Facilities should assess the difference in kV and MV latency, to enable meaningful interpretation of triggered kV images.

References

1. Klein, EE et al. (2009) Task group 142 report: Quality assurance of medical accelerators. Med Phys 36:4197–4212.
2. Hanley J, et al.(2021) AAPM Task Group 198 Report: An implementation guide for TG 142 quality assurance of medical accelerators. Med Phys 48:e830–e885.
3. Woods, K, Rong Y (2015) Technical Report: TG-142 compliant and comprehensive quality assurance tests for respiratory gating. Med Phys 42:6488–6497.

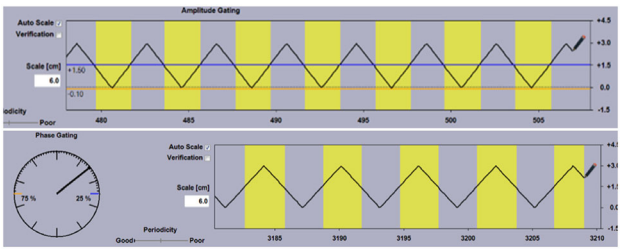

Fig. 1. Motion trace and gating window for measuring at exhale in amplitude-gating treatment mode (top) and at inhale in phase-gating treatment mode (bottom).

Table 1. Summary of measurement results following both methods – average across all target velocities ± 1 standard deviation. Note that beam-off latency was measured at one velocity only.

Modality	Gating type	Beam-on latency (ms)			Beam-off latency (ms)
		Method 1	Method 2	Method 2 Woods et al	Method 1
kV	Amplitude	112.2 ± 22.2	77.4 ± 34.8	92 ± 11	109.0 ± 22.4
	Phase	106.1 ± 24.2	102.1 ± 70.0	–	114.0 ± 24.0
MV	Amplitude	107.5 ± 12.1	127.4 ± 19.9	139 ± 10	28.0 ± 12.3
	Phase	96.9 ± 15.2	107.6 ± 16.0	–	8.5 ± 7.1

P19. Development of quality assurance procedures for the Integral Quality Monitor (IQM)

Alison Gray[1,2,3], Aitang Xing[1,2,3,*], Vaughan Moutrie[1], Kilian Michel[4], Gary Goozee[1,2,3]

[1]South Western Sydney Cancer Services, NSW Health, Sydney, Australia, [2]Ingham Institute for Applied Medical Research, Liverpool,

Australia, [3]South Western Sydney Clinical School, UNSW, Sydney, Australia, [4]iRT Systems, Koblenz, Germany

Introduction The Integral Quality Monitor (IQM) is a large ionisation chamber, which attaches to the linear accelerator (linac) head, with an in-built inclinometer, thermometer and barometer. The sensitive volume encompasses the entire beam and the electrode spacing varies linearly in the direction of MLC motion so each beam segment creates a spatially dependent signal. It can be used for pre-treatment patient-specific quality assurance (PSQA), during-treatment QA and machine QA. The aim of this work was to develop a QA procedure to ensure the correct performance of the IQM.
Method Publications on ionisation chamber performance testing, the IQM acceptance testing procedure and recommendations from iRT Systems formed the basis of the QA protocol created [1–4]. Test methods were developed in conjunction with iRT where not possible in the clinical IQM software. The local use (PSQA) and potential causes of failure e.g. linac output variation were also considered. Fields were created in Raystation and exported to IQM. Baseline values were obtained.
Results The QA protocol is summarised in [P19] **Table 4**. It recommends that IQM response be assessed daily, and compared to linac output monthly. An iRT QA test field to assess consistency of chamber response with field position was recommended monthly as this is critical to its use. Inclinometer reading (gantry and collimator) was recommended monthly based on feedback from iRT. The Annual QA tests repeated selected acceptance tests and also included a selection of MLC QA [5] and test treatment fields [6] to assess consistency of PSQA results. Where a multi-room kit was installed, allowing IQM use on multiple linacs, linac and detector dependent tests were assigned.
Conclusion A protocol for daily, monthly and annual QA was developed. The results will be reviewed in the future to re-assess the frequency and the value of the PSQA consistency tests.
References

1. iRT Systems. White paper – IQM Detector Characteristics: Signal Linearity and Dose Rate (In-) Dependence. https://www.iqm-system.com/download/iqm-detector-characteristics-signal-linearity-and-dose-rate-in-dependence-white-paper/. Accessed 29 June 2022.
2. iRT Systems. White paper – IQM Detector Characteristics: Signal reproducibility. https://www.iqm-system.com/download/iqm-detector-characteristics-signal-reproducibility-white-paper/. Accessed 29 June 20,223.
3. Kutcher GJ, Lawrence C, Gillin M et al. (1994) Comprehensive QA for Radiation Oncology. AAPM Report no. 46. Report of Task Group no. 40. Med Phys 21:581–618. https://doi.org/10.1118/1.597316
4. Australian / New Zealand Standards (1999). AS/NZS 4537:1999 Medical electrical equipment – Dosimeters with ionization chambers as used in radiotherapy.
5. Klein EE, Hanley J, Bayouth J et al. (2009) Task Group 142 report: Quality assurance of medical accelerators. Med Phys 36:4197–4212. https://doi.org/10.1118/1.3190392
6. Ezzell GA, Burmeister JW, Dogan, N et al. (2009) IMRT commissioning: Multiple institution planning and dosimetry comparisons, a report from AAPM Task Group 119. Med. Phys. 36(11): 5359–5373. https://doi.org/10.1118/1.3238104

Table 4. IQM QA tests by frequency.

Frequency	Test
Daily	Reference field measurement compared to baseline value
Monthly	Reference field deviation from baseline compared to linac output
	QA test field with 18 segments sampling different areas of the field
	Inclinometer accuracy
Annual	Thermometer accuracy
	Barometer accuracy
	Battery capacity
	Leakage signal
	Reproducibility
	Linearity
	Dose rate dependence
	PSQA consistency using MLC QA and treatment fields

P20. Commissioning of a WoMed T105 kilovoltage x-ray unit: challenges, results, and long-term performance

Tom Kupfer[1,*], Sherly Saju[2], Kym Rykers[1,2], Leah McDermott[1]

[1]Austin Health, Radiation Oncology Department, Heidelberg, Australia, [2]Ballarat Austin Radiation Oncology Centre, Ballarat, Australia

Introduction Superficial x-ray radiotherapy (SXRT) plays an important role in skin cancer treatment in Australia. To improve patient access to SXRT, a WoMed T105 unit was installed in a regional hospital in 2019 (Fig. 1). We present technical challenges encountered during its commissioning, beam measurement data and long-term performance data.
Method Informed by SpekCalc® (commercial kV spectrum simulator), combinations of filtration and kVp were selected to yield HVL of 0.7, 1.0, 2.0 and 4.0 mmAl. Post-installation commissioning tasks followed ACPSEM guidelines.[1] This included PDD measurements using a PTW Roos chamber in a scanning water tank. Applicator factors and stand-off corrections were measured with a small-volume ionisation chamber in air. The steel inner-wall of the 4-cm diameter applicator was coated with nail varnish to reduce electron contamination. Absolute dose-rate and timer error of the timer–based unit was measured according to the TG-61 protocol.[2] The performance of the unit's internal solid-state detector, which functions as an MU-counter and dose-rate monitor, was assessed. The drift of dose-rate and MU-counter was recorded over three years.

Results SpekCalc predicted the measured HVL to within 0.1 mmAl. The measured PDD differed by up to 13% from the BJR-25 reference data.[3] Nail varnish reduced the surface dose by ~ 10%, without affecting the PDD or applicator factor. The output dose-rate showed no long-term drift and the timer error was negligible. However, the MU-counter was sensitive to pre-irradiation. Its maximum standard deviation and annual drift were 7.4% and –9.0%, respectively.
Conclusion SpekCalc is useful for initial beam selection. The PDDs tabulated in BJR-25 agree within limits with the measured PDD. Nail varnish can significantly reduce surface dose present with a steel-walled applicator. The unit's output is stable, however, the variability of the MU-counter demands additional testing and ongoing monitoring.
References

1. Hill R, Healy B, Butler D, Odgers D, Gill S, Lye J, Gorjiara T, Pope D, Hill B (2018) Australasian recommendations for quality assurance in kilovoltage radiation therapy from the Kilovoltage Dosimetry Working Group of the Australasian College of Physical Scientists and Engineers in Medicine. Australas Phys Eng Sci Med 41:781–808. https://doi.org/10.1007/s13246-018-0692-1
2. Ma CM, Coffey CW, DeWerd LA, Liu C, Nath R, Seltzer SM, Seuntjens JP (2001) AAPM protocol for 40–300 kV x-ray beam dosimetry in radiotherapy and radiobiology. Med Phys 28:868–893. https://doi.org/10.1118/1.1374247
3. Aird A, Burns JE, Day MJ, Duane S, Jordan TJ, Kacperek A. (1996) Central axis depth dose data for use in radiotherapy: 1996. A survey of depth doses and related data measured in water or equivalent media. Supp 25. London: Brit. Inst. Radiol.

Fig. 15. WoMed T105 therapeutic x-ray unit.

P21. A study of the polarity effect for ionization chambers in kilovoltage and megavoltage radiotherapy beams

Yousif Yousif[1], John Daniel[2], Jackson Zifodya[3], Brendan Healy[4], Robin Hill[5,6,*]

[1]North West Cancer Centre- Tamworth Hospital, Tamworth, Australia, [2]North West Cancer Centre- Tamworth Hospital, Tamworth, Australia, [3]North West Cancer Centre- Tamworth Hospital, Tamworth, Australia, [4]Australian Clinical Dosimetry Service, ARPANSA, Melbourne, Australia, [5]Department of Radiation Oncology, Chris O'Brien Lifehouse, Camperdown, Australia, [6]School of Physics, Institute of Medical Physics, University of Sydney, Sydney, Australia

Introduction Ionization chambers are considered the reference detectors of choice for the dosimetry of kilovoltage (kV) and megavoltage (MV) beams. Recommendations for applying polarity correction factors vary across different dosimetry codes of practice and beam energies. This work investigates the polarity effect in kV and MV beams for a range of ionization chambers.
Methods Five PTW ionization chambers were studies being the PTW Roos, Advanced Markus, 3D Pinpoint, Semiflex and the Farmer 30,010 detectors (PTW-Freiburg, Germany). All measurements were performed at the required reference depth in a PTW-MP1 water tank. Doses were acquired for different radiation beams: 60—300 kVp, 6 MV, 6 MV FFF, 18 MV and 9 MeV. The polarity effect was determined as per IAEA TRS 398 CoP methodology.
Results Results for polarity correction factor for low energy kV beams at field sizes $\leq$ 10 cm diameter were 2.5% and 3% for the advanced Markus and Pinpoint chamber respectively. While, for higher energy, polarity effects were up to 8.5% and 13% for the same chambers. The magnitude of the polarity effect increases with the increase in the field size, beam energy, and depends on the chamber's sensitive volume. For MV beams, the polarity effect varied with field sizes and measurement depth. The maximum polarity effects was observed for the smallest field size at the surface. As field size increase and depth increase, the polarity effects decreases. Polarity effects for Advanced Markus is 14%, 10%, and 16% for 6, 18 MV, and 6 FFF respectively. Whereas, 5%, 3%, and 13% for the pinpoint chamber for 6, 18 MV, and 6 FFF, respectively. For 9 MeV electron beams, the advanced Markus and Pinpoint gave polarity effects $< 1\%$ at the surface and about 3% at D_{max}. Overall, the results agreed well with the published literature [1].
Conclusion It was found that some ionization chambers exhibited very large polarity effects. These need to be considered for accurate radiation dosimetry measurements.
References

1. Dowdell S, Tyler M, McNamara J, Sloan K, Ceylan A, Rinks A (2016) Potential errors in relative dose measurements in kilovoltage photon beams due to polarity effects in plane-parallel ionisation chambers. Phys Med Biol 61:8395–8407.

P22. Early experience using a web application for radiotherapy quality assurance with a megavoltage device for kilovoltage therapy dosimetry QA

George Warr[1,*]

[1]Western Cancer Centre Dubbo, WNSWLHD, NSW Health, Dubbo, Australia

Introduction Regular dosimetry checks are recommended for kilovoltage therapy unit quality assurance [1]. Some constancy check devices previously used for this purpose are no longer available, including the Sun Nuclear Corporation (SNC) CHECKMATE™ 2™. Some departments have used the SNC Daily QA3™ (DQA3) device instead [2], however, it is designed for Co-60 and megavoltage linac photon and electron beams. We report on early experience using this device for kilovoltage therapy dosimetry with the SNC SunCheck™ web application.

Method Baselines for DQA3 output constancy checks for 100 kV and 150 kV beams on a Xstrahl 150 unit delivering 100MU were acquired in SunCheck using a previously acquired 6MV linac array calibration. Both the 10 cm diameter 30 cm FSD reference applicator and a 20 cm square 50 cm FSD applicator were evaluated, with the applicator end flush with the DQA3. Dose linearity response was evaluated by varying the delivered MU in subsequent measurement iterations. Reproducibility was evaluated by repeated 100MU deliveries in succession and over several days.
Results The 10 cm diameter 30 cm FSD reference applicator gave results that were insensitive to dose variations of up to 20%, rendering it unsuitable. The DQA3 LEDs didn't indicate a fault condition and the delivered dose rate is well below the device limit of 250 cGy/s. Using the 20 cm square 50 cm FSD applicator gave reproducible and linear dose responses up to 150 MU, with non-linear responses for 200 MU deliveries, as shown in Fig. 1.
Conclusion Early results indicate the DQA3 can be used in SunCheck for output constancy checks of 100 kV and 150 kV beams on a Xstrahl 150 unit using the 20 cm square 50 cm FSD applicator and 100 MU deliveries. However, the 10 cm diameter 30 cm FSD reference applicator is not suitable for this purpose as the system is insensitive to clinically relevant dose output variations.
Acknowledgements: It is a pleasure to acknowledge the support of Dr Dilli Banjade in performing this work and fruitful discussions with Dr Setayesh Behin-Ain, Mr Wen-Long Hsieh, Mr Anthony Karl and Dr Shiaw Juen (Eugene) Tan.
References

1. Hill R, Healy B, Butler D, Odgers D, Gill S, Lye J, Gorjiara T, Pope D, Hill B (2018) Australasian recommendations for quality assurance in kilovoltage radiation therapy from the Kilovoltage Dosimetry Working Group of the Australasian College of Physical Scientists and Engineers in Medicine. Australas Phys Eng Sci Med 41:781–808. https://doi.org/10.1007/s13246-018-0692-1.
2. Ceylan A, Butson M, Cullen A, Yu PK, Alnawaf H (2012) Variations in daily quality assurance dosimetry from device levelling, feet position and backscatter material. Australas Phys Eng Sci Med 35:485–489. https://doi.org/10.1007/s13246-012-0169-6.

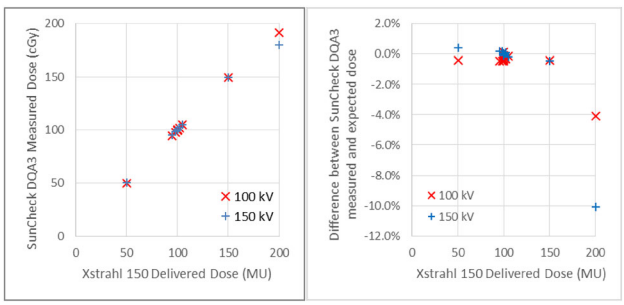

Fig. 1. SunCheck DQA3 linearity and reproducibility measurements following baselining with a 100 MU delivery on an Xstrahl 150 kilovoltage therapy unit using a 20 cm square 50 cm FSD applicator flush with the DQA3.

P23. Dosimetric evaluation of a tungsten eye shield for use during electron radiotherapy

Yousif Yousif[1], John Daniel[2], Jackson Zifodya[3], Robin Hill[4,5,*]

[1]North West Cancer Centre- Tamworth Hospital, Sydney, Australia, [2]North West Cancer Centre- Tamworth Hospital, Tamworth, Australia, [3]North West Cancer Centre- Tamworth Hospital, Tamworth, Australia, [4]Department of Radiation Oncology, Chris O'Brien Lifehouse, Camperdown, Australia, [5]School of Physics, Institute of Medical Physics, University of Sydney, Sydney, Australia

Introduction In radiotherapy, eye shields are used to protect critical structures like lens and cornea when treating lesions near to the eyes. This study evaluates the dosimetric behaviour of a commercial tungsten eye shield for 6 and 9 MeV electron beams.
Methods In this study, we used a tungsten eye shield (RPD Inc., Albertville, USA) with a thickness of 2 mm, internal and external diameters of 15 and 19.1 mm respectively, and 0.5 and 1 mm Aluminium (Al) caps. Transmission measurements were acquired with an Advanced Markus chamber in a solid water phantom (Gammex/RMI, Middleton, WI). The chamber was exposed with and without an eye shield for beam energies of 6 and 9 MeV and using field sizes of a 4×4 cm^2 and a 10×10 cm^2 at 100 cm SSD. Central depth doses and beam profiles were also measured using a PTW –MP3 scanning water tank with a 3D PinPoint (TM31016) ionization chamber (PTW, Freiburg, Germany). The depth dose profile data were normalized to 0 mm depth in an open field for all beams.
Results Even though the transmission factors measured for the 6 MeV beam were 2.5% and 2.6% for 4×4 cm^2 and 10×10 cm^2, respectively, it increased up to 10% for similar field sizes (see table 1) for 9 MeV. The difference in transmissions for 0.5 and 1 mm Al caps was minimal. The depth dose profiles showed a large reduction in the dose under the shield, followed by a gradual increase in dose outside the shield (see Fig. 1). The relative percentage dose under the shield increased from 6.9% to 6.7% for 6–9 MeV.
Conclusion The results of this study show that a 2 mm tungsten eye shield is adequate to protect OARs such as lens and cornea for a 6 MeV beam, which also agrees with manufacturer specifications[1].
References

1. Tungsten Eye Shields, Radiation Products Design Inc, 2019. www.rpdinc.com

Table 1. Measured Transmission factors of eye shield with the electron beam.

Applicator	Energy	2 mm Tungsten	2 mm Tungsten + 0.5 mm Al	2 mm Tungsten + 1.00 mm Al
4 × 4 cm^2	6 MeV	2.5	2.3	2.5
	9 MeV	10.2	8.9	7.7
10 × 10 cm^2	6 MeV	2.6	2.6	2.6
	9 MeV	10.0	8.8	7.7

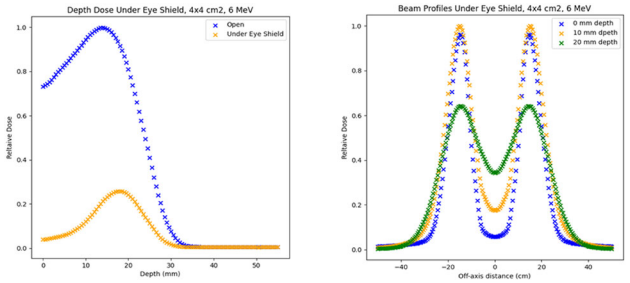

Fig. 1. Depth dose (a) and beam profiles measured under eye shield for a 4 × 4 cm^2 field size for 6 MeV.

P24. Abstract withdrawn

P25. Evaluation of a tungsten eye shield for kilovoltage X-ray beams using ionization chamber

Yousif Yousif[1], John Daniel[2], Jackson Zifodya[3], Robin Hill[4,5,*]

[1]North West Cancer Centre- Tamworth Hospital, Tamworth, Australia, [2]North West Cancer Centre- Tamworth Hospital, Tamworth, Australia, [3]North West Cancer Centre- Tamworth Hospital, Tamworth, Australia, [4]Department of Radiation Oncology, Chris O'Brien Lifehouse, Camperdown, Australia, [5]School of Physics, Institute of Medical Physics, University of Sydney, Sydney, Australia

Introduction Eye shields are used in radiotherapy to protect or reduce the radiation to ocular structures such as lens and the cornea. In this study, we performed a dosimetric evaluation of a tungsten eye shield in kV x-ray beams.

Methods A tungsten eye shield (RPD Inc., Albertville, USA), of diameter and thickness of 19.1 mm and 2 mm respectively, along with aluminium caps of thicknesses 0.5 and 1.0 mm were utilised. Data were acquired on an XStrahl 300 unit (XStrahl-Ltd., UK) for 60, 100, 150 and 300 KVp x-ray beams. All Transmission measurements were performed using an Advanced Markus ionization chamber (PTW, Freiburg, Germany) in a solid water phantom (Gammex/RMI, Middleton, WI) for field sizes 3 and 5 cm diameter with 30 cm focus to surface distance (FSD) and 10 × 10 cm^2 and 20 × 20 cm^2 with 50 FSD. Transmission measurements were performed for Tungsten, Tungsten with 0.5 Cap, and Tungsten with 1.0 mm Cap. In addition, depth dose profiles were acquired using a PTW –MP3 scanning water tank with a 3D PinPoint (TM31016) ionization chamber for a 5 cm diameter.

Results Transmission values increased from 3.3 to 34.6% and 3.3 to 28.3% for a 3 cm and 5 cm field sizes respectively over the range 60-300 kVp. Transmission for 10 × 10 cm^2, and 20 × 20 cm^2 were 16.8% and 23.8%, respectively. The depth dose profiles showed a significant dose under the shield, but, dose increased gradually away from the shield (see Fig. 1). As a result, the relative percentage dose under the shield increased from 6.7% to 12% for 60 -300 KVp.

Conclusion The eye shield was found to be suitable for low energies KVp x-ray beams, namely 60 and 100 KVp, but not for higher KV energies, which required alternative shield thickness. The findings, however, agreed with the previous studies[1].

References

1. Wang D, Sobolewski M, Hill R (2012) The dosimetry of eye shields for kilovoltage X-ray beams. Australas Phys Eng Sci Med 35:491–495. https://doi.org/10.1007/s13246-012-0166-9

Table 1. Transmission under the eye shield.

Applicator	kVp	2 mm Tungsten	2 mm Tungsten + 0.5 mm Al	2 mm Tungsten + 1.00 mm Al
3 cm Diam	60	3.3	2.9	2.5
	100	5.5	5.3	5.1
	150	10.1	9.9	9.8
	300	34.6	34.3	33.8
5 cm Diam	60	3.3	3.3	3.3
	100	6.5	6.3	6.1
	150	11.9	11.9	11.7
	300	28.9	29.0	28.9
10 × 10 cm^2	300	16.8	16.8	16.7
20 × 20 cm^2	300	23.8	23.8	23.8

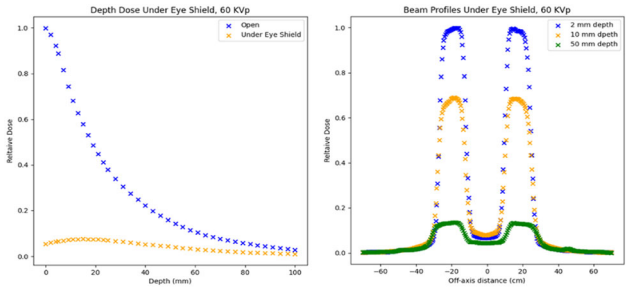

Fig. 1. Shows depth dose (a) and beam profiles under eye shield measured for a 5 cm dimeter applicator for 60 KVp.

P26. A new HVL jig for SXRT

Emma Dyce[1,2,*]

[1]Genesiscare Victoria, East Albury, Australia, [2]Murdoch University, Perth, Australia

Introduction GenesisCare Albury Wodonga implemented a new superficial and orthovoltage treatment program in 2021 after commissioning an XStrahl 200 X-ray therapy System (Gulmay Medical Ltd., Surrey, United Kingdom). A custom-made horizontal jig was designed and commissioned to measure the half-value layers (HVL) of each filter as specified by AAPM TG 61 [1]. The highest clinical energy is 150 kV.

Method A lead pinhole diaphragm was ordered from Antidote Biomedical (Preston, Australia) of external dimensions 10 cm × 10 cm with a 2 cm central hole and 9 mm thickness. Transmission testing was completed with the highest clinical energy of 150 kV using a Markus ionisation chamber in RW3 with a ring on. A local steel fabrication company (Albury Stainless Steel Pty Ltd., Albury, Australia) was commissioned to design and build the jig using the lead diaphragm to meet the AAPM specifications for a HVL jig. Measurements included distance from chamber to diaphragm tolerance ≥ 50 cm, transmission through diaphragm measured with a Markus chamber, tolerance < 0.1%, beam diameter less than 4 cm

and chamber centrally aligned. A holder for high purity attenuating materials and chamber holder for farmer chamber was included. HVLs were measured with the new jig and compared to existing baselines with tolerance of 2%.

Results Measurements confirmed the detector is 50 cm from diaphragm and attenuating material. Transmission through the diaphragm was measured to be 0.05% for 150 kV. The field size at the chamber was measured to be 3.4 cm, with the chamber centrally aligned and sensitive volume covered by the field. Measured HVLs were within 1.6% of baseline.

Conclusion A new HVL jig was commissioned and satisfied all requirements of AAPM TG 61 and has been released for clinical use.

Fig. 1. A new HVL jig.

P27. Commissioning of a 60-channel body coil for MRI utilized for radiotherapy planning

Aitang Xing[1,2,3,*], Doaa Elwadia[1,2], Robba Rai[1,2], Lois Holloway[1,2,3]

[1]Liverpool and Macarthur Cancer Therapy Centres, Liverpool, Australia, [2]Ingham Institute for Applied Medical Research, Liverpool, Australia, [3]South Western Sydney Clinical School, University of NSW, Liverpool, Australia

Introduction An MRI scanner (a Siemens 3 T Skyra) dedicated to radiotherapy was commissioned and integrated into the radiotherapy workflow in 2013. Recently a 60 channel body coil was purchased and installed. The aim of this work was to commission the coil for clinical use.

Method A series of checks and tests were performed: (1) visual and mechanical checks. The coil elements were visually checked and internally assessed by scanning the body coil using a CT simulator (Philips Brilliance); (2) phantom-based check to quantify the image quality. A Siemens Blue Sphere phantom D240 was filled with a solution containing 0.011 g MACROLEX blue per liter. The phantom was scanned using four clinical sequences: SE, GE, Dixon, and UTE. The phantom was placed on a headset and wrapped by the anterior and posterior components of the 60 channel body coil. Signal-to-noise ratio (SNR), uniformity, and the ghosting effect were calculated using the central slice as described in [1];(3) volunteer-based check. Volunteers were recruited to check the image quality of patients. The imaging region focused on the pelvis region including the liver and prostate. Clinical protocols were used and scanning parameters were adjusted to achieve optimal image quality.

Results No apparent damage were found on coil surface and cables. The coil elements were symmetrically distributed with no obvious defects observed. The image quality indices of phantom-based scan were presented in Table 1. The image quality of the volunteer scan was visually assessed and deemed clinically acceptable for radiotherapy planning purposes.

Table 1. Image quality indices from different sequences.

Sequence	SNR	Uniformity	Ghosting
SE	37.83	99.29	0.0016
GE	2.01	100	0.0301
UTE	4.725	93.372	0.0032
DIXON	7.436	92.868	0.0217

Conclusion The 60-channel body coil was successfully commissioned. Image quality quantified using a uniform phantom and volunteer images were found to be clinically acceptable.

References

1. Xing A, Holloway L, Arumugam S, Walker A, Rai R, Juresic E, Cassapi L, Goozee G, Liney G (2016) Commissioning and quality control of a dedicated wide bore 3 T MRI simulator for radiotherapy planning. Int J Cancer Ther Oncol 4:421.

P28. The variation of cryostat characterisation between three Unity MR-linacs

Katrina Biggerstaff[1,*], Luke Gilling[1], Urszula Jelen[2], Michael Jameson[2], John Baines[3]

[1]GenesisCare WA, Murdoch, Australia, [2]GenesisCare NSW, Alexandria, Australia, [3]Queensland Health, Townsville, Australia

Introduction The Unity (Elekta AB, Stockholm, Sweden) cryostat is a cylindrical container housing the coils of superconducting magnet and an active shimming system. Liquid helium in the cryostat maintains the coils in the superconductive state. The cryostat is built with low attenuating material, however variations in material thickness and helium levels at various gantry angles will cause changes in the attenuation of the radiation beam [1]. In this study, the transmission of three Unity MR-Linacs (each with different helium levels) were compared. The transmission effect of longitudinal offsets from the linac isocentre were also monitored to assess the homogeneity of the cryostat beam attenuation.

Methods For cryostat transmission measurements, a PTW Farmer chamber with a build-up cap was aligned to the MV isocentre with the patient couch top and posterior imaging coils removed. The same field was delivered and measured in 2-degree increments of gantry rotation to determine the transmission variation. This was completed for three Australian Unity MR-Linacs and the transmission variations were compared. For one MR-Linac, the measurements were repeated at isocentre and at 1 cm superiorly and inferiorly from the isocentre.

Results The variation in transmission (relative to gantry 90) ranged between 0.995 to 1.012, 0.991 to 1.009 and 0.981 to 1.010 for helium fills of 71.6%, 78.7% and 79.3%, respectively (shown in **Fig. 1**). Preliminary results show movement of 1 cm from the isocentre varied the transmission measurement by 0.5%, suggesting the homogeneity of the cryostat also varies with distance offset from the isocentre as shown in Fig. 1 (left).

Conclusion A Farmer chamber provided an averaged transmission with varying gantry angles, which is modelled in the treatment planning system. The clinical impact of dose variation with gantry angles can be significant due to the cryostat and variation in helium

fill. Careful evaluation of its construction will ensure accurate modelling in the treatment planning system.

Acknowledgements: The authors acknowledge Jason Arts, Armia George and Elekta for providing the beam model for testing.

References

1. Roberts DA et al. (2021) Machine QA for the Elekta Unity system: A Report from the Elekta MR-linac consortium Med. Phys. https://doi.org/10.1007/s001090000086

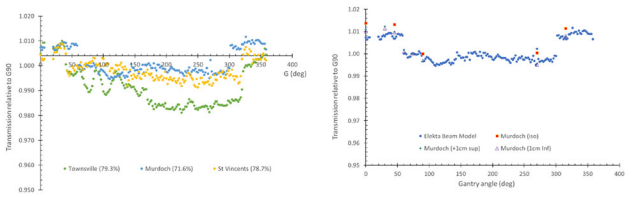

Fig. 1. (Left) Comparison of cryostat transmission values for three MR-Linacs with various Helium levels. (Right) Independent measurement of cryostat transmission at isocentre, 1 cm superior and 1 cm inferior of isocentre.

P29. A multi-centre study for implementation of MRI-only stereotactic prostate radiation therapy workflow

Peter Greer[1,2,*], Jae Hyuk Choi[2], Jason Dowling[2,3], Parnesh Raniga[3], Mark Sidhom[4], Tony Young[4], Dean Wilkinson[5], Laura O'Connor[1,2], Kate Skehan[1], Lee Wilton[1], Perry Hunter[1], Jarad Martin[1,2]

[1]Calvary Mater Newcastle Hospital, Newcastle, Australia, [2]University of Newcastle, Newcastle, Australia, [3]CSIRO, Brisbane, Australia, [4]Liverpool Hospital, Liverpool, Australia, [5]Illawarra Cancer Care Centre, Wollongong, Australia

Introduction The NINJA TROG18.01 clinical trial is comparing two schedules of stereotactic prostate treatments. A technical sub-study was incorporated to the trial to implement MRI-only treatment workflow in a multi-centre setting.

Method A comprehensive implementation and evaluation guide for MRI-only was developed as part of the trial RT QA guidelines. A staged three-phase implementation was developed:1) conventional treatment workflow with additional synthetic CT (sCT) evaluation against conventional CT dose (5 patients); 2) MRI-only workflow with quality assurance CT scan acquired for comparison of sCT dose to QA-CT dose (10 patients); 3) fully MRI-only workflow with QA of sCT dose using MRI-based bulk anatomical density (BAD) map (Fig. 1) calculation (1). Isocentre doses ($\Delta Diso$) were compared along with 3D Gamma evaluation with 3%/3 mm, 2%/2 mm, 2%/1 mm and 1%/1 mm criteria. PTV D98, D95, D50 and D2) and Rectum D50 were compared.

Results To date four centres are participating and two further centres are in development. At least 56 patients have received MRI-only workflow (Phase 3). While all patients had differences within 2.5%, only one patient had greater than 2% difference (-2.2%) between the sCT and BAD map isocentre dose calculations. Overall, the mean ± 1 SD $\Delta Diso$ between the scans was -0.95 ± 0.56%. All PTV dose differences were within 2.5% and the greatest difference was -2.3% for D2 (Fig. 2). The mean difference in Rectum D50 was -0.04 ± 0.62% and only one patient had greater than 2% difference (2.03%). Overall, the mean gamma pass rates at 3%/3 mm, 2%/2 mm, 2%/1 mm and 1%/1 mm criteria were 100.0 ± 0.1%, 100.0 ± 0.1%, 99.9 ± 0.1% and 96.8 ± 2.5% respectively.

Conclusion For MRI-only workflows sCT dose calculations were in close agreement to optimised bulk density calculations. MRI-only prostate workflow can be implemented in a multi-centre setting with appropriate quality assurance to validate sCT dose calculations.

References

1. Choi, JH, et al. (2019) Bulk anatomical density based dose calculation for patient-specific quality assurance of MRI-only prostate radiotherapy. Frontiers in Oncology, **9**.

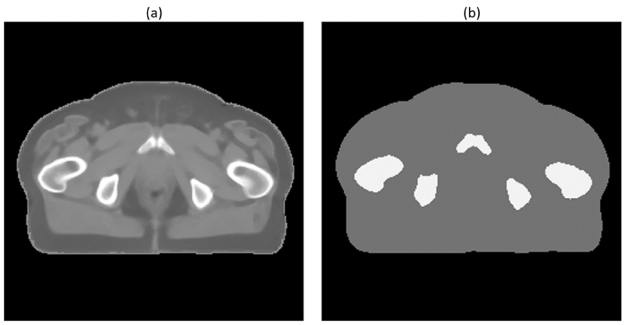

Fig. 1. Example sCT (a) generated using the multi-atlas local weighted voting method and its corresponding (b) two tissue class BAD map.

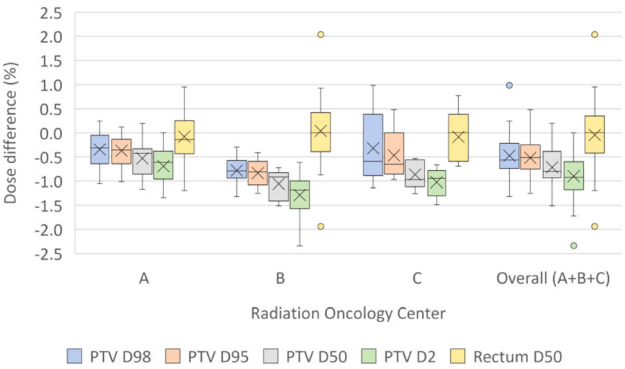

Fig. 2. Results of the dose volume histogram analysis. Differences in doses that cover 98%, 95%, 50% and 2% of the planning target volume (PTV D98, D95, D50 and D2) and 50% of the rectum (Rectum D50).

P30. 1.5 T MRI sequences assessment on Elekta Unity

Reza Alinaghizadeh[1], Nikki Shelton[1], Jessica Lye[1], Glenn Cahoon[1], Rob Behan[1,*], Sarah Elliott[1], Benjamin Harris[1], Sandra Fisher[1], Sweet Ping Ng[1]

[1]Olivia Newton John Cancer Research and Wellness Centre, Austin Health, Melbourne, Australia

Introduction The Unity MR-Linac provides high resolution and versatile soft tissue contrast imaging during the treatment process without extra dose to the patient. Since MR-linac images are used for both simulation and plan adaptation processes, the image quality and geometric integrity of sequences, which have a critical impact on treatment planning and dose delivery, must be critically assess across

a range of criteria [1]. The aim of this study was to evaluate and benchmark the MRI sequences of the Unity across multiple criteria prior to clinical use.
Method For this study, various methods and phantoms were used to baseline and check the MRI sequences. An ACR phantom was used and analysed with RIT software to evaluate the image quality parameters, like SNR, Uniformity, Ghosting, high contrast and low contrast [2]. To evaluate the geometric distortion, a 3D printed phantom (3DOne) was used, along with MIM Maestro software, to analyse the data using deformable registration tools. All the phantoms were scanned with similar coils and setup to the typical patient positioning during the scanning and treatment on the MR-Linac.
Results The ACR phantom results was acceptable in quality measures like SNR, Uniformity, ghosting and high contrast, however the low contrast results were not reliable since this test is designed for 1 cm slice thickness and the Unity system generates 0.1- 0.2 cm slice data. Geometric distortion analysis of the 3DOne phantom by MIM software showed a mean difference between transferred voxels of ≤ 1 mm within the 350 mm diameter area covered by phantom.
Conclusion Image quality measures and geometric distortion of individual sequences were assessed, and the results were well within recommended tolerances [1].
References

1. Carri K. Glide-Hurst, Eric S. Paulson2, Kiaran McGee3, Neelam Tyagi4, Yanle Hu5, James Balter6, John Bayouth AAPM TG 284 report: Magnetic Resonance Imaging Simulation in Radiotherapy: Considerations for Clinical Implementation, Optimization, and Quality Assurance Med Phys 2021 https://doi.org/10.1002/MP.14695
2. The American Association of Physicists in Medicine (AAPM) and the American College of Radiology (ACR) Phantom Test Guidance for Use of the Large MRI Phantom for the ACR – MRI Accreditation Program.

P31. Characterisation of a commercial head and neck immobilisation device for magnetic resonance guided adaptive radiotherapy

Claire Pagulayan[1,*], Maddison Picton[1], Conrad Loo[3], Charles Tran[1], Urszula Jelen[1], Nicolle Dunkerley[1], David Crawford[1], Tanya Twentyman[1], Jeremy de Leon[1], Dion Forstner[1,2], Michael Jameson[1,2]

[1]GenesisCare NSW, Sydney, Australia, [2]University of New South Wales, Sydney, Australia, [3]GenesisCare Vic, Melbourne, Australia

Introduction Head and neck (H&N) immobilization devices used in radiotherapy increase patient positioning reproducibility, and thus increase treatment precision. However, it is known from the literature that certain equipment can increase surface dose [1,2]. The purpose of this study was to dosimetrically characterise and model the iCAST head and shoulder (H&S) micro-mask and HeadSTEP headboard (Innovative Technologie Völp e.U, Innsbruck, Austria) for the Elekta Unity MR-Linac.
Method Measurements with and without the iCAST mask were performed on a Unity MR-Linac system. This included measuring the percentage depth dose (PDD) using EBT3 GafChromic film, comparing the surface doses and determining the masks' equivalent thickness of water. Similarly, transmission measurements using a Farmer chamber were performed with and without the HeadSTEP headboard on top of solid water. Lastly, the headboard was CT scanned for electron density information and exported to the TPS for modelling purposes. Modelled data was compared to that measured.
Results Through interpolation of the PDD, the water equivalence of the mask was found to be 2.08 mm for the 7FFF beam, and the surface dose was 38.8% higher when measured with the mask. However, this effect was minimised once the mask was stretched. Further, the headboard transmission was determined to be 97.6% and differences between the modelled and measured dose using the headboard was $< 1\%$. The main issues were found to stem from the couch model in the TPS itself which has been rectified in the most recent version of Monaco (v5.51 Elekta AB, Stockholm, Sweden).
Conclusion The iCAST H&S micro-mask and HeadSTEP headboard have been characterised dosimetrically. Approval has been given within the department for clinical release for patients requiring H&N immobilisation on the Unity MR-Linac.
References

1. Hadley SW, Kelly R, and Lam K (2005) Effects of immobilization mask material on surface dose. Journal of Applied Clinical Medical Physics 6:1–7.
2. Nolasco A, Faria LO (2020) Head and Neck Immobilization Masks: Increase in Dose Surface Evaluated by EBT3, TLD-100 and PBC Method. Precision Radiation Oncology 4: 73– 80.
3. Elekta. HeadSTEP: Head and Neck Immobilization. URL: https://ecatalog.elekta.com/oncology/headstep/products/0/22325/22312/20231/headstep.aspx. Accessed online 5/7/2022.

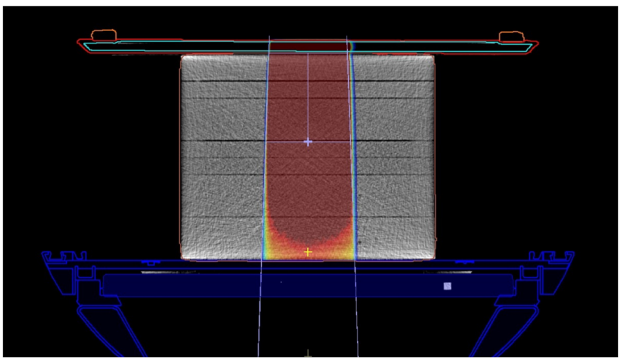

Fig. 1. Setup determining the relative electron density of the HeadSTEP in the TPS to compare to measured values.

P32. Quantifying the electron streaming effect in an MR-linac environment

Peter Stokes[1,*], Elizabeth Patterson[2], Marcus Powers[1], John Baines[1]

[1]Townsville Cancer Centre, Townsville, Australia, [2]Centre for Medical Radiation Physics, Wollongong, Australia

Introduction Magnetic resonance guided radiation therapy (MRgRT) can present clinically significant out-of-field dose due to the electron streaming effect (ESE). In the case of the Elekta Unity MRL, ESE can arise at both the patient entrance and exit surfaces [1,2] as well as at the anterior MR imaging coil that is present during all treatments [3]. This work aims to quantify the out-of-field dose resulting from ESE in an Elekta Unity MRL.
Method Solid water and lung slabs of 5 cm thickness were centred at isocentre and aligned 45° to an incident beam of field size 5 cm × 5 cm. Entrance and exit ESE doses were measured using EBT3 film for the solid water slab and a PTW microDiamond detector for the lung slab. Corresponding Monte Carlo ESE dose simulations were

performed using the GEANT4 platform [4] and vendor-provided phase-space files.

Results Fig. 1 shows simulated maximum entrance and exit ESE doses as functions of slab density. Relative to D_{max} in water (the maximum dose in a 30 cm × 30 cm × 30 cm water phantom with 133.5 cm SSD), out-of-field doses were found to be as large as 69% for entrance ESE and 89% for exit ESE. Figure 2 shows the ratio of the doses in Fig. 1, with the experimental results plotted alongside for comparison.

Conclusion For the setup considered, ESE results in an out-of-field dose as large as 89% of D_{max} in water. Promisingly, simulation and measurement were both found to agree to within 3%. In the near future, we plan to perform additional ESE measurements and simulations to better inform out-of-field dose mitigation strategies, such as shielding choice and thickness.

References

1. Liu H, Ding S, Wang B, Li Y, Sun Y, Huang X (2020) In-Air Electron Streaming Effect for Esophageal Cancer Radiotherapy with a 1.5 T Perpendicular Magnetic Field: A Treatment Planning Study. Front Oncol 10:607,061. https://doi.org/10.3389/fonc.2020.607061
2. Baines J, Powers M, Newman G (2021) Sources of Out-Of-Field Dose in MRgRT: an Inter-comparison of Measured and Monaco Treatment Planning System Doses for the Elekta Unity MR-Linac. Phys Eng Sci Med 44:1049–1059. https://doi.org/10.1007/s13246-021-01039-6
3. Powers M, Baines J (2022) Electron Streaming Effect Associated With the Elekta Unity Anterior Imaging Coil. Front Phys 10. https://doi.org/10.3389/fphy.2022.880121
4. 4. S. Agostinelli, et al. (2003) Geant4—a simulation toolkit. Nuclear Instruments and Methods in Physics Research Section A: Accelerators, Spectrometers, Detectors and Associated Equipment 506(3):250–303. https://doi.org/10.1016/S0168-9002(03)01368-8

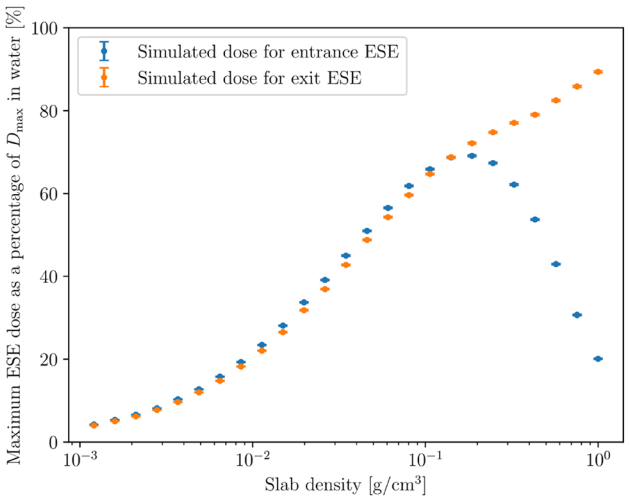

Fig. 1. Simulated entrance and exit ESE doses versus slab density.

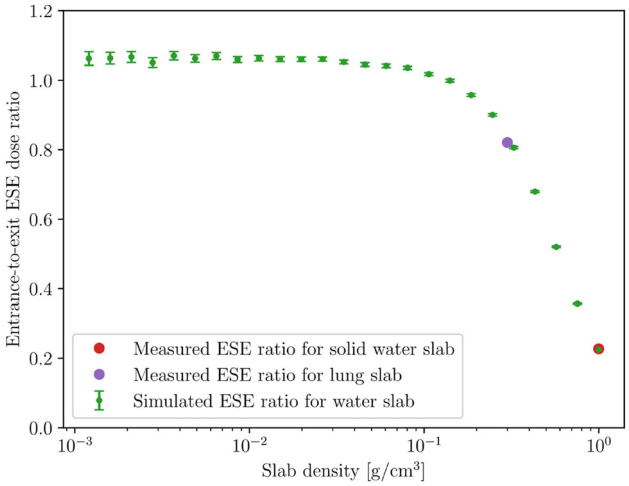

Fig. 2. Simulated and measured entrance-to-exit ESE dose ratios versus slab density.

P33. Accounting for inter-cell effects in single-cell Monte-Carlo simulations

Melissa McIntyre[1,*], Ayse Kizilersu[1], Anthony Thomas[1]

[1]University of Adelaide, Adelaide, Australia

Introduction The reproducibility and accuracy of scientific results is a major challenge for all fields of science. Monte-Carlo simulations of radiobiological systems such as cells and DNA are challenging to reproduce due to their complexity and large parameter space. As such, many simulations must be scaled-down due to high computational demand and the need to constrain the parameters. When inter-cell effects are neglected, deficiencies are introduced into the data, degrading its consistency with equivalent clinical data.

Method Here we present a comparative study of simulations performed using a multi-cell network and a more detailed single cell geometry. A parameter sensitivity study is performed at the multi-cell level using the Geant4-DNA Monte Carlo toolkit with a focus on contributions from charged particles. The results are compared with a single-cell geometry to assess the effect of dose contributions in the cell from its surroundings.

Results Single-cell simulations are shown to be a viable option in reproducing clinical radiobiological data at a reasonable computational expense. However, the correction procedure for modelling the response of cells within a multi-cellular network using a single-cell simulation is shown to significantly influence the results. This is illustrated through parameter sensitivity analyses and comparisons when inter-cell effects are considered and neglected.

Conclusion Designing reliable Monte Carlo simulations for biological systems is at the forefront of radiation research as treatment planning moves towards a radiobiological weighted approach. The importance of radiobiological simulations is therefore expected to increase. The desired low computational expense of simulations of this nature is achievable whilst preserving accuracy by considering effects that contribute to cell irradiation due to its surrounding environment and reproducibility through parameter sensitivity analyses.

P34. A review on the performance of different physics lists in TOPAS Monte Carlo simulation toolkit for megavoltage x-ray beams

Young woo Kim[1], Robin Hill[1,2,3,*]

[1]Department of Radiation Oncology, Chris O'Brien Lifehouse, Sydney, Australia, [2]Institute of Medical Physics, School of Physics, University of Sydney, Sydney, Australia, [3]Biomedical Innovation, Chris O'Brien Lifehouse, Sydney, Australia

Introduction Monte Carlo (MC) simulations are widely used to simulate photon and electron transport in different media. The TOPAS MC simulation toolkit is based on the Geant4 simulation toolkit. In TOPAS, the user can choose different "Physics Lists" which specify what particles and physics processes are defined, different cutoff parameters and other physics options [1,2]. In this work, we compared the performance of several physics lists for megavoltage x-ray beam dosimetry.
Method The geometry consisted of square water phantom (30 × 30 × 30 cm). The incident beam was a published IAEA phase-space file for a Varian Clinac iX 6MV x-ray beam with 4 × 4 cm field size. The number of incident particle used for simulation was 1e7 particles. Percentage depth doses (PDD) curve were calculated using 6 different physics lists available in TOPAS toolkit: G4EmStandardPhysics_option0 to 4 and G4EmPenelopePhysics. Calculated PDDs were compared to measured data obtained from a Varian 21IX linear accelerator.
Results The relative dose values at 10 and 20 cm depth and D_{max} are shown in table (1). The computing time required increased as the complexity of physics options in the list increases.
Conclusion There was acceptable agreement with measured data by the doses calculated by the different physics lists. The next step is to consider the performance of several physics lists for megavoltage x-ray beam dosimetry in geometry with tissue inhomogeneities such as bone, lung and high Z materials.
References

1. Perl J, Shin J, Schumann J, Faddegon B, Paganetti H (2012) TOPAS: an innovative proton Monte Carlo platform for research and clinical applications. Med Phys 39:6818–6837.
2. Faddegon B, Ramos-Mendez J, Schuemann J, McNamara A, Shin J, Perl J, Paganetti H (2020) The TOPAS Tool for Particle Simulation, a Monte Carlo Simulation Tool for Physics, Biology and Clinical Research, Physica Medica. https://doi.org/10.1016/j.ejmp.2020.03.019

Table 1. Depth of D_{max} and relative doses at 10 and 20 cm depth in water.

	Option 0	Option 1	Option 2	Option 3	Option 4	Penelope	Measured
D_{max} (cm)	1.25	1.25	1.25	1.25	1.75	1.25	1.5
D_10cm (%)	60.8	61.6	60.8	61.8	61.4	60.4	61.9
D_20cm (%)	32.9	32.7	32.5	33.7	32.2	32.5	33.7

P35. Beam dynamics studies for the NIMMS superconducting synchrotron for ion therapy

Hannah X.Q. Norman[1,2,3,*], Robert B. Appleby[1,2], Suzanne L. Sheehy[3,4], Elena Benedetto[5], Hywel L. Owen[2,6]

[1]University of Manchester, Manchester, United Kingdom, [2]Cockcroft Institute, Warrington, United Kingdom, [3]University of Melbourne, Melbourne, Australia, [4] Australian Nuclear Science and Technology Organisation (ANSTO), Australia, [5]SEEIIST Association, Geneva, Switzerland, [6]STFC Daresbury Laboratory, Warrington, United Kingdom

Introduction The Next Ion Medical Machine Study (NIMMS) is an international collaboration focused on the development of technology for future ion therapy facilities, driven by the need to improve the quality and accessibility of modern radiotherapy treatments. To realise such facilities, focus is placed on the particle accelerator, for which the footprint needs reduction while achieving beam intensities above 1 × 1010 particles per spill for efficient, effective treatment. A compact (27 m circumference) synchrotron, based on curved superconducting magnets has been designed to meet these requirements.
Method An accurate description of the magnet field errors is extracted from an electromagnetic model of the magnet using the finite element analysis software OPERA-3D. Carbon ions up to maximum treatment kinetic energy (430 MeV/u) are tracked using a model of the accelerator using the lattice code MAD-X and the Polymorphic Tracking Code, including magnetic field errors to evaluate the impact on the quality and stability of the beam.
Results The field errors of the curved magnet designed for the compact superconducting synchrotron are computed to sufficient accuracy. The results of tracking simulated particles through the accelerator with inclusion of magnetic field errors are presented, with considerations made for the clinical performance of the accelerator.
Conclusion A detailed study involving the simulation of therapeutic carbon ion beams tracked through the NIMMS superconducting synchrotron, subject to magnetic field errors, is presented. An accurate description of these field errors is essential to determine the impact on the beam dynamics of the accelerator and its suitability for treatment. This enables further work on the optimisation of the magnet and accelerator for implementation into future clinical facilities.
Disclosures This project has received funding from the Engineering and Physical Sciences Research Council (EPSRC) in the United Kingdom. We would also like to acknowledge our NIMMS collaborators for their valuable contributions to this work.

P36. Beyond synchrotrons: A fixed field accelerator for ion therapy

Adam Steinberg[1,2,3,*], Robert Appleby[2,3], Suzie Sheehy[1]

[1]University of Melbourne, Brunswick, Australia, [2]University of Manchester, Manchester, United Kingdom, [3]Cockcroft Institute, Daresbury, United Kingdom

Introduction Fixed Field Alternating Gradient Accelerators have been proposed as an alternative to current options for particle therapy [1], combining the rapid acceleration of cyclotrons with the variable extraction energy of synchrotrons. However, the magnetic field profile usually chosen to keep the beam stable during acceleration leads to large accelerators, and complex magnets. By relaxing the constraints on the magnetic field, we are able to reduce the complexity and size of the machine while maintaining stability during acceleration.

Method In Fixed Field Accelerators, the closed orbit trajectory varies significantly with energy. Although this increases the complexity of simulations, the extra freedom provides an opportunity to control the beam dynamics by the addition of nonlinear terms to the magnetic field. To avoid the loss of beam stability, these nonlinearities are tuned to ensure that the focusing experienced by the beam is approximately constant [2].
Results We present a design for an accelerator using nonlinear fixed magnetic fields that could be used to produce helium, carbon, and oxygen ions for particle therapy. The work investigates how the dynamic aperture – the stable volume in phase space – varies with beam energy, including realistic magnet errors to show that the accelerator could achieve the desired results if constructed. Initial studies on injection, extraction, and acceleration are also shown.
Conclusion As ion therapy evolves, new technologies will be required to keep up with the needs of clinicians. This work demonstrates that a Fixed Field Accelerator is a viable option for future treatment facilities, provides a method for designing them, and applies this method to give a realistically achievable novel accelerator for cancer treatment.
References

1. S. Verdu-Andres, U. Amaldi, & A. Faus-Golfe. (2011). Literature review on LINACs and FFAGs for hadron therapy. Int J of Mod. Phys. A, 26, 1659–1689. http://dx.doi.org/10.1142/S0217751X11053109
2. A.F. Steinberg, R.B. Appleby & S. L. Sheehy (2022) Tune Control in Fixed Field Accelerators. Proceedings of the 13th International Particle Accelerator Conference (IPAC'22). https://doi.org/10.18429/JACoW-IPAC2022-MOPOST02

The Melbourne and Manchester Graduate Research Group (GOLDEN Scheme) provides funding for the PhD that produced this work.

P37. Abstract withdrawn

P38. Potential effects due to variation in linear energy transfer definition and calculation method

Edward Smith[1,2,*], Carla Winterhalter[1,3], Tracy Underwood[1,3], Adam Aitkenhead[1,2], Jenny Richardson[1,2], Michael Merchant[1,3], Norman Kirkby[1,3], Karen Kirkby[1,3], Ranald Mackay[1,2]

[1]Division of Cancer Sciences, School of Medical Sciences, Faculty of Biology, Medicine and Health, The University of Manchester, Manchester, United Kingdom, [2]Christie Medical Physics and Engineering, The Christie NHS Foundation Trust, Manchester, United Kingdom, [3]The Christie NHS Foundation Trust, Manchester Academic Health Science Centre, Manchester, United Kingdom

Introduction The strong in vitro evidence that proton Relative Biological Effectiveness (RBE) varies with Linear Energy Transfer (LET) has led to an interest in applying LET within treatment planning. However, there is a lack of consensus on LET definition, Monte Carlo (MC) parameters or clinical methodology. This work aims to investigate how common variations of LET definition may affect clinical applications.
Method MC simulations (GATE/GEANT4) were used to calculate dose and different types of LET for a simple Spread Out Bragg Peak (SOBP) and for four clinical PBT plans covering a range of tumour sites. Variations in the following LET calculation methods were considered: (i) averaging (dose-averaged LET (LETd) & track-averaged LET); (ii) scoring (LETd to water, to medium and to mass density); (iii) particle inclusion (LETd to all protons, to primary protons and to particles); (iv) MC settings (hit type and Maximum Step Size (MSS)). LET distributions were compared using: qualitative, LET Volume Histograms (LVHs), single value criteria (maximum and mean values) and optimised LET-weighted dose models.
Results Substantial differences were found between LET values in averaging, scoring and particle type. These differences depended on the methodology, but for one patient a difference of $\sim$100% was observed between the maximum LETd for all particles and maximum LETd for all protons within the brainstem in the high isodose region (4 keV µm − 1 and 8 keV µm − 1 respectively). A model using LETd including heavier ions was found to predict substantially different LET-weighted dose compared to those using other LET definitions.
Conclusion The selection of LET definition may affect the results of clinical metrics considered in treatment planning and the results of an RBE model. The authors' advocate for the scoring of dose- averaged LET to water for primary and secondary protons using a random hit type and automated MSS.

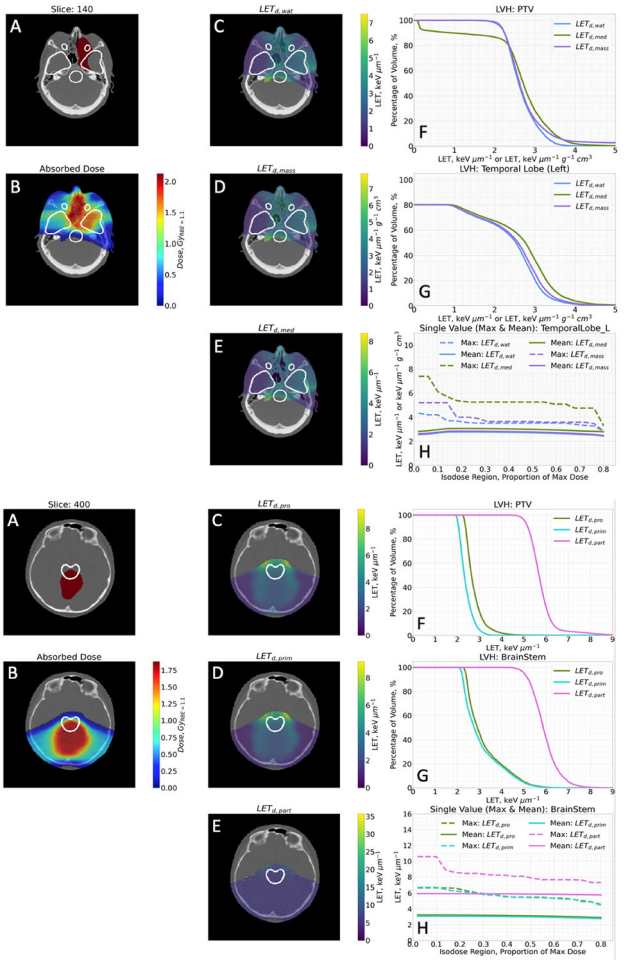

P39. A three-day scripting workshop for the Elekta Monaco treatment planning system

Jason Morton[1,*], Luis Munoz[1], Arek Mazurek[2], Peter McLoone[3]

[1]Genesiscare SA, Adelaide, Australia, [2]GenesisCare WA, Perth, Australia, [3]GenesisCare NSW, Sydney, Australia

Introduction Treatment planning automation via scripting can be leveraged to provide planner efficiency gains, reduced plan variability

and error reduction. Monaco version 6.0.1 (Elekta Inc. Atlanta, Georgia) has been released with a licensed scripting module accessed using an application program interface (API). A three-day Monaco scripting workshop was developed in-house for training Monaco scripting with the intent of being able to support automated planning within the clinic.
Method The three-day course covered essentials for becoming a competent Monaco scripter. At the end of the course the scripter was able to: 1. Work with the Monaco scripting API and Microsoft Visual Studio Version 16.11.16, 2. Import, load, and plan both prostate and head and neck plans, 3. Create data input forms, 4. Be able to import, export and manipulate planning data, and 5. Recursively optimize treatment plans based on planning criteria.
Results An initial cohort of 3 staff were trained, with all being able to achieve the workshop objectives for training proficiency.
Conclusion A three-day dedicated scripting workshop was created and delivered with the recipients being able to implement Monaco scripts that could support treatment planning automation.
Disclosures Genesiscare would like to acknowledge Elekta for an alpha agreement for scripting in Monaco 6.0.1

P40. User experience of remote TEAP supervision using instant messaging applications

Christopher Colyer[1,*], Manuel Carrillo-Serrano[2]

[1]Genesiscare, Kurralta Park, Australia, [2]Genesiscare, Murdoch, Australia

Introduction In radiotherapy departments treating patients takes priority over educational activities, such that there is little access to both machines and TEAP supervisors at reasonable times and scheduling practical activities can be extremely challenging. To further complicate matters, the COVID-19 pandemic forced registrars off-site for lengthy periods of time and emphasised working alone to minimise the risk of losing multiple staff members simultaneously. Mobile devices with high quality cameras are commonplace nowadays and instant messaging applications are mainstream. Our department already used the WhatsApp instant messaging application for urgent communication, such that using this for direct registrar-supervisor was natural.
Method This work uses a case study approach to observe the experiences the supervisor and registrar had in conducting activities over instant messaging, to generate an in-depth understanding of this interaction in a real-life context.
Results Remote support from supervisors allowed the registrars to take responsibility for their work and gain independence. It may also strengthen their practical knowledge as registrars are encouraged to troubleshoot before consulting remotely. Registrars also gain confidence using equipment because they use it independently rather than observing others. Conversely, remote support may take longer because it requires the supervisor to be connected through the application, receive the information, and assess the registrar's questions with the help of videos and photos rather than observing the processes live. Some items may be missed because the supervisor cannot observe the full setup, however this is also an opportunity for the registrar to view the work holistically, understand the source of errors and formulate an explanation to the supervisor.
Conclusion This paper demonstrates the usefulness of instant messaging applications for providing remote TEAP supervision. As with other forms of distance education, the success of this approach is ultimately a combination of the registrar's attitude and the supervisor's mindset.

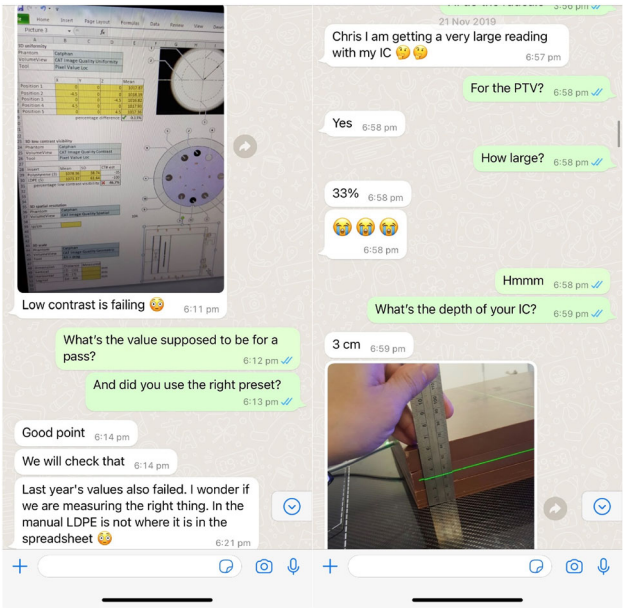

Fig. 1. Examples of registrar-supervisor interaction.

P41. Into the oblique: ExacTrac training for physicists and radiotherapists

Eireann Cosgriff[1,*], Alannah Kejda[2], Emma Sullivan[1], Rachel Stensmyr[1], Catherine Owen[1], Vanathy Manivasahan[1], Katrina West[3]

[1]Crown Princess Mary Cancer Centre, Westmead, Australia, [2]Royal North Shore Hospital, St Leonards, Australia, [3]Icon Group, Concord, Australia

Introduction Typical orthogonal pair two-dimensional kilovoltage images are readily understandable and provide recognisable visual information for correcting patient setup before radiotherapy. The image pairs provided by the ExacTrac™ system are acquired at oblique angles and are slightly more difficult to interpret. Matching to digital reconstructed radiographs also proceeds via automatic algorithm that requires human assessment or intervention before suggested couch moves are actioned. The major benefit of the ExacTrac system is the ability to image when a rotation is applied to the treatment couch as is common for cranial stereotactic radiosurgery treatments. Margins for these treatments are 1–2 mm and accurate patient positioning is paramount especially in single-isocentre multi-target treatments. System-specific training is essential for treatment staff to operate confidently and physicists to provide trouble-shooting advice.
Method A working group including physicists and radiotherapists was formed to improve ExacTrac training of treatment staff. A competency-based system in line with that currently in use in the department for cone-beam computed tomography image-guided radiotherapy training was created. The first stage involves the completion of an in-house, web-based moodle covering an introduction to stereotactic radiosurgery planning, the ExacTrac system components, and the basics of the matching algorithm. The second stage includes a session on an offline ExacTrac workstation with two trainers to guide the trainee through the software and demonstrate common problems through discussion of four training patients. The third stage involves

observation on the treatment console for a minimum of three patient treatments.
Results Over approximately 24 months, more than 25 radiotherapists and five physicists completed the training program. Training was hampered by restrictions in place during COVID outbreaks and related staff shortages.
Conclusion The implementation of a three-stage, competency-based assessment training program has proven beneficial to increasing staff knowledge and use of the ExacTrac system.

P42. Evaluation of continued professional development events: format, benefits and outcomes

Zoe Moutrie[1,*], Erin Seymour[2], Emma Dyce[3], Joel Poder[6,9], Alison Gray[1,4,5], Johnson Yuen[6], Laurel Schmidt[6], Ben Archibald-Hareen[7], Annette Haworth[8]

[1]South Western Sydney Cancer Services, NSW Health, Sydney, Australia, [2]Central Coast Cancer Centre, NSW Health, Gosford, Australia, [3]GenesisCare Victoria, East Albury, Australia, [4]Ingham Institute for Applied Medical Research, Liverpool, Australia, [5]South Western Sydney Clinical School, University of NSW, Sydney, Australia, [6]St George Hospital Cancer Care Centre, NSW Health, Kogarah, Australia, [7]Icon Cancer Centres, Sydney, Australia, [8]Institute of Medical Physics, University of Sydney, Sydney, Australia, [9]Centre for Medical Radiation Physics, University of Wollongong, Wollongong, Australia

Introduction Continuing professional development (CPD) is a career-long process where professionals build on existing knowledge and develop skills. Additional benefits of CPD include building relationships and networks for future collaboration. The Australasian College of Physical Scientists & Engineers in Medicine (ACPSEM) facilitates collaboration and professional development via special interest groups (SIG) and 6 regional branches. This work assessed whether there have been improved benefits to the ACPSEM membership with the increased utilisation of virtual CPD events organised by volunteers.
Method The attendance rates at over 30 CPD events hosted by the NSW/ACT branch and Medical Image Registration SIG (MIRSIG) were analysed. The following factors were compared: locality, attendee profession; notable outputs, opportunities for collaboration and networking. Member satisfaction surveys [1] were analysed to understand the desire for development opportunities and the formats that would provide the most benefit to the membership.
Results Virtual events were cost neutral to SIGs and branches and as a result are offered to members at no cost, unlike in person events which often attract overhead costs. In-person events were attended on average by 84 ± 38 compared to 130 ± 47 members for virtual. Virtual events had attendees from across Australia and New Zealand whereas in-person events were not as well attended by members outside the region where the event was hosted. In-person events have translated to consensus guidelines and the formation of needed special interest groups. Virtual events have resulted in current status publications [2].
Conclusion Virtual events are cost effective, promote inclusivity and provide improved access to regional members. Although networking opportunities may be limited, lively discussion panels, publications from surveys and reaching consensus is still achievable. Virtual events should continue to be utilised in addition to in-person events, as they have been shown to be popular and beneficial to the ACPSEM membership.
References

1. Barber, J, Vial P, White P. et al. (2017) A survey of modulated radiotherapy use in Australia & New Zealand in 2015. Australas Phys Eng Sci Med 40**:**811–822. https://doi.org/10.1007/s13246-017-0590-y
2. Pudsey L, Haworth A, White P. et al. (2022) Current status of intra-cranial stereotactic radiotherapy and stereotactic radiosurgery in Australia and New Zealand: key considerations from a workshop and surveys. Phys Eng Sci Med 45**:**251–259. https://doi.org/10.1007/s13246-022-01108-4

P43. Establishing a new and early career special interest group within the ACPSEM

Naasiha Cassim[1,*], Emily Simpson-Page[1]

[1]Royal Brisbane And Women's Hospital, Brisbane, Australia

Introduction A vital component of succession planning for any workforce is to support and nurture its early career members. A workforce survey in 2020 [1] indicated that many early career members were interested in expanding their skillset. Similarly, through informal discussions within the workforce it was found that there was also an interest to create a membership group for newly joined and early career members of the ACPSEM workforce. The purpose of the group was to support and nurture the professional development and enthusiasm of members, diversify career experience and foster networking among NESIG members and experienced members of the ACPSEM. With this in mind, the foundation of NESIG was laid.
Method NESIG was first established in 2021 through informal discussions with many ACPSEM members throughout Australia and New Zealand. A draft proposal of the group was created indicating the motivation behind establishing such a group. Once the foundation of NESIG was established, the Terms of Reference for the group was drafted to highlight the groups objectives.
Results NESIG was formalised into an official ACPSEM special interest group with support from the ACPSEM office and contributions from many ACPSEM members with experience ranging from less than a year to over 20 years. A leadership committee was appointed in 2022 to carry out the roles, responsibilities and missions of the newly found group.
Conclusion The new and early career special interest group, colloquially known as NESIG, was established to bring young and early career members of the ACPSEM workforce together. The journey through early career training and beyond can be a challenging process. Therefore, NESIG aims to support members through such transitions and facilitate collaboration, foster professional development and generally provide a safe and supportive environment for NESIG members within the ACPSEM workforce.
References

1. 1. Crowe S, Aland T, Fog L et al. (2021) Report of the ACPSEM radiation oncology medical physics workforce modelling project task group. Phys Eng Sci Med 44:1013–1025. https://doi.org/10.1007/s13246-021-01078-z

P44. Motion management of liver SBRT treatment: a local procedure incorporating all available techniques

Roger LI[1,*]

[1]Genesiscare Victoria, Melbourne, Australia

Introduction A SBRT liver treatment procedure combining all the available technologies locally has been developed to manage inter and intra-fractional motion for liver treatment. The challenge was not lacking technologies, rather how to incorporate available tools to develop an efficient and effective treatment procedure resulting in the best outcomes.
Method In preparation for the development of the SBRT liver treatment procedure, physics commissioning includes: 1. CT protocol for liver scans with IV contrast. 2. Varian RPM system on both CT simulation and treatment machines. 3. 4D CBCT and Gated CBCT on Varian machine. 4. Triggered imaging on fiducial markers. 5. AlignRT surface guided system. Expiration breath hold is used through CT simulation and treatment delivery using Varian RPM system.At CT simulation, the SmartPrep function in GE CT allows real-time monitoring of IV contrast enhancement in the area of interest and acquisition of no contrast images and IV contrast images. At treatment, AlignRT surface guided technique is used to manage intra-fractional motion. Triggered imaging takes verification images during the dose delivery to verify the lesion position by matching fiducial markers implanted in the target area to further reduce intra-fractional motion. Free breathing procedure has also been investigated for patients who have difficulty to perform expiration breath hold. The efficiency of the free breath procedures has been assessed using the factor:

$$\text{Duty cycle} = \frac{\text{Gated beam on time}}{\text{Gated beam on time + ungated time}}$$

Results A liver SBRT treatment procedure combining all the technologies available at local radiotherapy centre has been developed and implemented. The efficiency of breath hold techniques versus free breathing in CBCT imaging procedures is shown in the table 1.
Conclusion Expiration breath hold for liver cancer treatment allowing patients to proactively involve in the imaging and treatments, can significantly improve the efficiency of the procedures. It takes multidisciplinary efforts and expertise to ensure all the available technologies are used in a most efficient and effective way by designing a unique procedure to the centre.
Acknowledgements: I would like to thank the stereotactic team at GenesisCare Victoria to share their experience and expertise in developing a local SBRT liver treatment procedure.

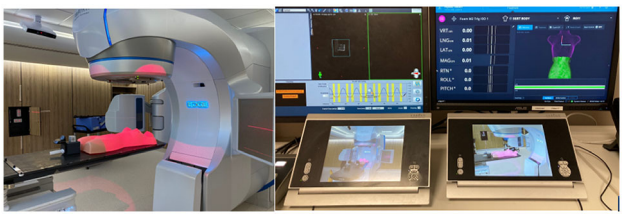

Fig. 1. Varian Edge, RPM gating and AlignRT.
Table 1. Time required for CBCT modes.

Acquisition Type	Breathing	Thresholds	Time of Acquisition (approximate)
CBCT	Breath hold		1:00 min
4D CBCT	Free breathing	10 Phases	2:00 min
Gated CBCT	Free breathing	Phase 40–60%	6:58 min

P45. Testing of SGRT tolerance limits using the HexaMotion with the ArcCHECK

Anthony Venning[1,*], Brett Waller[1]

[1]Mid North Coast Cancer Institute, Port Macquarie, Australia

Introduction Our centre installed the C-RAD surface guided radiation therapy (SGRT) system in 2020. We frequently use the system for treatments such as breast, lung, and liver SABR under deep inspiration breath hold (DIBH) conditions [1,2]. The tolerance window for breath hold is 4 mm and it is critical that we assess these tolerance limits to ensure the correct treatment is delivered.
Methods Our centre has the 6DoF HexaMotion® and ArcCHECK®. The HexaMotion was modified in-house to facilitate cradling the ArcCHECK and used to simulate in-hale and ex-hale patient breathing motion. A simple static rectangular breast treatment field was created in Monaco® on a virtual ArcCHECK phantom, and then delivered to the ArcCHECK under typical DIBH breathing conditions. The ArcCHECK acquired measurement was compared against the treatment plan created in Monaco using the Patient™ software gamma scoring system.
Results Below is the breathing trace used showing the tolerance levels where the machine went into beam hold as the ArcCHECK moved in and out of the specified tolerance limits. Both the upper and lower breath hold levels were tested. Using the ArcCHECK to measure the delivered plan on a dynamic phantom, the gamma pass rates were 98.8% at 3%/3 mm and 91.4% 2%/2 mm.
Conclusions Using the HexaMotion and ArcCHECK together is a useful tool for the clinical physicist when testing the upper and lower tolerance limits of an SGRT system. It is critical to the treatment delivery and patient outcome that these limits are correctly observed. Regular dynamic testing is an essential component of an SGRT system, which we strongly recommend is performed by the clinical physicist.
References

1. 1. Willoughby T, Lehmann J, Bencomo J, et al. (2012) Quality assurance for nonradiographic radiotherapy localization and positioning systems: Report of Task Group 147.
2. Al-Hallaq H, Cerviño L, Gutierrez et al. (2021) AAPM task group report 302: Surface- guided radiotherapy.

Fig. 1. ArcCHECK simulation delivery in DIBH breathing mode.

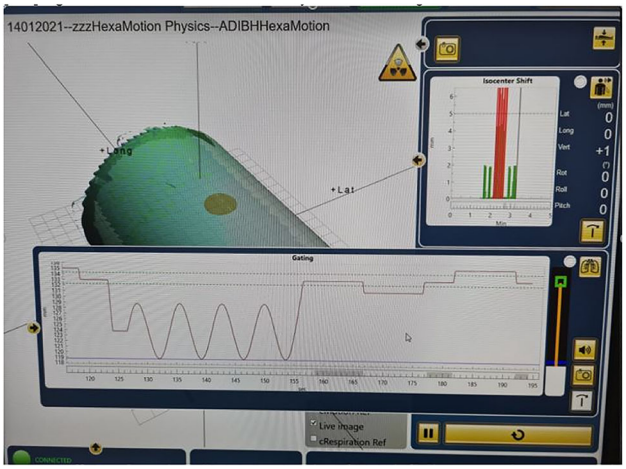

Fig. 2. ArcCHECK measurement in DIBH mode testing upper and lower tolerance limits.

P46. Commissioning of the PTW Octavius 1600 SRS™ array

Jaysree Ukath[1,*], Akash Mehta[1], Ben Perrett[1], Venkatakrishnan Seshadri[1], Prabhakar Ramachandran[1]

[1]Radiation Oncology Department Princess Alexandra Hospital, Woolloongabba, Australia

Introduction The Octavius 1600 SRS™ array has 1521 liquid-filled ionisation chambers spread over 15 cm × 15 cm area with a central high-density area with spacing of 2.5 mm and outer region with 5 mm. The PTW Octavius 1600 SRS™ [1] array has been commissioned for patient-specific quality assurance of SBRT plans.
Methods The array was characterized for dose linearity, dose rate dependence, reproducibility, uniformity and patient specific measurements in 6X and 6FFF beams [2]. The cross-calibration value was also determined independently using a Semiflex chamber and PinPoint 3D in the Octavius 4D phantom. The effect of cross calibration field size on QA results was also characterized.
Results The maximum variation of output of dose linearity was found to be 1.3% (2 MU) and 1.27% for (5 MU), for 6X and 6FFF beams respectively. For 6X beams, dose rate dependence was within ± 0.35%, and the array demonstrated maximum variation of 1.32% for 6FFF. In terms of reproducibility, the maximum variation was 0.36% for 6xFFF 15 × 15 field and 0.11% for 6X, 4 cm x 4 cm. The array was also tested for uniformity and leakage and was found to meet specifications. PSQA results was performed on a cohort of 20 SBRT plans that had been measured with Octavius 1000 SRS array. The results were found to be comparable.
Conclusion The Octavius 1600 array is found to be stable and consistent in its response to dose. Patient-specific type QA tests compared against the Octavius 1000 SRS have shown that the device is suitable for VMAT patient measurements.
References

1. OCTAVIUS Detector 1600 SRS—PTW Freiburg GmbH. (2022). Retrieved 12 July 2022, from https://www.ptwdosimetry.com/en/products/octavius-detector-1600-srs/
2. Benedict, Stanley H et al. "Stereotactic body radiation therapy: the report of AAPM Task Group 101." Medical physics vol. 37,8 (2010): 4078–101. https://doi.org/10.1118/1.3438081

P47. Commissioning of the Sun Nuclear™ advanced electron density phantom

Jaysree Ukath[1], Akash Mehta[1], Ryan Motley[1], Venkatakrishnan Seshadri[1], Ben Perrett[1], Sau Fan Liu[1], Peta Hanlon[1], Prabhakar Ramachandran[1]

[1]Radiation Oncology Department, Princess Alexandra Hospital, Woolloongabba, Australia

Introduction The Advanced Electron Density phantom (AEDP) is designed by Sun Nuclear corporation for conversion of CT numbers to electron density values. It comes with 16 inserts with 14 solid and 2 true water containers. The phantom has a large volume for body protocols and a smaller insert for head protocols. The phantom has an extended length to approximate full scatter conditions within a patient. This also facilitates use with kV CBCT. This phantom was commissioned for CT to ED conversions and annual QA purposes.
Methods Measurements were performed using five different configurations of inserts in the phantom. Each set was scanned with five departmental protocols (head & neck, pelvis, abdomen, chest, leg). For each set, an average HU of each rod for different protocol was calculated and compared with legacy phantom data (scanned using the Gammex 467 Tissue Characterisation Phantom). Data analysis was performed using the Sun Nuclear RapidCheck software.
Results CT to ED graph were compared for all phantom configurations and scan protocols. As the electron densities of rods were different between new and the old phantom, the HU values were interpolated. The maximum HU difference was calculated to be 62.5 HU for inner bone. The rest of the inserts had less than 30 HU difference.
Conclusion The advanced phantom is easy to setup with adjustable base. RapidCheck identifies scanned rods automatically and enables automated table completion. It also corrects for any discrepancies in the phantom position [1]. The AEDP phantom has been successfully used for clinical and annual QA purposes and approximates patient anatomy more closely.
References

1. Advanced Electron Density Phantom (Gammex™ Technology)—Sun Nuclear. Sunnuclear.com. (2022). Retrieved 15 July 2022, from https://www.sunnuclear.com/products/advanced-electron-density-phantom.

P48. The impact of magnetic field on ArcCHECK® density determination

Urszula Jelen[1], Katrina Biggerstaff[1], Valery Peng[1], Amrinder Chhabra[1], Aaron Fetin[1], David Waterhouse[1], Michael Jameson[1]

[1]Genesis Care, Sydney, Australia

Introduction For use within Monaco® treatment planning system (v5.51, Elekta AB, Sweden), the density assignment for the ArcCHECK® (Sun Nuclear, USA) device has to be determined via exit/entrance dose ratio measurement and should result with values between 1.14 and 1.16 [1]. This method has been applied to two MR-compatible ArcCHECK devices available at our institution for two MR-linacs (MRLs) and yielding 1.18 (AC1) and 1.25 (AC2). The latter result, being significantly outside of the manufacturers recommendation, prompted the present investigation of the diode angular response correction and its effect on density determination.
Method Measurement datafiles for 1010 cm^2 fields acquired with the two MR-compatible ArcCHECK units used clinically and with three

other MR-compatible units (AC3-AC5) used at either of the two MRLs (with $TPR_{20,10}$ agreeing within 0.9%) have been analysed. Factory array calibrations have been used for all devices.

Results The difference in the derived density for AC2 was due to the relatively lower response (-9.5%) of the diodes on the beam exit side (Fig. 1, top), i.e. irradiated at 180° angle, and was shown to be gantry direction independent and reproducible regardless of the device rotation. Compared to AC1, the relative dose profiles showed a good agreement of the relative exit doses for AC3 (-0.5%) and a lower response for AC4 (-4.9%) and AC5 (-5.2%) (Fig. 1, top). Without the angular corrections applied, the exit doses differences were slightly larger for unit AC3 (-1.6%) and AC4 (-6.8%) but smaller for unit AC2 (-7.1%) and AC5 (-3.2%) (Fig. 1, bottom).

Conclusion Magnetic field and diode angular corrections applied to the collected signal for the diodes at beams exit (irradiated at 180°) may lead to lower recorded exit doses and affect the entrance/exit ratio based density determination and, as consequence, patient specific QA (e.g. point dose calculations).

References

1. ArcCHECK Density, Application Note #05–12, Sun Nuclear corporation.

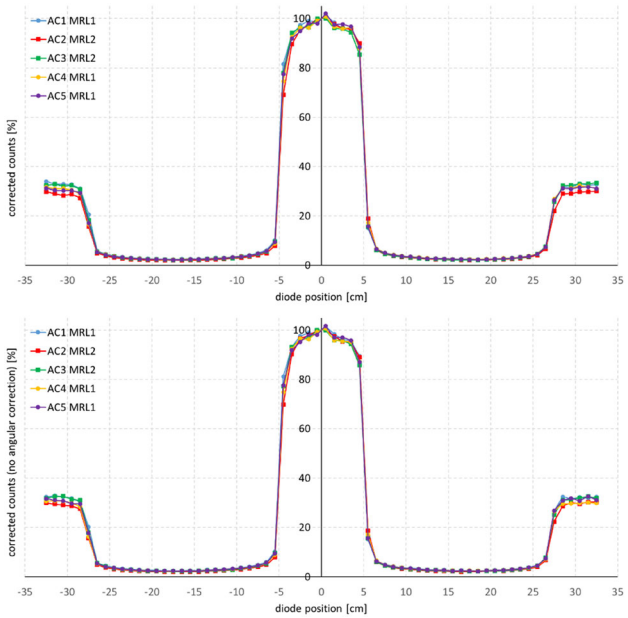

Fig. 1. Comparison of the relative diode responses with (top) and without (bottom) angular corrections applied, demonstrating how the angular corrections bring the profiles for devices AC1, AC3 and AC4 to better agreement, while recorded exit doses for devices AC2 and A5 remain 5–10% lower.

P49. Abstract withdrawn

P50. Application of statistical process control methods in the retrospective review and design of patient-specific quality assurance processes

Scott Crowe[1,2,3], Liting Yu[1,3], Samuel Peet[1,3], Tanya Kairn[1,2,3]

[1]Royal Brisbane & Women's Hospital, Herston, Australia, [2]University of Queensland, St. Lucia, Australia, [3]Queensland University of Technology, Brisbane, Australia

Introduction Pre-treatment patient-specific quality assurance (PSQA) measurements are frequently performed for intensity-modulated treatments, and statistical monitoring of the PSQA results across patients is recommended as best practice [1]. Similarly, when new technologies or techniques are introduced, a statistical analysis of PSQA results for a cohort of test plans is recommended to establish appropriate tolerance limits. In response to the introduction of new treatment and QA technologies within our department, retrospectively and prospectively calculated PSQA results were reviewed and analysed with statistical process control methods, to inform future practice.

Method In-house Python code was developed to retrospectively extract gamma evaluation data from PSQA reports generated using PTW Verisoft. This data was reviewed for process inconsistencies using histograms and control charts, and tolerance limits and process performance indices were calculated. Subsequently, these approaches were used for newly generated data, including gamma analysis pass rates calculated using multiple pairs of gamma criteria, for past patient PSQA results, and for treatments optimised for delivery on two new treatment systems, the Varian Edge and Accuracy Radixact.

Results Variations in reporting of gamma results were identified for historical plans, leading to a more consistent approach to both reporting and investigation of out-of-tolerance results. The results of control chart assessment resulted in the adoption of new gamma criteria and tolerance limits, following discussion within our physics group. Calculated process performance indices indicated that the treatment planning and PSQA process could reliably produce results within tolerance.

Conclusion Statistical process control tools including histograms and control charts facilitated quantitative review of historical PSQA data and allowed determination of suitable tolerance limits. Future work will include development of universal action limits based on sensitivity and specificity of PSQA processes to clinically relevant dose delivery errors, and the application of statistical process control tools at a site-specific level.

References

1. Miften M, Olch A, Mihailidis D, Moran J, Pawlicki T, Molineu A, Li H, Wijesooriya K, Shi J, Xia P, Papanikolaou N, Low DA (2018) Tolerance limits and methodologies for IMRT measurement-based verification QA: Recommendations of AAPM Task Group No. 218. Med Phys 45:e53–e83. https://doi.org/10.1002/mp.12810

P51. Dosimetric impact of tumour rotation during real-time adaptive prostate stereotactic body radiation therapy

Chandrima Sengupta[1], Simon Skouboe[2], Thomas Ravkilde[2], Per Poulsen[2], Doan Trang Nguyen[1], Ricky O'Brien[1], Jeremy Booth[3], Peter Greer[4], Trevor Moodie[5], Nicholas Hardcastle[6], Amy Hayden[5], Sandra Turner[5], Shankar Siva[6], Keen-Hun Tai[6], Jarad Martin[4], Paul Keall[1]

[1]ACRF Image X Institute, Sydney, Australia, [2]Aarhus University Hospital, Aarhus, Denmark, [3]Royal North Shore Hospital, Sydney, Australia, [4]Calvary Mater Newcastle, Waratah, Australia, [5]Crown Princess Mary Cancer Centre, Sydney, Australia, [6]Peter MacCallum Cancer Centre, Melbourne, Australia

Introduction In prostate stereotactic body radiation therapy (SBRT), intra-fractional tumour motion deteriorates the planned dose distribution [1]. So far, most of the major advances have focussed only on one aspect of tumour motion, translation. However, significant intra-fractional tumour rotation has been observed for prostate. The dosimetric impact of prostate rotation is not well understood yet. In this study, we quantified the dosimetric impact of prostate rotation for 32 prostate cancer patients treated on TROG SPARK trial [2].
Methods The motion-induced dose was reconstructed including intra-fractional dynamic (a) translation and rotation and (b) translation measured with a 6 degrees-of-freedom (DoF) tumour motion monitoring technology [3]. Patients received 7.25 Gy in each fraction over 5 fractions. Intra-fractional translation was corrected using a gating strategy and the residual translation is denoted as T_{res}. Intra-fractional rotation (R) remained uncorrected. The dose differences from the planned dose including 6DoF motion ($\Delta D(T_{res} + R)$) and including 3DoF motion ($\Delta D(T_{res})$) were determined for clinical target volume (CTV) D98, planning target volume (PTV) D95, bladder V6Gy and rectum V6Gy. Residual dose error due to uncorrected rotation was determined as: $\Delta D(T_{res} + R)$-$\Delta D(T_{res})$.
Results $\Delta D(T_{res})$ was always within 5% of the planned dose for all four organs for all patients. $\Delta D(T_{res} + R)$ was within 5% for CTV for all patients, however was $> 5\%$ in one fraction for PTV, in one fraction for bladder and in 5 fractions for rectum(Fig. 1).
Conclusions The dosimetric impact of tumour rotation on a large prostate cancer patient cohort was quantified in this study. These results suggest that the standard CTV-PTV margin was sufficient to account for the intra-fractional prostate rotation, provided an appropriate gating threshold was applied to correct for translation. Residual dose errors due to uncorrected prostate rotation were small in magnitude which may be corrected using different treatment adaptation strategies to further improve the dosimetric accuracy.
References

1. Keall PJ, Nguyen DT, O'Brien R et al. (2020) Real-Time Image Guided Ablative Prostate Cancer Radiation Therapy: Results From the TROG 15.01 SPARK Trial. Int J Radiat Oncol Biol Phys 107:530–538. https://doi.org/10.1016/j.ijrobp.2020.03.014
2. Keall P, Nguyen DT, O'Brien R. et al. (2017) Stereotactic prostate adaptive radiotherapy utilising kilovoltage intrafraction monitoring: the TROG 15.01 SPARK trial. BMC Cancer 17:180. https://doi.org/10.1186/s12885-017-3164-1
3. Hewson EA, Nguyen DT, O'Brien R et al. (2019) The accuracy and precision of the KIM motion monitoring system used in the multi-institutional TROG 15.01 Stereotactic Prostate Ablative Radiotherapy with KIM (SPARK) trial. Med Phys 46:4725–4737. https://doi.org/10.1002/mp.13784

P52. Abstract withdrawn

P53. IGRT setup residual errors for linac based Neuro SRS

Jeremy Hughes[1], [1]Micah Barnes, David Taylor[1], Phillip Tai[1,*], Glen Osbourne[1], Karen McGoldrick[1], Kenton Thompson[1], Derrick Wanigaratne[1]

[1]Peter Maccallum Cancer Centre, Melbourne, Australia

Introduction Stereotactic Radiosurgery (SRS) has been commissioned at Peter MacCallum Cancer Centre using Varian Truebeams with on board imaging/Cone beam CT (CBCT) IGRT and 6 degree of freedom (6DOF) couch. CBCTs are taken at Couch 0° and MV-kV paired imaging are used for positioning at Couch 45°/315°. The patient is immobilised in a Freedom X system (CDR Systems, CA, Canada) in a closed face mask. More recently surface monitoring has been integrated into SRS treatments which requires the patients are treated with open face masks. An in-depth analysis of image and positioning shifts was undertaken to compare the immobilisation of the two mask setups.
Method A total of 22 SRS treatments were analysed as a part of this study, 12 closed and 10 open face masks. The shifts and registration proposed shifts were recorded for each patient. If these shifts were above the threshold 0.05 cm, they would be repositioned and a verification image would be taken. Patient positioning was also replicated on an anthropomorphic phantom, STEEV.
Results The vector of the image registration of the verification images captures how well the system positions and immobilises the patient. The image registration vector for verification MV-kV images for closed face mask patients, open face mask patients, and replicated on a phantom can be seen in Fig. 1. For closed face masks, Average: 0.05 cm, standard deviation: 0.02 cm. For open face masks, Average: 0.06 cm, standard deviation: 0.04 cm. For phantom setup, Average: 0.02 cm, standard deviation: 0.01 cm.
Conclusion Patient motion contributed significantly to the residual setup error. Patient immobilisation is patient dependent. However generally the closed face mask immobilised patients more than the open face mask.
Acknowledgements: We would like to thank Elena Ungureanu, Adam Yeo, Atousa Montaseri, Nick Hardcastle, and Tomas Kron for their insight and knowledgeable discussion.

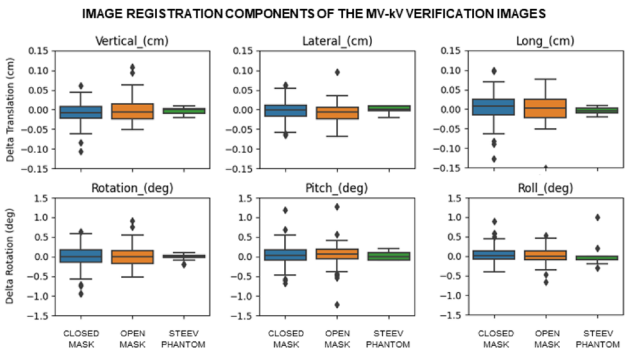

Fig. 1. The registration vector (cm) of MV-kV imaging after patient repositioning for patients with closed face masks (n = 63), open face masks (n = 43), and replicated on a phantom delivery (n = 12). Normalised frequency.

P54. Abstract withdrawn

P55. Evaluation of coplanar vs non-coplanar SRS and SRT plans for multiple brain metastases

Sergei Zavgorodni[1,2,*], Evan Maynard[3], Isabelle Vallieres[1]

[1]BC Cancer Agency, Victoria, Canada, [2]University of Victoria, Victoria, Canada, [3]BC Cancer Agency, Prince George, Canada

Introduction Linac-based SRT can be delivered with single-isocentre VMAT using coplanar as well as non-coplanar arcs. Non-coplanar treatments are expected to improve plan quality but this comes at the cost of increased workload in planning, QA, and delivery. These treatments also have increased image guidance requirements and can introduce additional patient positioning errors. Therefore, non-coplanar arcs would ideally be used in cases where plan quality

improvement outweighs associated overheads, and this study was aimed to determine predictors for such scenario. Potential predictors included the number of metastases, PTV size, and the proximity of PTVs to each other.

Method Thirty-one previously treated SRS and hypo-fractionated SRT coplanar plans were re-planned using non-coplanar arcs. A plan quality index (PQI) was developed and used to compare coplanar and non-coplanar treatments. This index was derived from retrospective analysis of 127 clinical plans previously delivered at our institution, and is comprised of conformity index, gradient measure, V20% and number of MUs delivered.

Results Our retrospective analysis has shown that PQI for non-coplanar plans improved in 77% (24/31) of all considered cases. The superior plan quality was primarily achieved due to reduction of the gradient measure, which reduced by 1.0 mm [95% CI 0.7, 1.4] on average. Plans with a larger average PTV diameter ($\geq$ 1.3 cm) saw the greatest improvement, while plans which became worse or showed no improvement tended to have smaller targets. When plans had a small number of targets ($<$ 5) the average V20% decreased for non-coplanar plans by 38 cc [95% CI 13, 62] but when the number of PTVs was large ($\geq$ 5), V20% increased by 62 cc [95% CI 22, 101].

Conclusion Patients with targets larger than 1.3 cm in diameter and with fewer than 5 targets were identified as more likely to receive a significant benefit from non-coplanar treatments.

P56. Abstract withdrawn

P57. Feasibility study: Replacing stereotactic cones with a fixed MLC field dynamic arc on Elekta and Varian linacs

Peter Mc Loone[1], Leon Dunn[1], Luis Muñoz[1]

[1]GenesisCare, Alexandria, Australia

Introduction Stereotactic cones have proven to be useful for the treatment of very small intracranial targets [1]. High definition multileaf collimators (MLC) has allowed the delivery of fields that can achieve similar dosimetric characteristics, when compared to small diameter cones [2–5]. Using a combination of both the Monaco (Elekta AB, Stockholm, Sweden) and Eclipse (Varian Medical Systems, Palo Alto, CA) treatment planning systems (TPS) a solution can generated for both vendor's linacs.

Method Fields were generated in Monaco 6.0.1 using 5 couch positions, 2 collimator angles with 90-degree separation and fixed MLCs and jaws depending on the virtual cone size desired. The fields were inversely optimised allowing for variable spaced and weighted control points. For Elekta linacs plans a dose distribution with similar characteristics to a physical 7.5 mm cone were generated with the jaws fixed to 6 mm and the MLCs at 3 mm. For Varian linacs an initial plan was generated in Monaco, the jaws were adjusted in Eclipse and the plan recalculated using both the AAA and Acuros beam model. The MLCs were fixed to 2.1 mm and the jaws to 5 mm to produce a dose distribution like a 5 mm cone. Plans were delivered to a phantom and analysed to check deliverability.

Results A Monaco generated virtual cone plan and the profiles, Fig. 1, and dosimetric characteristics, Table 1, were compared to a 7.5 mm cone for an Elekta linac. With the combination of Monaco and Eclipse a dose distribution was generated that showed good agreement with a 5 mm Varian cone. All plans delivered will high passing gamma rates above 95% for 3%/1 mm.

Conclusion Using an inverse planning technique in Monaco a dose distribution was generated using MLCs comparable to a 7.5 mm and 5 mm cone plan for an Elekta and Varian linac respectively. The plans were delivered on the linacs and showed good gamma passing rates.

References

1. Shukaili, K.A., et al., Characterization of ELEKTA SRS cone collimator using high spatial resolution monolithic silicon detector array. Journal of applied clinical medical physics, 2018. 19(4): p. 114–124.
2. Popple, R.A., et al., The virtual cone: A novel technique to generate spherical dose distributions using a multileaf collimator and standardized control-point sequence for small target radiation surgery. Advances in radiation oncology, 2018. 3(3): p. 421–430.
3. Brezovich, I.A., et al., Stereotactic radiosurgery with MLC-defined arcs: Verification of dosimetry, spatial accuracy, and end-to-end tests. Journal of applied clinical medical physics, 2019. 20(5): p. 84–98.
4. Brown, T.A., et al., Determination of commissioning criteria for multileaf-collimator, stereotactic radiosurgery treatments on Varian TrueBeam and Edge machines using a novel anthropomorphic phantom. Journal of Applied Clinical Medical Physics, 2022: p. e13581.
5. Brown, T.A., R.G. Ayers, and R.A. Popple, Commissioning a multileaf collimator virtual cone for the stereotactic radiosurgery of trigeminal neuralgia. Journal of Applied Clinical Medical Physics, 2022. 23(5): p. e13562.

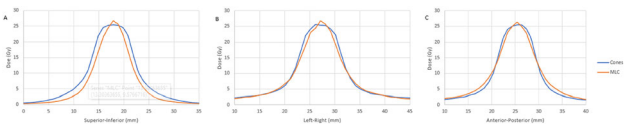

Fig. 1: Profiles for 7.5 mm Cone versus Virtual Cone dose distribution with 3 mm MLC gap in Monaco for (A) Superior-Inferior, (B) Left–Right and (C) Anterior-Post.

Table 1. Volume as calculated by Monaco for a 7.5 mm cone and virtual cone.

Volume	Cone/cm^3	Virtual Cone/cm^3
V50%	0.404	0.32
V25%	1.2	1.188
V10%	5.312	5.489

P58. State of the nation: a survey of NZ SABR programs

Suzanne Lydiard[1,*], Rowen de Vries[1], Sally Baker[1]

[1]Kathleen Kilgour Centre, Tauranga, New Zealand

Introduction SABR requires rigorous commissioning, on-going quality assurance, and adequate multidisciplinary expertise to ensure treatment safety. The UK NHS recommends centres treat more than 25 patients annually to ensure the SABR treatment team maintains competency [1]. RANZCR recognizes that this may not be achievable in Australasia and in the absence of large patient caseloads, encourages active collaboration and the development of regional networks to

maintain SABR quality [1]. This work aimed to conduct a survey about SABR programs within NZ to improve collaboration.
Method A survey was distributed amongst NZ Chief Physicists in October 2021, enquiring about the clinical status of SABR, patient caseloads in the past year, SABR equipment and techniques, confidence levels, and interest in further collaboration.
Results All ten NZ Radiation Oncology centres completed the survey. SABR is used to treat lung (n = 10), brain (n = 9), spine (n = 8), prostate (n = 4) and soft tissue (n = 6) cancers. Whilst all centres treated more than 25 SABR patients in the past year, Fig. 1 illustrates that many centres treated less than 25 patients for individual SABR sites. 86% and 43% of centres who provided patient numbers treated less than 10 and 5 patients respectively for a SABR site. As seen in Fig. 2, the average confidence score was lowest for contouring and highest for PSQA. All centres expressed interest in a SABR workshop and NZ inter-departmental SABR dosimetry verification to aid confidence and/or quality improvements.
Conclusion Every NZ centre utilizes SABR but patient caseloads are low. There is strong desire for further collaboration.
Acknowledgements: Thank you to the NZ Radiation Oncology centres and the ACPSEM NZ Branch for their support.
References

1. Foote, M., Bailey, M., Smith, L., et al. Guidelines for stereotactic body radiation therapy. Journal of Medical Imaging and Radiation Oncology 2015; 59: 646–653. https://doi.org/10.1111/1754-9485.12336

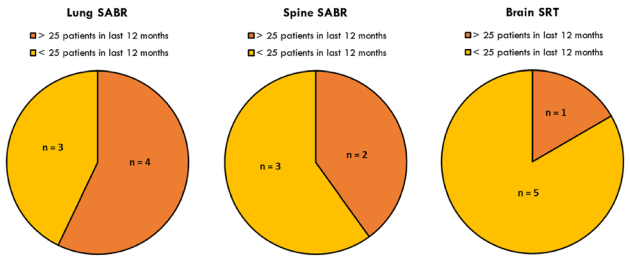

Fig. 1. Pie charts of NZ centre SABR patient numbers in the past year.

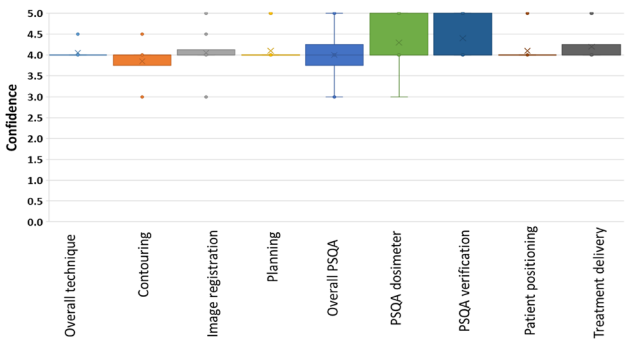

Fig. 2. Box and whisker plot of confidence levels within the SABR workflow. 1 = not confident, 2 = confident some of the time 3 = confident most of the time, 4 = confident but room for improvement, 5 = confident and no further improvements required.

P59. Patient specific quality assurance for SABR: How is NZ doing this?

Suzanne Lydiard[1,*], Rowen de Vries[1], Sally Baker[1]

[1]Kathleen Kilgour Centre, Tauranga, New Zealand

Introduction SABR treatment plans are often highly modulated to ensure the target volume is adequately treated whilst critical structures are adequately spared. Patient specific quality assurance (PSQA) to verify treatment deliverability is a critical step in ensuring efficacious SABR treatments but limitations in dosimetry equipment, detector sizes, detector resolutions, planar orientations and staff capacity can challenge this. This work aimed to better understand the SABR PSQA and film dosimetry methods currently used in NZ.
Method A survey was distributed amongst NZ Chief Physicists in October 2021, enquiring about SABR PSQA equipment, technique, processes and challenges.
Results All ten NZ Radiation Oncology centres completed the survey. SABR PSQA methods varied between centres and often within centres for different SABR anatomical sites. Seven centres performed software-based independent MU verification. All centres performed point dose measurements using ion chambers ranging from 0.007–0.13 cc. The use of film dosimetry or electronic planar measurements usually varied within a centre for SABR sites or predefined criteria, with nine centres utilizing film dosimetry and nine centres also utilizing electronic phantoms. As seen in Fig. 1, film dosimetry processes varied amongst centres. Five centres used EPID dosimetry for PSQA and two centres used EPID in-vivo dosimetry. Multiple centres mentioned a desire to replace film dosimetry with faster electronic PSQA techniques to sustain current and future SABR PSQA workloads.
Conclusion SABR PSQA and film dosimetry equipment and methods varied amongst NZ centres. There is a desire for faster SABR PSQA methods.
Acknowledgements: Thank you to the NZ Radiation Oncology centres for completing the survey.

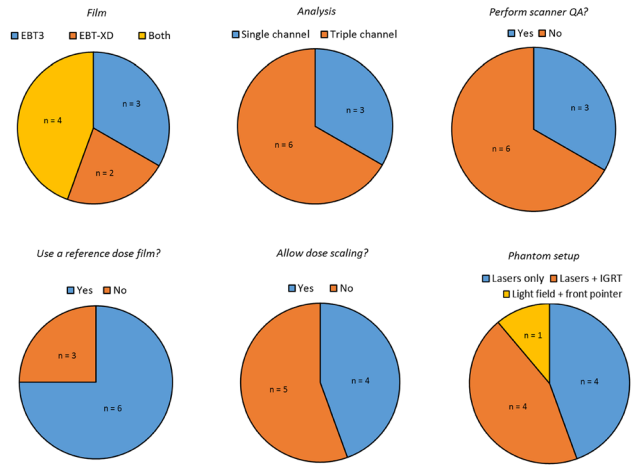

Fig. 1. Pie charts illustrating the variations in film dosimetry methods used for SABR PSQA within NZ Radiation Oncology centres.

P60. Dosimetric characterization of SRS MapCHECK under challenging static and VMAT fields

Elena Timakova[1,2,*], Sergei Zavgorodni[1,2]

[1]University of Victoria, Victoria, Canada, [2]BC Cancer Agency, Victoria, Canada

Introduction SRS MapCHECK is a high resolution dosimetry tool designed for patient specific quality assurance of stereotactic radiosurgery (SRS) treatments. In this study, the dosimetric performance, including under highly modulated VMAT fields, of SRS MapCHECK was characterized. Its performance as a small field dosimeter was also investigated.
Methods A series of static fields with varying characteristics including MLC-defined field size 0.5 × 0.5 cm^2 to 10 × 10 cm^2, off-axis distance (0 to 6 cm), energy (6MV and 10MV-FFF) and a series of VMAT fields with modulation factors 2.7–10.2 MU/cGy, designed to cover 2 cm diameter PTV, were delivered to SRS MapCHECK via Varian TrueBeam STx. The dose distributions for these fields were calculated with Eclipse AAA algorithm. Results were analyzed based on absolute dose gamma criterion of 3% dose-difference and 1 mm distance-to-agreement calculated by analysis software provided with SRS MapCHECK.
Results For static fields on-axis with field sizes 5 × 5 cm^2 down to 0.5 × 0.5 cm^2, the 3%/1 mm gamma pass rates exceeded 99% for both 6MV and 10MV-FFF energies, with the exception of 1 × 1 cm^2 field size which scored 94% for 6MV and 91% for 10MV-FFF. The lowest gamma pass rates for off-axis static fields were found to be 94% for 6MV (6 cm off-axis) and 84% for 10MV-FFF (1 cm off-axis) in the superior-inferior direction. For modulation factors below 3, all gamma pass rates were above 99%. For modulation factors between 3 and 5.5, all gamma pass rates were above 92%. For modulation factors above 5.5, only 33% of gamma pass rates were above 90% and mean gamma pass rate was 83%.
Conclusions Overall, SRS MapCHECK demonstrated excellent agreement with AAA calculated dose for static fields down to 0.5 × 0.5 cm^2 and VMAT fields with modulation factors below 3.

P61. Sensitivity of film and SRS Mapcheck to known delivery errors for SABR spine patient-specific QA

Peta Lonski[1], Jidi Sun[1], Joerg Lehmann[2,3,4], Nicholas Hardcastle[1], Mohammad Hussein[5], Catharine Clark[5,6,7], Tomas Kron[1]

[1]Peter MacCallum Cancer Centre, Melbourne, Australia, [2]Cavary Mater, Newcastle, Australia, [3]University of Newcastle, Newcastle, Australia, [4]The University of Sydney, Sydney, Australia, [5]National Physical Laboratory, London, UK, [6]University College London Hospital, London, UK, [7]University College London, London, UK

Introduction Accurate delivery is essential to the success of stereotactic ablative radiotherapy of vertebral metastases (SABR spine), characterised by high dose gradients to complex shaped targets adjacent to the spinal cord. Patient-Specific Quality Assurance (PSQA) involves measurement of a treatment plan on a suitable phantom and detector system to verify delivery prior to treatment. This work compared gamma pass rates, a common measure for comparison of plans and measurements, of two high-resolution detectors (film and SRS MapCheck) for SABR spine with known errors introduced as part of the SEAFARER study [1].
Method Known delivery errors were introduced into a SABR spine plan [1]. Twelve variations of the plan were delivered to film (axial plane) in a Perspex body Phantom 'Rod' [2] and again to the Sun Nuclear SRS Mapcheck (sagittal plane) with comparison to the original plan's dose distribution. The ability of each system to detect known errors was investigated and plan impact assessed by re-calculating on the original CT dataset.
Results Gamma pass rates for each delivery error and their corresponding clinical impact are shown in Table 1. Film measured on the axial plane detected 5 out of 9 clinically impactful (indicated in red) treatment errors using a 5%/1 mm 90% pass rate gamma criteria. The SRS MapCheck on the sagittal plane was more sensitive to delivery errors, failing 7 out of 9 plans with errors using the same criteria. MLC position errors resulted in potentially significant clinical impact, as was mixed combinations of errors. Collimator rotation errors of ± 1 degree had smaller impacts.
Conclusion Sensitivity of different PSQA tools to known delivery errors have been investigated for the purposes of SABR Spine QA. The SRS MapCheck showed higher sensitivity to treatment errors compared to film. Further work is ongoing to determine which system is appropriate for PSQA at our centre.
References

1. Lehmann, J., Hussein, M., Barry, M. A., Siva, S., Moore, A., Chu, M., … & Clark, C. H. (2022). SEAFARER–A new concept for validating radiotherapy patient specific QA for clinical trials and clinical practice. Radiotherapy and Oncology, 171, 121–128.
2. Kron, T., Ungureanu, E., Antony, R., Hardcastle, N., Clements, N., Ukath, J., … & Haworth, A. (2017). Patient specific quality control for Stereotactic Ablative Body Radiotherapy (SABR): it takes more than one phantom. In Journal of Physics: Conference Series (Vol. 777, No. 1, p. 012,017). IOP Publishing.

					Plan Impact (relative to original plan, %)	
Plan details	Film (5%/1mm)		SRSMC (5%,1mm)		PTV D90%	Spine PRV D0.03cc
Unedited	Pass	100%	Pass	100%	-	-
All MLC 0.5 mm retracted	Pass	99%	Pass	100%	2.86	6.3
Central 1 cm MLC 2 mm retracted	Pass	98%	Fail	87%	2.67	15.5
All MLC 1 mm retracted	Fail	84%	Fail	86%	5.34	14.1
All MLC 1.5 mm retracted	Fail	76%	Fail	47%	7.57	22.3
Central 1 cm MLC 5 mm retracted	Fail	67%	Fail	82%	2.72	31.3
MU reduced by 2%, coll angle -1 deg, all MLC 1 mm inwards	Pass	97%	Fail	73%	-8.42	-11.6
MU increased by 2%, coll angle +1 deg, all MLC 1 mm retracted	Fail	68%	Fail	54%	7.47	16.7
All MLC 0.5 mm inwards	Pass	99%	Pass	100%	-3.11	-5.4
All MLC 1 mm inwards	Pass	99%	Fail	93%	-6.45	-10.1
Coll angle -1 deg	Fail	89%	Pass	100%	-0.1	0.4
Coll angle +1 deg	Pass	100%	Pass	100%	0.05	-0.1

Table 1.

P62. The impact of using flattening filter-free energies on treatment efficiency for prostate SBRT

Tagreed Alalawi[1], Nesreen Shorbahi[1], Elham Rashaidi[1], Maha Alidrisi[1]

[1]King Abdullah Medical City, Jeddah, Saudi Arabia

Introduction Prostate cancer remains the second most common malignancy in men worldwide, with rising incidence particularly in developed countries. Volumetric modulation radiation therapy VMAT prostate treatment planning is done with a beam energy from 6 to 10MV. The main purpose of this study is to analyse the planning of Stereotactic Body Radiotherapy SBRT treatments for localized prostate cancer with 6FFF and 10FFF (flattening filter free) energies to see if there is a dosimetric difference between the two energies, and how we can increase the plan efficiency and reduce its complexity.
Method Two treatment plans generated for 15 patients with localized prostate cancer retrospectively using the CT planning image acquired for radiotherapy purposes. Each plan contains two/three complete arcs with two/three different collimator angle sets. The clinical target volume (CTV) consists of the entire prostate for organ-confined disease. The planning target volume (PTV) involve a margin of 5 mm. A 3-mm margin is favoured posteriorly. Organs at risk identified and contoured. The prescription dose is to deliver 35 Gy in five fraction to the PTV.

Results In terms of CI = 0.99, HI = 0.7 and GI = 4.1, it was observed that they all same for both energies 6FFF and 10FFF with no differences, but the total delivered MUs are much less for the 10FFF plans. There were no dosimetric differences between 6FFF, 10FFF in terms of PTV coverage and mean doses, the mean doses for the bladder, rectum, femoral heads, penile bulb and small bowel are collected, and they were in favor of the 10FFF. Integral doses ID in (Gy.L) were recorded for all OAR and they were lower with the 10FFF plans.
Conclusion High energy 10FFF has lower treatment time and lower delivered MUs 10FFF showed lower integral and mean doses to organ at risk. In this study, we suggest to use 10FFF beam for SBRT prostate treatment which has the advantage of lowering the treatment time and that lead to less plan complexity with respect 6FFF beams.

P63. Portal dosimetry (PDIP) for patient specific QA of Varian hyper-arc multi-met SRT

Dean Wallace[1,*]

[1]Icon Cancer Centre Mulgrave, Mulgrave, Australia

Introduction Current process for Hyper-arc stereotactic radiation therapy treatments (SRT) patient specific quality assurance traditionally requires the use of radiographic film. In this research it was investigated if the time-consuming radiographic film measurements could be replaced with the Varian portal dose image prediction (PDIP) software for Hyper-arc patient specific QA. In addition to this it was investigated if any additional machine or patient specific quality assurance tasks are required to compliment this change.
Method To assess the suitability of (PDIP) for patient specific QA with Hyper-arc the limitations of the portal dose model were identified by reviewing the current (PDIP) model against test plans & clinical plans that were delivered/treated within our departments. Modifications to the (PDIP) model was made to evaluate and investigate improvements gained in the forementioned plans.
Results The results showed a configuration limitation in the current Varian (PDIP) model for Hyper-arc treatments. However, it was identified that the major difference in gamma pass rates occurred due to predicted transmission through the MLCs by the TPS and that a reduction of the transmission factor from 0.148 to 0.1 showed improvements in the PDIP analysis for Hyper-arc. Configuration limitations and our departments jaw limitations of 3 cm x 3 cm it was noted that for PTV diameters < 1 cm often used for Hyper-arc there was difference between the TPS & (PDIP). The output factor for the 3 cm x 3 cm was changed from 0.942 to 0.952 to match the portal doses predicted output factors more accurately for PTVs < 1 cm.
Conclusion In conclusion it was shown that the Varian portal dose image prediction (PDIP) can be improved to allow for patient specific QA measurements using the (PDIP) and is comparable to radiographic film for Hyper-arc measurements using traditional SRT gamma criteria.
Table 1. Gamma results 2%/2 mm at 10% threshold for old and the new PDIP model.

Treatment Plan	Gamma Analysis (2%/2mm 10% Threshold)		
PDIP Model	Old PDIP Model		New PDIP Model
0.5cm Static MLC	73.9		95.8
0.5cm Hyper Arc Plan (Individual Arcs)	Field 1	82.2	97
	Field 2	56	89.6
	Field 3	54	89.7
	Field 4	54.9	99.6
0.5cm Hyper Arc Plan (Composite)	63.4		98.5
Clinical Hyperarc Plan (Individual Arcs)	Field 1	97.3	96.9
	Field 2	92	95.3
	Field 3	90.9	97.2
	Field 4	99.5	99.6
Clinical Hyperarc Plan (Composite)	91.3		97.5

P64. Matched linac stereotactic radiotherapy: delivery similarity and feasibility of distributive patient specific quality assurance

Simon Goodall[1,2,*], **Leon Dunn**[3], **Jonathan Dunning**[3], **Luis Munoz**[4,7], **Pejman Rowshanfarzad**[2], **Martin Ebert**[2,5,6]

[1]GenesisCare, Perth, Australia, [2]School of Physics, Mathematics, and Computing, Faculty of Engineering and Mathematical Sciences, University of Western Australia, Crawley, Perth, Australia, [3]GenesisCare, Melbourne, Australia, [4]GenesisCare, South Australia, Australia, [5]Department of Radiation Oncology, Sir Charles Gardiner Hospital, Nedlands, Australia, [6]5D Clinics, Perth, Australia, [7]Centre for Medical Radiation Physics, University of Wollongong, Wollongong, Australia

Introduction Within a clinical department patients may be treated on different linacs daily, if matched to a common set of baseline data. In addition, patient-specific quality assurance (PSQA) could be completed on any linac. Stereotactic body radiotherapy (SBRT) requires higher levels of accuracy than routine radiotherapy, consequently, linac matching should be deeply evaluated before distributive treatments or PSQA are implemented. This investigation proposed metrics for defining SBRT linac matching and assessed twelve linacs against these criteria. A potential distributive PSQA model was evaluated by reviewing rates of false PSQA results.
Method Ten SBRT spine plans were delivered by twelve matched Elekta linacs and measured using one of seven SRS MapCHECK devices. The measured dose distributions and gamma scores were evaluated across the entire dose distribution and on a detector location level.
Results Equivalent location detectors showed a range of gamma values ≤ 1.0 for 96.9%, 92.1% and 80.2% of detectors, using criteria of 3%2 mm, 3%1 mm and 2%1 mm respectively. Standard deviations were < 0.5 for 99.9%, 99.3%, and 95.7% of detectors. Dose differences showed 43.6%, 82.7%, and 91.4% of detectors had a dose range of $\leq 3.0\%$, $\leq 5.0\%$, and $\leq 6.0\%$, respectively. Standard deviations of dose differences were 1.5%, 2.5%, and 3.0% for 94.1%, 98.3%, and 99.5% of detectors, respectively. For the fleet of linacs, distributive PSQA yielded false results for 0.0%, 17.7%, and 33.0% of plans, equivalent to 1.2%, 3.5%, and 9.4% of detectors when using gamma criteria of 3%2 mm, 3%1 mm and 2%1 mm respectively.
Conclusion Linacs could be considered matched allowing a distributive treatment and PSQA program to be implemented when gamma analysis using criteria of (3%, 2 mm) was adequate. For stricter criterion PSQA and treatments should be completed on the same linac.

P65. Can a combinatorial measurement replace complete film measurement for SRT multimet patient specific QA?

Alessia Tamborriello[1,*], Leon Dunn[1]

[1]GenesisCare, Melbourne, Australia

Introduction Treating Single Isocentre Multiple Target (SIMT) cases with stereotactic radiotherapy (SRT) requires a substantial amount of patient specific QA (PSQA) to verify the geometric and dosimetric accuracy of the treatment. Radiochromic film (RCF) is commonly used to perform PSQA measurements for each lesion in the plan [1, 2, 3], however this is a time consuming and resource heavy option. This project investigates whether a combinatorial measurement with multiple detectors can replace complete film PSQA for these cases.
Methods RCF, the Sun Nuclear ArcCHECK (AC) and EPID PortalDose (PD) were used to measure an SRT treatment plan with 22 PTVs using gamma criteria of 3%/3 mm, 2%/1 mm, 1%/1 mm, 5%/1.5 mm and 5%/1 mm, respectively. The original plan was then artificially modified using Python introducing systematic MLC offsets and random variations, dose scaling and collimator miscalibrations to the plan DICOM MLC control points & fields. The PSQA results for the altered plans were compared to the original results for all measurement techniques.
Results All three detectors can determine errors in MLC systematic and random performance / calibration, dose output calibration and collimator calibration. Of course, the degree to which depends on the criteria used for determining a pass or fail. [P65] **Table 5** shows the results for AC and PD ranked according to the percentage decrease in clinical goals achieved.
Conclusion Combinatorial QA where the overall result for the plan is determined from a combination of PD/AC and RCF measurements is feasible and could reduce the pre- and post-measurement labour time by > 10 h whilst maintaining sensitivity and specificity to physical Linac performance variations. Optimised device-specific tolerances are required to maintain this sensitivity and specificity.
References

1. Popple, RA, Brown, MH, Thomas, EM, Willey, CD, Cardan, RA, et al. (2021), Transition from manual to automatic planning and delivery of volumetric modulated arc therapy stereotactic radiosurgery: clinical, dosimetric, and quality assurance results, *Practical Radiation Oncology*, vol. 11, pp. e163-e171, https://doi.org/10.1016/j.prro.2020.10.013
2. Decabooter, E, Swinnen, A & Canters, R (2019), Dosimetric verification of single isocenter VMAT for multiple brain metastases, *Radiotherapy and Oncology*, vol. 133, pp. S935-S936, https://doi.org/10.1016/S0167-8140(19)32155-3
3. Lagerwaard, FJ, Van Der Hoorn, EA, Verbakel, WF, Haasbeek, CJ, Slotman, BJ & Senan, S (2009), Whole-brain radiotherapy with simultaneous integrated boost to multiple brain metastases using volumetric modulated arc therapy, *International Journal of Radiation Oncology, Biology, Physics*, vol. 75, no. 1, pp.253–259, https://doi.org/10.1016/j.ijrobp.2009.03.029

Table 5. Results for PortalDosimetry and ArcCheck measurements for the altered plans when compared to the original plan. The plans are ranked according to the %of clinical goals passing.

Portal Dose							
Plan Name	Description	1%/1mm	2%/1mm	3%/3mm	5%/1.5mm	5%/1 mm	% of clinical goals passing
N03 Brain 0:0	Original Plan	100	100	100	100	100	98%
N03 Brain 0:1	1% scaling of MU	100	100	100	100	100	96%
N03 Brain 0:2	2% scaling of MU	99.5	100	100	100	100	93%
N03 Brain 0:3	3% scaling of MU	96.7	99.6	100	100	100	92%
N03 Brain 9	0.01-0.1 mm random offset of MLC positions	100	100	100	100	100	92%
N03 Brain 10	Systematic 0.1 mm shift of MLC positions	99.9	100	100	100	100	91%
N03 Brain 7	0.1- 0.25 mm random offset of MLC positions	97.9	99.7	100	100	100	86%
N03 Brain 0:7	7% scaling of MU	64.3	80.2	99.3	98.7	97.2	85%
N03 Brain 12	1 deg Collimator increase all fields	97.7	99.6	100	100	100	85%
N03 Brain 5	Systematic 0.25 mm shift of MLC positions	82	93.1	100	100	99.8	83%
N03 Brain 8	0.25-0.50 mm random offset of MLC positions	71.1	85.3	100	99.9	98.7	82%
N03 Brain 11	2 deg Collimator increase all fields	66.8	77.1	100	99.2	95.5	74%
N03 Brain 4	0.1 -1 mm random offset of MLC positions	42.8	54.4	98.5	89.3	83	63%
N03 Brain 6	Systematic 0.50 mm shift of MLC positions	47.9	59.7	99.5	92.3	86.7	60%
N03 Brain 1	Systematic 1 mm shift of MLC positions	24.6	32.1	72.3	62.2	56.3	40%
N03 Brain 3	1 - 2 mm random offset of MLC positions	17.5	22.5	52	44.1	39.5	29%
ArcCheck							
Plan Name	Description	1%/1mm	2%/1mm	3%/3mm	5%/1.5mm	5%/1 mm	% of clinical goals passing
N03 Brain 0:0	Original Plan	100	100	100	100	100	98%
N03 Brain 0:1	1% scaling of MU	83.3	93.7	99.8	100	99.4	96%
N03 Brain 0:2	2% scaling of MU	79	91.5	99.6	99.8	99.1	93%
N03 Brain 0:3	3% scaling of MU	74	88.5	99.3	99.6	98.3	92%
N03 Brain 9	0.01-0.1 mm random offset of MLC positions	85.8	94	99.9	100	99.6	92%
N03 Brain 10	Systematic 0.1 mm shift of MLC positions	82.9	92.8	99.9	99.6	99.3	91%
N03 Brain 7	0.1- 0.25 mm random offset of MLC positions	79.6	90.5	99.9	100	98.8	86%
N03 Brain 0:7	7% scaling of MU	44	69	96.1	96.3	93	85%
N03 Brain 12	1 deg Collimator increase all fields	77.9	89.2	99.8	99.4	97.8	85%
N03 Brain 5	Systematic 0.25 mm shift of MLC positions	72.3	84.5	99.9	99.6	96.6	83%
N03 Brain 8	0.25-0.50 mm random offset of MLC positions	67.8	80.2	99.9	99	95.2	82%
N03 Brain 11	2 deg Collimator increase all fields	65.2	78.7	98.4	96.5	93.1	74%
N03 Brain 4	0.1 -1 mm random offset of MLC positions	48.2	64.3	97.9	91.4	85.1	63%
N03 Brain 6	Systematic 0.50 mm shift of MLC positions	51.8	67.4	99.1	95.2	88.8	60%
N03 Brain 1	Systematic 1 mm shift of MLC positions	32.6	47.9	80	76.7	72.6	40%
N03 Brain 3	1 - 2 mm random offset of MLC positions	23.1	34.7	65.2	64.5	60.9	29%

P66. Abstract withdrawn

P67. Dose Variation in Pancreas SBRT – A planning study based on daily MR imaging

Tony Young[1,2,3,*], Mark Lee[1], Meredith Johnston[1], Theresa Nguyen[1], Rebecca Ko[1], Sankar Arumugam[1,2,4]

[1]South Western Sydney Cancer Services, NSW Health, Sydney, Australia, [2]Ingham Institute, Sydney, Australia, [3]Institute of Medical Physics, School of Physics, University of Sydney, Sydney, Australia, [4]South Western Clinical School, University of New South Wales, Sydney, Australia

Introduction Pancreatic Cancer is associated with significant morbidity and mortality, with the treatment outcomes remaining poor compared to other cancers. Even in patients with resectable disease, the 5 year overall survival is less than 25% [1]. The use of SBRT (1–5 fractions) to treat pancreatic cancer has improved survival [2]. The aim of this study was to investigate dosimetric variations that occur over a simulated SBRT course for pancreatic cancer using daily MR images.
Method Five healthy volunteers were scanned on a Siemens Skyra 3 T MRI over two sessions, approximately 3 h apart, per day over 5 days to simulate an SBRT daily simulation scan for treatment planning, and a pretreatment scan for patient setup and treatment. A 4D MRI scan was taken at each session for ITV generation and assessment. For each volunteer a treatment plan was generated in the Raystation TPS following departmental protocols on the day one, first session dataset, with bulk density overrides applied to enable dose calculation. This treatment plan was propagated through other imaging sessions, and the calculated dose, as well as the deformed dose for the second session of each day was accumulated as per treatment. These accumulated mock treatment doses were assessed

against the original treatment plan through DVH comparison of the PTV and OAR volumes.
Results The generated ITV varied on average 18.4% (1.6%—43.2%) between imaging sessions compared to the first session ITV. The PTV D95 varied from -53.8% to -2.7% for the rigid accumulated dose and -32.7% to + 0.1% considering the deformed dose. Surrounding OARs had large variations in delivered dose, with the duodenum D0.5 cc differences ranging from + 3.5% to + 17.1% for the rigid accumulated dose and + 0.6% to + 10.5% considering the deformed dose.
Conclusion Pancreas SBRT would benefit from daily adaptive planning to account for changes in anatomy.
References

1. Mahadevan A, Moningi S, Grimm J, Li XA, Forster KM, Palta M, et al. Maximizing Tumor Control and Limiting Complications With Stereotactic Body Radiation Therapy for Pancreatic Cancer. International Journal of Radiation Oncology* Biology* Physics. 2021;110:206–16.
2. de Geus SW, Eskander MF, Kasumova GG, Ng SC, Kent TS, Mancias JD, et al. Stereotactic body radiotherapy for unresected pancreatic cancer: A nationwide review. Cancer. 2017;123:4158–67.

P68. Clinical performance of a mono-chain algorithm for breast planning automation in Monaco treatment planning system

Luis Munoz[1,*], David Hughes[2], Peter McLoone[2], Matthew Price[3]

[1]Genesiscare Flinders Private, Bedford Park, Australia, [2]Genesiscare Sydney, Alexandria, Australia, [3]Genesiscare Fiona Stanley Hospital, Murdoch, Australia

Introduction Treatment planning automation within radiotherapy allows for improvements in workflow efficiencies [1] and minimizes the potential for error [2]. For fully automated treatment plans, algorithms can make inference to plan parameters using decision making tools that capture an optimal result to achieve clinical intent. Inverse planned tangential breast planning using dynamic multileaf collimator (DMLC), or Volumetric Modulated Radiotherapy (VMAT), is routinely used for treatment providing ideal target coverage and reduced doses to organs at risk [3]. An optimal gantry position is critical to the delivery of dose, this work utilised a mono-chain algorithm to inform on gantry position. This enabled the selection of the optimal gantry angles for breast planning in the Monaco treatment planning system (TPS). Providing a fully automated workflow that utilized an application programming interface (API) provided with Monaco 6.0.1.
Method Breast plans (left and right sided) of a variety of target size and separation were generated using an in-house developed automation module. Planning target volume (PTV) RT-Structure were extracted, and had a convex hull generated from contour points using a mono-chain algorithm. 2D projections within a limited set of gantry angles found the optimal angle for the medial beam; this informed on the calculated tangential one. Both angles were parsed to automation workflows for template based planning. Plans were evaluated against clinical dosimetric criteria for target coverage (D95% and V105%) and OAR sparing.
Results Of 10 automated plans, 5 left and 5 right sided, gantry angles elected by the algorithm were found to be acceptable. Solutions achieved the target coverage and the OAR sparing; V105% was also found to be within clinically acceptable limits.
Conclusion A mono-chain algorithm was used to ascertain the optimal gantry angle, enabling a fully automated solution for inverse planned tangential breast planning.
Acknowledgements: Genesiscare would like to acknowledge Elekta for an alpha agreement for scripting in Monaco 6.0.01.
References

1. Mitchell, R.A., et al., Improving the efficiency of breast radiotherapy treatment planning using a semi-automated approach. Journal of applied clinical medical physics, 2017. 18(1): p. 18–24.
2. Covington, E.L., et al., Improving treatment plan evaluation with automation. Journal of applied clinical medical physics, 2016. 17(6): p. 16–31.
3. Teoh, M., et al., Volumetric modulated arc therapy: a review of current literature and clinical use in practice. The British journal of radiology, 2011. 84(1007): p. 967–996.

P69. Quality improvement of intravenous-contrast use in radiotherapy CT simulation

Adam Yeo[1], Sally Soteriou[1], Brigid Moran[1], Lisa Hall[1], Alan Turner[1], Karen McGoldrick[1], Nicholas Hardcastle[1]

[1]Peter MacCallum Cancer Centre, Melbourne, Australia

Introduction Intravenous (IV) contrast is a key tool for enhancing visualisation of blood flow in diagnostic CT imaging. IV-contrast protocols are specific to the anatomical region and disease, and must also be customised to the scanning equipment. IV-contrast improves visualisation of tumours and critical structures, but has typically been used sparingly in radiotherapy planning compared with diagnostic imaging. We performed a multi-disciplinary review with the aims of understanding the requirements for IV-contrast in our radiotherapy CT-simulation workflow and create and modify IV-contrast CT protocols.
Methods A multi-disciplinary group of radiation therapists, radiation oncologists, radiologists, radiographers, nurses and medical physicists were consulted on IV-contrast protocols for a range of anatomical sites from the brain down to the pelvis. Four key protocols were identified which would cover the requirements for contrast phase, taking into account the image acquisition time of 3D and 4DCTs used in CT-simulation.
Results Specific protocols for brain, head and neck, 4DCTs and upper abdominal sites were created as shown in Table-1. The head and neck protocol was modified to 4:6 ratio bi-phase injection with 90 s delay. Liver and pancreas included a non-contrast 3D- or 4D-scan followed by arterial and portal venous phases timed using bolus tracking. A specific 4DCT protocol was created to provide a low level of contrast enhancement that includes both arterial and portal venous phases, applicable to thoracic and upper abdominal anatomy. Lastly, a 3D-printed phantom was designed to assist in staff training and protocol rollout. Remaining issues include calculation of dose on CT-simulation with IV-contrast and nursing and medical staff availability.
Conclusion IV-contrast is a valuable tool in radiotherapy CT-simulation. We formed a multi-disciplinary group to review and update our IV-contrast protocols for CT-simulation, resulting in improved consistency and quality of IV-contrast use in radiotherapy CT-simulation.

Table 1. A summary of IV-contrast protocols and intended use.

Body Site	Volume(mL) / Flow Rate (mL per sec) / time delay (sec)	Intended outcome of IV contrast use
Liver/	Pancreas	100 mL / 3.0 mL/s 45 secs delay for ART & 70 secs delay for PV, initiated using bolus tracking
Phase 0: No	contrast (as a planning CT) Phase 1: Late arterial visualisation (ART) Phase 2: Portal venous visualisation (PV) * Bolus tracking triggered with 150HU threshold in aorta at level of diaphragm	
Head & Neck	100 mL (= 40 + 60) / 2.5 mL/s 90 secs delay post 1st injection (40 mL) & 30 secs delay post 2nd injection (60 mL)	Bi-phase injection combines vascular and delayed phases into one acquisition The first bolus is performed to achieve a good venous contrast (e.g. for neck tumour) whereas the second bolus is used for vascular opacification (e.g. neck arteries)
Neuro	65 mL / 2.0 mL/s 5 min delay post injection	The identification of abnormal contrast enhancement, such as in brain metastases, some primary brain tumours, and brain abscesses
4D Slow	Contrast	100 mL / 1.2 mL/s 30 s delay post injection
Better	visualisation of moving tumour adjacent lung vessels or other OARs like cardiac wall, mediastinal structures and kidney 4DCT needs to be acquired during the contrast injection across the long acquisition (e.g. 100 s). Minimum 1.2 mL/sec, up to 1.5 mL/sec for large patients	

P70. Commissioning electron beam models within the Monaco TPS for a network of linacs

Simon Goodall[1,*], Jonathan Dunning[1]

[1]Genesiscare, Melbourne, Australia

Introduction Our institution recently transitioned to the Monaco Treatment Planning System (Elekta, Stockholm, Sweden) from Pinnacle. A significant part of this changeover was the commissioning of the Monte Carlo electron beam models to service our network of 40 matched Elekta Linacs.

Method Profiles and PDDs were calculated in Monaco for 6, 9, 12 and 15 MeV for the open fields with the 6 × 6, 10 × 10, 14 × 14 and 20 × 20 electron applicators. These PDDs and profiles were then compared to beam data measured on a subset of machines and to Elekta AGL data, a standard data set, generated by Elekta and used to create the beam models. The calculated and measured data was compared in the Monaco Commissioning Utility Software. Output factors measured for a variety of open fields and inserts in the four applicators at three SSDs (98, 100 and 110 cm) for all energies across a variety of Linacs were also compared to those calculated in Monaco. Finally, a selection of spot check measurements, including various shaped inserts, were also analysed.

Results The PDDs and profiles were analysed using a global gamma analysis criterion of 1%/1 mm. In general, all the curves matched well. Failing comparison points were due to the noisy nature of the Monte Carlo calculations and uncertainty in the build-up measurements rather than any global trend. For all field sizes, energies and SSDs tested, the average output and spot check reading across all Linacs matched with Monaco to within ± 3.0%. Any outliers were found to be due to differences in the beam profile measurement detectors used.

Conclusion Beam models for 6 MeV, 9 MeV, 12 MeV and 15 MeV have been evaluated and released for clinical use across our network of matched Elekta Linacs. Monaco accurately simulates dose deposition with electron beams accurately to within 3.0% of measured data.

P71. A multidisciplinary model for the commissioning and implementation of a new radiotherapy treatment planning system

Philip Vial, Gary Goozee[1], Josip Juresic[1], Joanne Veneran[1], Odette King[1], Sankar Arumugam[1], Shrikant Deshpande[1,*], Viet Do[1]

[1]South Western Sydney Cancer Services, Sydney, Australia

Introduction The demands of safely commissioning and implementing a modern treatment planning system (TPS) has outgrown traditional approaches. While the fundamentals addressed by established guidelines [1] remain important, the sophistication of many new functionalities present new risks that go beyond what a medical physicist can validate in isolation from the rest of the clinical Radiation Oncology team. Conversely, for the typical Radiation Therapist or Oncologist TPS user, there is very little structured guidance or experience on how to safely develop, validate and implement the complex tools and techniques at their disposal. This work describes a formalized structure that acknowledges and supports the shared roles and responsibilities of Radiation Oncology team members in the implementation of a modern TPS.

Method Radiation Oncology management at Liverpool and Macarthur Cancer Therapy Centres (LMCTC) proposed a structured model

for the commissioning of the newly acquired TPS (RayStation®) based on the division of key tasks into the multidisciplinary 'Task Groups' (TG) described in Table 1.

Results The multidisciplinary TGs were successfully formed and continue to function as clinical planning is transitioned to RaySta-tion®. Each TG meets regularly to report and manage progress. Each TG formed sub-groups for specific tasks within their areas of responsibility. TG representatives report to other TG and department meetings to manage issues of mutual dependence. Regular newsletters are used to communicate progress more broadly. The TGs continue to oversee improvements and system upgrades as treatment planning techniques transition through development, testing, implementation and clinical routine phases.

Conclusion A multidisciplinary TG model for TPS commissioning and clinical implementation has been established at LMCTC. The model will undergo review at the completion of all tasks.

References

1. Technical Reports Series no. 430, Commissioning and quality assurance of computerized planning systems for radiation treatment of cancer. International Atomic Energy Agency, Vienna, 2004.

Table 1. Task group (TG) structure outline. Multidisciplinary membership includes Medical Physics Specialist (MPS), Radiation Therapist (RT), Radiation Oncologist (RO), Information Technology (IT), and Computer Scientist (CS).

Task Groups	Responsibilities	Membership
TG 1	• Steering Committee – project management (priorities and resources) • IT support, hardware/software installation, architecture, connectivity, access & security • License management	MPS, IT, RT, RO
TG 2	• Processing of images for treatment planning • Policies and procedures • Contouring and image registration tools (all modalities)	MPS, RT, RO
TG 3	• Compliance with TRS 430 • Beam modelling and validation (all machines and energies, CTs) • Accuracy of tools, displays, scales, etc. • Reporting	MPS, RT
TG 4	• Site specific technique development. Templates & scripts (TG6) • Patient Specific Quality Assurance policies and procedures • Develop and document clinical planning work instructions • Staff training	RT, MPS, RO
TG 5	• Assess, advise and commission tools for advanced applications • Oversee clinical implementation of advanced tools (TG4) • e.g. adaptive replanning & dose accumulation, Robustness tools	MPS, RT, RO
TG 6	• Develop RS scripting environment, tools, policies and procedures • Provide scripting support for all TGs.	MPS, RT, CS

P72. Assessment of junctions for VMAT treatments with long abutting fields in Monaco

***[1]Manuel Carrillo Serrano, [1]Arek Mazurek**

[1]Genesiscare, Murdoch, Australia

Introduction Volumetric modulated radiation therapy (VMAT) for lesions covering limbs, craniospinal irradiation (CSI) [1], and in total body irradiation (TBI) [2]; involve long targets. Due to physical constraints of linear accelerators, treatment plans are divided into long abutting fields. The junctions of those abutting fields are usually formed with the multileaf collimators (MLC), and if not assessed properly, they could affect PTV coverage. Here, we study dosimetric effects in the junction region by introducing artificial shifts in four clinical plans created in the Monaco 6® treatment planning system (TPS), and in measurements using the ArcCHECK phantom [3, 4].

Method Four plans were selected from patients treated previously, and multiple longitudinal shifts were introduced in the isocentre location of the inferior fields. The plans were compared by evaluating DVH metrics of each shift. ArcCHECK measurements were also artificially shifted and compared to TPS dose distributions.

Results Preliminary results show that our current patient specific QA gamma criterium is not rigorous enough to assess the effects of having a shift of less than 7 mm between the two sets of abutting fields, in some cases. As expected, the largest difference in the dose distributions with and without shifts, occurs in the junction region and in the lower extreme of the inferior field. DVH comparisons for the clinical plans, show that the metrics worsen with shifts of 3 mm, making some plans clinically unacceptable.

Conclusion This work assessed the dosimetric effects in the junctions of abutting fields using Monaco and our local patient specific QA program with the ArcCHECK phantom. Preliminary results show that, even with passing rates above our locally accepted gamma criterium, failing points in the junction region are indications of non-optimal treatments, based on DVH statistics.

References

1. Studenski M, Shen X, Yu Y, et al. Intensity-modulated radiation therapy and volumetric-modulated arc therapy for adult craniospinal irradiation–a comparison with traditional techniques. Med Dosim. 2013 Spring; 38:1; 48–54.

Symons K, Morrison C, Parry J, et al. Volumetric Modulated Arc Therapy for Total Body Irradiation: A Feasibility Study using Pinnacle3 Treatment Planning System and Elekta AgilityTM Linac. J Appl Clin Med Phys 2018; 19:2; 103 – 110.

3, Morrison C, Symons K, Woodings S, et al. Verification of Junction Dose between VMAT Arcs of Total Body Irradiation using a Sun Nuclear ArcCheck Phantom. J Appl Clin Med Phys 2017; 18:6; 177 – 182.

4. Sun Nuclear Corporation. ArcCHECK® & 3DVH®; 2017; Available from: https://www.sunnuclear.com/solutions/patientqa/arccheck3dvh.

P73. Computerised planning for total body irradiation; retrospective review of in vivo doismetry

Iliana Peters[1], Dale Roach[1], Phillip Vial[1], Shrikant Deshpande[1,2,*], Andrew Wallis[1], Minh Ngo[1], Joshua Hiatt[1], Alicia Haman[1], Vinh Luong-Poole[1], Caroline Round[1], Eng-Siew Koh[1,2]

[1]South West Sydney Cancer Services, NSW Health, Australia, [2]South Western Sydney Clinical School, Faculty of Medicine, University of New South Wales, Australia

Introduction Total body irradiation (TBI) planning traditionally utilised manual monitor unit (MU) calculations based on dosimetric data collected at extended Source-to-Axis Distance (SAD). As heterogeneities and internal patient scatter cannot be accounted for in manual planning in vivo dosimetry (IVD) is recommended for TBI to maintain dosimetric accuracy of ± 10% [1,2]. Computerised treatment planning systems (TPS) can provide 3D dose distribution to predict organs at risk (OAR) dose and allow customization [3,4], however they are isocentrically commissioned and require verification for extended distance TBI geometry. Our centre recently transitioned to TPS based TBI planning and this study reports a retrospective review of TBI IVD for TPS based treatment plans.

Method Between 2018–2022 each TBI patient was concurrently planned via manual calculation and in Pinnacle[3] TPS. Patients were positioned supine on a couch at 365 cm SAD and irradiated laterally at a fixed gantry angle with a 180° couch rotation halfway through treatment. *IVD* was performed with an ionisation chamber at patient midline between thighs and thermoluminescent detectors (TLDs) for entrance and exit dose at four locations plus one placed at chamber. Measured data was subsequently compared against TPS and manually calculated dose.

Results Agreement of chamber measurement to manual and TPS calculated dose for 18 patients was 9.9% ± 4.7% and 3.5% ± 3.5% respectively ([P73] **Fig. 1**). The distribution of TLD measurements with respect to TPS dose is shown in [P73] **Fig. 2**. Chest and neck measurements showed the largest variation in agreement (± 11.6% and ± 9.9% respectively).

Conclusion This review verified our isocentrically commissioned TPS a suitable option for TBI planning. The TBI IVD showed a better chamber agreement with TPS compared to manual calculations. The relatively large IVD spread at chest and neck highlights the increased inhomogeneous dose distribution and setup variability in those areas. The retrospective review will assist in future TBI planning technique development.

References

1. Bloemen-van Gurp, E. J., Mijnheer, B. J., Verschueren, T. A., & Lambin, P. (2007). Total body irradiation, toward optimal individual delivery: dose evaluation with metal oxide field effect transistors, thermoluminescence detectors, and a treatment planning system. International journal of radiation oncology, biology, physics, 69(4), 1297–1304. https://doi.org/10.1016/j.ijrobp.2007.07.2334
2. van Dyk, J.; Galvin, J.M.; Glasgow, G.P.; et al. AAPM Report No 17: The physical aspects of total and half body irradiation. New York: American Institute of Physics; 1986.
3. Nelligan, R., Bailey, M., Tran, T. et al. (2015) ACPSEM ROSG TBI working group recommendations for quality assurance in total body irradiation. Australas Phys Eng Sci Med 38, 205–215 https://doi.org/10.1007/s13246-015-0344-7
4. Fog, L. S., Hansen, V. N., Kjær-Kristoffersen, F., Berlon, T. E., Petersen, P. M., Mandeville, H., & Specht, L. (2019). A step and shoot intensity modulated technique for total body irradiation. Technical innovations & patient support in radiation oncology, 10, 1–7. https://doi.org/10.1016/j.tipsro.2019.05.002

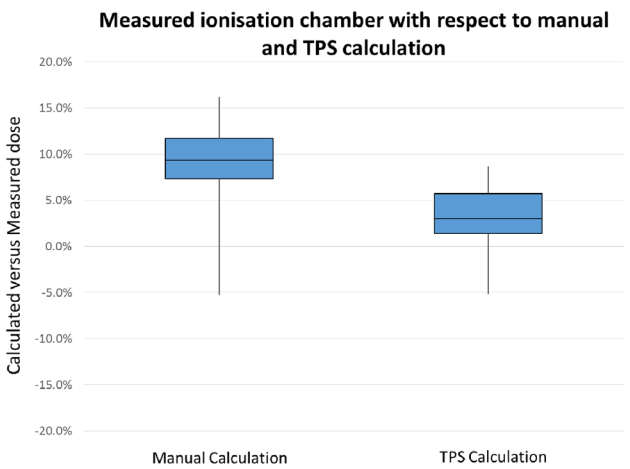

Fig. 1. Ionisation chamber measurements representing midpoint dose captured during 2018–2022 TBI treatments in comparison to expected dose determined via manual calculation and via TPS.

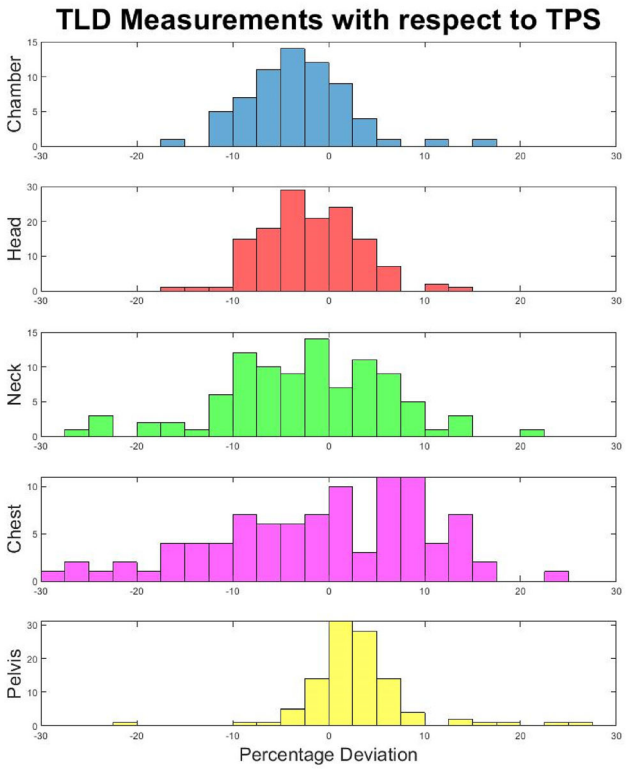

Fig. 2. Variation between measured TLD in vivo dosimetry and calculated TPS dose for patients undergoing TBI between 2018–2022.

P74. Commissioning of BrainLab 4PI couch overlay in Raystation treatment planning system (TPS)

Kamlesh Gupta[1], Zoë Moutrie[1,*], Joshua Hiatt[1], Anthony Espinoza[1], Gary Goozee[1]

[1]Liverpool And Macarthur Cancer Therapy Center, Campbelltown, Australia

Introduction Brainlab 4PI Couch overlay is designed for Stereotactic treatments. Comprising of a carbon fiber high density sandwiched we set out to assess the impact of this on patient dosimetry.

Method Dose attenuation through high density material of 4Pi couch overlay was measured for both 6MV and 10FFF PDD [1] in a Gammex RMI457 solid water with PTW 34,045 advanced Markus chamber, while skin dose measurements were completed using EBT3 film [2]. CIRS anthropomorphic head- and CIRS IMRT freepoint-phantoms were CT scanned with in the 4PI overlay. An in house script was used to contour 4Pi overlay as part of the external contour. Coplanar and non-coplanar VMAT plans were created in Raystation (v10b) for our Elekta VersaHD linacs. Each plan was delivered to the anthropomorphic head phantom, with EBT3 film placed in axial slices and repeated with Thermoluminescent dosimeter [3] (TLD-100 ^{TM}) placed at the isocentre. Each plan was delivered to the CIRS freepoint phantom measured with an IBA cc13 ion chamber at key locations.

Results The greatest variation in dose was 11% and 8.5% dose attenuation at 5 cm depth for 6MV and 10FFF MV respectively. Skin dose showed an increase of 13% while PDD changed by 1% and 2.4% after dmax for 6MV and 10FFF MV respectively. Local point dose measurement within 3% with respect to TPS dose. TLD skin dose measurement shows good agreement (< ± 5%) with TPS predicted

doses. Fluence was assessed in terms of gamma agreement [4] (3% 2 mm) between measured and predicted doses was greater than 95% for both energies (coplanar and non-coplanar beam arrangement).
Conclusion Dosimetric assessment of the immobilization systems shows this tool must be accounted for in the TPS, modelling of the 4PI couch overlay in Raystation shows clinically acceptable variations when an in house script was used to include the 4Pi couch overlay as a part of external contour.
References

1. Imae T, Takenaka S, Watanabe Y, Aoki A, Matsuda K, Sasaki K, Saegusa S, Nawa K, Nakagawa K. Surface and build-up dose comparison between Elekta 6 MV flattening filter and flattening-filter-free beams using an advanced Markus ionization chamber and a solid water-equivalent phantom 12 November 2020; https://doi.org/10.1002/acm2.13094
2. Toossi MTB, Ghorbani M, Khorshidi F, Mohammadi M, Mohamadian N, Akbari F, Dayani M. Skin dosimetry with EBT3 radiochromic film in radiotherapy of parotid cancer. J Biomed Phys Eng 2021 11:573–582.
3. Ganapathy K, Kurup PGG,Murali V et al. Patient dose analysis in total body irradiation through in vivo dosimetry. J Med Phys. 2012 37:214–218. https://doi.org/10.4103/0971-6203.103607
4. Low DA, Harms WB, Mutic S, Purdy JA. A technique for the quantitative evaluation of dose distributions. Med Phys. 1998 25:656–61. https://doi.org/10.1118/1.598248

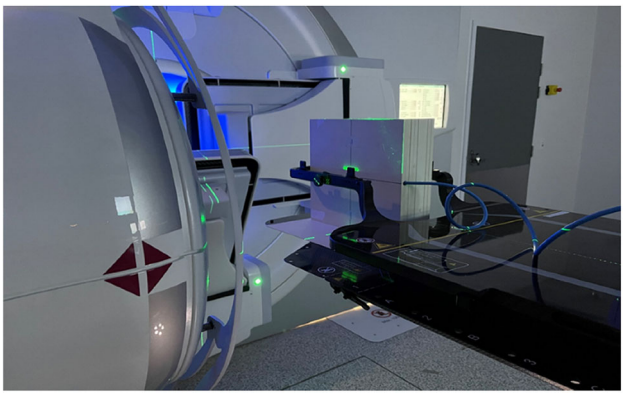

Fig. 1. Markus chamber setup at surface on solid water phantom with cranial 4PI overlay.

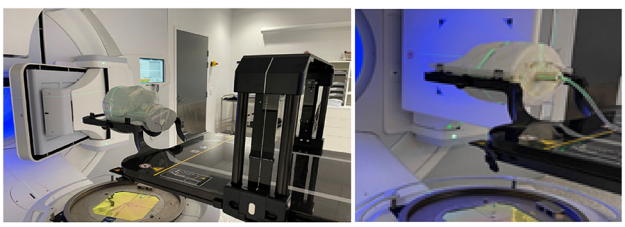

Fig. 2. EBT3 film sandwiched in axial plane of anthropomorphic phantom and point dose measurement setup in CIRS phantom.

P75. Review of the "Hype" associated with treatment planning systems that use the Monte Carlo computation method and report results as "dose to medium"

Nick Bennie[1,*]

[1]Northern NSW Cancer Institute, Lismore, Australia

Introduction This paper reviews, with reference to the article Hype Cycle in Radiotherapy [1], some of the claims made regarding Radiotherapy TPS that make use of MC methods and report results as the quantity Dm. Hype (a derivation of Hyperbole, Exaggeration) is a method whereby commercial companies draw attention to and stimulate interest in their product in order to progress commercial transactions. In this context it refers to the reaction of the radiotherapy community. It is generally considered fair practice. However, such claims should be regularly clarified, such that clinical practice is based on established data. It is claimed there is an intrinsic link between the MC method and Dm. This only means the clinical algorithm can calculate Dm slightly more efficiently. Accuracy: For the requirements of a Clinical system to achieve equivalent accuracy, a MC method is orders of magnitude slower than analytic methods. Relevance to clinical effect: Dm is chosen for MC methods as it improves the efficiency of these methods, not for relevance to clinical effect, which is not established. Correlation/comparison to established standard Convolution algorithm: The standard Convolution algorithm is a very stable and bounded algorithm. Due to the random nature of MC methods they are unbounded. Noise generated from noise inherent in CT data results in equivalent noise in Dm and Dw, both are first order dependent on CT data. The natural variation of certain tissues, eg breast, appear as noise. This is as a result of real variation in the material composition of the tissue. Problems with optimization, linked to step changes at material boundaries.
Conclusion It is concluded that the commercial companies that promote planning systems that use MC methods and report Dm use significant "Hype" as defined in [1]. Care should be taken in the evaluation of these systems to determine they are the most suitable system for purpose.
References

1. Bortfeld T, Marks LB (2013). Hype cycle in radiation oncology. Int J Radiat Onc Bio Phys 86:819–821.

P76. A semi-automated tool for extracting radiomic features from Dicom datasets

Prabhakar Ramachandran[1,*], **Ryan Motley**[1], **Margot Lehman**[1]

[1]Princess Alexandra Hospital, Woolloongabba, Australia

Introduction This study aims to develop a tool to automate the process of extracting radiomic features from Dicom datasets.
Methods The commercially available MATLAB™ programming platform was used to develop an App to extract radiomic features. The key principle of operation of the application is the correlation between the contours found in the RT structure set with their position relative to each image slice. The pixels outside of the contour were

masked out in each image slice allowing for segmentation of only the relevant pixel values, which were then stacked to make a pseudo-3D representation of the entire contour with reference to the original image volume. The creation of the pseudo-3D structure aided in decreasing the computation time by allowing simultaneous feature calculation instead of one slice at a time. Altogether, 109 radiomic features divided into seven categories were extracted and compared against radiomic features extracted from the 3D-slicer software. For single patient analysis, input is of the form of a single folder containing all patient images and RT Structure Sets. A simple batch processing option was incorporated into the software to extract features in one go, eliminating a large amount of the manual processing and human labour required to analyse patients individually. Output from batch processing is an excel spreadsheet containing the radiomics data for each selected contour for each patient.

Results The extracted radiomic features from the developed tool agreed closely with the feature values extracted from 3D-slicer for all the 109 radiomic features.

Conclusion The semi-automated tool developed in MATLAB reduces the time required to import, process, extract and populate the output in a user-readable format. It allows seamless extraction of radiomic features found in CT and MR images for use in machine learning projects.

Acknowledgements: SERTA, Queensland Health.

P77. Abstract withdrawn

P78. Accuracy limits on small field SBRT dosimetry

Febrian Kachina[1], Robin Hill[1,*], Samara Alzaidi[1]

[1]Chris O'Brien Lifehouse, Haymarket, Australia

Introduction SBRT is now commonly used in radiotherapy to treat cancer many of which can have small target sizes. A challenge of SBRT is to accurately measuring the delivered doses for Quality Assurance (QA) purposes. In this work, we evaluated the suitability of a range of selected dosimeters for SBRT dosimetry.

Method Treatment plans were created with 7 PTV sizes ranging from 1.1 to 7.2 cm equivalent sphere diameter. These were calculated for the 6 MV and 10 MV x-ray beams with the corresponding Free-Flattening Filter (FFF) mode using the Varian Eclipse treatment planning system. The dose of various target sizes was measured using a PTW PinPoint ionization chamber, the Electronic Portal Imaging Dosimetry (EPID) on the Truebeam linac and an ArcCHECK phantom representing 1D, 2D, and 3D dosimeters, respectively. The planned doses from Eclipse were recalculated using the secondary dose check program PlanCHECK (Sun Nuclear, USA).

Results Ionization chamber measurements showed a small percentage dose difference at isodose point with average dose difference ranging from -1.7% to 2.3%. EPID measurements had high gamma passing rate with more than 99% of the measurements have more than 95% gamma pass rate for 1%/1 mm gamma criteria. For clinical purposes, where the gamma index used for small target is 2%/2 mm, the passing rate for ArcCheck declined sharply from target smaller than 3 cm equivalent sphere diameter. PlanCHECK^{TM} results proved to have 100% gamma pass rate for almost all the plans with the lowest gamma pass rate was 98.5%

Conclusion Measurements from ionization chamber and EPID showed good agreement with the planned dose. The ArcCHECK was effective for measuring dose for target sizes no smaller than 3 cm eqivalent sphere diameter. PlanCHECK^{TM} results showed a great agreement to the calculated dose from Eclipse^{TM} TPS.

P79. What is an acceptable level of uncertainty: Minimal reportable dose and what is an acceptable level of uncertainty in personal dosimetry

Stephen Marks[1,*]

[1]Arpansa, Yallambie, Australia

Introduction Nearly 55 years ago, Lloyd Currie published his seminal paper [1], which now underpins international standards for reporting measurements. In that paper, he rigorously defined three characteristic limits for a measurement: the critical limit, the detection limit, and the quantification limit. This last characteristic, the quantification limit, defined as the "the smallest signal of interest which has an acceptable uncertainty" generally dictates what is set as the minimum reportable value.

Method The occupational dose (D_o) reported by ARPANSAs personal radiation monitoring service is the gross measured wearer dose (D_W) minus the gross background dose (D_C) as measured on a control monitor. $D_O = D_W - D_C$. Using the personal radiation monitoring service's historic data, the average background signal for a typical wearing period was calculated. Using this value as the background signal the relative uncertainty was calculated as a function of the occupational dose.

Results Unsurprising we can clearly see that there is an increase in the relative uncertainty as the occupational dose decreases, this exceeds 100% at around 20μsv against the average background level of 270 μSv. We can now use these results as a tool to set a minimum reportable dose at a level that balances the want for reporting lowest possible dose and ensuring that the results and associated uncertainty makes sense and is not misleading to clients.

Conclusion In personal radiation monitoring the relative high background signal and what is an "acceptable" uncertainty are the two biggest factors when calculating the minimum reportable dose. As the background signal cannot be changed the defining factor becomes what do we deem as acceptable level of uncertainty.

Reference

1. Currie, L.A., Analytical Chemistry, volume 40, issue 3, pp 586–593, 1968.

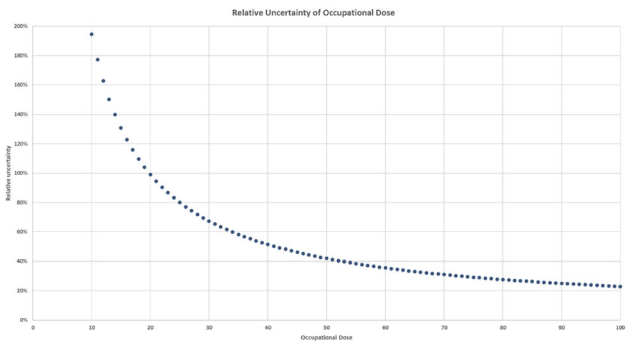

Fig. 1.

P80. Remote dosimetric auditing for trials

Peter Greer[1,2,*], Joerg Lehmann[1,2,3], Therese Standen[1], Annette Haworth[3], Andrew Grose[4], Alisha Moore[4]

[1]Calvary Mater Newcastle Hospital, Newcastle, Australia, [2]University of Newcastle, Newcastle, Australia, [3]University of Sydney, Sydney, Australia, [4]TROG Cancer Research, Newcastle, Australia

Introduction Centres participating in Australian led clinical trials, with TROG radiation therapy credentialing requirements, must show evidence of recent independent dosimetric audits, including a higher level audit if intensity modulated treatments are used. This can be a barrier to participation for international centres. The Virtual Epid Standard Phantom Audit (VESPA) was pioneered in Australia to alleviate major local backlogs in dosimetric auditing [1,2]. Recently the VESPA remote audit method has been extended to overseas centres to facilitate participation in locally led clinical trials.
Methods The centres transfer their trial plan to a cylindrical phantom model in the treatment planning system (TPS) and calculate dose in the phantom. The plan is delivered, and images are recorded in-air on the electronic portal imaging device. The data is sent to Calvary Mater Newcastle for analysis. The dose in the (virtual) cylindrical phantom is reconstructed using an image to 3D dose conversion algorithm and compared to the TPS dose (Fig. 1). Software and methods to handle newer jpg format image frames from Elekta have been developed.
Results Currently 18 international centres from 8 different countries (Fig. 2) have completed or are undertaking the VESPA audit process as part of a TROG led quality assurance program for five separate clinical trials (TOPGEAR, EXPERT, DECREASE, NINJA, DASL-HICAP). Both Varian and Elekta delivery platforms are now assessable except for older Elekta iView software that cannot acquire cine images for VMAT. A dosimetry license must be requested from Elekta if this is not already present as the dosimetry information in the image is encoded.
Conclusions The VESPA method can provide a high level of confidence that trial IMRT and VMAT doses are being delivered accurately. Application of the method to international sites can facilitate adherence to TROG quality assurance standards and participation in Australian led trials.
References

1. Miri, N., et al., Virtual EPID standard phantom audit (VESPA) for remote IMRT and VMAT credentialing. Physics in Medicine and Biology, 2017. 62(11): p. 4293–4299
2. Miri, N., et al., A remote EPID-based dosimetric TPS-planned audit of centers for clinical trials: Outcomes and analysis of contributing factors. Radiat. Oncol. 2018. **13**(1).

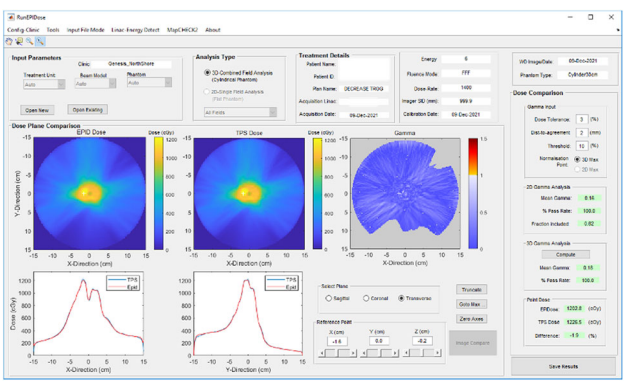

Fig. 1. Example of a VESPA dosimetry assessment for the DECREASE trial.

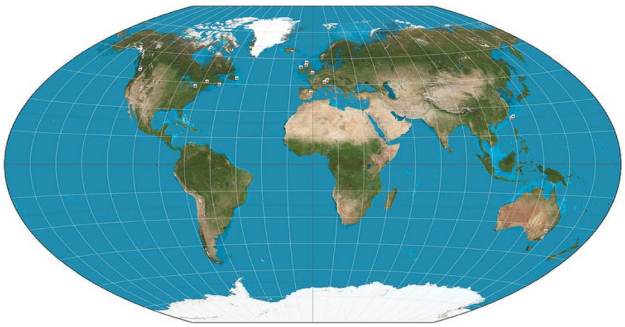

Fig. 2. International centres being audited with VESPA for TROG led clinical trials.

P81. International comparison of air kerma for low energy kilovoltage x-rays

Shahrzad (Sara) Shoyookhi[1,*], Duncan Butler[1], Max Hanlon[2], Tracey Bailey[1], [1]Chris Oliver[1]

[1]Australian Radiation Protection and Nuclear Safety Agency, Yallambie, Australia, [2]William Buckland Radiotherapy Centre, Melbourne, Australia

Introduction The Bureau International des Poids et Mesures (BIPM) is an international standards laboratory established under the Metre Convention. For radiation dosimetry the BIPM maintains primary standards against which standards laboratories compare to establish their international equivalence. In 2022 ARPANSA performed this comparison for air kerma for four x-ray beam qualities.
Method Two PTW 23,344 thin window ionization chambers were calibrated at ARPANSA, then at the BIPM in Paris, and returned for a second set of measurements. The result of the comparison is the ratio of the ARPANSA calibration coefficients N_K to the BIPM values. In both laboratories the primary standard is a free air chamber. At ARPANSA a Philips RT100 x-ray tube was used to establish the four radiation qualities.
Results The following table shows the ARPANSA beams and air kerma calibration coefficients.The ARPANSA results include changes made as a result of data published in ICRU Report 90.
Conclusion The calibration coefficients are consistent between pre and post-transfer measurements. BIPM's results will be presented at the conference. Based on the chamber history the ARPANSA results are expected to be consistent with BIPM within the expanded (k = 2) uncertainties.
References

1. ICRU Report 90.

Table 1

Radiation quality	10 kV	30 kV	50 kV b	50 kV a
Added filtration / mm of Al	-	0.205	1.0	4.0
Half Value Layer / mm of Al	0.038	0.17	1.00	2.35
PTW23344 sn 0858				
Nk (ARPANSA-2008) mGy/nC	83.91	83.46	81.65	81.32
Nk (Pre-transfer) mGy/nC	85.59	83.07	81.31	80. 64

Table t continued

Radiation quality	10 kV	30 kV	50 kV b	50 kV a
Nk (Post-transfer) mGy/nC	85.56	82.97	81.22	80.79
PTW23344 sn 0967				
Nk (ARPANSA-2008) mGy/nC	92.40	89.67	87.82	87.93
Nk (Pre-transfer) mGy/nC	92.43	88.87	86.52	86.51
Nk (Post-transfer) mGy/nC	92.84	88.89	86.78	86.66
Combined standard uncertainty (%)	0.76	0.46		

P82. Summary of ARPANSA diagnostic reference level program data for 2021

Peter Thomas[1,*], Masoumeh Sanagou[1], Toby Beveridge[1], Kam Lee[1]

[1]Australian Radiation Protection and Nuclear Safety Agency, Yallambie, Australia

Introduction ARPANSA's Diagnostic Reference Level (DRL) program supports optimisation of medical exposures by providing guidance on typical dose for common imaging procedures. Routine comparison against DRLs is included in regulatory requirements such as the Medical Exposure Code [1] and the Diagnostic Imaging Accreditation Scheme [2].

Method ARPANSA's National Diagnostic Reference Level Service (NDRLS) collects CT survey data through a web portal. Data on image-guided interventional procedures (IGIP) is collected using spreadsheet templates. Median dose metrics from each survey are reported as facility reference levels (FRLs). Surveys include data for up to 20 patients in CT and 30 patients for IGIP. National DRLs are based on the third quartiles of the FRL distributions.

Results In 2021, 3829 CT surveys from 550 scanners were completed. Third quartiles of the FRL distributions are shown in Table 1 and compared with the national DRLs [3]. For several scan categories the third quartile for 2021 is $> 10\%$ below the national DRL. A general review of the CT DRLs will commence shortly. Ninety-two (92) surveys were submitted for image-guided procedures. Of these, 40 were for coronary angiography and the third quartiles of the FRL distributions were consistent with the national DRLs [4]. Data for other procedures were quite sparse and more submissions are needed to establish national DRLs. A survey of radiopharmaceutical administered activity and metrics for associated CT scans in nuclear medicine and positron emission tomography was conducted between September 2021 and March 2022. The data are being discussed with a liaison panel and recommendations for updates to the national DRLs are expected to be released by the end of 2022.

Conclusion Australia's DRL program is well established. Work is underway to update the DRLs for adult and pediatric CT. Recommendations for updates to the DRLs for nuclear medicine will be released by the end of 202More data is needed for image-guided procedures.

References

1. Australian Radiation Protection and Nuclear Safety Agency (2019). Code for Radiation Protection in Medical Exposure. ARPANSA. https://www.arpansa.gov.au/regulation-and-licensing/regulatory-publications/radiation-protection-series/codes-and-standards/rpsc-5 Accessed 14 July 2022.
2. Australian Commission on Safety and Quality in Health Care (2016). Diagnostic Imaging Accreditation Scheme Standards. ACSQHC. https://www.safetyandquality.gov.au/standards/diagnostic-imaging/diagnostic-imaging-accreditation-scheme-standards Acces sed 14 July 2022.
3. Australian Radiation Protection and Nuclear Safety Agency (2021). Current Australian national diagnostic reference levels for multi detector computed tomography. ARPANSA. https://www.arpansa.gov.au/research-and-expertise/surveys/national-diagnostic-reference-level-service/current-australian-drls/mdct Accessed 14 July 2022.
4. 4. Australian Radiation Protection and Nuclear Safety Agency (2021). Current Australian national diagnostic reference levels for image guided and interventional procedures. ARPANSA. https://www.arpansa.gov.au/research-and-expertise/surveys/national-diagnostic-reference-level-service/current-australian-drls/igip Accessed 14 July 2022.

Table 1. Third quartiles of the 2021 CT FRL distributions for adult patients and comparison with the national DRLs, categorised by scan region.

Scan Region	Surveys	$CTDI_{vol}$ (mGy)		DLP (mGy.cm)	
		3rd Quartile (2021)	DRL	3rd Quartile (2021)	DRL
Head	555	45.9	52	818	880
Cervical Spine	459	18.9	21	401	470
Soft-Tissue Neck	353	14.4	15	406	450
Chest	514	8.4	10	339	390
Chest-Abdo-Pelvis	444	10.2	11	787	940
Abdo-Pelvis	549	10.3	13	505	600
Kidney-Ureter-Bladder	408	9.0	10	412	460
Lumbar Spine	516	21.2	26	591	670

P83. Dose to cardiac implantable electronic devices: comparison between GammaKnife and LINAC intracranial SRS

Atousa Montaseri[1,*], Elena Ungureanu[1], Peta Lonski[1], Tomas Kron[1]

[1]Peter MacCallum Cancer Centre, Melbourne, Australia

Introduction Patients with cardiac implantable electronic devices (ICDs) increasingly receive advanced radiation therapy (RT) at Peter MacCallum Cancer Centre (PMCC). Depending on patient dependency precautionary investigations, documentations, device checks, and monitoring during RT are performed. In general, ICDs should always be located out of radiation field. Since external beam treatment planning systems don't calculate the out-of-field dose accurately, verification dose measurements are performed before treatment to ensure patient safety.
Method A pituitary adenoma patient who had a cardiovascular defibrillator received stereotactic radiotherapy at Gamma Knife (ELEKTA). A single dose of 21 Gy was prescribed. A verification plan was created and delivered in GK on STEEV anthropomorphic phantom (CIRS). Dose at ICD location was measured using thermoluminescent dosimeters (TLD100H). ICD dose was also measured in-vivo during patient treatment. For comparison to a similar treatment on LINAC, patient dataset was transferred to Varian Eclipse treatment planning system and 10FFF co-planar VMAT plans were created. Dose to ICD location was measured on STEEV phantom using TLDs. Additional co-planar VMAT plans with jaws retracted to 10cmx10cm were created to simulate single-iso multiple-target scenarios.
Results Phantom and patient in-vivo measurement in GK agreed with each other and showed about 10 mGy to ICD (0.05% of prescribed dose). ICD dose in VMAT plans was similar to GK, while setting collimator at 90° provided out-of-field dose reduction by a factor of 2, compared to collimator 0°, demonstrating the reduction of leakage dose through the MLC bank. Increasing the jaw settings to 10 × 10cm2 with similar MLC patterns increased the does to ICD by a factor of 3-5 highlighting MLC transmission and the need to optimise jaw settings to minimise the dose to ICDs in SRS.
Conclusion Dose to ICD in GK and co-planar VMAT intracranial SRS is similar. GK beam geometry is non-coplanar. ICD dose in LINAC non-coplanar SRS is being investigated.

P84. Abstract withdrawn

P85. Effect of scanner lens on lateral response artefact in radiochromic film dosimetry

Tarafder Shameem[1,*], Nick Bennie[1], David Thwaites[2], Martin Butson[3]

[1]NCCI, Lismore Base Hospital, Lismore, Australia, [2]University of Sydney, Sydney, Australia, [3]EPA, Sedney, Australia

Introduction Radiochromic film is a good dosimeter choice for patient QA for complex treatment techniques because of its near tissue equivalency, very high spatial resolution and established method of use. Commercial scanners are typically used for film dosimetry, among which EPSON scanners are the most common. Radiochromic film dosimetry is not straightforward as there are some well-defined problems which must be considered, one of the main ones being the Lateral Response Artefact (LRA) effect. Previous studies showed that the contributing factors to LRA are due to the structure of the active ingredients of the film and to the components and construction of the flatbed scanner. The purpose of this study is to investigate the effect of the scanner lens on the LRA effect.
Method EBT3 films were irradiated with 40 × 40cm^2 field size 6 MV beams. Films were analysed using images captured by a Canon 7D camera utilising 18 mm, 50 mm and 100 mm focal length lenses compared to images scanned with a conventional EPSON V700 scanner.
Results The magnitude of the LRA was observed to be directly related to the focal length of the lens used to image the film. A substantial reduction in LRA was seen with the use of the 50 mm and 100 mm lenses, by factors of 3-5 for the 50 mm lens and 4-20 for the 100 mm lens compared to conventional desktop scanner techniques.
Conclusion This is expected to be from the longer focal length camera lens system being able to collect more light from distant areas compared to the scanner-based system and provides an opportunity to design film dosimetry systems that minimise this artefact.

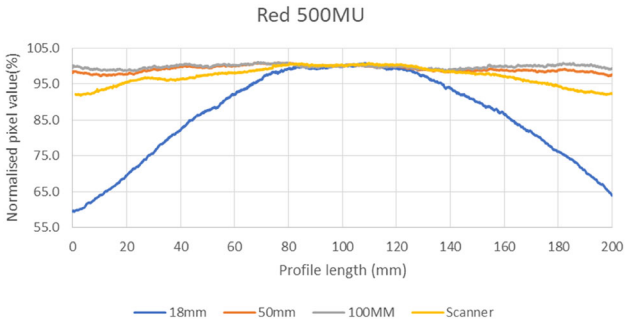

Fig. 1. The four profiles in the figure are based on the red channel analysis of images of the film acquired with the Epson V700 flatbed scanner and with a Canon DSLR 7D camera equipped with an 18 mm, 50 mm and 100 mm focal length lens.

P86. Identification of source of extra cameral response in radiation detectors

Duncan Butler[1,*], Max Hanlon[1], Chris Oliver[1]

[1]ARPANSA, Yallambie, Australia

Introduction Understanding the response of radiation detectors is key to using them accurately and recognising situations where they might give erroneous results. It has long been known that in most detectors the response comes mostly from the active volume but there is an additional "extra cameral" signal arising from other structures. For example, in ionisation chambers the stem and cable have a (usually small) co ntribution to the overall signal.
Method Different parts of a Farmer-type ionisation chamber were irradiated with a 1 mm × 20 mm 90 keV photon beam generated by a synchrotron. This beam was scanned over the length of the chamber so that only 1 mm of the chamber was irradiated at a time. The signal from the thimble (present even with the beam is not irradiating the cavity, due to scatter) was reduced by lowering the bias voltage.
Results The results at -2 V and + 2 V are shown in Fig. 1. There is a region in the chamber stem where the signal is independent of bias, indicating a component of extra cameral response. The intention was to subtract these scans to isolate the bias-independent component, however a difference in the magnitude of the signal from the cavity was observed, so this method could not be used. Further work is required to determine if this difference is a feature of the chamber or a change in the air kerma rate between the scans.
Conclusion A region at the base of the active volume was isolated as one source of extra cameral signal.

Disclosures
This work was performed at the ANSTO Australian Synchrotron.

Fig. 1. Signal from the chamber as 1 mm wide beam is scanned along the length.